

Geophysical Investigations of the North Scotia Ridge

A thesis submitted by Alexander Peter Cunningham to the University of London

External Programme for the degree of Doctor of Philosophy

Geoscience Division
British Antarctic Survey
High Cross
Madingley Road
Cambridge CB3 0ET

November 1998



ABSTRACT

The North Scotia Ridge (NSR) is a series of islands and submarine ridges extending 2000 km from Tierra del Fuego to South Georgia in the western South Atlantic. The ridge forms the elevated northern tectonic margin of the Scotia Sea, and accommodates east–west sinistral strike-slip motion at the South American–Scotiaplate boundary. Existing studies have shown that the northern flank of the NSR is a large and continuous accretionary prism, formed during presumed mid–late Cenozoic north–south convergence. This report describes results of three related marine geophysical studies of the NSR region: (1) a long-range side-scan sonar survey of the southern Falkland Plateau, Falkland Trough and NSR between 40 and 58°W; (2) a multi-channel seismic reflection survey of the NSR near 46°W (Aurora Bank); and (3) a 3.5 kHz sub-bottom profile and bathymetry survey of the Falkland Trough east of 50°W. Data presented in these studies describe the structure and tectonic evolution of this former convergent margin. In particular, multi-channel seismic reflection profiles show the structure of the arc-plateau collision zone near 46°W, and demonstrate that north–south convergence has ceased at the toe of the accretionary prism. Accompanying gravity measurements reveal intermediate-to-oceanic crustal thicknesses beneath the southern Falkland Plateau and Falkland Trough, and show that Aurora Bank is formed principally of deformed accreted sediment, overriding a north-dipping basement backstop. Side-scan sonographs show the structural style of the NSR accretionary prism for the first time, and better constrain the locus of modern South American–Scotia decoupling beneath more southerly, elevated parts of the ridge. Sonographs also show geological features consistent with current control of deposition, non-deposition and erosion beneath the Antarctic Circumpolar Current. In particular, this report describes current-influenced sedimentation in the Falkland Trough, and steep-sided eroded depressions and diffuse scour fabric on the elevated Falkland Plateau.

ACKNOWLEDGEMENTS

I would like to thank several individuals for their help and support in the production of this thesis. In particular, Dr. Peter Barker, my supervisor at the British Antarctic Survey, who conceived the project and supervised my work, and Dr. Robert Larter who provided additional guidance. I also wish to thank Dr. Joseph Cartwright, my University of London Adviser, for his patience and support.

My colleagues in the Geoscience Division, Jeremy Tomlinson, Dr. Richard Woollett, Lieve Vanneste, Dr. Peter Morris, Dr. John Howe, Dr. Carol Pudsey, Marion Barber and Dr. Roy Livermore, assisted with data collection and processing. I am grateful to the British Antarctic Survey for providing facilities and funding for my research, and to the director Prof. Chris Rapley for permission to include the results in this report.

I am also indebted to the officers, crew and scientists who participated in RRS *Shackleton*, RRS *Discovery*, RRS *Charles Darwin* and RRS *James Clark Ross* research cruises for assistance in obtaining the original data. Research Vessel Services and GLORIA personnel at the Southampton Oceanography Centre provided technical support, and the Institute of Terrestrial Ecology, Monks Wood provided image processing facilities.

Finally, I would like to thank my wife and family for their encouragement and support over the years.

CONTENTS

	Page
Chapter 1. Introduction	1
Chapter 2. Long-range side-scan sonar investigation of the North Scotia Ridge	
2.1 Synopsis	2
2.2 Introduction	3
2.3 GLORIA side-scan sonar data acquisition and processing	8
2.4 Interpretation of GLORIA and seismic reflection data	10
2.5 Discussion	28
2.6 Conclusions	36
Chapter 3. Multi-channel seismic reflection investigation of the North Scotia Ridge near 46°W	
3.1 Synopsis	39
3.2 Introduction	40
3.3 Multi-channel seismic reflection data acquisition and processing	44
3.4 Interpretation of seismic reflection data	47
3.4.1 MCS profile BAS878-03	48
3.4.2 MCS profile BAS878-04	57
3.4.3 MCS profile BAS923-S26	64
3.4.4 MCS profile BAS878-05	70
3.4.5 MCS profile BAS878-06	73
3.4.6 MCS profile BAS878-07	76
3.5 BAS878-04 gravity model	79
3.6 Discussion	84
3.7 Conclusions	93
Chapter 4. 3.5 kHz sub-bottom profile and bathymetry investigation of the eastern Falkland Trough	
4.1 Synopsis	96
4.2 Introduction	97
4.3 Geophysical data acquisition and processing	102
4.4 Geophysical data interpretation	105

4.5 Discussion	114
4.6 Conclusions	117

Appendix A. Publications

Appendix B. MAP_SYS map projection software

LIST OF FIGURES

Figure		Page
1(a)	The Scotia Sea region of the western South Atlantic with 3000–m bathymetry and tectonic inset map	
(b)	Negative free-air gravity anomalies in the Scotia Sea region plotted with 3000–m bathymetry	
(c)	North Scotia Ridge region of the western South Atlantic, plotted with 1000, 2000 and 3000–m bathymetry, earthquake epicentres and focal mechanisms, and GLORIA side-scan sonar survey area	4
2	Seismic reflection profile tracks and GLORIA side-scan sonar coverage in the North Scotia Ridge region	9
3(a)	Digital mosaic of GLORIA sonographs obtained in the North Scotia Ridge region west of 50°W	11
(b)	Digital mosaic of GLORIA sonographs obtained in the North Scotia Ridge region east of 50°W	12
4(a)	GLORIA lineaments west of 50°W plotted with bathymetry	
(b)	GLORIA lineaments west of 50°W plotted with free-air gravity	14
5(a)	GLORIA lineaments east of 50°W plotted with bathymetry	
(b)	GLORIA lineaments east of 50°W plotted with free-air gravity	16
6(a)	Single-channel seismic reflection profile BAS889–S01	
(b)	Coincident 3.5 kHz sub-bottom profile	18
7(a)	Single-channel seismic reflection profile SHA734–6	
(b)	Single-channel seismic reflection profile SHA801–1	20
(c)	Multi-channel seismic reflection profile BAS878–03	
(d)	Multi-channel seismic reflection profile BAS878–04	22
8	Tectonic summary of the North Scotia Ridge region	29

9	Single and multi-channel seismic reflection profile tracks crossing the North Scotia Ridge region	41
10	Single and multi-channel seismic reflection profile tracks crossing the Aurora Bank section of the North Scotia Ridge	43
11(a)	Interpreted line drawing of seismic reflection profile BAS878-03	49
(b)	Profile BAS878-03 data panel	50
12(a)	Interpreted line drawing of seismic reflection profile BAS878-04	58
(b)	Profile BAS878-04 data panel	59
13(a)	Interpreted line drawing of seismic reflection profile BAS923-S26	65
(b)	Profile BAS923-S26 data panel	66
14(a)	Interpreted line drawing of seismic reflection profile BAS878-05	71
(b)	Profile BAS878-05 data panel	72
15(a)	Interpreted line drawing of seismic reflection profile BAS878-06	74
(b)	Profile BAS878-06 data panel	75
16(a)	Interpreted line drawing of seismic reflection profile BAS878-07	77
(b)	Profile BAS878-07 data panel	78
17	Falkland Plateau interval velocity–depth functions	81
18	Model of free-air gravity anomaly along seismic reflection profile BAS878-04	83
19	The western South Atlantic Ocean with 3000–m bathymetry and bottom current flow directions	98
20	Bottom potential temperature in the western South Atlantic (after Locarnini <i>et al.</i> 1993)	100
21	Bathymetry ship tracks crossing the central and eastern Falkland Trough	103

22	3.5 kHz sub-bottom profile tracks crossing the central and eastern Falkland Trough	104
23	Bathymetry of the central and eastern Falkland Trough, with area of east Falkland Trough sediment drift shaded, and +0.2°C bottom potential temperature contour	106
24	3.5 kHz sub-bottom profile A–A'	109
25(a)	3.5 kHz sub-bottom profile B–B'	
(b)	3.5 kHz sub-bottom profile C–C'	111
26	Single-channel seismic reflection profile D–D' (profile 'B' of Ludwig & Rabinowitz 1982)	113

Chapter 1

Introduction

This report describes results of marine geophysical surveys of the North Scotia Ridge (western South Atlantic) conducted by the Geoscience Division of the British Antarctic Survey (BAS). These investigations were initiated as part of a wider programme of research into Scotia Sea tectonic evolution and palaeo-circulation (BAS project B6153). The data which form the basis of this work were obtained on BAS scientific cruises between 1987 and 1993, and include bathymetric soundings, high-resolution sub-bottom profiles, multi-channel seismic reflection profiles, long-range side-scan sonographs and marine gravity measurements. For clarity, interpretations have been arranged into three separate studies: (1) a long-range side-scan sonar survey of the southern Falkland Plateau, Falkland Trough and North Scotia Ridge between 40 and 58°W; (2) a multi-channel seismic reflection survey of the North Scotia Ridge near 46°W (Aurora Bank); and (3) a 3.5 kHz sub-bottom profile and bathymetry survey of the Falkland Trough east of 50°W. Essential background information describing the tectonic, sedimentary and oceanographic framework of the North Scotia Ridge region has been included, so that each study may be considered separately. Some of the work described in this thesis has been completed with the assistance of others, and these contributions have been acknowledged in the text. Published results are reproduced in Appendix A of this report.

Chapter 2

Long-range side-scan sonar investigation of the North Scotia Ridge

2.1 SYNOPSIS

The North Scotia Ridge is a series of islands and submarine ridges extending 2000 km from Tierra del Fuego to South Georgia in the western South Atlantic. The ridge forms the elevated northern tectonic margin of the Scotia Sea, and accommodates east–west sinistral strike-slip motion at the South American–Scotiaplate boundary. Existing studies have shown that the northern flank of the North Scotia Ridge is a large and continuous accretionary prism, formed during presumed mid–late Cenozoic north–south convergence. In this study, I present long-range side-scan sonar (GLORIA) images and seismic reflection profiles which show the structural style of the accretionary prism for the first time. The youngest accreted sediments show a uniform fabric of initial deformation (symmetric–gently asymmetric folds of 1–4 km wavelength), which has been subsequently disrupted at shallower depths by additional shortening and uplift. Between 52°45'W and 50°30'W, the deformation front is exposed at the sea floor, and the Falkland Trough retains the appearance of an active convergent margin. Elsewhere however, the deformation front is buried beneath younger, undeformed drift sediments indicating that convergence has ceased. GLORIA sonographs also show geological features consistent with current control of sedimentation, non-deposition, and erosion beneath the Antarctic Circumpolar Current. In particular, this study describes current-influenced sedimentation in the Falkland Trough, and steep-sided, eroded depressions and diffuse slope-parallel fabric on the elevated Falkland Plateau.

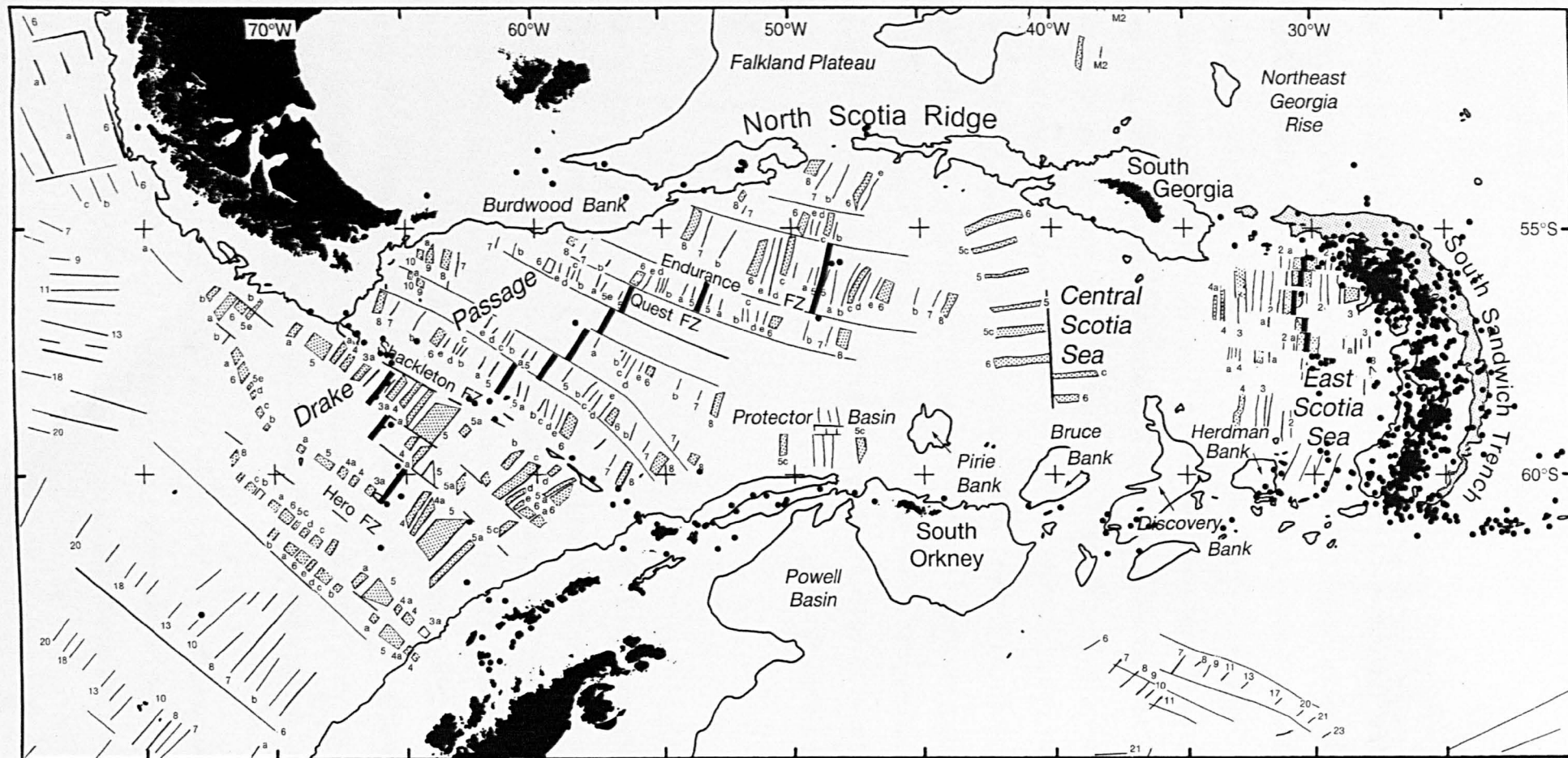
2.2 INTRODUCTION

Studies of arc accretion have shown that arc-continent collision may lead to a cessation of convergent deformation in an accretionary prism, and relocation of the zone of convergence elsewhere. The Banda arc collision zone provides an example of this process (Genrich *et al.* 1996; Snyder *et al.* 1996), where the locus of convergence between the Australian and southeast Asian plates may have moved from a site south of Timor to the Wetar thrust after collision. This study describes the similar development of the North Scotia Ridge in the western South Atlantic (Fig. 1a), where mid-late Cenozoic north-south convergence of the South American and Scotia plates led to collision of an east-west limb of the Scotia arc with the partly continental Falkland Plateau. Here, GLORIA and seismic reflection profiles show clearly that convergence has ceased, and reveal the style of pre-collision deformation. The Banda arc remains in a convergent tectonic setting, but collision of the North Scotia Ridge with the Falkland Plateau has given way to east-west strike-slip motion some 50–100 km south of the original deformation front.

Tectonic setting

The North Scotia Ridge consists of a series of islands and submarine ridges extending 2000 km from Tierra del Fuego to South Georgia, in the western South Atlantic (Fig. 1a). Submerged parts of the ridge have appreciable bathymetric relief: summit regions lie less than 1000 m below sea level, and slopes exceed 15° along its southern margin (Tectonic Map 1985). The North Scotia Ridge is bordered to the north by the Falkland Trough, an east-west bathymetric deep extending from the South American continental margin to the Malvinas Outer Basin, and to the south, by ocean floor exceeding 3000 m depth. The southern flank of the ridge forms the northern topographic boundary of the Scotia Sea.

The North Scotia Ridge is a component of the Scotia arc, an eastward-closing loop of submarine ridges and islands which connects the Andean Cordillera of South America to the Antarctic Peninsula, and encloses the Scotia Sea (Barker & Dalziel 1983; Barker *et al.* 1991).



Tectonic map of the Scotia Arc (adapted from Fig. 2 of Livermore *et al.* 1994). The 2000-m contour is shown, and sea floor which lies > 6000 m below sea level at the South Sandwich Trench is shaded (bathymetry after GEBCO). Magnetic anomaly isochrons are taken from the BAS Tectonic Map of the Scotia Arc (Tectonic Map 1985). Bold line segments correspond to the extinct spreading centres in Drake Passage (Phoenix Ridge and West Scotia Ridge), and the active East Scotia Ridge in the East Scotia Sea. Earthquake epicentres are marked with black dots, and describe the margins of the Scotia plate (along the Shackleton Fracture Zone, North Scotia Ridge, South Scotia Ridge and East Scotia Ridge). Intense seismicity beneath the South Sandwich Islands is associated with westward subduction of the South American plate beneath the east-migrating Sandwich plate.

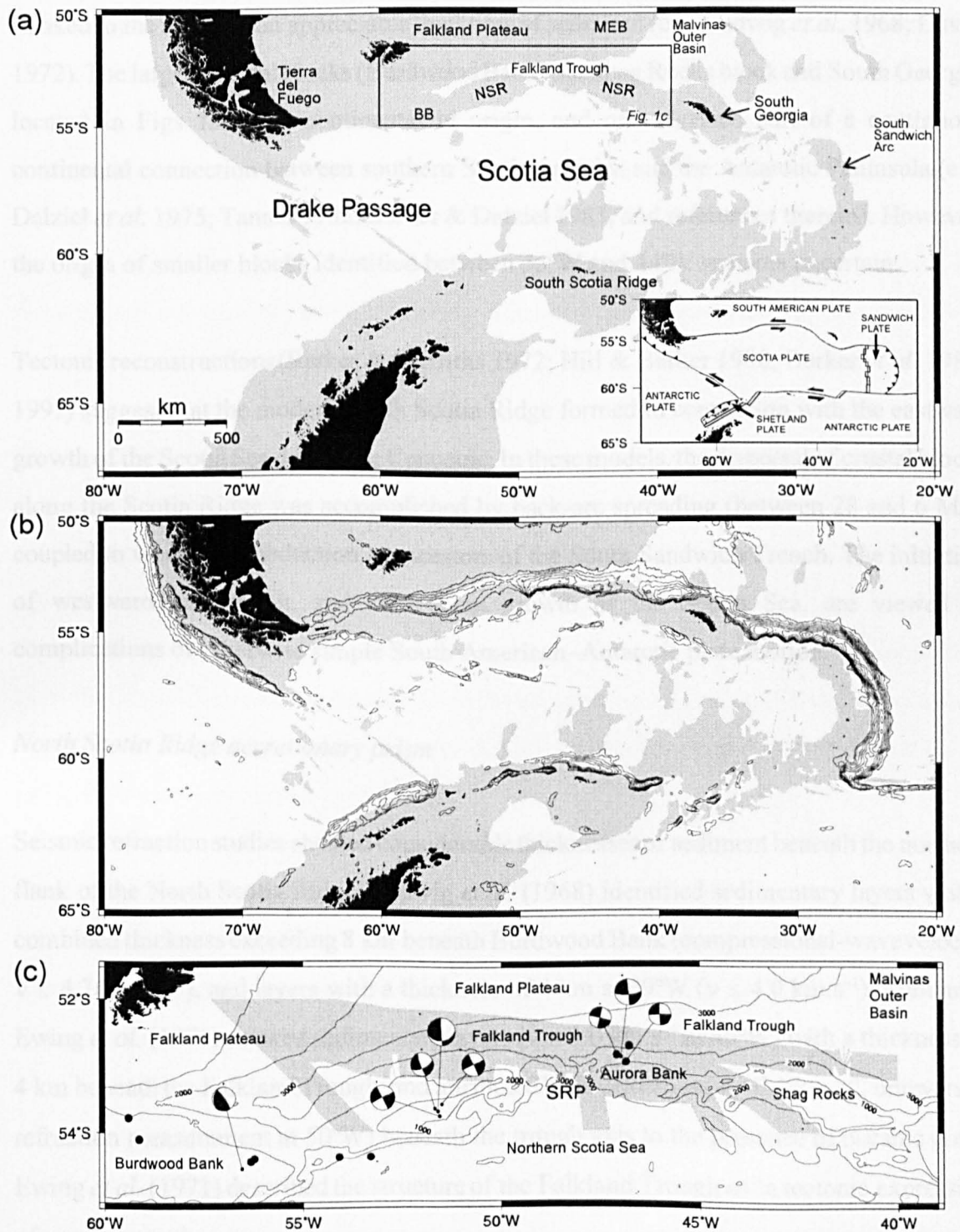


Fig. 1 (a) The Scotia Sea region of the western South Atlantic. Sea floor above 3000 m is shaded, and the area shown in (c) and Fig. 2 is outlined. Inset map shows tectonic setting of the Scotia Sea. NSR, North Scotia Ridge; BB, Burdwood Bank; MEB, Maurice Ewing Bank. (b) Negative free-air gravity anomalies (contour range 0 to -250 mGal, contour interval 25 mGal; Sandwell *et al.* 1995) in the Scotia Sea region plotted with 3000 m bathymetry. The North Scotia Ridge accretionary prism is marked by the east-west gravity low extending east from Tierra del Fuego to South Georgia. (c) North Scotia Ridge region of the western South Atlantic. Earthquake epicentres (Forsyth 1975; Pelayo & Wiens 1989) are marked with black dots, and Harvard centroid moment tensor solutions (e.g. Dziewonski *et al.* 1995) are plotted as equal-area projections of the lower focal hemisphere, with solid quadrants representing compressional *P* wave first motions. 1000 m, 2000 m and 3000 m isobaths (Tectonic Map 1985) are marked, and the area of GLORIA survey is shaded. SRP, Shag Rocks passage.

The ridge is principally composed of small, discrete crustal blocks, partly overlain and flanked to the north by an appreciable thickness of sediment (e.g. Ludwig *et al.* 1968; Davey 1972). The largest crustal blocks (Burdwood Bank, the Shag Rocks block and South Georgia, located in Figs 1a,c) are continental in origin, and once formed part of a continuous continental connection between southern South America and the Antarctic Peninsula (e.g. Dalziel *et al.* 1975; Tanner 1982; Barker & Dalziel 1983, and references therein). However, the origin of smaller blocks identified between 55°W and 44°W remains uncertain.

Tectonic reconstructions (Barker & Griffiths 1972; Hill & Barker 1980; Barker *et al.* 1984, 1991) suggest that the modern North Scotia Ridge formed in connection with the eastward growth of the Scotia Sea during the Cenozoic. In these models, the dispersal of crustal blocks along the Scotia Ridge was accomplished by back-arc spreading (between 28 and 6 Ma), coupled to westward subduction at ancestors of the South Sandwich Trench. The initiation of westward subduction, and subsequent growth of the Scotia Sea, are viewed as complications of otherwise simple South American–Antarctic plate motion.

North Scotia Ridge accretionary prism

Seismic refraction studies showed considerable thicknesses of sediment beneath the northern flank of the North Scotia Ridge. Ludwig *et al.* (1968) identified sedimentary layers with a combined thickness exceeding 8 km beneath Burdwood Bank (compressional-wave velocity $v \leq 4.76 \text{ km.s}^{-1}$), and layers with a thickness of 4 km at 49°W ($v \leq 4.0 \text{ km.s}^{-1}$). Similarly, Ewing *et al.* (1971) showed sedimentary layers ($v \leq 3.0 \text{ km.s}^{-1}$ at 40°W) with a thickness of 4 km beneath the Falkland Trough, and attributed high velocities ($v = 7.1 \text{ km.s}^{-1}$, unreversed refraction measurement at 50°W) beneath the trough axis to the presence of oceanic crust. Ewing *et al.* (1971) described the structure of the Falkland Trough as ‘a tectonic expression of convergence’.

The strike extent of the wedge of sediments became apparent in regional compilations of seismic refraction and gravity data (Rabinowitz 1977; Ludwig *et al.* 1978a,b). Rabinowitz

(1977) showed an east–west belt of large amplitude, negative gravity anomalies (less than -150 mGal) coinciding with the sediment wedge. Similarly, more recent satellite-derived gravity data (Livermore *et al.* 1994; Sandwell *et al.* 1995) have shown a continuous east–west low extending from Tierra del Fuego to the South Sandwich Trench (Fig. 1b). The gravity low is bounded to the south by a steep gravity gradient (locally exceeding 10 mGal.km $^{-1}$), which principally reflects the north-dipping surface of dense underlying basement (e.g. Davey 1972; Barker *in press*). More southerly summit regions of the ridge show large positive gravity anomalies which coincide with elevated topography and outcrops of dense basement material (e.g. Davey 1972).

Using multi-channel seismic reflection data, Ludwig & Rabinowitz (1982) showed that the deformed sediment wedge constitutes a large and continuous accretionary prism. In places west of $50^{\circ}30'W$, the deformation front is exposed at the sea floor, and the Falkland Trough has the appearance of a convergent margin (Ludwig & Rabinowitz 1982; Ludwig 1983; Barker *et al.* 1991). Ludwig & Rabinowitz (1982) inferred active convergence extending from Burdwood Bank to Shag Rocks from the deformation of Falkland Trough sediments, and more recent studies confirmed active deformation at Burdwood Bank (Platt & Philip 1995; Richards *et al.* 1996).

South American–Scotia plate boundary

Earthquake studies have shown that east–west relative motion of the South American and Antarctic plates is partitioned between the North and South Scotia Ridges (Forsyth 1975; Pelayo & Wiens 1989). Along the North Scotia Ridge, a component of South American–Antarctic motion is accommodated at the South American–Scotia plate boundary, which extends from continental South America to South Georgia (inset, Fig. 1a). In Tierra del Fuego, South American–Scotia slip occurs at fault zones crossing the Magallanes foreland fold and thrust belt (Winslow 1982; Klepeis 1994; Diraison *et al.* 1997; Klepeis & Austin 1997). Farther east, the plate boundary lies beneath the North Scotia Ridge, although sparse seismicity does not permit its detailed delineation (Fig. 1c). Forsyth (1975) attributed

earthquakes beneath the ridge to eastward movement of Scotia sea floor with respect to the South American plate. Pelayo & Wiens (1989) confirmed sinistral strike-slip motion, with a component of convergence increasing to the east. Harvard centroid moment tensor focal mechanisms (e.g. Dziewonski *et al.* 1995) describe four earthquakes near 51°30'W (Fig. 1c). Three of these focal mechanisms are consistent with sinistral strike-slip along steep fault planes striking 070–250°T.

Objectives of this study

During cruise CD37 of RRS *Charles Darwin* (1989), the British Antarctic Survey conducted GLORIA survey of a part of the Falkland Plateau, Falkland Trough and North Scotia Ridge, opportunistically on passage from the Falkland Islands to more distant GLORIA target areas. This survey provides new information concerning the past and present tectonic environment of the North Scotia Ridge, and the pattern of sediment deposition and erosion in this region. The main objectives of this study are:

(1) To describe the extent of modern convergence at the toe of the accretionary prism: earthquake studies suggest that South American–Scotia motion is now sinistral strike-slip beneath the central North Scotia Ridge (e.g. Pelayo & Wiens 1989). However, these results are contrary to studies which imply that significant north–south convergence is accommodated in the Falkland Trough between Burdwood Bank and Shag Rocks (Ludwig & Rabinowitz 1982). In this study, I reconcile these conflicting views by using GLORIA and seismic reflection data to identify, and assess the extent of modern convergence at, the toe of the accretionary prism.

(2) To describe the structural record of past north–south convergence preserved within tectonic fabric of the accretionary prism. Field studies have shown distinct phases of shortening and later strike-slip motion across the South American–Scotia boundary in Tierra del Fuego (e.g. Klepeis 1994). However, prior to this study, marine geophysical data were insufficient to establish the structural style of the submerged accretionary prism. As part of this investigation, I use sonographs to map individual folds and faults, and elucidate structural relationships for the first time.

(3) To better constrain the locus of decoupling east of 55°W. Although earthquake studies show that the South American–Scotia plate boundary extends beneath the northern flank of the North Scotia Ridge, data are insufficient to delineate it. In this study, I better constrain the northern extent of the neotectonic zone from its surface expression.

(4) To examine the effects of the vigorous Antarctic Circumpolar Current on sedimentation within the region. In particular, I describe young bottom current-controlled sediment drift deposits in the Falkland Trough, and surficial structures and bedforms in more elevated areas of non-deposition.

2.3 GLORIA SIDE-SCAN SONAR DATA ACQUISITION AND PROCESSING

During cruise CD37, the British Antarctic Survey conducted the first long-range side-scan sonar survey of the North Scotia Ridge (Tomlinson *et al.* 1992) using the GLORIA *Mk II* side-scan sonar (Somers *et al.* 1978). GLORIA data were acquired along four principal ship tracks extending east–southeast across the Falkland Plateau, Falkland Trough and North Scotia Ridge (Fig. 1c). The data constitute *c.* 11 days of continuous GLORIA survey, and cover an area exceeding 100,000 km². During CD37, the GLORIA swath width was 45 km (30 s recording), and survey speeds of 15–18 km.h⁻¹ resulted in cross-line spatial sampling resolutions of *c.* 45 m, and in-line resolutions of *c.* 120 m at close range, degrading to *c.* 900 m at far range (Searle *et al.* 1990). Cruise CD37 also acquired gravity and magnetic data, 3.5 and 10 kHz echo soundings, and two-channel seismic reflection profiles. Seismic reflection profiles from published studies and the British Antarctic Survey archive (Fig. 2) have also been used to support interpretations.

GLORIA side-scan sonar data processing

GLORIA sonographs presented in this study were processed by Jeremy Tomlinson (formerly of British Antarctic Survey Geoscience Division). GLORIA data were initially corrected for ray path geometry (slant-range correction), variations in ship speed (anamorphic correction), and beam sensitivity and refraction effects (shading correction: Searle *et al.* 1990). Pixel



Fig. 2 Single-channel seismic and multi-channel seismic tracks (seismic data sources described in the text). Thin tracks correspond to single-channel seismic reflection profiles, bold tracks correspond to multi-channel seismic reflection profiles, and profiles reproduced in Figs 6 and 7a-d are highlighted. 1000 m, 2000 m and 3000 m isobaths are marked with dotted lines, and the area of the GLORIA survey is shaded.

positions were then transformed onto a Lambert Conformal Conic projection, and coincident sonographs were digitally edited and combined using Mini Image Processing Software (Chavez 1986). A linear contrast stretch was applied before display. The digital mosaicking of the images was supervised by the author.

Artefacts and inherent limitations of the GLORIA image are few, but should be noted. Along-track resolution is decreased at far range, and artefacts may appear along track, either from the poorly synchronised output pulse of a different acoustic system (airgun, 3.5 kHz) or as interference fringes at extreme range. The ship track appears as a diffuse central zone, resulting from the zero sensitivity of the system in the vertical plane. When interpreting the image, care must be taken to consider the insonification direction, which will generally change between adjacent swaths and across the ship track, and the insonification angle, which will vary from the centre to edge of a swath. Fabric perpendicular to track will be relatively poorly insonified.

For convenience, the GLORIA mosaic has been split at 50°W into western and eastern parts. Figures 3a and 3b show the separate parts of the mosaic, plotted so that areas of high backscatter appear bright, and areas of low backscatter appear dark. Figures 3a and 3b also include interpreted line drawings of features apparent in the sonographs. In general, these lineaments mark boundaries separating areas of contrasting backscatter, discontinuities in fabric, and narrow areas of very high backscatter.

2.4 INTERPRETATION OF GLORIA AND SEISMIC REFLECTION DATA

GLORIA sonographs have been interpreted with reference to Birmingham University and British Antarctic Survey seismic reflection profiles (Fig. 2) obtained during RRS *Shackleton* cruises 734, 756 and 801 (1973–1981), RRS *Discovery* cruise 172 (1988), cruise CD37 (1989) and RRS *James Clark Ross* cruise JR04 (1993). I also refer to profiles acquired by the Lamont-Doherty Earth Observatory (Ludwig & Rabinowitz 1982) during RV *Robert D. Conrad* cruises 1606 (1973) and 2106 (1978). These data help to determine the internal

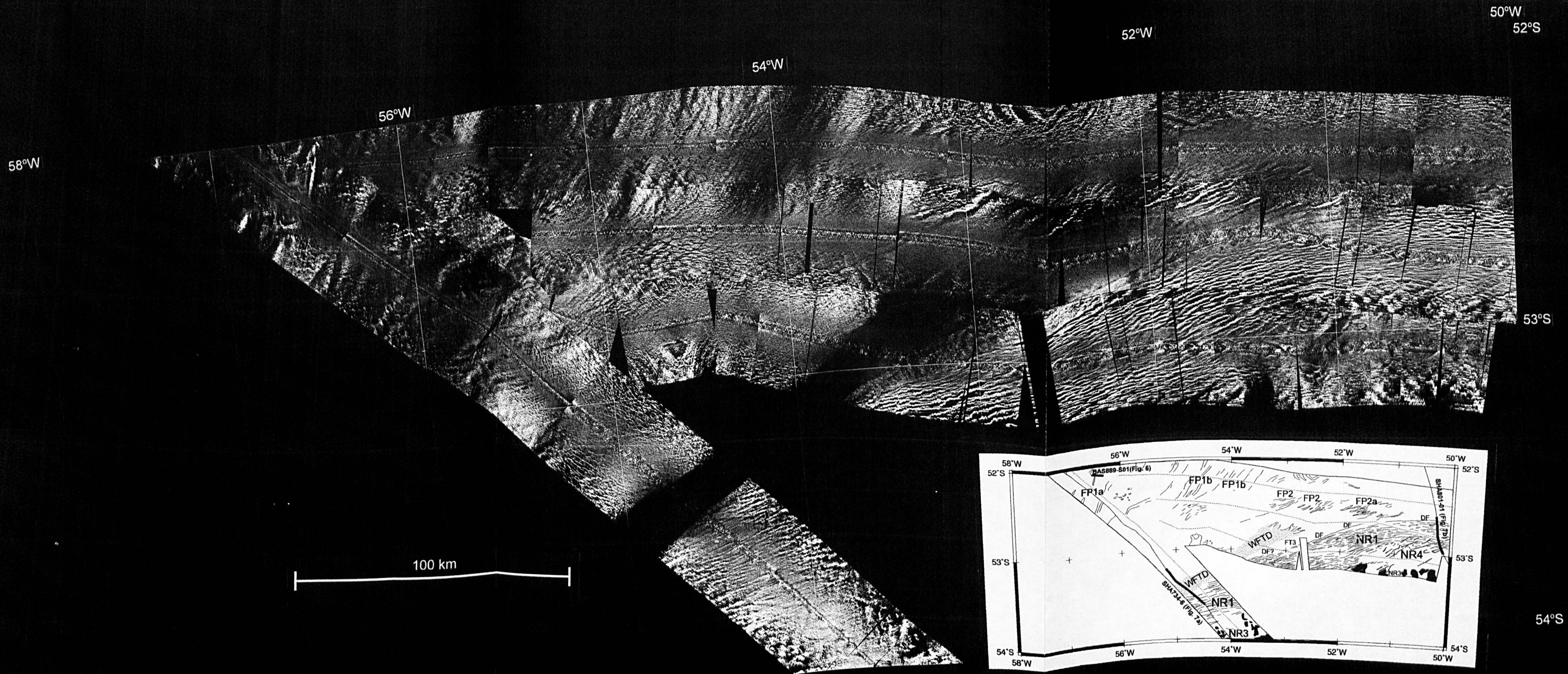


Fig 3a. Digital mosaic of GLORIA sonographs acquired west of 50°W. Inset shows interpreted lineaments traced from the GLORIA data. Labels locate sea-floor features described in the text, and tracks of seismic reflection profiles (Figs 6 and 7a,b) are labelled. Solid black areas on the inset correspond to areas of high backscatter in the side-scan sonographs. Dotted lines on the inset mark GLORIA survey tracks.

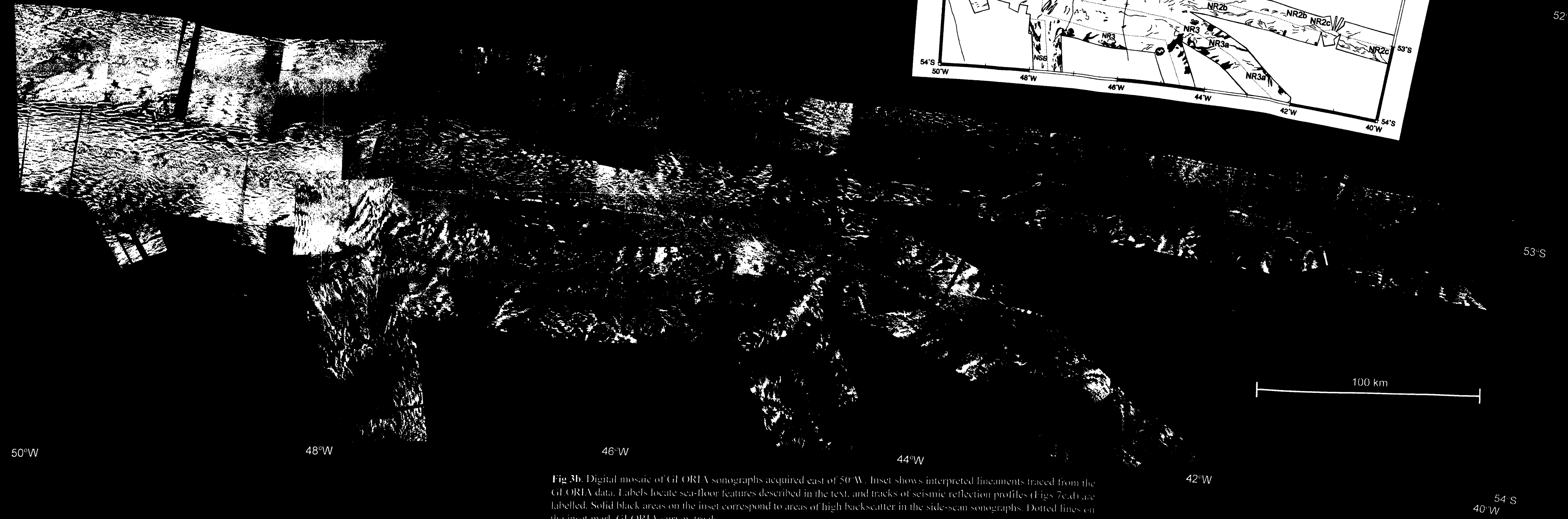


Fig 3b. Digital mosaic of GLORIA sonographs acquired east of 50°W. Inset shows interpreted lineaments traced from the GLORIA data. Labels locate sea-floor features described in the text, and tracks of seismic reflection profiles (Figs 7c,d) are labelled. Solid black areas on the inset correspond to areas of high backscatter in the side-scan sonographs. Dotted lines on the inset mark GLORIA survey tracks.

structure and origin of sea-floor features apparent in the sonographs. Figures 3–5 show interpreted GLORIA lineaments with seismic tracks, regional bathymetry (Tectonic Map 1985) and satellite-derived gravity anomalies (Sandwell *et al.* 1995).

This study is concerned principally with tectonic fabric, but also describes bottom current-related bedforms and sediment drift deposits, which are prominent in the sonographs. The GLORIA mosaic includes four distinct geological provinces: the Falkland Plateau, Falkland Trough, North Scotia Ridge and northern Scotia Sea (Fig. 1c).

Falkland Plateau

The GLORIA survey extends across a triangular area of the Falkland Plateau, southeast of the Falkland Islands. This area lies almost entirely within the western mosaic, north of the Falkland Trough (Fig. 1c). Here, Falkland Plateau sea floor is smooth, and dips southeastward with gradients of up to 0.8° (Fig. 4a). Sonographs show a strongly textured sea floor, with broad areas of moderate backscatter, adjacent shadow and prominent lineaments. Most lineaments are sub-parallel to the bathymetric contours (Fig. 4a).

FP1 acoustic fabric

A group of bright lineaments ('FP1a', Fig. 3a) lies near the western limit of survey at 800–1400 m depth. FP1a are elongate areas of very high backscatter, broadly aligned with the bathymetric contours. The most prominent FP1a lineament can be traced over 17 km in the sonographs. Single-channel seismic reflection and 3.5 kHz profiles (Fig. 6, and profile SHA734–6, Barker *in press*) show that this particular lineament is a steep-sided asymmetric depression, created by differential erosion at the thinning up-slope termination of a sediment sequence that is widespread over the Falkland Plateau slope. Although the steep eastern flank of the depression resembles a fault scarp, profile BAS889-S01 shows that deeper bedding plane reflections extend continuously beneath it (at c. 2.35 STWT, Fig. 6a).

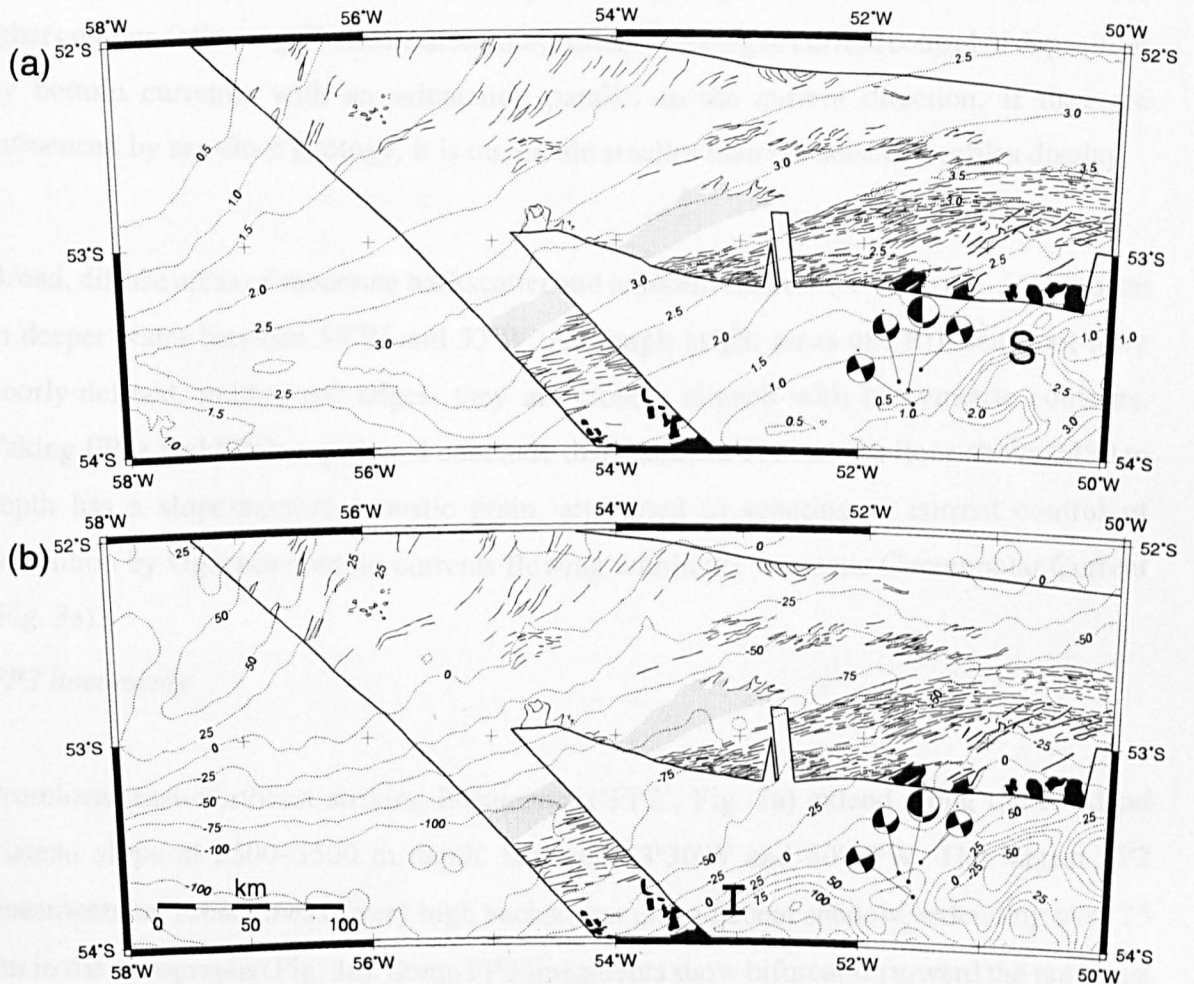


Fig. 4. Western GLORIA mosaic lineaments plotted with (a) bathymetry (contour interval 0.5 km: Tectonic Map 1985). 'S' marks steep NE-SW trending southern flank of the North Scotia Ridge (b) free-air gravity anomaly derived from satellite altimetry data (contour interval 25 mGal: Sandwell *et al.* 1995). Earthquake focal mechanisms are from the Harvard centroid moment tensor catalogue (e.g. Dziewonski *et al.* 1995). Solid black areas correspond to areas of very high backscatter in sonographs. 'I' marks steep gravity gradient corresponding to the northern flank of basement beneath the North Scotia Ridge (modelled by Barker *in press*).

Other outcropping geological boundaries are seen downslope on seismic reflection profile SHA734-6, but are not similarly eroded. The more subdued FP1a lineaments have a topographic origin: on CD37 seismic reflection and 3.5 kHz profiles they appear as changes in surface roughness, but the 3.5 kHz profiles are acoustically-opaque (indicating a hard sea floor) and the seismic profiles show no systematic changes in sediment thickness. These other contour-following FP1a lineations may reflect scouring or current control of deposition by bottom currents, with an orientation parallel to the current direction. If they are influenced by sea-floor geology, it is on a scale smaller than the seismic profiles display.

Broad, diffuse areas of moderate backscatter and adjacent shadow ('FP1b', Fig. 3a) are seen in deeper water between 55°W and 53°W. Although bright areas of FP1b sea floor have poorly-defined, gradational edges, they are closely aligned with bathymetric contours. Taking FP1a and FP1b together, I conclude that Falkland Plateau sea floor above 2250 m depth has a slope-parallel acoustic grain, attributed to scouring or current control of deposition by vigorous contour currents flowing within the Antarctic Circumpolar Current (Fig. 3a).

FP2 lineaments

Prominent east-northeast striking lineaments ('FP2', Fig. 3a) extend along the Falkland Plateau slope at 2500-3500 m depth, between 53°30'W and 50°30'W. The largest FP2 lineaments are broad lines of very high backscatter and adjacent shadow, extending over 25 km in the sonographs (Fig. 3a). Some FP2 lineaments show bifurcation toward the northeast (e.g. 'FP2a', Fig. 3a). FP2 lineaments straddle an east-west boundary between GLORIA swaths, and appear consistently brighter on the more southerly (up-slope) sonograph (Fig. 3a). This may reflect over compensation of backscatter amplitude at far range during processing, since the farthest ranges were preserved on the southernmost swath during editing. However, these characteristics are also consistent with backscatter from steep, south-facing bathymetric scarps.

FP2 fabric is crossed obliquely by one 3.5 kHz profile, and by two Lamont-Doherty single-

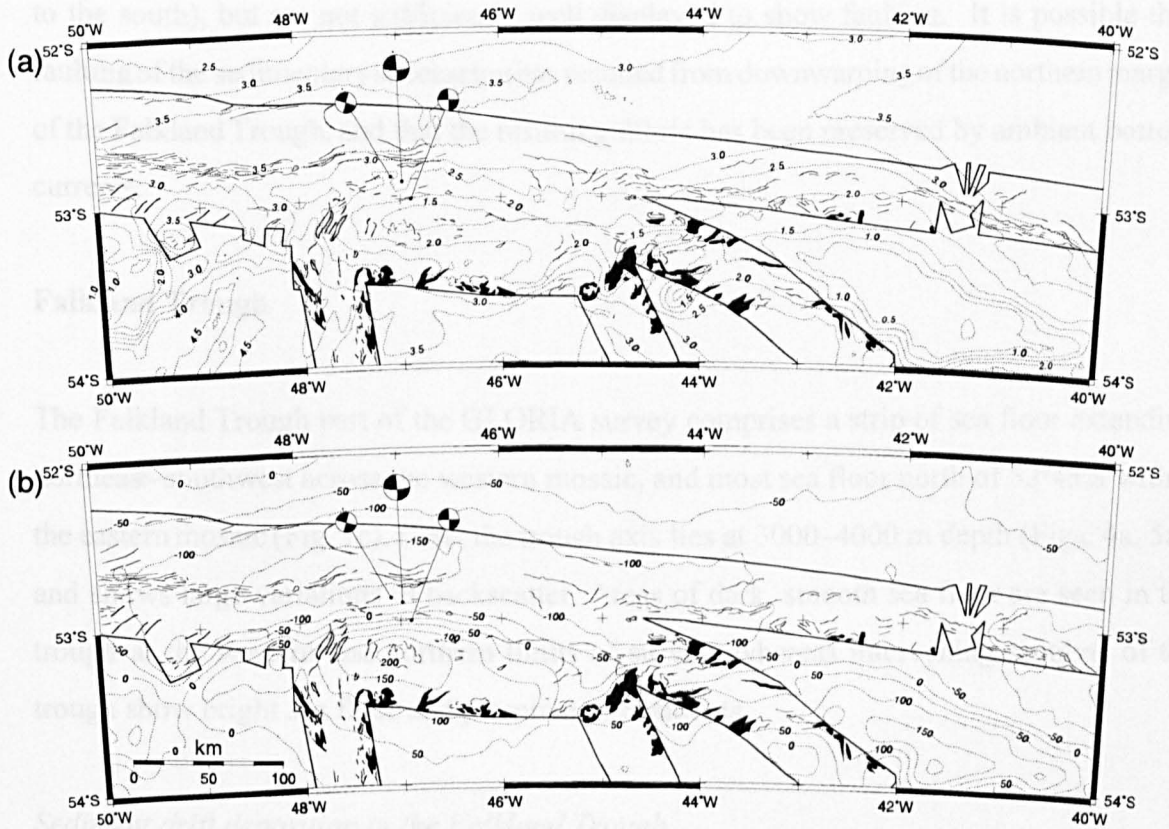


Fig. 5. Eastern GLORIA mosaic lineaments plotted with (a) bathymetry (contour interval 0.5 km; Tectonic Map 1985), (b) free-air gravity anomaly derived from satellite altimetry data (contour interval 50 mGal; Sandwell *et al.* 1995). Earthquake focal mechanisms are from the Harvard centroid moment tensor catalogue (e.g. Dziewonski *et al.* 1995). Solid black areas correspond to areas of very high backscatter in sonographs.

channel seismic reflection profiles (cruises RC1606 and IO1578). The 3.5 kHz profile (Fig. 5a of Howe *et al.* 1997) shows a south-facing fault scarp (*c.* 75 m height). Similarly, the seismic profiles show sea-floor scarps with comparable scale and asymmetry (steeper flank to the south), but are not sufficiently well displayed to show faulting. It is possible that faulting of the sedimentary succession has resulted from downwarping of the northern margin of the Falkland Trough, and that the resulting fabric has been preserved by ambient bottom currents.

Falkland Trough

The Falkland Trough part of the GLORIA survey comprises a strip of sea floor extending northeast–southwest across the western mosaic, and most sea floor north of 52°45'S within the eastern mosaic (Fig. 1c). Here, the trough axis lies at 3000–4000 m depth (Figs. 4a, 5a), and shows large variations in backscatter. Areas of dark, smooth sea floor are seen in the trough at the western and northern limits of survey, whereas intervening sections of the trough show bright sea floor and prominent lineaments.

Sediment drift deposition in the Falkland Trough

Between the western limit of survey and about 53°W, the Falkland Trough shows extremely low backscatter (described in this study as the west Falkland Trough sediment drift (WFTD), Fig. 3a). At 54°30'W, WFTD sea floor contrasts with the bright, textured sea floor of the adjacent Falkland Plateau and North Scotia Ridge, and can be traced eastward across a gap in sonographs over 160 km. The low backscatter suggests a smooth, well-sedimented sea floor, since a rough surface buried beneath weakly-scattering sediment may yield significant backscatter to *c.* 20 m depth (at 6.5 kHz, Mitchell 1993). Between 54°W and 53°W, WFTD sea floor widens to the east and shows steadily increasing backscatter. Coincident 3.5 kHz profiles (Howe *et al.* 1997) show thinning of surficial trough sediments to the east. The thinning eastern end of the WFTD lies on the northern trough slope, adjacent to a separate, flat-bottomed deep ('FT3', Fig. 3a).

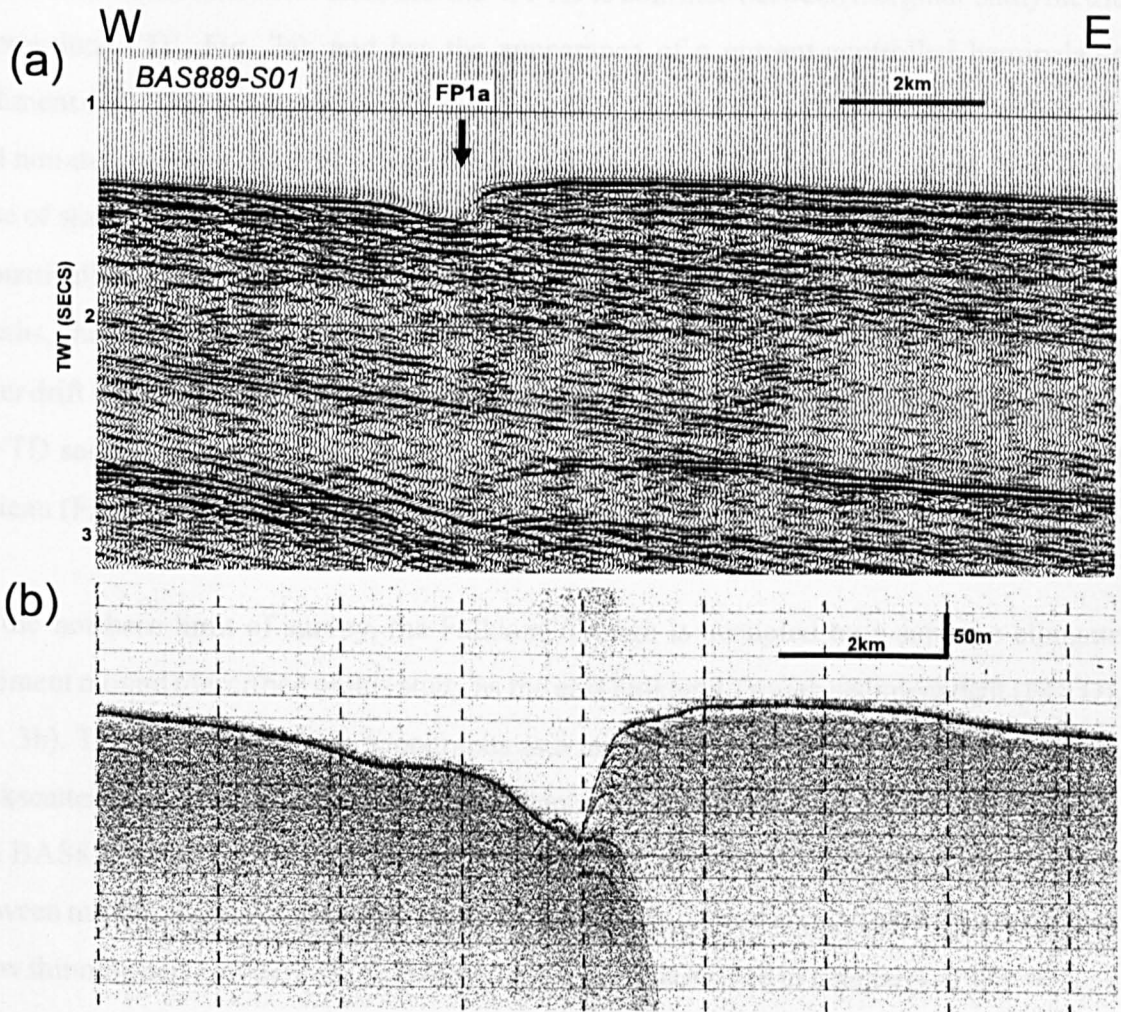


Fig. 6. (a) Single-channel seismic reflection profile BAS889-S01 (located in Fig. 3a inset, vertical exaggeration (VE)= *c.* 4:1 in water) showing eroded depression on Falkland Plateau sea floor (FP1a, Fig. 3a). (b) Coincident 3.5 kHz sub-bottom profile (VE= *c.* 10:1 in water).

Seismic reflection profile SHA734–6 (Fig. 7a) shows that WFTD sea floor corresponds to the surface of a thick, mounded sequence characterised by bright, fairly continuous reflections. These data show also, that the WFTD is confined between marginal bathymetric depressions ('D', Fig. 7a), and has the appearance of a current-controlled hemipelagic sediment drift. This is supported by 3.5 kHz profiles (Howe *et al.* 1997) which show thinning and non-deposition at the drift margins in response to intensified bottom-current flow at the base of slope. Beneath the southern flank of the trough, WFTD sediments overlie deformed, acoustically-opaque sediments of the North Scotia Ridge accretionary prism. At greater depths, the boundary between drift and accretionary prism becomes indistinct, and some older drift sediments may have been incorporated within the accretionary prism. To the north, WFTD sediments overlie acoustically-stratified, south-dipping sediments of the Falkland Plateau (Fig. 7a).

At the northern limit of survey, the Falkland Trough is occupied by a separate elongate sediment mound (described in this study as the east Falkland Trough sediment drift (EFTD), Fig. 3b). The EFTD appears in sonographs as a faint but discernible eastward reduction in backscatter near 47°30'W (Fig. 3b). Multi-channel seismic reflection profiles BAS878–03 and BAS878–04 (Figs. 7c,d) show thick, acoustically-stratified EFTD sediments confined between marginal bathymetric depressions ('D', Figs. 7c,d), and coincident 3.5 kHz profiles show thinning and non-deposition at the drift margins (described in chapter 4 of this report). On these grounds, the mounded external geometry of the EFTD is attributed to bottom current-control of deposition.

Between the WFTD and EFTD lies an area of the Falkland Trough with moderate to high backscatter, in which such lineaments as are seen are characteristic of the Falkland Plateau. This area probably has only a thin and patchy cover of modern sediments. At the eastern end of the WFTD, the rougher sea floor of the Falkland Trough deep ('FT3', Fig. 3a) is also Falkland Plateau sediment, essentially unburied.

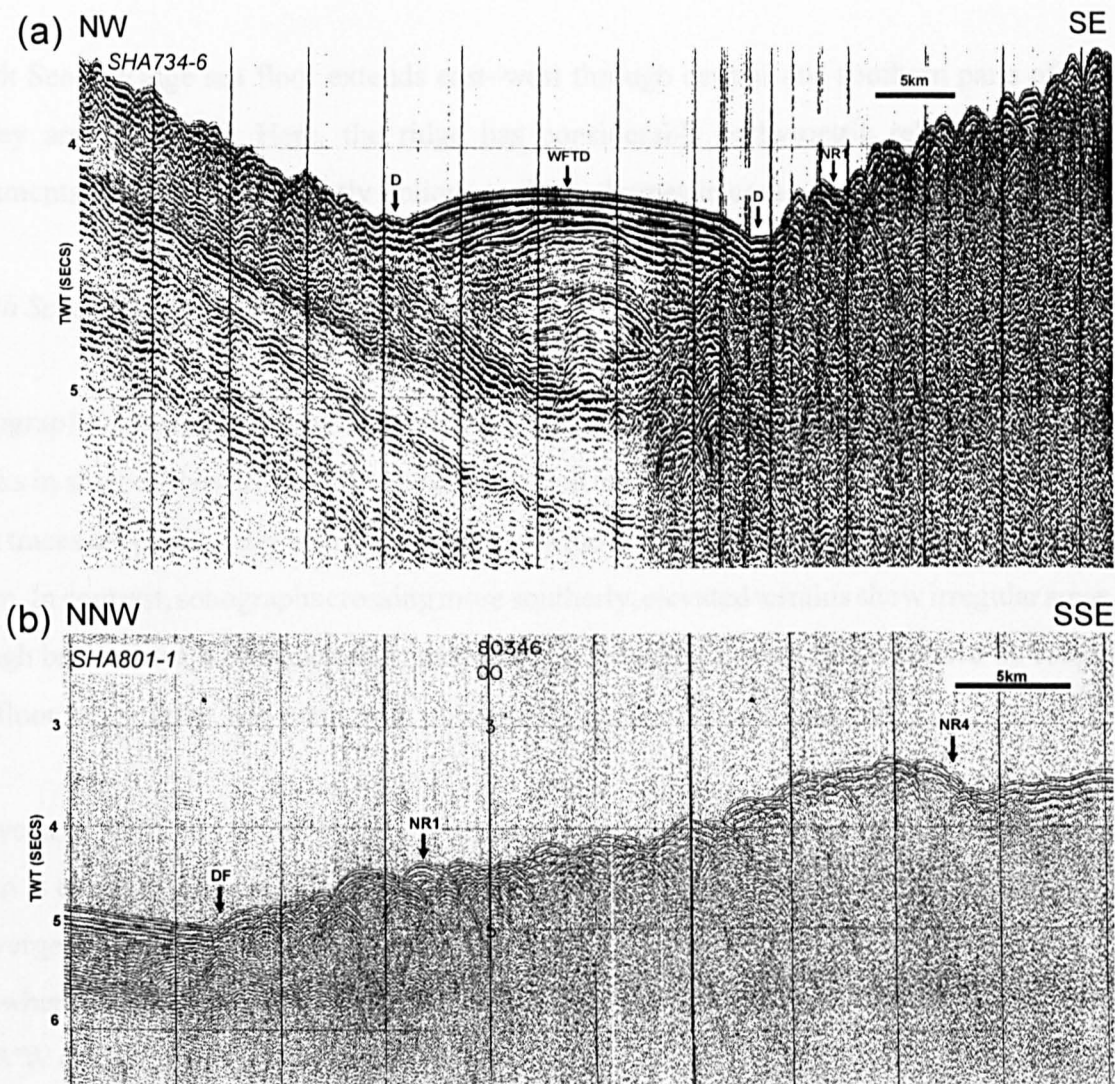


Fig. 7 (a) Single-channel seismic reflection profile SHA734-6 (located in Fig. 3a inset, VE = *c.* 18:1 at the sea floor). Broad, shallow, high-amplitude reflections which parallel the sea floor beneath WFTD are airgun source bubble reverberations; primary geological reflections appear as higher frequency arrivals which cut across these events. Profile shown is a bandpass filtered single-channel monitor record acquired using a single Bolt 1500C airgun (chamber capacity=4.8 l). (b) Single-channel seismic reflection profile SHA801-1 (located in Fig. 3a inset, VE = *c.* 6:1 at the sea floor). Acquisition and processing parameters as for SHA734-6. (c) Multi-channel seismic reflection profile BAS878-03 (located in Fig. 3b inset, VE = *c.* 6:1 at the sea floor). BAS878-03 was acquired using a source of 3 Bolt airguns (combined chamber capacity=15.1 l) and a 48-channel hydrophone streamer (50 m group interval), and processed to 24-fold common-mid-point stack using standard procedures. The profile shown has been imaged using a Stolt F-K time migration algorithm. (d) Multi-channel seismic reflection profile BAS878-04 (located in Fig. 3b inset, VE = *c.* 6:1 at the sea floor). Acquisition and processing procedures as for BAS878-03. WFTD, west Falkland Trough sediment drift; EFTD, east Falkland Trough sediment drift; D, marginal bathymetric depressions, DF, deformation front; NR1, fabric of initial deformation; NR2a, outcrops of thrust faults; NR4, young southward-dipping fault scarp; TH, thrust plane reflection.

North Scotia Ridge

North Scotia Ridge sea floor extends east–west through central and southern parts of the survey area (Fig. 1c). Here, the ridge has considerable bathymetric relief, and most lineaments are parallel or slightly oblique to the bathymetric contours (Figs. 4a, 5a).

North Scotia Ridge accretionary prism

Sonographs show linear–curvilinear fabric, attributed to backscatter from folds, faults and breaks in slope at the surface of the North Scotia Ridge accretionary prism. Fold fabric and fault traces are particularly well preserved across the northernmost 50 km of the accretionary prism. In contrast, sonographs crossing more southerly, elevated terrains show irregular areas of high backscatter, low backscatter and shadow. These regions are characterised by rough sea-floor topography, and areas with outcrops of dense basement material.

Between 52°45'W and 50°30'W, the deformation front of the North Scotia Ridge accretionary prism is exposed at the sea floor, and the Falkland Trough axis retains the appearance of a convergent margin (Ludwig & Rabinowitz 1982; Ludwig 1983; Barker *et al.* 1991). Elsewhere however, the deformation front is buried beneath undeformed drift sediments west of 53°W (WFTD) and east of 48°W (EFTD).

Deformation front

Between 52°45'W and 50°30'W, a thin, continuous line ('DF', Fig. 3a) marks the northern edge of the accretionary prism. Seismic reflection profiles (single-channel profile SHA801–1, Fig. 7b and profile 143 of Ludwig & Rabinowitz 1982) show that DF separates smooth Falkland Plateau sea floor from rougher North Scotia Ridge sea floor lying to the south (marked with diffractions in Fig. 7b). These data show also, that DF is accompanied by a southward reduction in the continuity of near-surface reflections, attributed to the deformation and uplift of Falkland Plateau sediments at the foot of the North Scotia Ridge

Long-range side-scan sonar investigation of the North Scotia Ridge

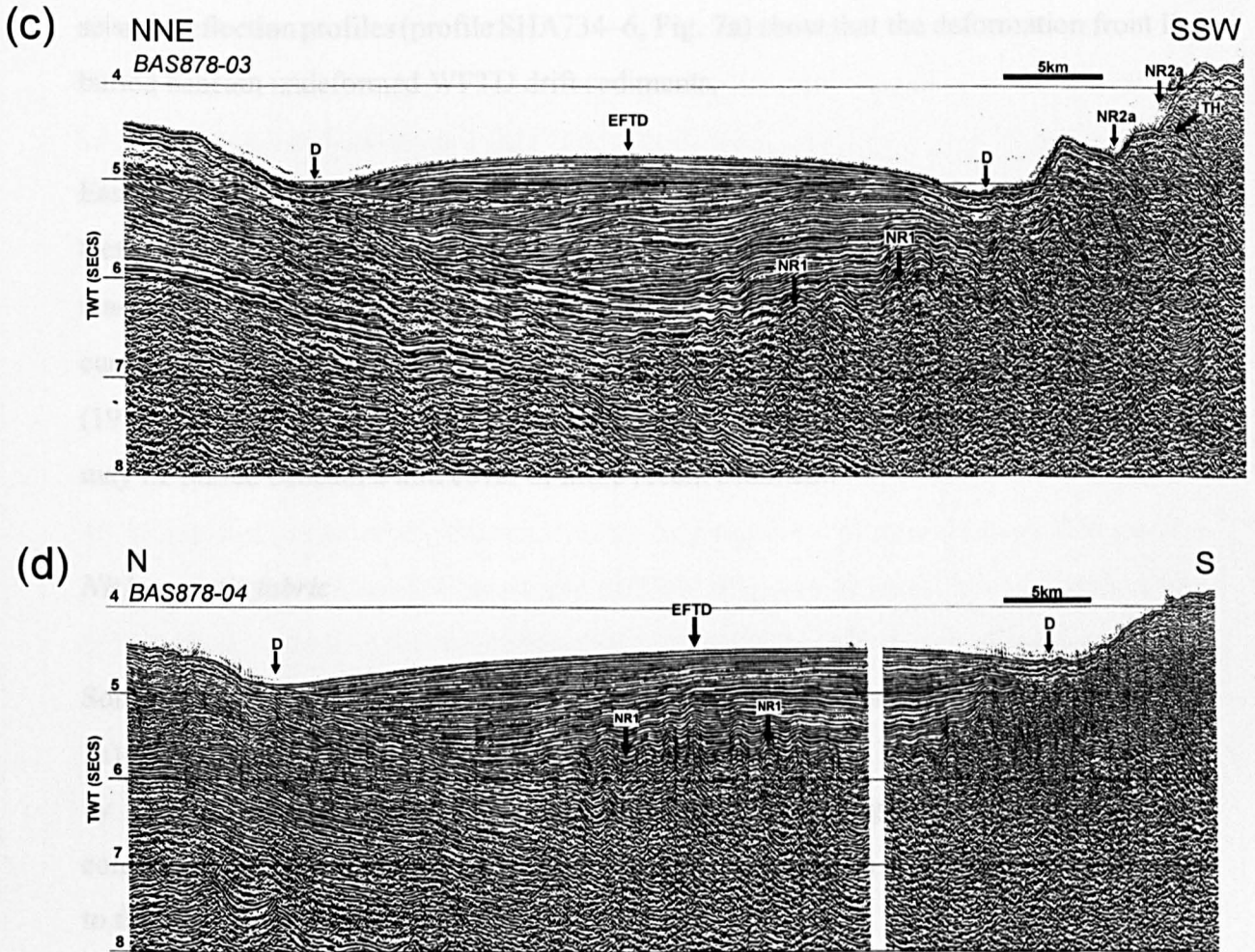


Fig. 7 (c and d)

(Ludwig & Rabinowitz 1982; Ludwig, 1983; Barker *et al.* 1991). Hence, DF marks the exposed deformation front of the accretionary prism, which can be traced in sonographs over 250 km. Near 54°W, DF converges to the west with the WFTD (Fig. 3a), although the point of intersection lies in a gap between sonographs. At 54°30'W, sonographs (Fig. 3a) and seismic reflection profiles (profile SHA734–6, Fig. 7a) show that the deformation front lies buried beneath undeformed WFTD drift sediments.

East of about 50°W, DF becomes less distinct, and is replaced by a broader zone where tectonic fabric terminates against smooth Falkland Trough sea floor (e.g. 49°W, Fig. 3b). The reason for this is unclear; the accretionary prism may have been eroded by strong bottom currents flowing in the vicinity of Shag Rocks passage, as inferred by Ludwig & Rabinowitz (1982) from their nearby seismic reflection profile 142. However, it is also possible that DF may lie buried beneath a thin cover of more recent sediment.

NR1 acoustic fabric

Sonographs of the western North Scotia Ridge show a striped acoustic fabric ('NR1', Fig. 3a) within 50 km of the deformation front (below 2000 m depth). NR1 fabric is characterised by very bright, sub-parallel lineaments which are closely aligned with the bathymetric contours (Fig. 4a). NR1 lineaments can be traced across a gap in sonographs from 48°30'W to the western limit of survey.

Migrated seismic reflection profiles crossing exposed NR1 fabric were not available for this study. However, time-migrated data obtained farther east help to describe this fabric. Profiles BAS878–03 and BAS878–04 (Figs. 7c,d) obtained between 47°W and 46°W show a wavy reflection configuration within the lower layers of the EFTD ('NR1', Figs. 7c,d), which is attributed to drape across well-formed, open, symmetric–gently asymmetric folds developed at the surface of the accretionary prism. Farther west, these folds are unburied, and are represented in sonographs by NR1 (Figs. 3a,b). The striped fabric results from large, regular variations in acoustic grazing angle across successive folds; bright lineaments correspond to

fold limbs facing the insonification direction, and opposing fold limbs occupy intervening areas of low backscatter. The lack of dependence of brightness on insonification direction suggests that the folds are symmetric–gently asymmetric. Hence, NR1 represents a broad area of regular folds extending south from the deformation front, and in this respect, resembles the most recently accreted sections of the Makran accretionary prism (e.g. White & Ross 1979) and the Barbados Ridge accretionary prism (Biju-Duval *et al.* 1982; Stride *et al.* 1982; Brown & Westbrook 1987).

NR1 fold wavelengths are between 1 and 4 km, and appear consistently larger (*c.* 3.5 km) on the westernmost GLORIA track at 54°30'W (Fig. 3a). Individual folds can be traced in sonographs over 20 km, and generally thin at their limit, suggesting a steady reduction in fold amplitude. The folds show few discontinuities, although minor lateral offsets are observed where NR4 lineaments (described below) cut shallow NR1 fabric near 50°30'W (Fig. 3a). NR1 fold axes are generally aligned with the bathymetric contours, although folds appear slightly oblique to bathymetric strike near 54°30'W (Fig. 4a). There is little variation in fold trend with distance from the deformation front, across any given section of the accretionary prism.

NR2 acoustic fabric

Near 48°W, NR1 fabric is replaced to the east by a thin band of sinuous acoustic fabric ('NR2', Fig. 3b) extending along the North Scotia Ridge to the Shag Rocks block at 2000–3500 m depth. NR2 is characterised by sinuous, curvilinear bands of moderate and low backscatter, parallel or slightly oblique to the bathymetric contours (Fig. 3b). This fabric is attributed to backscatter from folds, faults and breaks in slope at the surface of the accretionary prism, although it does not have the linearity or regularity of NR1.

NR2 fabric is particularly well developed at 47°W ('NR2a', Fig. 3b). Here, seismic reflection profile BAS878–03 (Fig. 7c) shows large breaks in slope, and I note a similarity between NR2a and sinuous sonar fabric attributed to slope breaks elsewhere (e.g. near 7°N, 79°30'W

off Panama, Plate 2 of Westbrook *et al.* 1995). The breaks in slope mark the surface trace of south-dipping thrust faults, with faint thrust plane reflections apparent in the near surface ('TH', Fig. 7c). Hence, NR2a represents backscatter from the exposed surface of thrust fault-bound slices of accreted sediment, resulting from secondary (post-NR1) uplift and shortening within the accretionary prism. Thrust fault-controlled breaks in slope have been associated with compressional loading of the foreland north of Burdwood Bank (Platt & Philip 1995), and are a common feature of accreting forearc terrains (e.g. in the west Gulf of Oman, White & Ross 1979; Middle America Trench, Moore & Shipley 1988; Nankai Trough, Moore *et al.* 1990).

On profile BAS878-03 (Fig. 7c), NR2a structures mark the southern limit of NR1 folds. From this, I infer that the regularity of NR1 generated at the frontal fold has been disrupted at shallower depths by secondary deformation and uplift. Also, MCS profiles BAS878-03 and BAS878-04 (Figs 7c,d) show that NR1 sea floor is entirely buried beneath EFTD sediments between 47°W and 46°W. Therefore, the transition from NR1 to NR2 fabric observed in sonographs at 48°W reflects the burial of NR1 folds east of 48°W, and does not necessarily indicate a change in structural style.

Similar but smaller lineaments ('NR2b', Fig. 3b) extend at 2250–3000 m depth along the northern slope of the Shag Rocks block. Here, Ludwig & Rabinowitz (1982) described incipient thrusting and uplift of near-surface sediments, and NR2b may therefore represent backscatter from convergent deformation at the surface of the accretionary prism.

East of 42°W, the tectonic environment is different: to the north lies thick ponded sediment overlying ocean floor of the Malvinas Outer Basin, rather than the narrow Falkland Trough and (probably continental) eastern Falkland Plateau. Here, sonographs show a prominent fabric ('NR2c', Fig. 3b) along the northeast flank of the Shag Rocks block, attributed to backscatter from slopes steepened by shortening and uplift of the accretionary prism. NR2c fabric is separated from adjacent dark sedimented ocean floor by a lobate boundary which runs close to the base of slope. The lobate character of NR2c appears similar to that observed

in sonographs of active deformation fronts (e.g. Masson & Scanlon 1991; Maldonado *et al.* 1994; Westbrook *et al.* 1995).

NR3 acoustic fabric

Above 2250 m depth, the North Scotia Ridge shows chaotic fabric ('NR3', Figs. 3a,b), with irregular areas of high backscatter, low backscatter and shadow. Near 44°30'W, bright NR3 fabric coincides with broad, steep-sided summit ridges (Fig. 5a). Narrow, very bright NR3 lineaments near 42°30'W may represent backscatter from fault scarps along the southern flank of the Shag Rocks block ('NR3a', Fig. 3b). The brightness of NR3 owes something to the virtual absence of sedimentation over the crest of the North Scotia Ridge under the influence of a vigorous Antarctic Circumpolar Current.

NR4 lineaments

Near 50°30'W, a set of faint lineaments ('NR4', Fig. 3a) extends across the North Scotia Ridge at 2000–3000 m depth. NR4 lineaments appear as thin, faint but continuous lines, with 060–240°T trending curvilinear trajectories which cut NR1 folds. This subdued fabric crosses shallowest NR1 sea floor and adjacent NR3 sea floor near 50°30'W. Individual NR4 structures can be traced in sonographs over 35 km. Near 52°50'S, NR4 structures have an échelon pattern and terminate *c.* 20 km south of the deformation front (Fig. 3a).

Seismic reflection profile SHA801–1 crosses NR4 structures near 52°30'S (Fig. 3a) where they define a horst, with a south-facing scarp at its southern end ('NR4', Fig 7b). On these grounds, NR4 lineaments are interpreted as fault traces which cut North Scotia Ridge tectonic fabric. The faults are broadly aligned with east northeast–west southwest trends in gravity and bathymetry; in particular, the nearby southern flank of the North Scotia Ridge ('S', Fig. 4a), and the steep gravity gradient ('I', Fig. 4b), that in places corresponds to the northern flank of North Scotia Ridge basement (e.g. Barker *in press*).

The linearity and continuity of NR4 suggest that the faults are young, relative to the development of the accretionary prism, and possibly active. Nearby earthquakes showing sinistral strike-slip along near-vertical fault planes (oriented at 070–250°T, Fig. 4) suggest that this section of the ridge is being actively dissected by South American–Scotia motion. NR4 faults are closely aligned with the fault planes (Fig. 4), although an absence of GLORIA data in the vicinity of the earthquakes means that their relationship with NR4 remains uncertain. The NR4 faults and earthquakes could reflect separate components of slip, occurring near the northern and southern boundaries of basement.

Alternatively, NR4 could reflect merely a stage in the continued deformation of the accretionary prism; this tectonism may have occurred during the development of older NR1 folds, or after the formation of youngest NR1 folds. The faults lie 40 km north of the few earthquakes which describe South American–Scotia slip, and die out steadily northeastward, which is more a feature of normal faulting than of strike-slip. They might be oblique to NR1 here because of the curve in the overall trend of the accretionary prism, but more commonly aligned with NR1, and therefore almost impossible to detect.

South American-Scotia plate boundary

West of 50°W, earthquakes show South American–Scotia slip south of the survey area (Fig. 4). Across Aurora Bank however, earthquakes lie within the survey area (Fig. 5, and Pelayo & Wiens 1989), allowing any sea-floor fabric associated with South American–Scotia motion to be examined. Here, an east–west zone of short (up to 10 km), curvilinear, low-amplitude lineaments extends across the area of epicentres. It can be traced only with difficulty, possibly from 48°W–45°W along the same line. The northern (down-slope) edge of the zone is indistinct, lying close to a swath boundary, and possibly merging with NR2 fabric. Up-slope to the south the seabed appears smooth. Hence, sea-floor fabric in the epicentral region is minor, not warranting specific identification in Fig. 3b.

Northern Scotia Sea

The GLORIA data include two swaths that extend south onto Scotia Sea ocean floor (south of 53°30'S and west of 44°W, Fig. 3b). Bathymetric relief within this area is subdued, and ocean floor ages range between 28 and 18 Ma in the vicinity of the westernmost swath (Tectonic Map 1985). Sonographs show bright, chaotic fabric, lying adjacent to broad areas of smooth, almost featureless sea floor ('NSS', Fig. 3b). Unpublished CD37 profile data show that bright NSS fabric coincides with slightly elevated ocean floor, where basement has negligible sediment cover. Intervening, featureless areas have a variable thickness of weakly-scattering sediment.

2.5 DISCUSSION

North Scotia Ridge accretionary prism: convergent deformation, and neotectonics of the South American–Scotia plate boundary

Between 65°W and 31°W, the Scotia Sea is floored by a single, independent Scotia plate, and the South American–Scotia plate boundary accommodates slow, sinistral, mainly east–west strike-slip motion (Forsyth 1975; Pelayo & Wiens 1989), although sparse seismicity prevents its detailed delineation beneath the North Scotia Ridge. While the few published earthquakes suggest that the plate boundary lies close to the crustal fragments which support the accretionary prism, several tens of km south of the deformation front (shown in Fig. 8, with the deformation front, 3000–m bathymetry, and small circles of South American–Scotia motion), relative motion need not be confined solely to this area; it could be distributed diffusely across the ridge, or strain could be partitioned between sites beneath the northern and southern flanks of the ridge.

Relict North Scotia Ridge deformation front

Seismic profiles have been used to argue that north–south convergence persists, with continued deformation at the toe of the accretionary prism. In particular, Ludwig & Rabinowitz (1982) inferred active convergence extending from Burdwood Bank to Shag

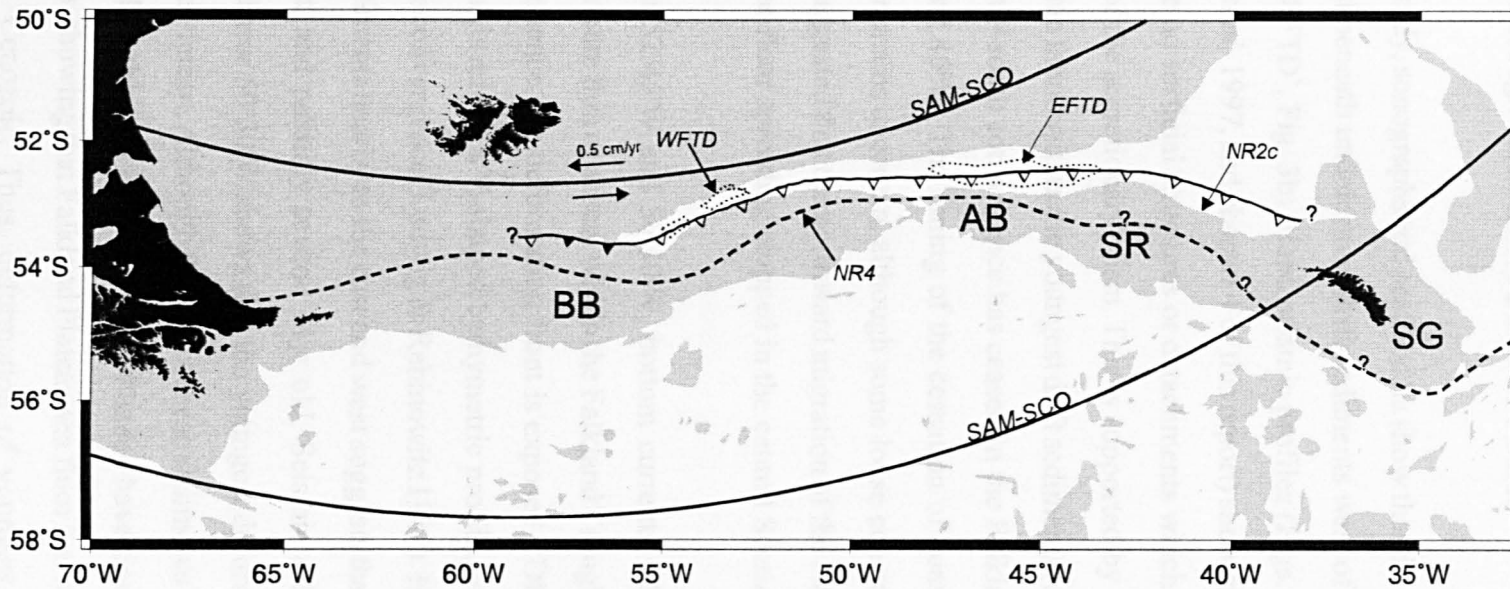


Fig. 8 Tectonic summary of the North Scotia Ridge region. Sea floor above 3000 m is shaded. BB, Burdwood Bank; AB, Aurora Bank; SR, Shag Rocks block; SG, South Georgia. The position of the North Scotia Ridge deformation front (inferred from sonographs and seismic reflection profiles) is marked with a solid line, with barbs on the overriding plate. Inactive sections of the deformation front are marked with open barbs, and solid barbs delineate active thrusting of Falkland Trough sediments at Burdwood Bank. A possible path of the South American-Scotia plate boundary (inferred from gravity and earthquake data, and adjusted with reference to sonographs) is marked with a bold dashed line. Small circles of South American-Scotia relative motion (pole at 18.7degS, 58.9degW: Pelayo & Wiens 1989) with co-latitudes of 34 and 39deg relative to the rotation pole are labelled SAM-SCO. Fine dotted lines (labelled WFTD, EFTD) enclose areas of known drift deposition in the Falkland Trough. NR4 and NR2c locate tectonic fabric described in the text.

Rocks from the deformation of the youngest preserved Falkland Trough sediments. More recent studies (Platt & Philip 1995; Richards *et al.* 1996) confirmed active thrusting of Falkland Trough sediments at Burdwood Bank.

In this study, sonographs and profile data show that the North Scotia Ridge deformation front is buried beneath undeformed drift sediments west of 53°W ('WFTD', Fig. 3a) and east of 48°W ('EFTD', Fig. 3b). Here, seismic profiles (Figs. 7a,c,d) and 3.5 kHz sub-bottom data (Howe *et al.* 1997, and chapter 4 of this report) show an exceptionally smooth sea floor, and there are no surficial structures or detachments which might indicate active deformation at the toe of the accretionary prism. This is supported by sonographs which show no evidence of tectonic fabric within the youngest drift sediments (e.g. 'WFTD', Fig. 3a). Hence, I infer that north–south convergence has ceased in the Falkland Trough at 54°30'W, and between 47°W and 46°W. The timing of the cessation of convergence within the central Falkland Trough remains uncertain, although some loose constraint is available. Barker *et al.* (1984; 1991) suggested that the northward migration of the North Scotia Ridge ceased *c.* 6 Ma ago, when sea-floor spreading stopped in the central Scotia Sea and Drake Passage.

Between 52°45'W and 50°30'W, bottom currents inhibit sedimentation, and young drift sediments are thin or absent within the Falkland Trough (e.g. Fig. 3 of Howe *et al.* 1997). As a consequence, the deformation front is exposed ('DF', Figs 3a and 7b), and the Falkland Trough axis retains a V-shaped bathymetric profile, sometimes interpreted as an indication of active convergence (Ludwig & Rabinowitz 1982). However, the presence of undeformed drift sediments nearby to the east and west suggests that the exposed deformation front may be relict, and possibly several Myr old. Seismic reflection profile SHA801–1 (Fig. 7b) obtained near 50°30'W shows that the youngest deformed sediments extend south from the Falkland Plateau. Although the age of these sediments is uncertain, piston and gravity cores acquired on this part of the Falkland Plateau have Eocene–Miocene core top ages (Saito *et al.* 1974), showing that Falkland Plateau sea floor has been non-depositional during much of the late Cenozoic. Thus, deformation of youngest Falkland Plateau sediments is not necessarily indicative of recent convergence, and the deformation front is probably inactive

at 50°30'W. On the basis of available data, an inactive deformation front may extend eastward from about 54°30'W to the northern margin of South Georgia (marked with open barbs, Fig. 8).

These findings conflict with the conclusions of Ludwig & Rabinowitz (1982) who argued that young Falkland Trough sediments are 'quickly incorporated into the collision complex' where the trough retains a V-shaped bathymetric profile.

Transpression at Burdwood Bank

Multi-channel seismic reflection profiles (Ludwig & Rabinowitz 1982; Platt & Philip 1995; Richards *et al.* 1996) show active thrusting of Falkland Trough sediments at the foot of Burdwood Bank. Because Burdwood Bank lies beyond the western limit of GLORIA survey, I cannot properly account for this apparent change in the stress regime at the toe of the accretionary prism. This region may accommodate a northerly component of South American–Scotia slip (marked with solid barbs, Fig. 8), possibly associated with a change in the trend of the plate boundary inferred near 55°W (eastward from 058–238°T to 103–283°T, Fig. 8).

Convergent deformation style

Sonographs show east–west variation in convergent deformation style. West of 48°W, regular NR1 fabric records the northward advance of the frontal fold, whereas farther east, NR1 is replaced by sinuous, less continuous NR2 fabric (Fig. 3b). Near 47°W, this reflects the eastward burial of NR1 beneath the EFTD, where NR2 represents a second phase of deformation. East of 42°W, lobate NR2c fabric resembles that of a modern deformation front, although Fig. 8 shows that it lies midway between the inferred positions of the North Scotia Ridge deformation front and the South American–Scotia plate boundary. Additional profile data are required to determine if NR2c represents relict tectonic fabric, or fabric related to modern plate motion.

Faults within the North Scotia Ridge accretionary prism

Sonographs provide little evidence of recent tectonic activity at the surface of the accretionary prism. However, near $50^{\circ}30'W$, faults ('NR4', Fig. 3a) which cut NR1 tectonic fabric have well-defined, fairly continuous curvilinear traces, suggesting that they are young relative to the development of the accretionary prism, and possibly active. Seismic reflection profiles show that a prominent NR4 trace corresponds to a normal fault scarp ('NR4', Fig. 7b), suggesting an extensional component of slip. Also, nearby earthquakes show that this part of the ridge is being actively dissected by South American–Scotia motion (Fig. 4). Hence, NR4 faults may accommodate slip across a transtensional section of the North Scotia Ridge, where the vector of relative motion is rotated clockwise relative to the local trend of the plate boundary (between Burdwood Bank and $50^{\circ}30'W$, Fig. 8). However, other interpretations are possible, and the faults could merely reflect gravitational collapse of the accretionary prism, coeval with its late-stage (post-NR1) development.

Active faulting may have been detected on Aurora Bank around the earthquake epicentres at $47^{\circ}W$ (Figs 3b and 5). Here, a minor, low-amplitude, discontinuous fabric occupies a median zone of the accretionary prism, where sediments are several km thick (see chapter 3 of this report). It is difficult to reconcile this subdued fabric with continued east–west strike-slip motion at this locality over 6 Myr or so (at 0.5 cm.yr^{-1} , Pelayo & Wiens 1989), producing a total offset of *c.* 30 km. Possibly, sediment sliding down slope has buried older surface fabric, or the locus of strike-slip may have migrated to this region only recently. Alternatively, South American–Scotia motion could be distributed diffusely across this section of the ridge. In Fig. 8, the South American–Scotia plate boundary has been drawn through the earthquake epicentres on Aurora Bank and the NR4 fault zone (north of earthquakes, Fig. 4a).

Controls on sedimentation

Oceanographic data show that the North Scotia Ridge lies in the path of the Antarctic Circumpolar Current, which flows eastward through Drake Passage, and then northward across the North Scotia Ridge, Falkland Trough and Falkland Plateau (e.g. Nowlin & Klinck 1986; Peterson & Whitworth 1989; Peterson 1992; Orsi *et al.* 1995). Here, the ridge topography forms a barrier to flow: shallower water flows across the western North Scotia Ridge as the Falkland Current (Peterson 1992), whereas deeper water is confined within the northern Scotia Sea until Shag Rocks passage (Fig. 1c). Estimates of Antarctic Circumpolar Current flow through Drake Passage average 134 Sv (e.g. Grose *et al.* 1995).

Non-deposition beneath the Antarctic Circumpolar Current

Although the Antarctic Circumpolar Current is principally wind-driven, studies demonstrate the influence of Antarctic Circumpolar Current bottom flow on sedimentation in the North Scotia Ridge region. Piston and gravity cores show pre-Quaternary sediments exposed across the Falkland Plateau (Saito *et al.* 1974; Ciesielski *et al.* 1982; Howe *et al.* 1997), where vigorous bottom currents inhibit sedimentation. Similarly, DSDP cores show that Falkland Plateau sea floor has been subject to prolonged non-deposition or erosion since the inception of the Antarctic Circumpolar Current in the early Miocene (Barker, Dalziel *et al.* 1976).

In this study, sonographs and profile data show steep-sided, eroded depressions ('FP1a', Fig. 3a), and diffuse slope-parallel fabric ('FP1b', Fig. 3a) on the Falkland Plateau which is attributed to persistent non-deposition and scour beneath the Antarctic Circumpolar Current. By inhibiting sedimentation, the Antarctic Circumpolar Current also preserves tectonic fabric across the North Scotia Ridge ('NR1-NR4', Figs. 3a,b) and in the northern Scotia Sea ('NSS', Fig. 3b).

Current-influenced sedimentation

Existing studies also demonstrate current control of deposition beneath the Antarctic

Circumpolar Current (e.g. Barker & Burrell 1977; Pudsey & Howe 1998). In the North Scotia Ridge region, young, fine-grained sediments are best preserved in deep, sheltered areas of the Falkland Trough and Malvinas Outer Basin, where bottom currents have remained comparatively slack. Here, sonographs and profile data show young, partly biogenic drift sediments, which have been deposited in the presence of sluggish southern-origin bottom water, or deepest Antarctic Circumpolar Current flow ('WFTD' and 'EFTD', Fig. 8).

West Falkland Trough sediment drift (WFTD)

The western Falkland Trough is occupied by a well-developed sediment drift ('WFTD', Figs 3a, 7a). Sediment cores obtained at the drift surface contain a 0.1–0.4 m layer of foraminiferal sand, underlain by fine-grained diatomaceous hemipelagites. These incorporate a significant (up to 55%) terrigenous component, of reworked sediment transported down-slope from Burdwood Bank, the Falkland Islands and southern South America, with a small proportion of ice-rafted material (Howe *et al.* 1997). The average sedimentation rate is 3–4 cm.ka⁻¹.

Although WFTD sediments incorporate a significant terrigenous component, the external geometry of the drift suggests that ambient bottom currents, rather than down-slope flows, have maintained a controlling influence on its formation. At 54°30'W, its bounding bathymetric depressions result from sediment thinning and non-deposition toward the drift margins. Farther east, drift sediments lie not within the deepest part of the trough, but along the Falkland Plateau slope. Profiles crossing the adjacent trough deep show no equivalent accumulations of coarse material as may have been expected if gravity flow maintained a controlling influence on drift formation. In the Falkland Trough, ponded sediments (and mass wasting) occur at 56°W (profile 144 of Ludwig & Rabinowitz 1982; Fig. 4c of Howe *et al.* 1997), mounded drift sediments occur at 54°30'W ('WFTD', Fig. 7a), and thin plastered drift sediments are seen at 53°30'W ('WFTD', Fig. 3a). This lateral change in depositional style is attributed to an eastward increase in bottom current activity, acting on a relatively small volume of terrigenous sediment transported down-slope.

It follows that WFTD sediments are confined west of 53°W because bottom currents there have remained sufficiently sluggish to permit prolonged hemipelagic sedimentation. At 54°30'W, the drift flanks are symmetrically disposed within the trough axis, and sediment thinning suggests intensified bottom current flow toward the base of slope (Howe *et al.* 1997). These characteristics may be explained by sedimentation within a cyclonic loop of Circumpolar Deep Water, with westward flow at the southern margin of the drift, and eastward flow at its northern margin; similar flow has been inferred at shallower depth by Piola & Gordon (1989). Alternatively, WFTD sediments may have been deposited within a loop of Weddell Sea Deep Water, extending even farther westward along the Falkland Trough from the Malvinas Outer Basin than for the EFTD (described in chapter 4 of this report). However, this is considered less likely, since thick drift sediments do not extend continuously across Shag Rocks passage, and Weddell Sea Deep Water appears confined within the eastern Falkland Trough by the Antarctic Circumpolar Current (Locarnini *et al.* 1993).

Howe *et al.* (1997) inferred a reduction in bottom current flow across the WFTD, and an increase in terrigenous sedimentation during the Last Glacial Maximum. A reduction in Circumpolar Deep Water flow may have accompanied the fall in sea level at the Last Glacial Maximum, since the ocean section accommodating northward Antarctic Circumpolar Current flow above the western North Scotia Ridge would have been significantly reduced, and parts of Burdwood Bank would have been subaerial. However, existing studies suggest also that Weddell Sea Deep Water activity was reduced, and that Antarctic Circumpolar Current activity increased at glacial maximum (Pudsey 1992; Pudsey & Howe 1998); as a consequence, westward flow of Weddell Sea Deep Water in the Falkland Trough may have been suppressed further by a more vigorous Antarctic Circumpolar Current during the Last Glacial Maximum. Hence, the origin of the water mass which controls sedimentation in the western Falkland Trough remains uncertain.

East Falkland Trough sediment drift

Sonographs and profile data show that the eastern Falkland Trough is occupied by a well-developed sediment drift ('EFTD', Figs. 3b, 7c,d). Piston core PC 036 of Jordan & Pudsey (1992) shows that youngest EFTD sediments are predominantly biogenic, with an average diatom content of 70–80%, 10% carbonate near the top and base of the core, and a small (partly ice-rafted) terrigenous component. This contrasts with the substantial terrigenous component of drift sediments in the western Falkland Trough (e.g. GC062 of Howe *et al.* 1997), and reflects increased biogenic productivity in the vicinity of the Antarctic Polar Front, and a virtual absence of local terrigenous sources. EFTD sediments have an estimated sedimentation rate of 5 cm.ka⁻¹ (Shimmield *et al.* 1993). An absence of carbonate in the central part of core PC 036 suggests that the Polar Front lay farther north in this region during the Last Glacial Maximum.

2.6 CONCLUSIONS

New side-scan sonographs and profile data provide insights into the tectonic development of the North Scotia Ridge, and the neotectonics of the South American–Scotia plate boundary. In particular, these data describe the extent of modern convergence at the toe of the accretionary prism, and relict deformation fabric resulting from past north–south convergence. Erosional sea-floor fabric, and young sediment drift deposits are also prominent in the sonographs. More specific findings are listed below:

(1) North–south convergence has ceased along much of the central Falkland Trough. Here, the deformation front is buried beneath undeformed drift sediments west of 53°W and east of 48°W. In the intervening region, where drift sedimentation is thin or absent, the toe of the accretionary prism is preserved at the sea floor, and the trough axis retains the appearance of a convergent margin (e.g. Ludwig & Rabinowitz 1982; Barker *et al.* 1991). However, the exposed deformation front is considered inactive, since the youngest deformed Falkland Plateau sediments may be several Myr old, and earthquakes suggest a more southerly locus of slip. These findings conflict with conclusions of previous studies (Ludwig & Rabinowitz 1982) that suggested continuing north–south convergence within the survey

area, but do not necessarily conflict with a notion of continued transpression at Burdwood Bank to the west.

(2) Sonographs and seismic reflection profiles show that the North Scotia Ridge accretionary prism has a well-ordered elongate primary deformational fabric created by past north–south convergence of the Scotia Sea and Falkland Plateau. A linear–curvilinear fabric ('NR1', elongate folds of wavelength 1–4 km, up to 20 km in length) extends up to 50 km south of the deformation front (exposed between 52°45'W and 50°30'W), and is also seen buried beneath younger drift sediments. East of 48°W this fabric is replaced by a more sinuous, curvilinear sea-floor fabric ('NR2'). In this region, NR1 is buried, and it is possible that NR2 developed farther from the frontal fold, overprinting NR1. Along the northern flank of Shag Rocks block (east of 42°W), a prominent lobate fabric ('NR2c', Fig. 3b) lies midway between the inferred line of the deformation front and the South American–Scotia plate boundary. The lobate character of NR2c appears similar to that observed in sonographs of active deformation fronts (e.g. Masson & Scanlon 1991). However, additional profile data are required to determine if NR2c represents relict tectonic fabric, or fabric related to modern plate motion.

(3) East of 52°W, sparse earthquake data suggest that South American–Scotia strike-slip occurs beneath southerly elevated parts of the North Scotia Ridge, close to the fragmented crustal blocks which support the accretionary prism. Near 50°30'W, sonographs show a set of relatively young faults ('NR4', Fig. 3a) which extend across deformation fabric. The origin of these faults is uncertain; they may result from gravitational collapse of the accretionary prism coeval with its late-stage (post-NR1) development. Alternatively, the faults could be active, and accommodate slip across a transtensional part of the South American–Scotia plate boundary. Farther east, on the northern slope of Aurora Bank (47°W) where the locus of strike-slip is defined by earthquake epicentres, its sea-floor expression in the GLORIA image is less prominent than expected, and cannot be followed far.

(4) Sonographs show large, steep-sided, depressions ('FP1a', Fig. 3a), and diffuse, slope-parallel acoustic fabric ('FP1b', Fig. 3a) on the Falkland Plateau which reflect persistent non-deposition and scour by bottom currents flowing within the Antarctic Circumpolar Current. Also, these data show well-formed sediment drift deposits in the

Falkland Trough east of 48°W and west of 53°W. Here, thick sequences of pelagic and hemipelagic sediment have accumulated in the presence of comparatively sluggish bottom currents associated with southern-origin bottom water, or deepest Antarctic Circumpolar Current flow. The composition of these sediments reflects increased biogenic productivity in the vicinity of the Antarctic Polar Front, and the limited contributions of more westerly sources of terrigenous sediment.

Chapter 3

Multi-channel seismic reflection investigation of the North Scotia Ridge near 46°W

3.1 SYNOPSIS

The North Scotia Ridge (NSR) consists of a series of islands and submarine ridges extending 2000 km from Tierra del Fuego to South Georgia in the western South Atlantic. Existing studies suggest that the ridge is principally composed of small, discrete crustal fragments, overlain to the north by a large and continuous accretionary prism. The largest crustal blocks are continental in origin, and once formed part of a continuous continental connection between southern South America and the Antarctic Peninsula. However, the origin of smaller crustal fragments which underlie the ridge between 44 and 55°W remains uncertain. This study describes results of a multi-channel seismic reflection (MCS) survey of the NSR near 46°W (Aurora Bank). These data show compressional deformation in the Falkland Trough where Falkland Plateau and oldest Falkland Trough sediments have been uplifted and deformed at the toe of the NSR accretionary prism. The inactive deformation front lies beneath a mounded, gently-asymmetric sediment drift; diverse seismic reflection patterns within the drift reflect current control of sedimentation, and drape across the deformed topography of the underlying accretionary prism. The youngest drift sediments show no signs of recent tectonism, indicating that north-south convergence has ceased at the toe of the accretionary prism. A model of free-air gravity anomaly constrained with MCS data describes deep structure and suggests that: (1) the southern Falkland Plateau Basin is floored by intermediate-thickness crust; (2) the southern Falkland Trough and the northern flank the NSR are floored by oceanic-thickness crust; and (3) Aurora Bank is formed principally of uplifted, accreted sediment, overriding a dense, north-dipping basement backstop.

3.2 INTRODUCTION

The North Scotia Ridge consists of a series of islands and submarine ridges extending 2000 km from Tierra del Fuego to South Georgia in the western South Atlantic (see chapter 2 of this report for tectonic setting). Existing studies suggest that the ridge is principally composed of small, discrete crustal fragments, overlain and flanked to the north by an appreciable thickness of sediment (e.g. Ludwig *et al.* 1968; Ewing *et al.* 1971; Davey 1972; Ludwig *et al.* 1978a,b). The largest crustal blocks (Burdwood Bank, the Shag Rocks block and South Georgia, located in Fig. 1c of this report) are continental in origin, and once formed part of a continuous continental connection between southern South America and the Antarctic Peninsula (e.g. Dalziel *et al.* 1975; Tanner 1982; Barker & Dalziel 1983, and references cited therein). However, the origin of the smaller submarine ridges which form the North Scotia Ridge between Burdwood Bank and the Shag Rocks block remains uncertain. This study describes one such component of the North Scotia Ridge located near at 46°W (Aurora Bank, labelled in Fig. 10), which extends east–west over 170 km, and which rises above 1200 m below sea level.

Previous geophysical studies

The topography of Aurora Bank is described in bathymetry (e.g. Rabinowitz *et al.* 1978; Tectonic Map 1985; GEBCO: IOC, IHO & BODC 1997) and free-air gravity studies (Rabinowitz 1977; Livermore *et al.* 1994) of the Scotia Sea. However, geophysical profile data are sparse in this region, and published sources describe only two unprocessed (bandpass filtered, with no additional digital enhancement) single-channel profiles across Aurora Bank (profiles ‘A’ and ‘B’ of Ludwig & Rabinowitz 1982).

Objectives of this study

During RRS *Discovery* cruise 172 (D172, 1988), the British Antarctic Survey obtained 680 line-km of 24–fold multi-channel seismic reflection (MCS) data across the southern Falkland



Fig. 9. Single-channel and multi-channel seismic tracks crossing the North Scotia Ridge region (area located in chapter 2, Fig. 1c). Thin tracks correspond to single-channel seismic profiles and bold tracks correspond to multi-channel seismic profiles. These data were obtained by the British Antarctic Survey during RRS *Shackleton* cruises 734, 756 and 881, RRS *Bransfield* cruise 778, RRS *Discovery* cruise 172, RRS *Charles Darwin* cruise 37 and RRS *James Clark Ross* cruise 04 (conducted between 1974 and 1993). Additional profiles were obtained by the Lamont-Doherty Earth Observatory during RV *Robert D. Conrad* cruise 1606 and 2106 (conducted between 1973 and 1978). 1000 m, 2000 m and 3000 m isobaths (Tectonic Map 1985) are marked with thin dotted lines. Area shown in Fig. 10 is outlined.

Plateau, Falkland Trough and Aurora Bank (located in Fig. 10, and shown in Figs 11,12,14,15 and 16). These data represent the first digitally-recorded MCS profiles to be acquired across this part of the North Scotia Ridge. The D172 lines are supplemented by an additional 134-km 4-channel seismic reflection profile BAS923–S26 (located in Fig. 10, and shown in Fig. 13) obtained during RRS *James Clark Ross* cruise 04 (JR04, 1993). The main objectives of this study are:

(1) To describe the structure of Aurora Bank. Published seismic reflection profiles (Ludwig *et al.* 1978b; Ludwig & Rabinowitz 1982) are sparse in this region, and do not describe the deep structure of the North Scotia Ridge near 46°W. In this study, I use MCS profiles and gravity data to describe the deep structure Aurora Bank for the first time.

(2) To describe and account for the seismic reflection character of sediments within the eastern Falkland Trough, and to assess evidence for continued north–south convergence at the toe of the North Scotia Ridge accretionary prism. Previous workers (Ludwig & Rabinowitz 1982) attributed the complex seismic character of Falkland Trough sediments to ‘buckling, folding and uplift’ resulting from continued north–south tectonic convergence. In this study, I reassess these findings in the light of more recent published studies describing current control of sedimentation.

(3) To determine crustal thickness beneath the southern Falkland Plateau Basin and Falkland Trough. Previous workers (Ludwig & Rabinowitz 1980; Ludwig, Krasheninnikov *et al.* 1983; Lorenzo & Mutter 1989) suggested that the Falkland Plateau Basin is underlain by intermediate thickness crust, and that the central Falkland Trough is underlain by oceanic crust (Ewing *et al.* 1971; deWit 1977; Ludwig *et al.* 1978b). In this study, I use gravity measurements to estimate crustal thickness beneath the Falkland Trough for the first time, and consider implications for its origin, and the mode of deformation of the sediments preserved within it.

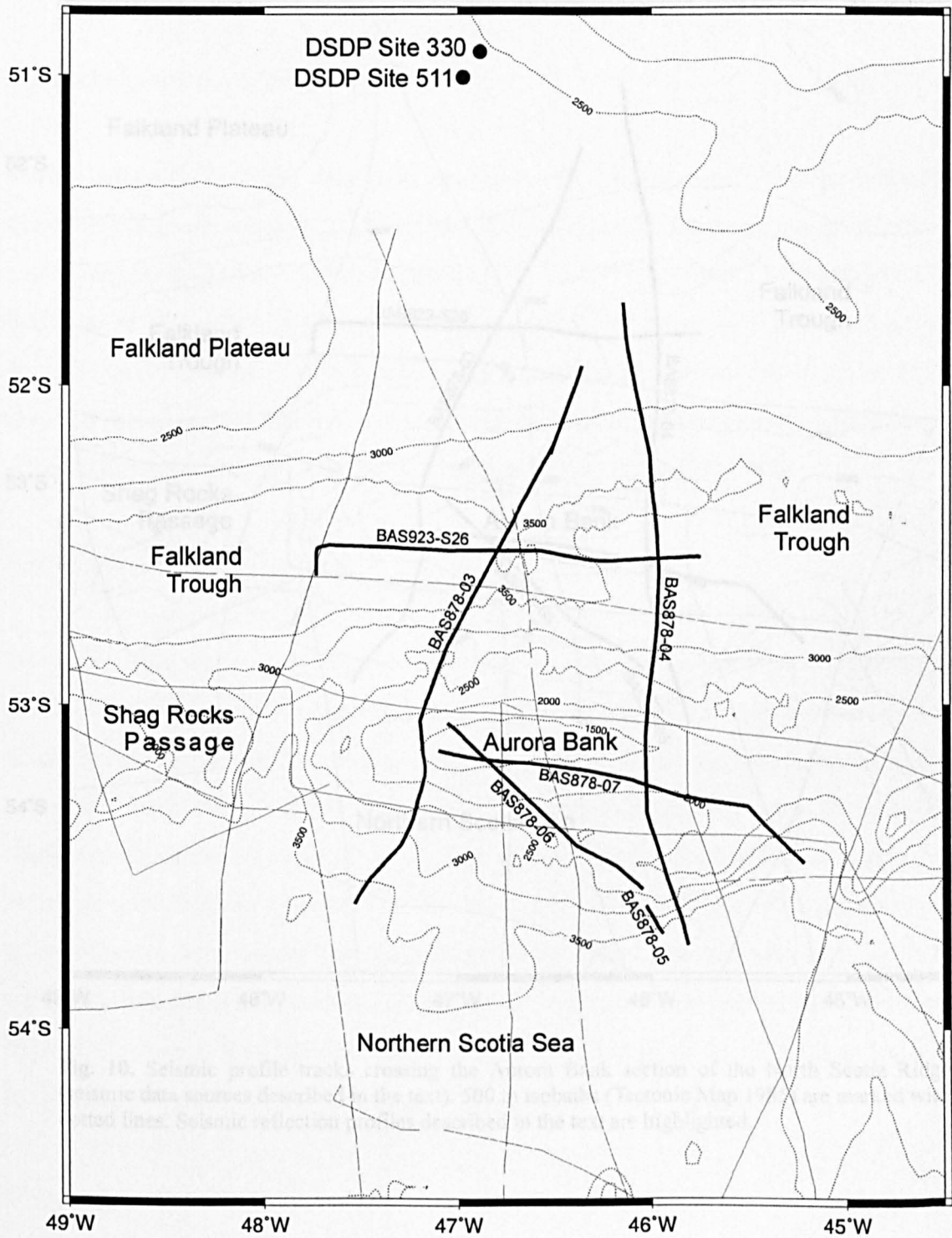


Fig. 10. Seismic profile tracks crossing the Aurora Bank section of the North Scotia Ridge (seismic data sources described in the text). 500 m isobaths (Tectonic Map 1985) are marked with dotted lines. Seismic reflection profiles described in the text are highlighted. DSDP sites located on the Falkland Plateau are described in the text.

3.3 GEOPHYSICAL DATA ACQUISITION AND PROCESSING

Multi-channel seismic reflection data

During cruise D172, MCS data were obtained with a 48-channel, 2400-m hydrophone streamer (maximum source-receiver offset = 2575 m), and a source consisting of three *Bolt* 1500C airguns with a total chamber capacity of 15.8 l. D172 profiles presented here include BAS878-03, -04, -05, -06 and -07 (located in Fig. 10, and shown in Figs 11,12,14,15,16). An additional 4-channel profile BAS923-S26 (located in Fig. 10, and shown in Fig. 13) was obtained during cruise JR04 with a 200-m hydrophone streamer (maximum source-receiver offset = 329 m), and a single *Bolt* 1500C airgun with a capacity of 4.8 l.

Navigation data processing

D172 and JR04 shotpoint navigation data were computed by relating geodetic position to seismic station number via time. Initially, shot times were recovered from SEG-B shot headers, and used to determine and assign live station locations for each seismic line. Times were then interpolated for all station locations, and tied to positions delivered by the shipboard navigation system (derived from GPS and TRANSIT satellite navigation, with electromagnetic log and gyro, British Antarctic Survey 1978; 1993). Shotpoint position was taken to be the source-near group midpoint for each shot, and corrections were made to compensate for the offset between the satellite navigation antenna and the true shot location beyond the stern of the ship. Geodetic positions were computed for all stations and output in the *UKOOA-P1/90* digital exchange format (*UKOOA-P1/90* 1991).

Seismic reflection data processing

Seismic reflection data presented in this study were processed to common-mid-point stack by the author using *MicroMAX* software. D172 profiles were also imaged using a Kirchoff

post-stack time migration algorithm within *ProMAX*. Prior to processing, filter and deconvolution parameter tests were applied to the data to determine an optimum processing scheme for each data set.

Processing strategy for D172 multi-channel seismic reflection data.

Stages in the processing scheme for D172 MCS were as follows:

- (1) *SEG-B shot demultiplex*. Raw SEG-B shot records were demultiplexed and transcribed to 32-bit trace-sequential floating point SEG-Y.
- (2) *Geometry assignment*. Shot-receiver midpoints were calculated from live station locations and shooting geometries recorded in the field observer's logs. Traces were binned at 25 m intervals.
- (3) *Recording block delay*. -40 ms delay correction.
- (4) *Amplitude recovery*. A partial gain recovery was applied to compensate for amplitude decay with time.
- (5) *Bandpass filter (corner frequencies 8–60 Hz)*. Spectral analyses showed that shot gathers were contaminated with periodic low frequency (*c.* 4 Hz) swell and towing noise. Filter tests suggested that a low-cut filter with a corner frequency of 8 Hz effectively suppressed the towing noise without seriously affecting primary reflections.
- (6) *Statistical deconvolution before stack*. Autocorrelations of raw shot gathers showed a prominent peak at *c.* 120 ms lag generated by correlation between airgun bubble pulse oscillations. Deconvolution tests showed that these periodicities could be suppressed by applying a predictive deconvolution operator before stack. A deconvolution operator length = 300 ms, a prediction gap = 24 ms and 1% whitening was chosen on the basis of tests applied to shot gathers and stack panels.
- (7) *Common-mid-point sort*. Prestack processed traces were sorted into 24-fold CMP gathers (binning interval = 25 m).
- (8) *Velocity analyses*. Stacking velocity functions were picked from semblance

displays, and checked by plotting normal moveout-corrected CMP gathers.

(9) *Normal moveout*. Applied using semblance-derived stacking velocities.

(10) *Normal moveout mute*.

(11) *24-fold CMP straight mean stack*.

(12) *Kirchoff post-stack time migration*. Applied using semblance-derived stacking velocities. Velocities reduced to 80% at > 8.0 STWT, and smoothed with operator half-width = 50 CMPs, half-height = 200 ms.

(13) *Time and space variant bandpass filter*. Filter corner frequencies $F1 = 8\text{--}110$ Hz, $F2 = 8\text{--}35$ Hz. $F1$ and $F2$ windowed from the sea floor.

(14) *Automatic gain control*. Operator length = 500 ms.

(15) *3-trace running mix*. Trace weights 1:2:1.

Processing strategy for JR04 4-channel seismic reflection data

Stages in the processing scheme for JR04 profile BAS923–S26 were follows:

(1) *SEG–Y recovery*. Field data files recorded on BAS PC-based acquisition system concatenated and written to 16-bit trace-sequential integer SEG–Y.

(2) *Geometry assignment*. Shot–receiver mid-points were calculated from live station locations and shooting geometries recorded in the field observer’s logs.

(3) *Amplitude recovery*. A partial gain recovery was applied to compensate for amplitude decay with time.

(4) *Bandpass filter (corner frequencies 10–80 Hz)*. Profile BAS923–S26 was acquired at *c.* 8 knots and spectral analyses showed that shot gathers were contaminated with periodic low frequency swell and towing noise. Filter tests suggested that a low-cut filter with a corner frequency of 10 Hz effectively suppressed the towing noise without seriously affecting primary reflections.

(5) *Statistical deconvolution before stack*. Autocorrelations of raw shot gathers showed a prominent peak at *c.* 110 ms lag generated by correlation between airgun bubble pulse oscillations. Deconvolution tests showed that these periodicities could

be suppressed by applying a predictive deconvolution operator before stack. A deconvolution operator length = 300 ms, a prediction gap = 24 ms and 1% whitening was chosen on the basis of tests applied to shot gathers and stack panels.

(6) *Normal moveout correction.* Profile BAS923–S26 was acquired using a short seismic streamer in water depths of *c.* 3000 m, across sea floor with subdued topography. As a consequence, reflections on shot gathers showed little moveout, and shot gathers have been treated as CMP gathers during processing. Normal moveout was applied in the shot domain using a simple 2-layer velocity field (stacking velocities above sea floor = 1480 m.s⁻¹, stacking velocities below sea floor = 2000 m.s⁻¹).

(7) *4-fold mean shot stack.*

(8) *Time and space variant bandpass filter.* Filter corner frequencies F1 = 10–110 Hz, F2 = 10–35 Hz. F1 and F2 windowed from the sea floor.

(9) *Automatic gain control.* Operator length = 500 ms.

(10) *3-trace running mix.* Trace weights 1:2:1.

Gravity data

Free-air gravity anomaly data presented in this study were acquired with a Lacoste-Romberg marine gravity meter (no. *S84*) during RRS *Discovery* cruise 172. These data have been corrected for instrumental drift and Eötvös effects, and tied to the IGSN71 gravity network by means of base station ties in the Falkland Islands at the start and end of the cruise leg (British Antarctic Survey 1988). Free-air gravity anomalies were calculated using the 1967 Geodetic Reference System Formula (Woollard 1979).

3.4 INTERPRETATION OF SEISMIC REFLECTION DATA

The following section describes profiles BAS878–03, –04, –05, –06, –07 and BAS923–S26 (located in Fig. 10, and shown in Figs 11–16). For clarity, sequences characteristic of the Falkland Plateau, Falkland Trough and North Scotia Ridge are considered separately. Where

possible, acoustic stratigraphic sequences have been identified in accordance with Mitchum *et al.* (1977). In the interpretations, 'start of line' and 'end of line' are described by the main orientation of the profile (quoted in °T) and increasing shot number in the seismic sections.

3.4.1 MCS profile BAS878–03

MCS profile BAS878–03 lies along 020°T and crosses the Falkland Plateau, Falkland Trough and North Scotia Ridge near 47°W (Fig. 10). The northernmost part of BAS878–03 (north of shotpoint (SP) 2750, Fig. 11) extends across smooth, southward-dipping Falkland Plateau sea floor. Between SPs 2050 and 2750, BAS878–03 crosses Falkland Trough sea floor at > 3500 m depth, which is very smooth and shows appreciable curvature. The southernmost part of profile BAS878–03 (between SP 2050 and the start of line, SOL) crosses rough, elevated sea floor of the North Scotia Ridge, which shoals to *c.* 1200 m depth near SP 1080 (Fig. 11). Profile BAS878–03 intersects four-channel profile BAS923–S26 at SP 2490 (equivalent to SP 1658 on BAS923–S26, Fig. 13).

Falkland Plateau acoustic basement

On profile BAS878–03, Falkland Plateau basement can be traced southward from the end of line (EOL) to *c.* SP 2025 (Fig. 11). Beneath the southern flank of the Falkland Plateau (north of SP 2750, Fig. 11), the top of basement is interpreted at depths of between 5.5 and 6.5 STWT. This surface is poorly defined in the profiles, and has been identified on the basis of reflection character: basement rocks appear acoustically-chaotic to opaque, with few laterally-persistent reflections (e.g. below 6.0 STWT near SP 3550, Fig. 11), whereas the oldest overlying sediments (Falkland Plateau lower sequence, described below) show moderate to high amplitude, coherent, continuous reflections (e.g. at 5.5 STWT near SP 3550, Fig. 11). Beneath the lower Falkland Plateau slope (at 5.95 STWT near SP 2900, Fig. 11), faint reflections have been erosionally truncated at the top of basement.

Farther south, moderate amplitude, coherent reflections describe basement topography

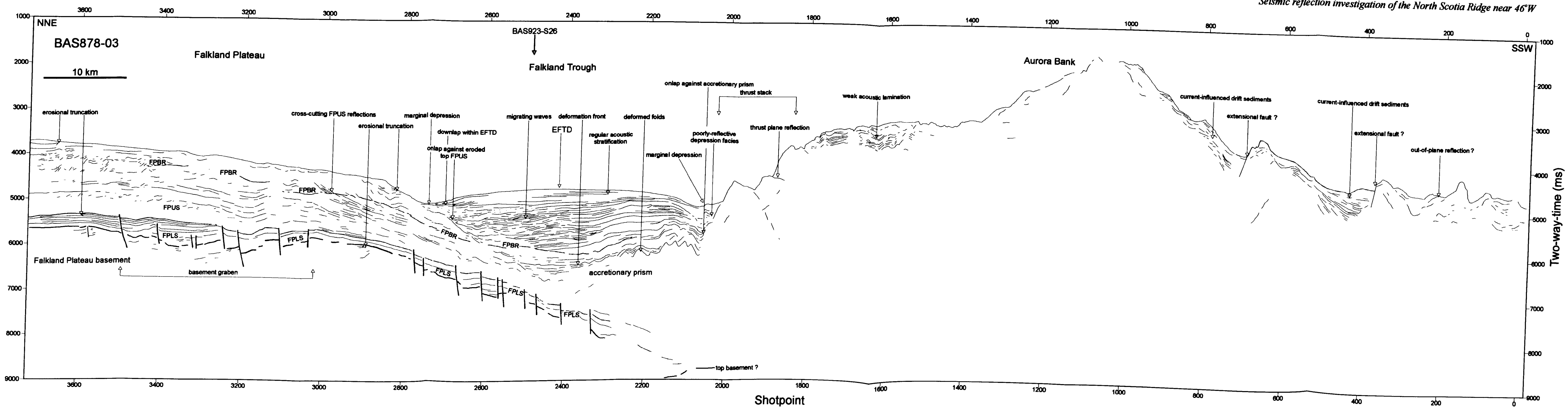
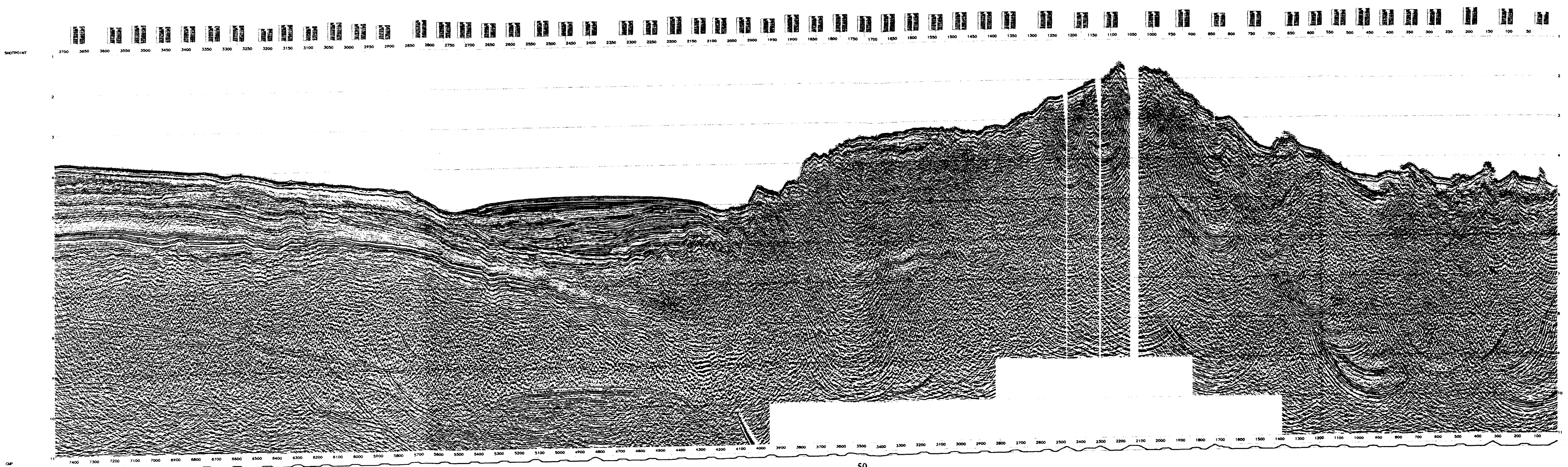


Fig. 11. (a) Interpreted line drawing of multi-channel seismic reflection profile BAS878-03 (located in Fig. 10). Horizontal scale = 1:300 000, vertical exaggeration = c. 6.6:1 at the sea floor. (b) Profile BAS878-03 data panel.



South West

**BAS
D172
Kirchoff Migration
BAS878-03**

FIELD PARAMETERS

WELL ID: 172
FALGARD PLATEAU-NORTH SCOTIA RIDGE

NAVIGATION

Survey Name: BAS D172
Project: Kirchoff Migration
Operator: Schlumberger

SOURCE

Shot Point: 3700
Shot Interval: 100
Shot Length: 1000

RECORDING

Receiver: 24
Receiver Interval: 20
Receiver Length: 2000

PROCESSING SEQUENCE

1. SEG-B DEMULTIPLEX
2. RECORDING DELAY
3. GEOMETRY ASSIGNMENT
4. ANTI-ALIAS FILTERING
5. DATA CHECKS AND REPAIRS
6. STATISTICAL DECONVOLUTION BEFORE STAGE
7. CMP GATHER
8. INTERACTIVE VELOCITY ANALYSIS
9. NORMAL MOVEMENT CORRECTION
10. NORMAL MOVEMENT STRETCH MITING
11. 3000 STRAIGHT MEAN CMP STACK
12. GROUP VELOCITY TIME CORRECTION
13. TIME AND SPACE VARIATION REMOVAL FILTERING
14. AUTOMATIC GAIN CONTROL
15. 800 m operator length

DISPLAY PARAMETERS

Time Scale: 1000 ms
Gain: 100
Filter: 10-100 Hz

ADVANCE PHOENIX

Fig 11(b)

beneath the Falkland Trough (extending to > 8.5 STWT at SP 2025, Fig. 11). Some of these deeper reflections may have been generated near the top of basement within overlying sediments, since the reflection character of these events resembles that of the Falkland Plateau lower sequence (described below). Similarly, some reverberant reflections near the top of basement (at *c.* 7.2 STWT near SP 2600, Fig. 11) may have been generated by interbed multiple reflection within overlying sediments. Occasional reflections at greater depth (e.g. at 6.8 STWT near SP 2850, Fig. 11) may represent primary intra-basement events.

Profile BAS878–03 shows that Falkland Plateau basement has been offset by extensional faults. Between SPs 3050 and 3550, the top surface of basement has been down-faulted into a graben, and basement faults also penetrate and offset overlying sedimentary strata beneath the Falkland Trough (e.g. at > 6.0 STWT, between SPs 2025 and 2800, Fig. 11).

Falkland Plateau lower sequence

MCS profile BAS878–03 shows that Falkland Plateau acoustic basement is overlain by a sedimentary sequence with moderate to high amplitude, coherent, laterally-continuous reflections. In this study, this unit is termed the Falkland Plateau lower sequence (FPLS). Near the EOL, the FPLS is marked by a series of high amplitude, coherent reflections (e.g. between 5.35 and 5.60 STWT at SP 3550, Fig. 11). At SPs 3300 and 3575 (at 5.6 and 5.37 STWT respectively, Fig. 11), shallowest FPLS strata have been erosionally truncated, which suggests that the upper surface of the FPLS constitutes an acoustic sequence boundary. Elsewhere (on MCS profile BAS878–04, described below), the FPLS onlaps Falkland Plateau basement. Hence, on these grounds, the FPLS is defined as a seismic stratigraphic sequence in this study.

MCS profile BAS878–03 shows that the thickness of the FPLS is related to underlying basement structure. In particular, the FPLS thickens within the basement graben (to > 0.2 STWT, near SP 3460, Fig. 11), and thins across an adjacent basement high (to < 0.1 STWT, near SP 2900, Fig. 11). The FPLS also thins across a small basement high beneath the

Falkland Trough (at 6.8 STWT near SP 2525, Fig. 11), which suggests that FPLS deposition was partly controlled by underlying topography. There are also subtle indications of reflection divergence within older FPLS strata, suggesting syn-tectonic deposition (at 5.7 STWT near SP 3350, Fig. 11). On profile BAS878–03, basement faults penetrate the top FPLS boundary (e.g. at 5.45 STWT near SP 3500, Fig. 11) which suggests that basement tectonism continued after the cessation of FPLS deposition.

Falkland Plateau upper sequence

MCS profile BAS878–03 shows that the FPLS is overlain by a thick sedimentary succession characterised by discontinuous reflection configurations. In this study, this unit is termed the Falkland Plateau upper sequence (FPUS). BAS878–03 shows that the base of the FPUS (top FPLS) is an acoustic sequence boundary, and that its upper bounding surface coincides in places with the sea floor. On these grounds, the FPUS is defined as an acoustic stratigraphic sequence in this study.

On profile BAS878–03, the FPUS shows diverse internal reflection configurations. According to position and depth, FPUS sediments show fine acoustic stratification, or appear disrupted, irregular or nearly reflection-free. Near the EOL, shallow FPUS sediments show disrupted acoustic facies (e.g. at 4.1 STWT near SP 3700, Fig. 11), whereas farther south, FPUS sediments at equivalent sub-bottom depth (at 4.6 STWT near SP 2950, Fig. 11) are nearly reflection-free (the broad reflection at *c.* 0.14 STWT below sea floor represents an airgun bubble pulse). At greater depth (> 0.5 STWT below sea floor, Fig. 11), FPUS sediments show bands of disrupted, discontinuous reflections (e.g. between 4.85 and 5.00 STWT near SP 3650, Fig. 11).

Beneath the lowermost Falkland Plateau slope and Falkland Trough, the FPUS thins rapidly southward from a time-thickness of *c.* 1.3 STWT at SP 2850 to *c.* 1.0 STWT at SP 2685 (Fig. 11). Thinning of this sequence is thought to have resulted from erosion by bottom currents flowing in the vicinity of Shag Rocks passage. Profile BAS878–03 also shows erosional

truncation of FPUS strata at the sea floor, which suggests that this part of the Falkland Plateau is presently non-depositional. Near SP 2810, reflections from truncated FPUS strata interfere with the sea-floor reflection resulting in disruption of the sea-floor wavelet (at 4.8 STWT, Fig. 11).

On MCS profile BAS878–03, basement faults terminate within the lower FPUS (e.g. above 5.45 STWT at SP 3500, Fig. 11). However, the poor reflection continuity of these older FPUS strata prevents reliable identification of the most recent fault displacements.

Falkland Plateau bottom-simulating reflection

MCS profiles crossing the southern Falkland Plateau and Falkland Trough show a diffuse, laterally-extensive but discontinuous, faint to high amplitude band of reflectivity within the upper FPUS. Beneath the Falkland Plateau, this reflection lies within a fairly narrow range of depths (0.3 to 0.6 STWT below sea floor), and as a consequence, is termed the Falkland Plateau bottom-simulating reflection (FPBR) in this study. On profile BAS878–03, the FPBR is prominent beneath the lower Falkland Plateau slope (e.g. at 5.0 STWT at SP 2880, Fig. 11) where it cuts across more steeply dipping FPUS strata. Here, the FPBR lies at *c.* 0.5 STWT below the sea floor, and dips southward to increasing sub-bottom depth beneath the Falkland Trough. On BAS878–03, the FPBR has been tentatively traced to *c.* 6.15 STWT (near SP 2415, Fig. 11), where it cuts across younger, acoustically-stratified Falkland Trough sediments (described below). This interpretation is supported by correlation with east–west profile BAS923–S26 (described below) which crosses BAS878–03 in the Falkland Trough (at SP 2490, Fig. 11). It is notable therefore, that the FPBR does not always mimic the topography of the overlying sea floor, and hence is not strictly bottom-simulating.

Near SP 2880 (at 5.0 STWT, Fig. 11), the FPBR coincides with a vertical change in reflection configuration: sediments below the FPBR show distinct acoustic stratification whereas overlying sediments are less reflective, and appear nearly reflection-free in the near-surface. However, this adjustment in reflection character is of local extent on profile

BAS878-03.

North Scotia Ridge accretionary prism

Existing MCS studies (e.g. Ludwig & Rabinowitz 1982; Ludwig 1983; Barker *et al.* 1991; Platt & Philip 1995) have shown that the northern flank of the North Scotia Ridge is underlain by a thick wedge of deformed sediment. On profile BAS878-03, the sediment wedge appears to extend northward from the SOL to *c.* SP 2450 (Fig. 11). At its northern limit, the wedge is represented by a north-tapering, acoustically-opaque body of sediment beneath the Falkland Trough (e.g. at 7.0 STWT near SP 2300, Fig. 11).

On profile BAS878-03, the buried top surface of the wedge is marked by an abrupt vertical change in acoustic facies: sediments incorporated within the wedge are acoustically-opaque with few laterally-persistent reflections (e.g. below 6.15 STWT at SP 2250, Fig. 11), whereas overlying Falkland Trough sediments (described below) show distinct acoustic stratification (e.g. above 6.15 STWT at SP 2250, Fig. 11). Falkland Trough strata also onlap the upper surface of the wedge (e.g. at 5.7 STWT near SP 2055, Fig. 11).

Profile BAS878-03 shows compressional tectonic structures within the sediment wedge. In particular, the upper surface of the wedge shows well-formed, regular, open folds (apparent wavelengths of 1 to 3 km) which are mimicked by wavy reflections within the overlying trough sediments (at 6.1 STWT near SP 2300, Fig. 11). It is also possible that the oldest preserved Falkland Trough sediments have been incorporated within the wedge (below *c.* 6.4 STWT at SP 2450, Fig. 11). At shallower depth, BAS878-03 shows abrupt changes in sea-floor slope (at SPs 1885 and 1935, Fig. 11) which appear to mark the surface trace of south-dipping thrust faults, with faint fault plane reflections in the near-surface (e.g. at 4.45 STWT near SP 1885, Fig. 11). Hence, these structures are interpreted as a stack of thrust fault-bound slices of accreted sediment. GLORIA sonographs presented in chapter 2 of this report show that these structures extend over 100 km along the North Scotia Ridge.

Beneath the Falkland Trough, the base of the sediment wedge lies close to the top FPLS sequence boundary (e.g. at 7.5 STWT near SP 2300, Fig. 11). Here, most of the thinned FPUS section has been uplifted, deformed and incorporated within the accretionary prism, whereas the FPLS, and perhaps some of the deepest FPUS sediments, extend relatively undeformed beneath. Hence, a former decollement surface must have existed near the base of the FPUS, and in places, may have extended along the top FPLS sequence boundary itself.

Farther south, the sea floor rises steadily toward the summit of the Aurora Bank (at *c.* 1200 m depth near SP 1080, Fig. 11), and then dips southward across its southern flank (reaching >3500 m depth at the SOL, Fig. 11). Here, the North Scotia Ridge appears mainly acoustically opaque, with few laterally-persistent reflections. On profile BAS878-03, accreted sediments are overlain by younger, acoustically-stratified strata (e.g. at 3.6 STWT near SP 1750, and 4.8 STWT near SP 450, Fig. 11). These surficial sediments are thickest within topographic lows (e.g. near SP 420, Fig. 11), and show weak to moderate acoustic stratification, or appear nearly reflection-free. Reflections within these sediments show considerable relief, interpreted as an indication of current control of sedimentation.

On MCS profile BAS878-03, acoustic basement has not been clearly imaged beneath the southern flank of Aurora Bank. The reason for this is uncertain, although basement rocks commonly appear acoustically-opaque in the MCS profiles, and are not easily distinguished from accreted sediment on the basis of reflection character alone. Similarly, reflections from the top of basement may have been obscured by sea-floor multiple reverberations which overprint weaker primary events deep in the section.

On the southern flank of Aurora Bank (between SP 1080 and the SOL, Fig. 11), the sea-floor reflection describes rough topography, and it may be partly obscured by coincident out-of-plane reflections (suggested by bifurcation of the sea-floor reflection near SP 200, Fig. 11). It is possible that exposed tectonic fabric on this part of the ridge trends obliquely to the profile. Near SPs 365 and 690 (Fig. 11), the sea floor is offset by steep scarps which could represent north-dipping extensional faults.

East Falkland Trough sediment drift

MCS profile BAS878–03 shows that the eastern Falkland Trough is occupied by a thick, highly reflective sediment mound which overlies older sediments of the Falkland Plateau and North Scotia Ridge. This sediment body is termed the east Falkland Trough sediment drift (EFTD) in this study. On profile BAS878–03, the EFTD is confined to >3500 m depth, and its top surface is exceptionally smooth and shows appreciable curvature. The mound is bordered to the north and south by bathymetric depressions (at SPs 2050 and 2750, Fig. 11) which extend along the base of slope, and has an apparent width of *c.* 35 km.

On profile BAS878–03, the oldest preserved EFTD sediments lie buried beneath the Falkland Trough near SP 2450 (at *c.* 6.5 STWT, Fig. 11). These older sediments may have been incorporated within the North Scotia Ridge sediment wedge, although younger overlying EFTD strata show no indications of recent convergence. At shallower depth, EFTD sediments onlap (e.g. at 5.7 STWT near SP 2055, Fig. 11) or passively drape (e.g. wavy reflections at 6.2 STWT near SP 2310, Fig. 11) the deformed surface of the wedge. Farther north, onlap is also seen where EFTD strata thin and pinch-out against a more steeply dipping top FPUS boundary (at 5.4 STWT near SP 2680, Fig. 11). However, this onlap surface is of local extent, and cannot be traced with confidence to the sea floor. Therefore, some EFTD sediments may be coeval with FPUS strata.

On profile BAS878–03, EFTD sediments show a range of internal reflection configurations including: regular, wavy, sub-parallel and divergent, or show migrating-wave acoustic facies. Between SPs 2200 and 2680 (at 5.0 to 6.0 STWT, Fig. 11), the EFTD shows a migrating-wave reflection configuration, with lenticular acoustic packages containing cross-bedded sets of north-dipping reflections (e.g. at 5.4 STWT near SP 2500, Fig. 11). This distinctive reflection pattern is best developed beneath the crest and northern flank of the drift (north of SP 2200, Fig. 11). At shallower depth, sediments directly overlying the migrating-wave units show comparatively poor reflection continuity (e.g. between 5.1 and 5.3 STWT near SP

2550, Fig. 11), whereas youngest overlying EFTD sediments show high amplitude, coherent, continuous reflections (e.g. above 5.1 STWT near SP 2550, Fig. 11). These younger strata thin beyond seismic resolution toward the northern and southern margins of the EFTD (e.g. at 4.9 STWT near SP 2230, Fig. 11), which suggests that its mounded external form results from long-term lateral variations in sedimentation rate. At shallower depth beneath the southern Falkland Trough, EFTD sediments pass laterally southward into poorly reflective sediments deposited within the southern marginal depression (e.g. at 5.3 STWT near SP 2090, Fig. 11).

3.4.2 MCS profile BAS878–04

MCS profile BAS878–04 (located in Fig. 10, and shown in Fig. 12) lies along 180°T and crosses the Falkland Plateau–North Scotia Ridge collision zone near 46°W. North of SP 1125 (Fig. 12), profile BAS878–04 crosses smooth, south-dipping Falkland Plateau sea floor, and between SPs 1125 and 2025, Falkland Trough sea floor at > 3300 m depth. Farther south (between SP 2025 and EOL, Fig. 12) BAS878–04 crosses rough, elevated sea floor of Aurora Bank, and ocean floor of the northern Scotia Sea. Profile BAS878–04 intersects four-channel profile BAS923–S26 at SP 1610 (equivalent to SP 380 on BAS923–S26, Fig. 13), and MCS profile BAS878–07 at SP 3220 (equivalent to SP 1522 on BAS878–07, Fig. 16).

Falkland Plateau acoustic basement

Between SOL BAS878–04 and SP 825 (Fig. 12), the top surface of Falkland Plateau basement lies at depths of between 5.7 and 6.6 STWT, and is tilted northward into the Falkland Plateau Basin. Near SP 825, basement is offset by an extensional boundary fault with a throw of at least 0.8 STWT. The position and scale of this fault suggests that tilting of basement to the north could represent footwall uplift in response to extensional collapse of basement to the south. Between SPs 825 and 1910, moderate to high amplitude coherent reflections describe basement topography beneath the lowermost Falkland Plateau slope and Falkland Trough (e.g. at 8.0 STWT near SP 1240, Fig. 12). Here, reflections generated at or

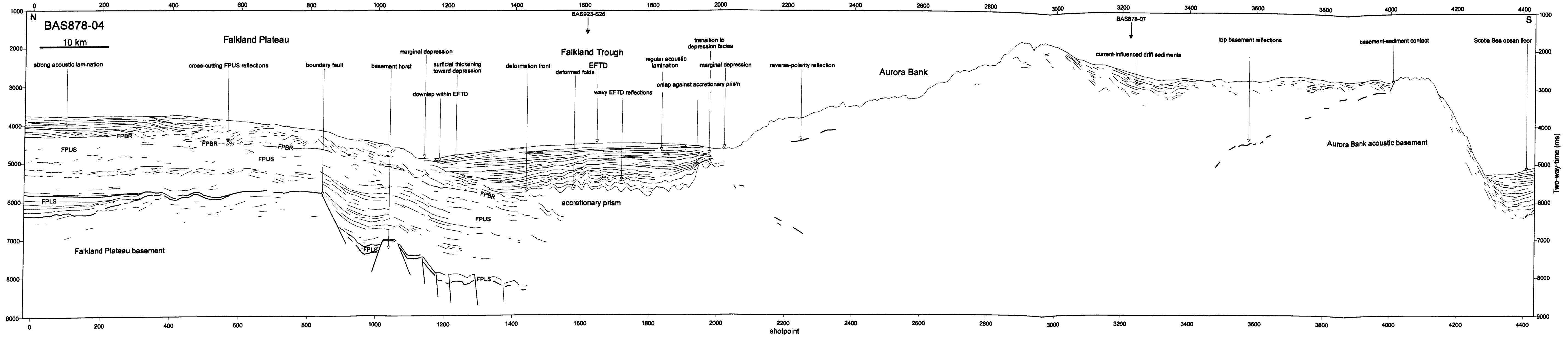


Fig. 12 (a) Interpreted line drawing of multi-channel seismic reflection profile BAS878-04 (located in Fig. 10). Horizontal scale = 1:300 000, vertical exaggeration = c. 6.6:1 at the sea floor. (b) Profile BAS878-04 data panel.

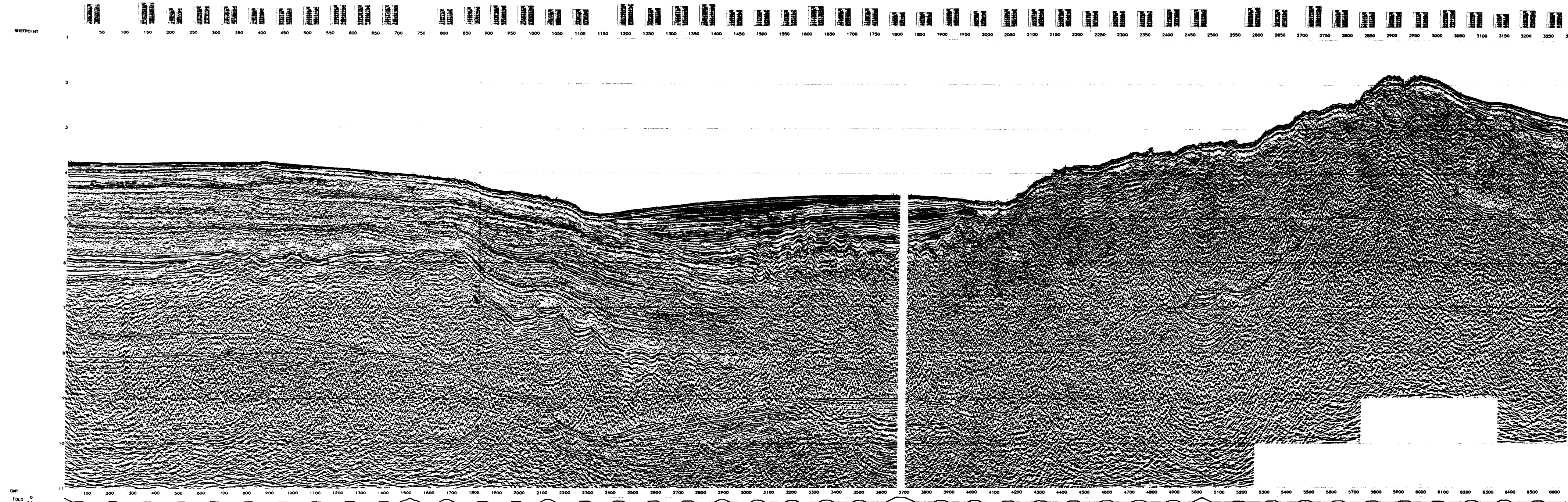
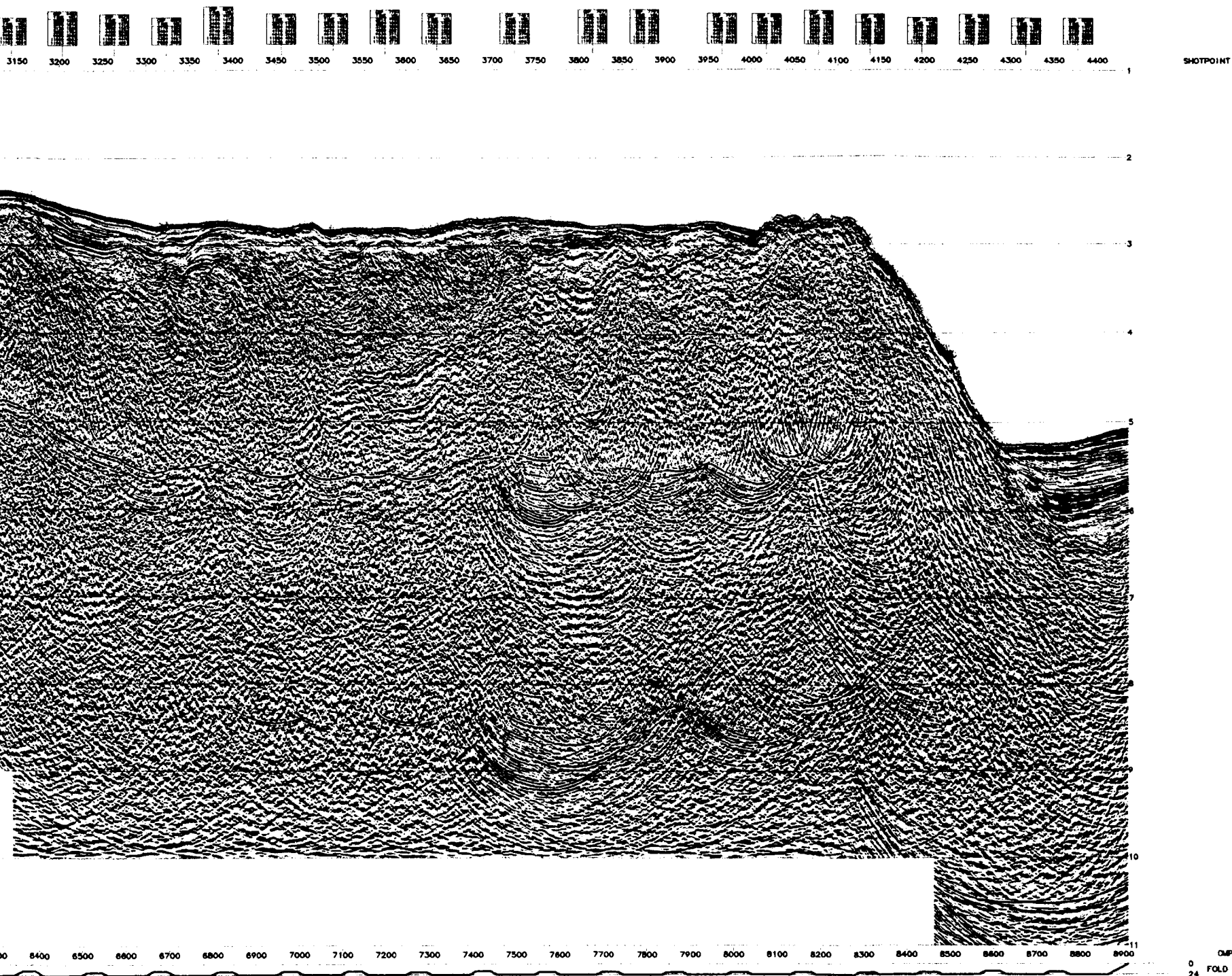


Fig 12(b)

Seismic reflection investigation of the North Scotia Ridge near 46°W



South

BAS D172 Kirchoff Migration BAS878-04

FIELD PARAMETERS

RIS DISCOVERY CRUISE 172
FALKLAND PLATEAU-NORTH SCOTIA RIDGE

NAVIGATION
 Primary navigation = GPS + SATNAV
 Secondary navigation = Deppar Log, S.M. Log and Gyro
 Seismic shotpoint = Source-NEPT trace midpoint location

SOURCE
 Source type = BOLT 300C airguns
 Combined chamber capacity = 15.8
 Airgun chamber size (cu. ins) = 180, 300, 466
 Shotpoint interval = 50 m
 Nominal source depth = 10 m

STREAMER
 Number of active groups = 48
 Group interval = 20 m
 Estimated source-to-rear group offset = 2570 m
 Estimated source-to-front group offset = 2570 m
 Nominal streamer depth = 10 m

SEISMIC RECORDING
 Recording system = Sercel 38306/055 V
 Primary data channels = 48
 Auxiliary channels = 8
 Sampling interval = 4 ms
 Anti-alias corner frequency = 27.0 Hz
 Field tape format = 27.0 Hz

PROCESSING SEQUENCE

1. SEG-B DEMULTIPLY
2. RECORDING DELAY
-50 ms delay removal
3. GEOMETRY ASSIGNMENT
4. BANDPASS FILTERING
Zero phase Omnis bandpass filter
Corner frequencies 8-28 Hz
5. Partial Gain Recovery
Proportional to 1/amp at 1800 m/s
6. STATISTICAL DECONVOLUTION BEFORE STACK
Wiener-Levinson Least Squares Operator
Operator length = 300 ms
Operator gain = 24 ms
Migration = 10
Design window = 3000-4000 ms length including sea-floor reflection
7. CMP GATHER
8. INTERACTIVE VELOCITY ANALYSIS
9. NORMAL MOVEOUT CORRECTION
Using semblance-derived stacking velocities
10. NORMAL MOVEOUT STRETCH EDITING
11. 2400S STRAIGHT MEAN CMP STACK
12. KIRCHHOFF POST-STACK TIME MIGRATION
Using semblance stacking velocity field
Smoothing operator half-width = 50 ms
Smoothing operator half-height = 200 ms
13. TIME AND SPACE VARIANT BANDPASS FILTERING
Filter corner frequencies F1 = 8-110 Hz
F1 and F2 windowed from sea floor
14. WEIGHTED TRACE MIX
3-trace running mix
Trace weights = 1,2,1
15. AUTOMATIC GAIN CONTROL
500 ms operator length

ARC 2/94

DISPLAY PARAMETERS

Thu Nov 10 17:20:14 1994
 Tracks/Channels = 40
 Bias Percent = -15
 Gain = 0
 Gain Constant = 700

Static Shift = 0
 Continents/Seas = 8
 Clip Limit = 2
 RMS Amplitude = 1

ADVANCE **ProMAX**

0
24 FOLD

near the top of basement can be traced at increasing depth beneath the Falkland Trough (to *c.* 9.5 STWT near SP 1910, Fig. 12.). Some of these deeper events may have been generated within overlying FPLS sediments. Here also, profile BAS878-04 shows that the top of basement has been offset by extensional faults, marked by abrupt changes in the slope of reflections (e.g. at 7.9 STWT near SP 1170, Fig. 12). A basement horst is also seen near SP 1040 at *c.* 7.0 STWT.

Profile BAS878-04 shows few laterally-persistent intra-basement reflections. Reverberant events at shallow sub-basement depths may result from inter-bed multiple reflection within overlying sediments (e.g. at 8.3 STWT near SP 1210, Fig. 12).

Falkland Plateau lower sequence

On profile BAS878-04, Falkland Plateau acoustic basement is overlain by a sedimentary sequence characterised by high-amplitude, coherent, laterally-persistent reflections. Although profiles BAS878-03 and BAS878-04 do not intersect, comparison between these lines suggests strongly that these strata represent the FPLS, as high-amplitude, laterally-continuous reflections are confined solely to the FPLS on profile BAS878-03.

At the SOL BAS878-04, the FPLS is represented by a sequence of high-amplitude reflections (between 5.8 and 6.25 STWT, Fig. 12) which thins southward against north-dipping basement. Near SP 330 (at 5.7 STWT, Fig. 12), the FPLS thins close to the limit of seismic resolution, although a thin layer may continue farther south beyond this point (e.g. at 5.85 STWT near SP 575, Fig. 12). Profile BAS878-04 shows onlap of FPLS sediments against Falkland Plateau basement (at 5.9 STWT near SP 260, Fig. 12), which confirms that the base of the unit represents an acoustic sequence boundary. Gently divergent reflections apparent near SP 100 (at 6.1 STWT, Fig. 12) suggest that basement tectonism accompanied the deposition of the FPLS. Similarly, thinning of this sequence against elevated basement shows that FPLS deposition was controlled in part by pre-existing basement topography. Hence, profile BAS878-04 confirms that basement tectonism preceded FPLS sedimentation,

and accompanied deposition of the sequence.

Falkland Plateau upper sequence

MCS profile BAS878–04 shows that the FPLS is overlain by a thick sedimentary succession with a variable acoustic character, which extends in places to the sea floor. Comparison with MCS profile BAS878–03 suggests strongly that this sequence represents the FPUS. At the SOL BAS878–04, FPUS sediments directly overlie youngest FPLS strata (at *c.* 5.8 STWT, Fig. 12). Near SP 800 however, it is possible that the FPUS lies in contact with uplifted basement, where the intervening FPLS thins to the limit of seismic resolution (e.g. at 5.75 STWT, Fig. 12). North of SP 1125, the upper surface of the FPUS coincides with the sea floor. Farther south however, the FPUS is buried, and its upper limit coincides in places with the base of the EFTD (marked by occasional onlaps, e.g. at 5.25 STWT near SP 1240, Fig. 12).

On profile BAS878–04, the FPUS shows a range of internal reflection configurations including fine acoustic stratification, disrupted or chaotic reflections, and weakly-reflective facies. Between the SOL and SP 250 (at < 0.5 STWT below sea floor, Fig. 12), shallow FPUS strata show fine acoustic stratification, with moderate amplitude, fairly continuous reflections. Farther south however (e.g. at SP 800, Fig. 12), reflections at equivalent sub-bottom depth appear disrupted. Beneath the lower Falkland Plateau slope (between SPs 825 and 1435, Fig. 12), FPUS reflections dip southward and partly mimic the topography of underlying basement. This reflection geometry suggests that FPUS sediments progressively infilled and draped Falkland Plateau basement topography. Reflection terminations within the FPUS near SP 875 (at 5.45 STWT, Fig. 12) are thought to represent an internal unconformity. However, this boundary cannot be followed far in the MCS data, and consequently no attempts have been made to sub-divide this sequence. Profile BAS878–04 also shows erosional truncation of FPUS reflections at the sea floor (near SP 485, Fig. 12), which suggests that this part of the Falkland Plateau is presently non-depositional. In contrast to nearby profile BAS878–03, the FPUS on profile BAS878–04 thickens appreciably

Origin of the Falkland Plateau bottom-simulating reflection (FPBR)

Seismic reflection profiles BAS878-03, BAS878-04 and BAS923-S26 (Figs. 11-13) show that the FPBR has an anomalous reflection character. In particular, this diffuse, discontinuous reflection mimics the topography of the overlying sea floor beneath much of the southern Falkland Plateau (e.g. on profiles BAS878-03 and BAS878-04, Figs. 11 and 12), and cuts across bedding plane reflections beneath the Falkland Plateau (on BAS878-03 at 5.0 STWT near SP 2880, Fig. 11) and the Falkland Trough (on BAS923-S26 at 6.15 STWT near SP 2930, Fig. 13). Also, these data show that the FPBR has been incorporated within the North Scotia Ridge accretionary prism near 46°W (on BAS878-04 at 6.0 STWT near SP 1435, Fig. 12), but elsewhere, lies above the toe of the accretionary prism within EFTD sediments (on BAS878-03 at 6.15 STWT near SP 2415, Fig. 11). These characteristics suggest strongly that the FPBR is a time-transgressive event, which results from secondary geological processes. In previous studies, time-transgressive bottom-simulating reflections have been associated with the presence of solidified methane gas hydrate beneath continental slopes, rises (e.g. Shipley *et al.* 1979), and forearc terrains (e.g. Westbrook *et al.* 1995), and with silica diagenesis (e.g. Hein *et al.* 1978).

In the case of gas hydrate bottom-simulating reflections, the precipitation of solidified methane hydrate results in an increase in the rigidity and seismic velocity of the host sediments, and anomalous reflections are generated at the base of the hydrated section, where the substitution of fluid or gas in the underlying pore space results in an abrupt downward decrease in acoustic impedance. This is commonly described by a large-amplitude negative polarity reflection which mimics the topography of the overlying sea floor. Pressure-temperature relationships describing methane hydrate stability show that increasing hydrostatic pressure and decreasing water-bottom temperature will make hydrates stable to greater sub-bottom depths in sediments (Shipley *et al.* 1979). Hence, an additional diagnostic feature of methane hydrate reflections is that of increasing sub-bottom depth with increasing water depth (in the presence of a uniform thermal gradient).

In the case of reflections from silica diagenetic fronts, an increase in cementation associated with the transformation of inorganic opal-A to opal-CT results in an abrupt downward increase in acoustic impedance, which is commonly described by a large-amplitude positive

(continued facing p. 63)

southward beneath the lowermost Falkland Plateau slope (from a time-thickness of 1.6 STWT at SP 825 to 2.1 STWT at SP 1340, Fig. 12).

Falkland Plateau bottom-simulating reflection

On profile BAS878–04, the FPBR extends beneath the Falkland Plateau slope and Falkland Trough (from SOL to *c.* SP 1420, Fig. 12). At the SOL, the FPBR appears as a high amplitude, coherent normal-polarity reflection at *c.* 0.54 STWT below sea floor. Between SPs 400 and 550, the FPBR is faint, but becomes stronger again beneath the lowermost Falkland Plateau slope (e.g. at 4.6 STWT near SP 775, Fig. 12). Here also, the FPBR wavelet is disrupted by interference with coincident cross-cutting FPUS reflections (at 4.5 STWT near SP 580, Fig. 12). South of SP 1100, the FPBR lies at increasing sub-bottom depth, and appears to have been incorporated within the North Scotia Ridge accretionary prism near SP 1435 (at 6.0 STWT, Fig. 12). This contrasts with the interpretation of MCS profile BAS878–03 (Fig. 11), which shows the FPBR cutting across undeformed Falkland Trough sediments above the accretionary prism, but is confirmed by east–west profile BAS923–S26 (described below).

On profile BAS878–04, the FPBR separates FPUS sediments with contrasting internal reflection configurations. At the SOL, FPUS sediments above the FPBR show fine acoustic stratification, with moderate amplitude, fairly continuous reflections, whereas reflections below the FPBR show poor reflection continuity, and are disrupted and discontinuous.

North Scotia Ridge accretionary prism

On profile BAS878–04, the Falkland Trough and North Scotia Ridge are underlain by deformed, acoustically-opaque sediments (between SPs 1435 and 3950, Fig. 12). Here, the northern limit of deformation is interpreted at *c.* SP 1435 (below *c.* 5.7 STWT, Fig. 12), where FPUS sediments (and possibly oldest preserved EFTD sediments) have been shortened, uplifted, and incorporated within the North Scotia Ridge accretionary prism.

polarity reflection which mimics the topography of the overlying sea floor. Time-temperature relationships describing opal-A to opal-CT transformation (Hein *et al.* 1978) show that opal-CT forms rapidly regardless of burial depth at high temperatures, but may take more than 30 Myr to form at low temperatures and shallow burial depths.

At present, the origin of the FPBR remains uncertain because it has not been sampled by scientific drilling. However, I surmise that the FPBR represents a silica diagenetic front on the basis of the following observations:

(1) Seismic reflection data show that the FPBR is a time-transgressive event which cuts across bedding plane reflections. In areas where the FPBR is prominent beneath the southern flank of the Falkland Plateau, it clearly shows normal reflection polarity (described by its resemblance to the overlying sea-floor reflection). This is consistent with reflection from a silica diagenetic front rather than reflection from the base of a gas hydrated layer.

(2) Seismic reflection data show that the FPBR only partly mimics the topography of the overlying sea floor. In particular, the FPBR lies at greater sub-bottom depth within the EFTD, but does not show a consistent increase in sub-bottom depth with increasing water depth. These characteristics are inconsistent with the presence of methane gas hydrate (unless accompanied by local variations in the geothermal gradient), but could be explained by reflection from a silica diagenetic front.

(3) DSDP drill cores and piston cores obtained in the region contain Tertiary bio-siliceous sediments. In particular, cores from DSDP sites 327 and 329 (Falkland Plateau) contain Palaeocene-Eocene siliceous oozes, and diatom ooze of Upper Miocene age (Barker, Dalziel *et al.* 1976), and piston core PC 036 of Jordan & Pudsey (1992) shows that youngest EFTD sediments are predominantly biogenic, with an average diatom content of 70-80 %. Hence, sediments of the Falkland Plateau and Falkland Trough contain an abundance of the diatomaceous material necessary for the formation of a silica diagenetic front.

Additional references

Hein, J.R., Scholl, D.W., Barron, J.A., Jones, M.G. & Miller, J. 1978. Diagenesis of late Cenozoic diatomaceous deposits and formation of the bottom simulating reflector in the southern Bering Sea. *Sedimentology*, **25**, 155-181.

Farther south, well-formed, regular open folds (apparent wavelength 1.3–2.5 km) are developed at the upper surface of the wedge (e.g. at 5.7 STWT near SP 1700, Fig. 12), and are mimicked by wavy reflections within overlying EFTD sediments (at 5.4 STWT near SP 1700, Fig. 12). The upper surface of the wedge is also described by a vertical change in internal reflection configuration: sediments incorporated within the wedge appear acoustically-opaque, with few laterally-persistent reflections, whereas overlying EFTD sediments show high amplitude, fairly continuous reflections.

Farther south (between SPs 2050 and 3950, Fig. 12), BAS878–04 shows that Aurora Bank is underlain by considerable thicknesses of deformed, accreted sediment. In general, accreted sediments appear acoustically-opaque, with few laterally-persistent reflections, although isolated, fairly coherent reflections are seen beneath the northern flank of Aurora Bank. In particular, faint south-dipping events beneath the base of slope (at 6.2 STWT near SP 2150, Fig. 12) are tentatively interpreted as a relict thrust faults, and a reverse-polarity reflection at shallower depth (at 4.2 STWT near SP 2320, Fig. 12) may be attributed to the presence of solidified natural gas hydrate (e.g. Shipley *et al.* 1979; and elsewhere on the North Scotia Ridge, Platt & Philip 1995). Beneath the southern flank of Aurora Bank (between SPs 2950 and 4010, Fig. 12), profile BAS878–04 shows that the accreted sediments are overlain by acoustically-stratified current-influenced sediments (e.g. at 2.8 STWT near SP 3250, Fig. 12). These shallower strata have been erosionally truncated at the sea floor (e.g. near SP 3100, Fig. 12), which suggests that this part of the North Scotia Ridge is presently non-depositional.

North Scotia Ridge acoustic basement

South of SP 4010, North Scotia Ridge acoustic basement outcrops at the sea floor, and forms the steep southern flank of Aurora Bank. The contact between accreted sediments and basement dips northward from this point, and can be traced with confidence to *c.* SP 3490 (at 5.0 STWT, Fig. 12). Very faint, low-frequency reflections at greater depth (e.g. at 7.2 STWT near SP 3210, Fig. 12) are also interpreted as top basement reflections.

East Falkland Trough sediment drift

MCS profile BAS878–04 shows a thick succession of EFTD sediments within the Falkland Trough near 46°W. Here, the EFTD is wider than on profile BAS878–03 (c. 44 km between flanking depressions, Fig. 12), and its surface shows less curvature. On BAS878–04, oldest preserved EFTD sediments may have been incorporated within the North Scotia Ridge sediment wedge (note asymmetric over-thrust fold at c. 5.8 STWT near SP 1435, Fig. 12), although younger EFTD strata show no indications of recent north–south convergence. At shallower depth, EFTD strata show draped, wavy reflections which mimic the deformed folds of the wedge (e.g. at 5.4 STWT near SP 1700, Fig. 12), and onlap its upper surface (e.g. at 5.1 STWT near SP 1935, Fig. 12). Farther north, EFTD strata overlie sediments of the FPUS. In places, EFTD reflections onlap more steeply dipping FPUS strata (e.g. at 5.25 STWT near SP 1240, Fig. 12). However, as observed on profile BAS878–03, this onlap surface cannot be traced far, and some EFTD sediments may be coeval with FPUS strata. It is notable also, that the migrating-wave reflection configuration seen on profile BAS878–03 is absent on profile BAS878–04.

3.4.3 Four-channel profile BAS923–S26

Four-channel profile BAS923–S26 (located in Fig. 10, and shown in Fig. 13) extends along the Falkland Trough between 45°30' and 48°W. Between the SOL and SP 2890, BAS923–S26 lies along 270°T, nearly coincident with the Falkland Trough axis. However, near SP 2890 the orientation of the profile changes to 180°T, and the remaining part of the line extends southward toward Shag Rocks passage. Profile BAS923–S26 crosses MCS profile BAS878–03 at SP 1658 (equivalent to SP 2490 on BAS878–03, Fig. 11) and MCS profile BAS878–04 at SP 380 (equivalent to SP 1610 on BAS878–04, Fig. 12). In this study, profile BAS923–S26 is unmigrated.

Falkland Plateau Acoustic basement

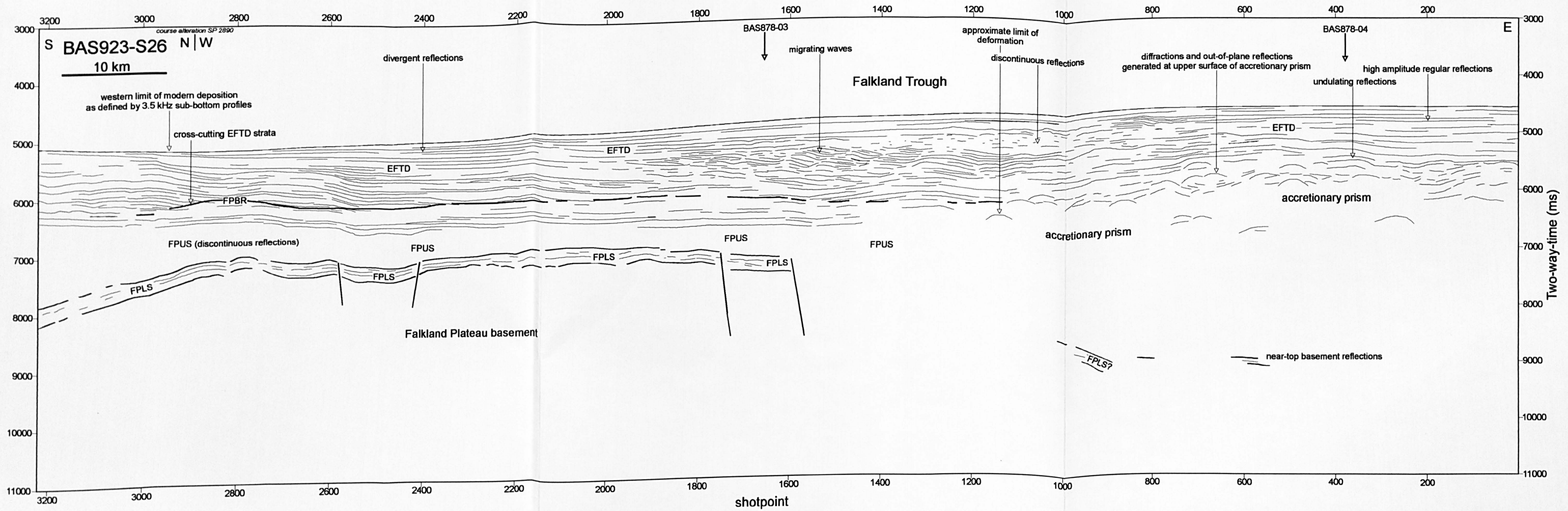
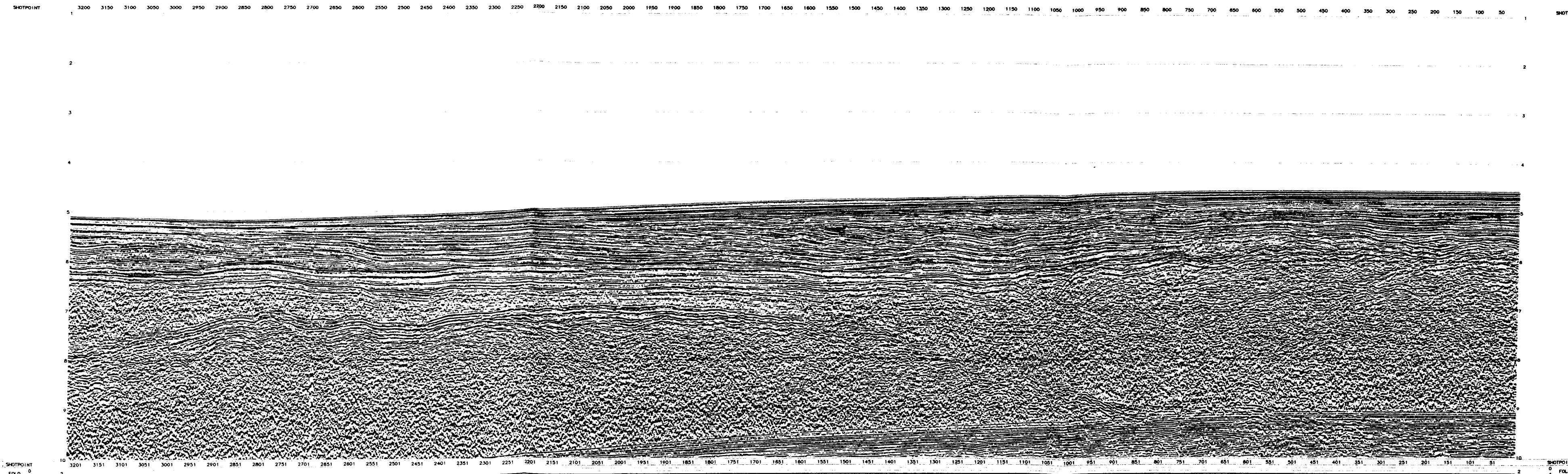


Fig. 13(a) Interpreted line drawing of four-channel seismic reflection profile BAS923-S26 (located in Fig. 10). Horizontal scale = 1:300 000, vertical exaggeration = c. 6.6:1 at the sea floor. (b) Profile BAS923-S26 data panel.



East

**BAS
JR04
4-Fold stack
BAS923-S26**

FIELD PARAMETERS

M/S JAMES CLARK ROSS CRUISE 04
FALKLAND TROUGH

NAVIGATION

Primary Position = GPS
Secondary Position = Starboard Log, F.M. Log and GPS
Datum: WGS84

SOURCE

Source Type = 0.5" 1500C airgun
Charge Weight = 1200 kg
Shot Interval = 10 s
Shot Depth = 10 m

STREAMER

Number of active groups = 16
Group Length = 1000 m
Estimated source-to-receiver group offset = 100 m
Streamers Depth = 10 m

SEISMIC RECORDING

Receiver System = BAS SENSORS 3000/3000
Sampling Interval = 4 ms
Shot Interval = 10 s
Shot Depth = 10 m
Data Type Format = SEG-Y

PROCESSING SEQUENCE

1. SEG-Y TRANSDUCTION
2. PARTIAL GAIN RECOVERY
3. BANDPASS FILTERING
Data Type Group: SEG-Y
Filter: Butterworth 10-100 Hz
4. STATISTICAL DECONVOLUTION BEFORE STACK
Deconvolution Length: 1000 samples
Operator: 0.5
Filter: 10-100 Hz
Deconvolution Length: 1000 samples including non-zero padding
5. NORMAL MOVEMENT CORRECTION
Applied using a 1000 m layer velocity field
Stacking velocity: 1500 m/s
4000 STRAIGHT NEAR-SHOT STACK
6. TIME AND SPACE VARIANT BANDPASS FILTERING
Filter corner frequencies: F1 = 10-150 Hz
F2 and F3 windowed from top trace
7. AUTOMATIC GAIN CONTROL
500 m operator length
8. WEIGHTED TRACE MIX
Program: WTAKE M2.1
Trace Length: 1000

DISPLAY PARAMETERS

File Name: 01_03_00_0001
Trace Length: 1000
Data Format: SEG-Y
Data Channel: C 000

Shot Point: 0
Time: 0.000
Time Scale: 0.000
Time Unit: s
Time Interval: 0.000
Time Offset: 0.000
Time Reference: 0.000
Time Scale: 0.000
Time Unit: s
Time Interval: 0.000
Time Offset: 0.000
Time Reference: 0.000

ADVANCE ProMAX

Fig 13(b)

(top FPLS boundary) is fairly well-defined at shallow depth (e.g. at 7.05 STWT near SP 2320, Fig. 13) and separates FPUS strata from contrasting, acoustically-stratified sediments of the FPLS. The top of the FPUS is less well-defined on profile BAS923–S26, and is represented by a broader zone where FPUS sediments pass upward into acoustically-stratified sediments of the EFTD (e.g. at c. 6.6 STWT near SP 2320, Fig. 13). Between SP 2890 and the EOL, profile BAS923–S26 shows that the FPUS thickens appreciably southward beneath the Falkland Trough toward Shag Rocks passage.

North Scotia Ridge accretionary prism

On profile BAS923–S26, the North Scotia Ridge accretionary prism is represented by acoustically-opaque sediments which lie between the SOL and c. SP 1140 (below c. 5.5 STWT, Fig. 13). Here, the top of the wedge is described by a broad, confused zone of diffractions and out-of-plane? reflections (e.g. at 5.9 STWT near SP 380, Fig. 13) which separates accreted sediments from overlying sediments of the EFTD. The poor definition of this boundary may be partly due to the trend of the profile, which is thought to lie close to that of tectonic fabric developed at the surface of the wedge. On BAS923–S26, the limit of convergent deformation is interpreted near SP 1140 (e.g. below c. 6.2 STWT, Fig. 13), although the deformation front is poorly defined in the MCS data. This interpretation is supported by north–south profiles BAS878–03 and BAS878–04, which suggest that the deformation front crosses the plane of section between SPs 380 and 1658. The poor definition of the deformation front is partly due to similarities in the acoustic character of undeformed FPUS and deformed North Scotia Ridge sediments on this profile.

On profile BAS923–S26, the base of the North Scotia Ridge sediment wedge is unclear, and is thought to lie at or close to the top of Falkland Plateau basement (e.g. dipping eastward at 9.0 STWT near SP 910, Fig. 13).

East Falkland Trough sediment drift

On profile BAS923–S26, the sediments of the FPUS and North Scotia Ridge sediment wedge are overlain by acoustically-stratified sediments of the EFTD. On this east–west profile, the base of the EFTD corresponds to a broad transition in reflection character from the discontinuous acoustic facies of the FPUS and North Scotia Ridge (described above), to the more continuous, acoustically-stratified facies of the overlying mound.

On BAS923–S26, EFTD reflections appear parallel to sub-parallel, divergent, wavy, or show a migrating-wave configuration. Near the SOL, shallow EFTD sediments (e.g. at 4.8 STWT near SP 200, Fig. 13) show regular, coherent, continuous reflections, whereas deeper EFTD strata (e.g. at 5.5 STWT near SP 200, Fig. 13) show greater relief, which is thought to mimic the topography of the underlying North Scotia Ridge sediment wedge.

Between SPs 1000 and 2100 (at *c.* 5.6 STWT, Fig. 13), profile BAS923–S26 shows a sediment wave field buried at intermediate depth within the EFTD. Here, at least seven sediment wave cycles are seen, with apparent wavelengths of between 3.8 and 4.6 km, and amplitudes of up to *c.* 90 m (assuming an acoustic velocity of 1800 m.s⁻¹). The sediment waves consistently show an eastward component of migration. North–south profile BAS878–03 crosses profile BAS923–S26 within the area of the sediment waves, and shows a more complex lenticular to migrating-wave configuration at equivalent depth (e.g. at 5.4 STWT near SP 2480, Fig 11). This complex configuration may indicate that the trend of profile BAS878–03 lies close to that of the sediment wave crests, since the bedforms should be imaged more clearly on profiles trending at a high angle to the wave crests. Near the top of the sediment wave field (e.g. at 5.3 STWT near SP 1560, Fig. 13), dipping migrating reflections pass abruptly upward into flat-lying strata, and some wave crests may have been erosionally truncated before the deposition of overlying sediments.

Farther west, EFTD sediments show laterally-continuous divergent reflections, which thin beyond seismic resolution, and pinch-out at the sea floor (e.g. near SP 2710, Fig. 13). Thinning and pinch-out of reflections is also seen at higher resolution on 3.5 kHz sub-bottom profiles, which suggest that modern EFTD sedimentation extends westward to *c.* SP 3000

(described in chapter 4 of this report).

Falkland Plateau bottom simulating reflection

On profile BAS923–S26, the FPBR extends between SPs 1140 and 2950 (Fig. 13), where it appears as a broad, faint, diffuse and discontinuous reflection. In places (e.g. at 6.15 STWT near SP 2930, Fig. 13), the FPBR cuts across coincident EFTD reflections.

At SP 1658, profile BAS923–S26 intersects north–south profile BAS878–03, which permits correlation of the FPBR between profiles within the Falkland Trough. Here, the FPBR is poorly defined, and is interpreted on profile BAS923–S26 at *c.* 6.1 STWT. On profile BAS878–03 however, the FPBR is better defined, and cuts across EFTD strata (at 6.1 STWT near SP 2490, Fig. 11). Farther east, profile BAS923–S26 crosses north–south profile BAS878–04 (at SP 380, Fig. 13). Profile BAS878–04 suggests that here, the FPBR has been incorporated within the North Scotia Ridge sediment wedge (at *c.* 6.0 STWT near SP 1435, Fig. 12). This interpretation is supported by profile BAS923–S26, which suggests that the FPBR meets the deformation front near SP 1140 (at *c.* 6.25 STWT, Fig. 13).

3.4.4 MCS profile BAS878–05

MCS profile BAS878–05 (located in Fig. 10, and shown in Fig. 14) lies along 316°T, and crosses the southern flank of Aurora Bank and the northern Scotia Sea near 46°W. During the MCS survey, data acquisition along this profile was halted after only 11.7 km due to engine failure.

The southernmost part of profile BAS878–05 shows smooth, sedimented sea floor of the northern Scotia Sea, which meets the southern slope of Aurora Bank near SP 25 (Fig. 14). At shallower depth (at 3.9 STWT near SP 100, Fig. 14), BAS878–05 shows a rough, acoustically-opaque structural high, which probably represents Aurora Bank basement, since basement rocks are exposed along the same slope only 8 km to the east (on profile

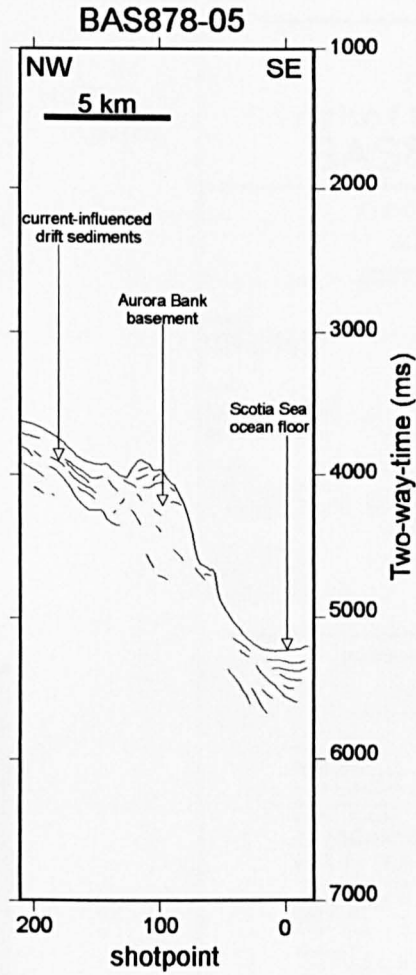
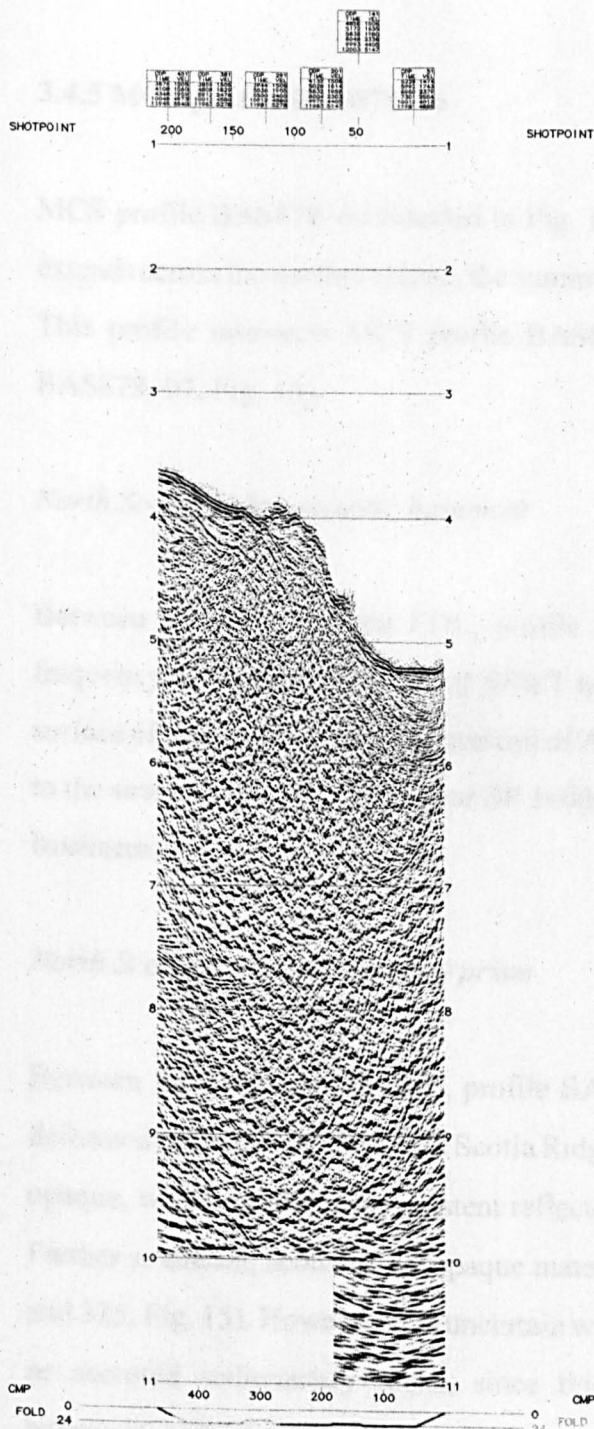


Fig. 14 (a) Interpreted line drawing of multi-channel seismic reflection profile BAS878-05 (located in Fig. 10). Horizontal scale = 1:300 000, vertical exaggeration = c. 6.6:1 at the sea floor. **(b)** Profile BAS878-05 data panel.

Seismic reflection investigation of the North Scotia Ridge near 46°W



South

BAS D172 Kirchoff Migration BAS878-05

FIELD PARAMETERS

RMS DISCOVERY CRUISE 172
FALKLAND PLATEAU-NORTH SCOTIA RIDGE

NAVIGATION

Primary navigation	= GPS + SATNAV
Secondary navigation	= Doppler Log, E.M. Log and Gyro
Seismic shotpoint	= Source-neof trace midpoint location

SOURCE

Source type	= BOLT 1500C airguns
Combined chamber capacity	= 15.8 l
Airgun chamber area (sq. in.)	= 150, 300, 466
Shotpoint interval	= 50 m
Nominal source depth	= 10 m

STREAMER

Number of active groups	= 48
Group interval	= 30 m
Estimated source-neof group offset	= 225 m
Estimated source-far group offset	= 175 m
Nominal streamer depth	= 10 m

SEISMIC RECORDING

Recording system	= Serac SN358/555 V
Primary data channels	= 1-48
Auxiliary channels	= 0
Sampling interval	= 4 ms
Anti-alias corner frequency	= 77 Hz
Field tape format	= SEG-B

PROCESSING SEQUENCE

1. SEG-B DEMULTIPLEX
2. RECORDING DELAY
-40 ms delay removal
3. GEOMETRY ASSIGNMENT
25 m common-mid-point bins
4. BANDPASS FILTERING
Zero phase Ormsby bandpass filter
Corner frequencies 8-60 Hz
5. Partial Gain Recovery
Proportional to time at 1500 m/s
6. STATISTICAL DECONVOLUTION BEFORE STACK
Wiener-Levinson Least Squares Operator
Operator length = 300 ms
Operator gap = 24 ms
Whitening = 18
Design window = 3000-4000 ms length including sea-floor reflection
7. CMP GATHER
8. INTERACTIVE VELOCITY ANALYSIS
9. NORMAL MOVEOUT CORRECTION
Using semblance-derived stacking velocities
10. NORMAL MOVEOUT STRETCH MATTING
11. 2400s STRAIGHT MEAN CMP STACK
12. KIRCHOFF POST-STACK TIME MIGRATION
Using smoothed stacking velocity field
Smoothing operator half-width = 50 ms
Smoothing operator half-weight = 200 ms
13. TIME AND SPACE VARIANT BANDPASS FILTERING
Filter corner frequencies F1 = 8-110 Hz
F1 and F2 windowed from sea floor
14. WEIGHTED TRACE MIX
3-trace running mix
Trace weights = 1,2,1
15. AUTOMATIC GAIN CONTROL
500 ms operator length

APC 6/98

DISPLAY PARAMETERS

Tue Oct 13 15:18:23 1998	Static Shift = 0
Traces/Channels = 48	Centimeters/Second = 5
Blas Percent = -15	Clip Limit = 5
Gain Set = 0.5	Max Amplitude = 1
Gain Constant = 700	

ADVANCE ProMAX

Fig 14(b)

BAS878-04, Fig. 14). These acoustically-opaque rocks are overlain to the northwest by acoustically-stratified sediments (e.g. at 4.0 STWT near SP 165, Fig. 14). Undulating reflections within these sediments are interpreted as an indication of current control of sedimentation.

3.4.5 MCS profile BAS878-06

MCS profile BAS878-06 (located in Fig. 10, and shown in Fig. 15) lies along 316°T, and extends across the southern slope, the summit, and part of the northern slope of Aurora Bank. This profile intersects MCS profile BAS878-07 at SP 1210 (equivalent to SP 340 on BAS878-07, Fig. 16).

North Scotia Ridge acoustic basement

Between SP 1120 and the EOL, profile BAS878-06 shows moderate amplitude, low frequency reflections (e.g. at 3.0 STWT near SP 1300, Fig. 15) which describe the upper surface of basement beneath the summit of Aurora Bank. Weaker reflections at similar depth to the southeast (at 3.3 STWT near SP 1000, Fig. 15) may also represent the top of acoustic basement.

North Scotia Ridge accretionary prism

Between SP 1120 and the EOL, profile BAS878-06 clearly shows basement overlain by deformed sediments of the North Scotia Ridge sediment wedge, which appear acoustically-opaque, with few laterally-persistent reflections (e.g. at 2.5 STWT near SP 1300, Fig. 15). Farther southeast, acoustically-opaque material outcrops at the sea floor (between SPs 110 and 335, Fig. 15). However, it is uncertain whether the sea floor here is formed of basement or accreted sedimentary rocks, since this part of the profile fails to show a clear basement-sediment contact.

Seismic reflection investigation of the North Scotia Ridge near 46°W

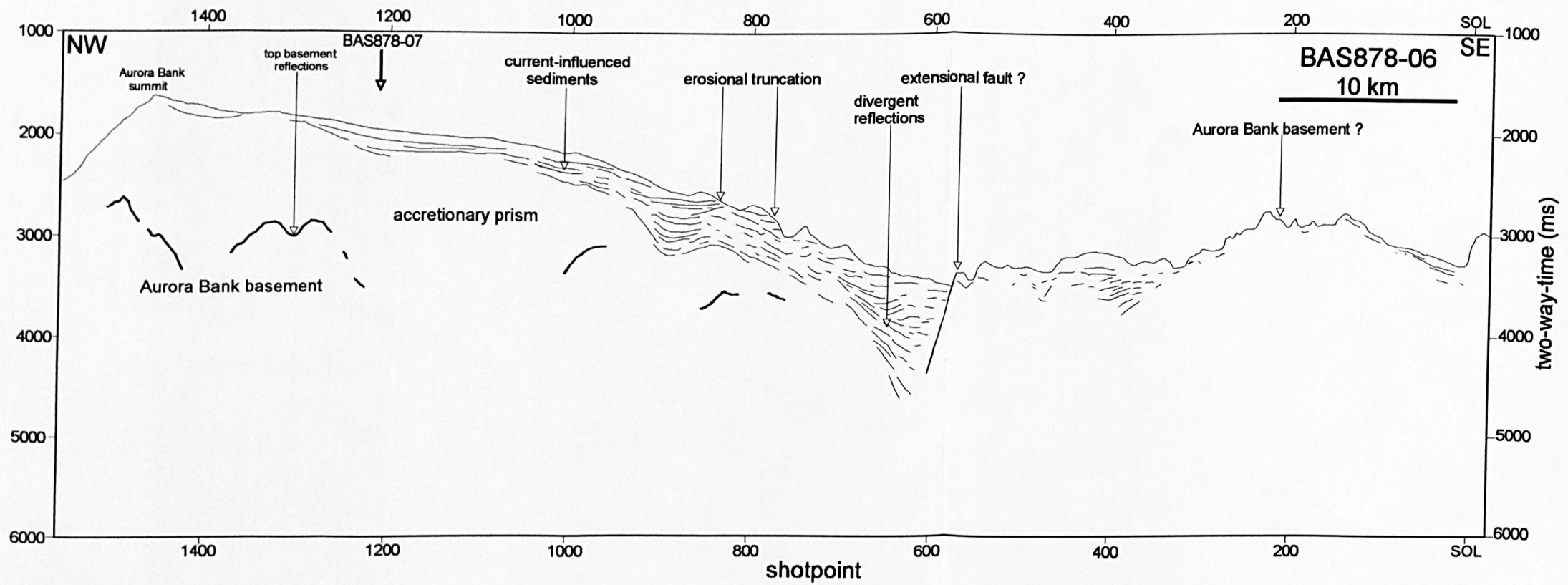
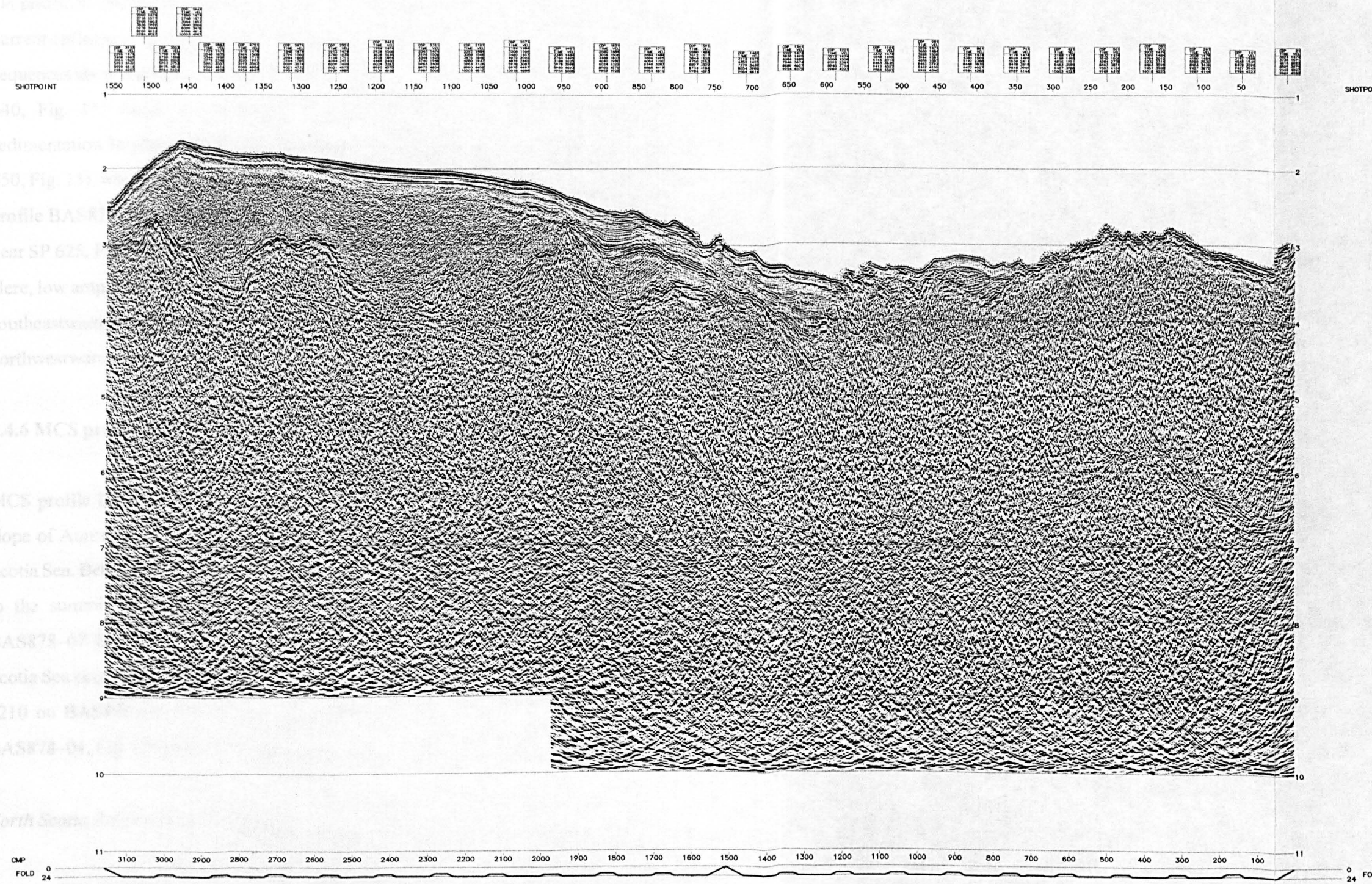


Fig. 15 (a) Interpreted line drawing of multi-channel seismic reflection profile BAS878-06 (located in Fig. 10). Horizontal scale = 1:300 000, vertical exaggeration = *c.* 6.6:1 at the sea floor. **(b)** Profile BAS878-06 data panel.



South East

**BAS
D172
Kirchoff Migration
BAS878-06**

FIELD PARAMETERS

RHS DISCOVERY CRUISE 172
FALKLAND PLATEAU-NORTH SCOTIA RIDGE

NAVIGATION

Primary navigation	= GPS + SATNAV
Secondary Navigation	= Doppler Log, E.M. Log and Gyro
Seismic Shotpoint	= Source-near trace midpoint location

SOURCE

Source type	= BOLT 1500C airguns
Combined chamber capacity	= 15.8
Airgun chamber sizes (cu. ins)	= 150, 300, 468
Shotpoint interval	= 50 m
Nominal source depth	= 10 m

STREAMER

Number of active groups	= 48
Group interval	= 50 m
Estimated source-near group offset	= 125 m
Estimated source-far group offset	= 1575 m
Nominal streamer depth	= 10 m

SEISMIC RECORDING

Recording system	= Sercel 3005/DSS V
Primary data channels	= 48
Auxiliary channels	= 0
Sampling interval	= 7 ms
Anti-alias corner frequency	= 7 Hz
Field tape format	= SEG-B

PROCESSING SEQUENCE

1. SEG-B DEMULTIPLEX
2. RECORDING DELAY
-40 ms delay removal
3. GEOMETRY ASSIGNMENT
20 m common-mid-point bins
4. BANDPASS FILTERING
Zero phase Ormsby bandpass filter
Corner frequencies 8-80 Hz
5. Partial Gain Recovery
Proportional to time at 1500 m/s
6. STATISTICAL DECONVOLUTION BEFORE STACK
Wiener-Levinson Least Squares Operator
Operator length = 300 ms
Operator gap = 24 ms
Winning = 14
Design window = 3000-4000 ms length including sea-floor reflection
7. CMP GATHER
8. INTERACTIVE VELOCITY ANALYSIS
9. NORMAL MOVEOUT CORRECTION
Using semblance-derived stacking velocities
10. NORMAL MOVEOUT STRETCH MUTING
11. 2400K STRAIGHT MEAN CMP STACK
12. KIRCHOFF POST-STACK TIME MIGRATION
Using semblance stacking velocity field
Smoothing operator half-width = 50 ms
Smoothing operator half-height = 200 ms
13. TIME AND SPACE VARIANT BANDPASS FILTERING
Filter corner frequencies F1 = 8-10 Hz
F2 = 8-30 Hz
F1 and F2 windowed from sea floor
14. WEIGHTED TRACE MIX
3-trace running mix
Trace weights = 1:2:1
15. AUTOMATIC GAIN CONTROL
500 ms operator length

Geopacience Division
British Antarctic Survey
High Cross Road
Madingley Road
Cambridge UK

APC 8/98

DISPLAY PARAMETERS

Static Shift = 0	Gain Constant = 100
Traces/Centimeters = 40	Gain Sel = 0.5
Blue Percent = -15	Gain Limit = 2
Clipping Limit = 5	RMS Amplitude = 1

ADVANCE ProMAX

Fig15(b)

On profile BAS878–06, accreted sediments are overlain by a cover of acoustically-stratified, current-influenced sediments which mantle the southern flank of Aurora Bank. These sequences show complex, discontinuous reflection configurations (e.g. at 3.7 STWT near SP 640, Fig. 15) which are interpreted as an indication of bottom current control of sedimentation. In places, these strata are erosionally truncated at the sea floor (e.g. near SP 850, Fig. 15), which suggests that this part of Aurora Bank is presently non-depositional. On profile BAS878–06, current-influenced sediments are thickest (TWT–thickness of *c.* 0.8 S near SP 625, Fig. 15) within a topographic depression on the southern flank of Aurora Bank. Here, low amplitude reflections (e.g. at 4.0 STWT near SP 605, Fig. 15) terminate abruptly southeastward beneath a small sea-floor scarp, which is tentatively interpreted as northwestward-dipping normal fault.

3.4.6 MCS profile BAS878–07

MCS profile BAS878–07 (located in Fig. 10, and shown in Fig. 16) crosses the southern slope of Aurora Bank between 45 and 47°W, and extends onto ocean floor of the northern Scotia Sea. Between SOL and SP 2310 (Fig. 16), profile BAS878–07 lies along 100°T, close to the summit of Aurora Bank. Farther east (between SP 2310 and EOL, Fig. 16), BAS878–07 lies along to 135°T, and crosses the southeastern slope of Aurora Bank and Scotia Sea ocean floor. Profile BAS878–07 crosses BAS878–06 at SP 340 (equivalent to SP 1210 on BAS878–06, Fig. 15) and BAS878–04 at SP 1522 (equivalent to SP 3220 on BAS878–04, Fig. 12) close to the summit of the North Scotia Ridge.

North Scotia Ridge acoustic basement

Near the SOL BAS878–07, acoustic basement outcrops close to the summit of Aurora Bank (at SPs 10 and 140, Fig. 16), and discontinuous basement reflections can be traced at increasing sub-bottom depth southeastward from this point (to *c.* 5.2 STWT at SP 800). Basement reflections are also seen on central and southeastern parts of the profile at sub-

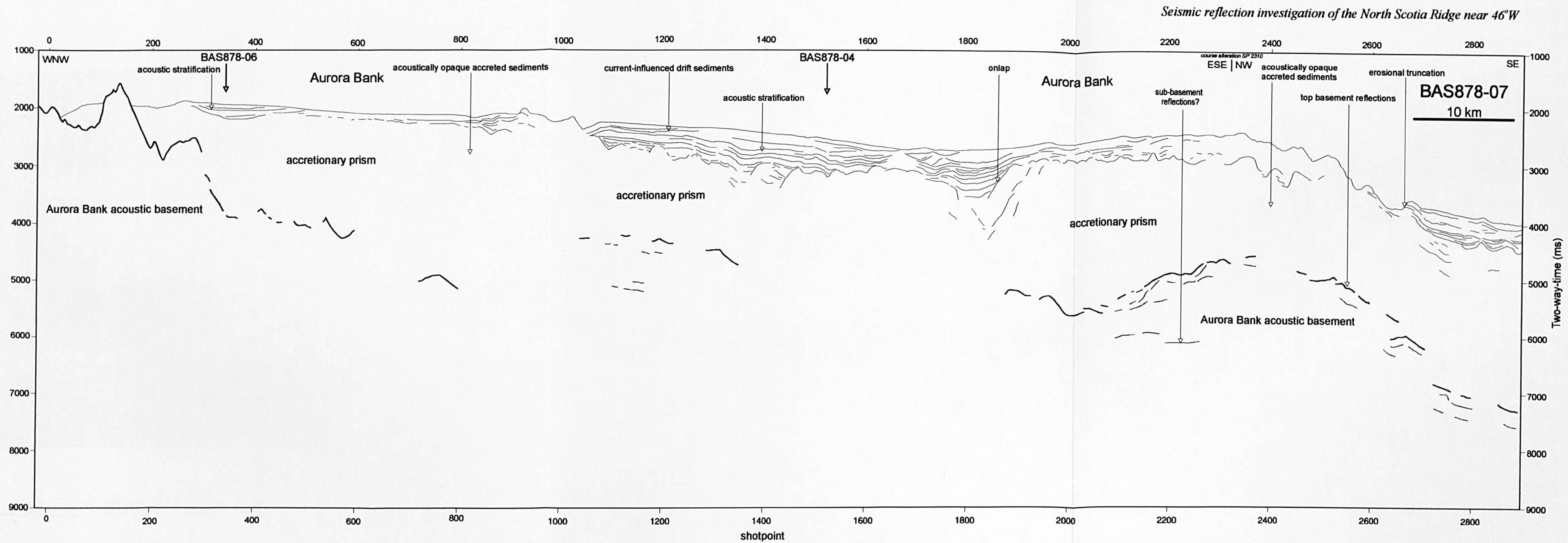


Fig. 16 (a) Interpreted line drawing of multi-channel seismic reflection profile BAS878-07 (located in Fig. 10). Horizontal scale = 1:300 000, vertical exaggeration = *c.* 6.6 at the sea floor. **(b)** Profile BAS878-07 data panel.

bottom depths of > 2.0 STWT. In particular, prominent reflections describe a broad acoustic basement high beneath the southeastern slope of Aurora Bank, which rises to *c.* 4.6 STWT at SP 2400 (Fig. 16). Beyond SP 2400, basement reflections dip steadily southeastward to *c.* 7.2 STWT depth at the EOL (Fig. 16), where they may describe the top of oceanic basement in the northern Scotia Sea.

North Scotia Ridge accretionary prism

MCS profile BAS878-07 shows that the summit and southern flank of Aurora Bank are underlain by deformed, accreted sediments of the North Scotia Ridge accretionary prism (e.g. at 3.0 STWT near SP 500, Fig. 16). On profile BAS878-07, accreted sediments appear acoustically-opaque, with few laterally-persistent reflections, and have a time-thickness exceeding 2.0 STWT beneath most parts of the ridge.

On profile BAS878-07, accreted North Scotia Ridge sediments are overlain by younger, acoustically-stratified sediments which cover the southern slope of Aurora Bank (e.g. at 2.5 STWT near SP 1350, Fig. 16). These sediments are thickest within a buried topographic low of the underlying accretionary prism (TWT-thickness of *c.* 0.8 S near SP 1810, Fig. 16), and show fairly complex lenticular reflection patterns (e.g. at 2.9 STWT near SP 1710, Fig. 16), interpreted as an indication of current control of deposition.

3.5 BAS878-04 GRAVITY MODEL

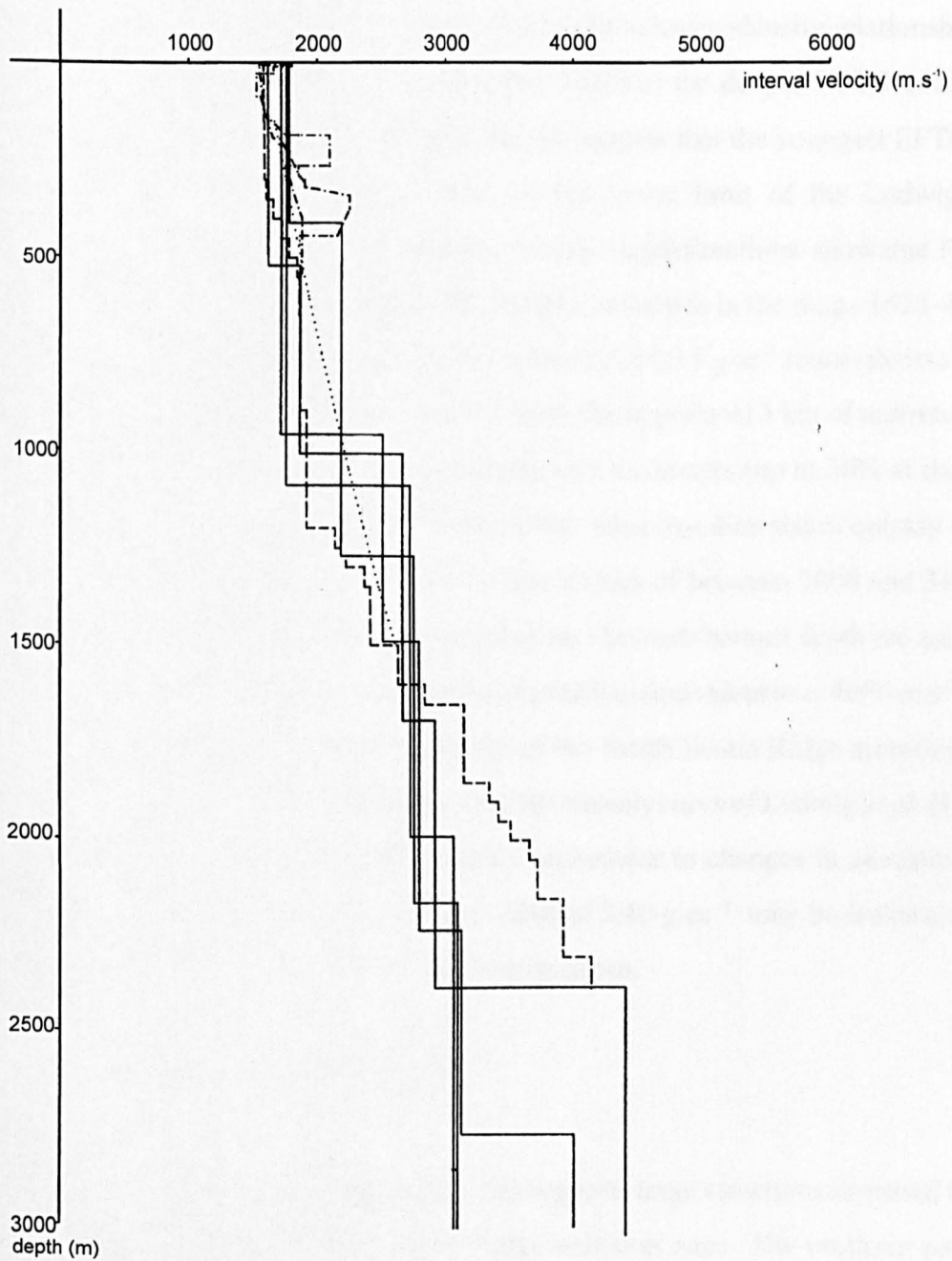
As part of this study, the free-air gravity anomaly along MCS profile BAS878-04 has been modelled to constrain better the crustal structure of the southern Falkland Plateau, Falkland Trough and North Scotia Ridge near 46°W. Prior to modelling, values of observed gravity anomaly and ship time (GMT) were resolved onto a track trending along 180°T (using a FORTRAN program 'RESOLVE'), which forms the horizontal axis of the model. Subsequently, the sea-floor reflection, the base of the EFTD and the top of acoustic basement were picked (in TWT) at 10 km intervals along profile BAS878-04, and SP positions for each pick were

converted to projected distance by relating shot time to projected values of ship time. TWT picks of the sea-floor reflection were used to construct a bathymetry profile, and sub-surface picks were converted to depth using a crude velocity function (described below). These data were combined and used to construct model polygons for input into the British Geological Survey 'GRAVMAG' gravity modelling program.

Velocity–density information

Densities have been assigned to model bodies on the basis of available data. Northern Scotia Sea ocean floor at the southern EOL (described as a 'fairly typical young oceanic section' by Hill 1978) was modelled using the standard oceanic crustal density profile of Worzel (1974): ocean floor sediments are represented by a variable thickness layer of 1.90 g.cc^{-1} , layer 2 is represented by a 1.5 km thick body of 2.55 g.cc^{-1} , and layer 3 is represented by a variable thickness body of 2.86 g.cc^{-1} . The crust beneath the Falkland Plateau and Falkland Trough has been modelled with the same density profile, since existing studies (Ewing *et al.* 1971; Ludwig *et al.* 1978b; Barker in press) suggest that these regions may also be underlain by oceanic crust. Mantle rocks have been modelled with a uniform density of 3.3 g.cc^{-1} .

Density estimates of Falkland Plateau–North Scotia Ridge sediments were made with reference to available velocity information. Initially, interval velocity functions derived from semblance analyses during MCS processing (via stacking velocities, using the equation of Dix 1956) were examined. However, these velocities showed considerable scatter, due to the relative insensitivity of normal moveout at depth, and to the poor definition in semblance of velocity trends within acoustically-opaque sediments of the North Scotia Ridge. Consequently, alternative sources of velocity information were considered (summarised in Fig. 17). In particular, four sonobuoy measurements (39C15, 41C15, 74C15 and 151C16 of Ludwig *et al.* 1978b) obtained close to profile BAS878–04 on the Falkland Plateau show a stepped increase in acoustic velocity from $1625\text{--}1790 \text{ m.s}^{-1}$ at the sea floor, to $3080\text{--}4415 \text{ m.s}^{-1}$ at sub-bottom depths exceeding 2750 m. For simplicity, Falkland Plateau–North Scotia Ridge sediments have been modelled with three layers which mimic this increase in velocity



- AMG878-04 mean velocity-depth
- Ludwig et al. (1978)
- DSDP Sites 327, 330
- Carlson et al. (1986)

Fig. 17 Falkland Plateau interval velocity-depth functions derived from seismic refraction profiles (Ludwig *et al.* 1978), semblance velocity analyses conducted on MCS profile BAS878-04, and sonic velocity measurements of cores obtained at DSDP sites. For comparison, these data are plotted with the empirical sediment velocity-depth function of Carlson *et al.* (1986).

(and hence density) with depth. The EFTD is represented by a layer with a density of 1.9 g.cc^{-1} (equivalent to 2000 m.s^{-1} , according to the velocity–density relationship of Ludwig *et al.* 1970). While this density is probably realistic for deeper EFTD sediments, interval velocities derived from semblance analyses suggest that the youngest EFTD strata are less dense, with densities ranging close to the lower limit of the Ludwig *et al.* (1970) velocity–density curve. The sonobuoy velocity–depth functions show that Falkland Plateau sediments above 3 km sub-bottom depth have velocities in the range $1625\text{--}4415 \text{ m.s}^{-1}$ (Fig. 17). On these grounds, I have assigned a density of 2.15 g.cc^{-1} (equivalent to an intermediate velocity of 2700 m.s^{-1} , Ludwig *et al.* 1970) to the uppermost 3 km of sediments. This has led to an overestimation of density for shallowest sediments (up to 30% at the sea floor), but velocity–depth functions (Fig. 17) show that this error diminishes quickly with depth, and that the density is realistic for sub-bottom depths of between 1000 and 2400 m. Falkland Plateau–North Scotia Ridge sediments below 3 km sub-bottom depth are assigned a density of 2.4 g.cc^{-1} on the basis of the sonobuoy profiles (equivalent to *c.* 4000 m.s^{-1} , Ludwig *et al.* 1970). Whilst deeply buried sediments of the North Scotia Ridge accretionary prism may have higher acoustic velocities, the velocity–density curve of Ludwig *et al.* (1970) shows that variations in density are comparatively insensitive to changes in acoustic velocity in the range $4 \text{ to } 6 \text{ km.s}^{-1}$. Hence, a density value of 2.40 g.cc^{-1} may be realistic for much of the sedimentary cover below 3 km sub-bottom depth.

Gravity model interpretation

The BAS878–04 gravity model (Fig. 18) suggests large variations in crustal thickness across the Falkland Plateau–North Scotia Ridge collision zone. The northern part of the model implies crustal thicknesses of between 9 and 13 km beneath the Falkland Plateau Basin, with thickest crust beneath the southern slope of the plateau (near 37 km along-track, Fig. 18). Farther south, Falkland Plateau crust thins rapidly southward, so that the southern Falkland Trough and the northern flank of the North Scotia Ridge are floored by crust with a thickness of between 4.8 and 6.4 km. Near 144 km along-track (Fig. 18), the gravity model suggests an abrupt change in the dip of the upper surface of basement, where flat-lying Falkland

Uncertainties in gravity modeling

The model of free-air gravity along BAS878-04 (Fig. 18) is not supported by reliable estimates of the thickness (or density) of sediment or crust, and the following points should be considered when assessing these results.

(1) The bathymetry profile is the only certain constraint in the model. In the absence of wide-angle seismic data, I have no reliable means to estimate the velocity (or density) of the sedimentary layers, or the velocity (or density) of the underlying crust. Interval velocities derived from MCS processing showed considerable scatter, and were not considered reliable for this purpose. The only constraint on the topography of the base of the crust is the long wavelength component of the observed free-air anomaly.

(2) In this study, the crust beneath the Falkland Plateau and Falkland Trough has only been modeled using oceanic crustal densities (from Ludwig *et al.* 1970). The substitution of a continental lower crustal density of 2.84 g.cc^{-1} (Ludwig *et al.* 1970) would require adjustments in crustal thickness to fit the observed anomaly, although these would be minor, because 2.84 g.cc^{-1} closely resembles the density used for oceanic layer '3' in the existing model.

(3) Published seismic refraction data are insufficient to distinguish between highly thinned continental crust or oceanic crust beneath the eastern Falkland Trough. Profile 'C-D' of Ewing *et al.* (1971) only provides a single unreversed seismic refraction velocity measurement of 7.1 km.s^{-1} , and gives no indication of the acoustic velocity gradient within the crust, or total crustal thickness (the estimate was not obtained using modern seismic modelling methods). Furthermore, if the Falkland Trough is floored by thinned continental crust, the gravity model suggests that it may have been extended to such an extent (up to a factor of 6) that it cannot be distinguished from oceanic crust, as it is generally believed that normal oceanic crust can only be distinguished from continental crust which has been stretched by factors of 3 or less on the basis of seismic velocity structure (Whitmarsh & Sawyer 1996).

Additional references

Whitmarsh, R.B. & Sawyer, D.S. 1996. The ocean/continent transition beneath the Iberia abyssal plain and continental-rifting to seafloor-spreading processes. In: Whitmarsh, R.B. Sawyer, D.S., Klaus, A. & Masson, D.G. (eds.), *Proceedings of the Ocean Drilling Program, Scientific Results*, 149, College Station, TX (Ocean Drilling Program).

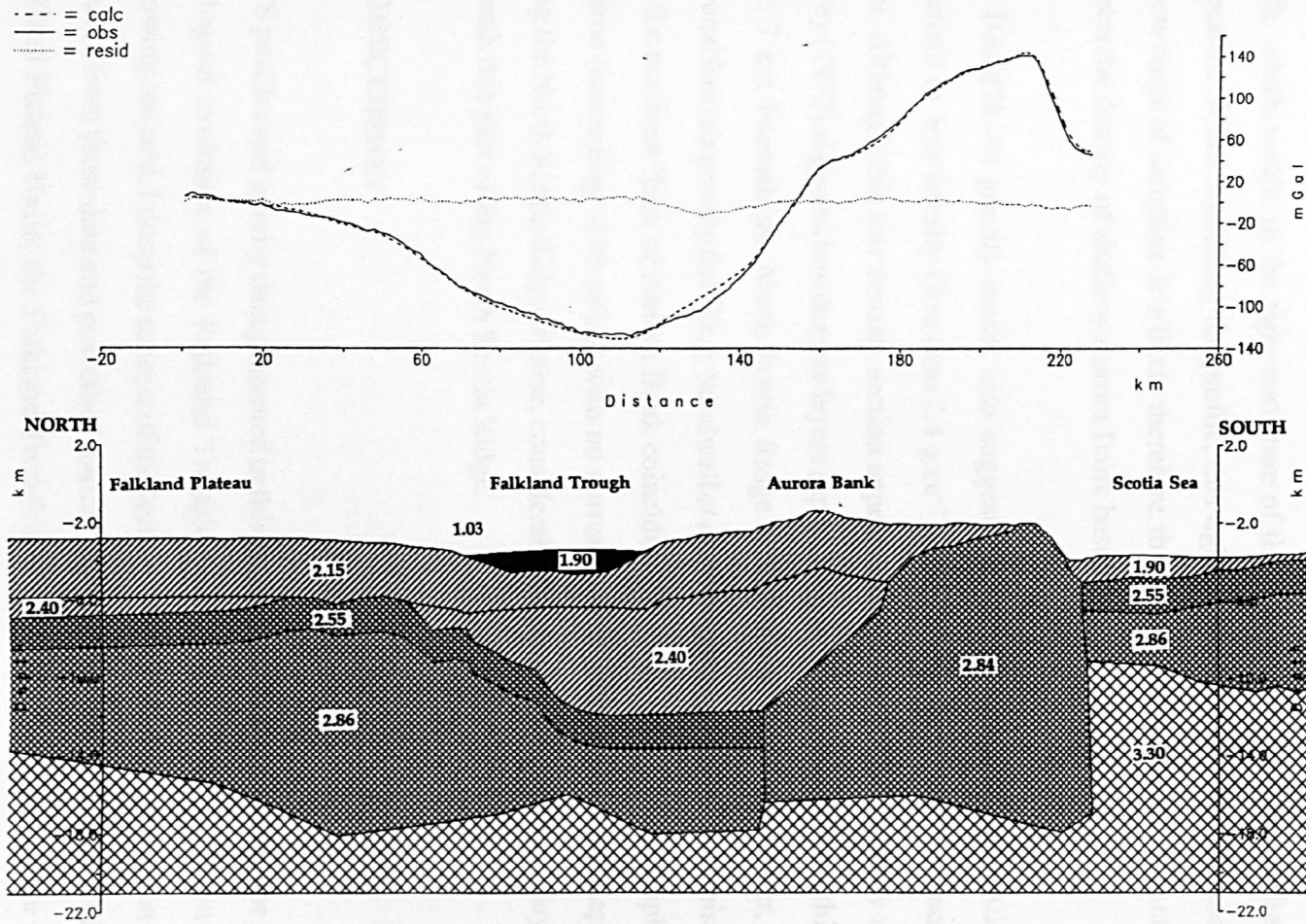


Fig. 18. Model of free-air gravity anomaly along MCS profile BAS878-04. Densities (g/cc) assigned to each model body are marked. Horizontal axis is projected distance (km) along 180 deg T.

Trough basement meets Aurora Bank basement. Farther south, the upper surface of Aurora Bank basement shallows southward, and becomes continuous with the sediment–basement contact apparent in the MCS data. Along the southern edge of Aurora Bank (at *c.* 213 km along-track, Fig. 18), the exposed basement high generates a large density contrast at shallow depth, which results in the tight curvature of the observed and calculated free-air gravity anomalies. When modelling the profile, this tight curvature could be matched only with a narrow range of densities. It is likely therefore, that the chosen value of 2.84 g.cc^{-1} accurately reflects the density of shallow Aurora Bank basement.

The BAS878–04 gravity model also suggests that the northern flank of Aurora Bank is underlain by low density (less than 2.4 g.cc^{-1}) layers with a combined thickness exceeding 9 km. Although this low density section appears exceptionally thick, gravity modelling by Davey (1972) suggests low density layers (up to 2.3 g.cc^{-1}) with a combined thickness of up to *c.* 7 km beneath the North Scotia Ridge at Burdwood Bank. Moreover, maps of the regional free-air gravity field (e.g. Sandwell *et al.* 1995, shown in Fig. 1b of this report) show that the northern flank of Aurora Bank coincides with one of the highest amplitude gravity minima (exceeding -150 mGal , with no corresponding increase in water depth) observed along the North Scotia Ridge. Hence, considerable thicknesses of sediment may be expected beneath this part of the North Scotia Ridge.

3.6 DISCUSSION

MCS profiles and gravity data presented in this study provide insights into the structure and geological evolution of the Falkland Trough–North Scotia Ridge collision zone. In the following account, I describe aspects of the tectonic and sedimentary evolution of this region deduced from these data and published sources. For clarity, the development of the southern Falkland Plateau Basin, the Falkland Trough and the North Scotia Ridge are considered in turn.

Falkland Plateau Basin

Mesozoic evolution

MCS profiles presented in this study show faulted Falkland Plateau acoustic basement overlain by a thick sedimentary succession composed of at least two seismic stratigraphic sequences. While studies (e.g. Rex & Tanner 1982; Barker, Dalziel *et al.* 1976) have shown that elevated parts of the Falkland Plateau are underlain by continental crust of the Gondwanaland craton, the age and origin of the intervening Falkland Plateau Basin is less certain. Previous workers (e.g. Barker, Dalziel *et al.* 1976; Martin *et al.* 1981; Lorenzo & Mutter 1988) have proposed that the Falkland Plateau Basin formed initially during the Middle–Upper Jurassic, in association with the breakup of Gondwanaland, and existing studies (e.g. Barker 1976; Ludwig & Rabinowitz 1980; Ludwig, Krashenninikov *et al.* 1983; Lorenzo & Mutter 1988) suggest that the basin is floored by highly extended continental or thickened oceanic crust. More recently, Barker (in press) suggested that the Falkland Plateau Basin formed as an area of sub-aerial sea-floor spreading. The BAS878–04 gravity model presented in this study provides further evidence of intermediate thickness crust beneath the southern Falkland Plateau Basin (suggesting a thickness of 9–13 km, when modelled as an oceanic section), but does not distinguish its mode of origin.

MCS data presented in this study lack reliable age control. However, comparison with published sources provides some loose constraint on the age of the sedimentary sequences overlying Falkland Plateau basement. The oldest overlying sequence is the FPLS, which is characterised by high-amplitude, coherent, laterally-continuous reflections. On the Falkland Plateau, this distinctive reflection configuration is confined wholly to the FPLS, and contrasts with the discontinuous seismic character of overlying FPUS sediments. In a previous MCS study conducted by the Lamont-Doherty Earth Observatory (LDEO), Lorenzo & Mutter (1988) described a similar acoustic sequence with ‘strong parallel reflectors’ on profiles crossing the Falkland Plateau Basin (their ‘first’ depositional sequence). The FPLS and the ‘first’ depositional sequence both overlie basement, and show a similar reflection configuration. On these grounds, the two sequences are considered equivalent in this study. Ties between the LDEO MCS data and DSDP site 330 showed that the base of the ‘first’

depositional sequence (unconformity 'U1' of Lorenzo & Mutter 1988) corresponds to the top of Falkland Plateau basement, where pre-Cambrian gneiss is overlain by sands, silts and sapropelic claystones of Middle–Upper Jurassic age (Barker, Dalziel *et al.* 1976), and that the top of the sequence (unconformity 'U2') separates sapropelic claystones of Upper Jurassic and Lower Cretaceous age. On these grounds, sediments of the FPLS are assumed to be Middle–Upper Jurassic in age in this study. Similarly, the upper bounding surface of the FPLS is thought to represent a Jurassic–Cretaceous unconformity.

MCS profile BAS878–04 (Fig. 12) shows that FPLS strata onlap tilted Falkland Plateau basement, which suggests that basement tectonism preceded the onset of FPLS deposition, and that FPLS deposition was controlled in part by pre-existing basement topography. This is also suggested by the relationship between the thickness of the FPLS and underlying basement structure (noted also by Lorenzo & Mutter 1988). Subtle divergent reflection configurations within the FPLS also imply that basement extension accompanied FPLS deposition. On MCS profile BAS878–03 basement faults extend upward through the top FPLS unconformity, which indicates that basement tectonism continued after the cessation of FPLS deposition. Hence, these data suggest that extension of the Falkland Plateau Basin had begun by the Middle Jurassic, and that it continued until the Lower Cretaceous. These findings are in broad agreement with results of existing studies, although Lorenzo & Mutter (1988) found no evidence for post-Jurassic basement faulting.

MCS profiles show that the style and intensity of basement faulting varies appreciably along-strike beneath the southern Falkland Plateau slope. Basement faults with large throws identified near 46°W (on profile BAS878–04, Fig. 12) may trend obliquely to the southern margin of the plateau, in common with northeast–southwest or southeast–northwest structural trends identified to the north (Lorenzo & Mutter 1988). Extension of southern Falkland Plateau basement may have occurred in connection with the opening of the Falkland Plateau Basin to the north (as described by Barker, Dalziel *et al.* 1976; Lorenzo & Mutter 1988; Marshall 1994), or the separation of the southern Falkland Plateau from its congruent margin in the southern Weddell Sea (during the Middle Jurassic, Livermore & Hunter 1996).

Both explanations are consistent with data presented in this study.

At shallower depth, the FPLS is overlain by the FPUS, a thick sedimentary succession which extends in places to the sea floor. The FPUS is probably composed of Cretaceous and Tertiary pelagic-hemipelagic sediments as sampled at DSDP sites 330 and 511 (located in Fig. 10). These sediments include mudstones, shales, claystones, chalks and calcareous oozes (Barker, Dalziel *et al.* 1976; Ludwig, Krashenninikov *et al.* 1983). DSDP drilling also revealed a major change in lithology from sapropelic claystones of Aptian age to nanno claystones of Albian age, reflecting less restricted ocean circulation in the western South Atlantic during the Albian. On MCS profiles, older FPUS sediments show discontinuous reflection configurations which resemble the laterally-incoherent and hummocky acoustic facies reported by Lorenzo & Mutter (1988) for their 'second' and 'third' depositional sequences (of Lower and Upper Cretaceous age respectively). Unpublished British Antarctic Survey seismic reflection profiles (located in Fig. 2 of this report) show that hummocky, discontinuous internal reflection configurations are widespread on the Falkland Plateau.

Tertiary evolution

During the Upper Cretaceous and Early Tertiary, the Falkland Plateau subsided steadily (Barker, Dalziel *et al.* 1976), and sedimentation conditions on the plateau were variable. Tertiary rocks sampled on the Falkland Plateau include siliceous and calcareous oozes, chalks and zeolitic clays. These sediments show widespread current control of deposition, reworking, non-deposition and erosion (Ciesielski & Wise 1977; Ciesielski *et al.* 1982; Wise *et al.* 1982; Barker, Dalziel *et al.* 1976).

Previous workers (Barker, Dalziel *et al.* 1976; Ludwig & Rabinowitz 1982; Ludwig 1983; Lorenzo & Mutter, 1988) have described a regional Cretaceous–Tertiary unconformity which extends across the Falkland Plateau Basin. However, MCS profiles presented in this study fail to show an acoustic stratigraphic surface at equivalent depth. If this unconformity extends across the survey area, it might coincide locally with the FPBR, where the FPBR is strong

and continuous, and there are no signs of coincident cross-cutting strata. A Tertiary sequence time-thickness map presented by Lorenzo & Mutter (1988) suggests that MCS profiles BAS878-03 and BAS878-04 cross the unconformity north of 52°S (north of *c.* SP 520 on profile BAS878-04, Fig. 12), where it lies at sub-bottom depths of up to 0.5 STWT. Lorenzo & Mutter (1988) also noted that the unconformity ('U4') has a 'two-fold nature: commonly it is a horizontal flat reflector, but in a few places it can be hummocky and discontinuous'. Hence the FPBR lies at a similar depth to the 'U4' boundary, and has a similar reflection character. The disruption the 'U4' reflection may be due to modification of the acoustic impedance contrast across the boundary by effects of silica diagenesis (e.g. Lonsdale 1990). A similar arrangement has been reported farther east in the Malvinas Outer Basin (Barker, Dalziel *et al.* 1976), where a Cretaceous-Tertiary unconformity coincides with an increase in compaction and diagenesis at DSDP site 328. Hence, the Cretaceous-Tertiary unconformity reported in previous studies may coincide in places with the FPBR. However, if such an association exists, it is of local extent, and the FPBR itself is not regarded as a chronostratigraphic surface.

In spite of this uncertainty, the reflection character of the uppermost FPUS resembles that of Tertiary sequences reported elsewhere on the Falkland Plateau. Barker (1976) described Tertiary Falkland Plateau sediments with discontinuous, undulating and irregular reflection configurations, which resemble those seen at shallow depth on profiles BAS878-03 and BAS878-04. Similarly, shallow sub-horizontal reflections at the northern EOL BAS878-04 may correspond to the 'oblique parallel, almost horizontal' configuration reported by Lorenzo & Mutter (1988). In this and previous studies, discontinuous, irregular reflection configurations within Falkland Plateau sediments are interpreted as an indication of bottom current control of sedimentation.

Falkland Trough

Mesozoic evolution

MCS profiles presented in this study show Falkland Trough basement dipping southward beneath the northern flank of the North Scotia Ridge. At its western limit (near Burdwood Bank, located in Fig. 1c) the Falkland Trough is underlain by continental crust (e.g. Ludwig *et al.* 1968; Davey 1972). However, seismic refraction studies (Ewing *et al.* 1971; Ludwig *et al.* 1978b) suggest that more easterly parts of the trough may be underlain by oceanic crust. The BAS878–04 gravity model suggests crustal thicknesses of up to 6.4 km beneath the southern Falkland Trough (when modelled as an oceanic section, Fig. 18) which falls within the range of ‘standard’ oceanic crustal thickness (listed as 6.1–7.6 km in table 2 of Carlson & Raskin 1984). Hence, these data are consistent with the presence of oceanic crust beneath this part of the Falkland Trough. The trough may be floored by a remnant sliver of oceanic crust which formed after the separation of the Falkland Plateau from its congruent margin in the Weddell Sea. Tectonic reconstructions (Barker & Lonsdale 1991; Barker *et al.* 1991) suggest that ocean floor south of the Falkland Plateau formed initially at a former South American–Antarctic ridge during the Upper Jurassic–Early Cretaceous, and that it was later overridden by the east-migrating Scotia arc. A more recent tectonic reconstruction by Livermore & Hunter (1996) suggests that the southern Falkland Plateau separated from its congruent margin in the southern Weddell Sea during the Middle Jurassic. Hence, the Falkland Trough near 46°W could be underlain by oceanic crust of Middle Jurassic age.

Cenozoic evolution: Falkland Plateau–North Scotia Ridge convergence

Previous workers (Ewing *et al.* 1971; Ludwig *et al.* 1978b; Ludwig & Rabinowitz 1982; Ludwig 1983; Barker *et al.* 1991; Platt & Philip, 1995) have shown that the northern flank of the North Scotia Ridge is underlain by a thick wedge of deformed sediment, and have interpreted this feature as an indication of tectonic convergence. MCS profiles presented in this study support this view, and show Falkland Plateau sediments deformed and uplifted to the south along the axis of the Falkland Trough.

MCS profiles show that the northern limit of the sediment wedge is described by a well-formed deformation front. This structure is most clearly apparent on MCS profile

BAS878-04, where it is described by an asymmetric over-thrust fold near the base of the EFTD, which coincides with a southward reduction in reflection continuity. Although the deformation front is less clear on other MCS profiles, it has nonetheless been traced continuously across the MCS survey area. On all MCS profiles, accreted North Scotia Ridge sediments appear acoustically opaque, with few laterally-persistent reflections.

MCS profiles (Figs 11-13) show well-formed, regular, open folds at the surface of the sediment wedge, which are mimicked at shallower depth by a wavy reflection configuration within the lower layers of the EFTD. This regular, primary deformation fabric is buried within the MCS survey area. However, convergent deformation is exposed at the sea floor nearby to the south (on profile BAS878-03, Fig. 11), where thrust fault-bound slices of accreted sediment have been imaged near the base of the North Scotia Ridge. These structures mark the southern edge of the regular folds generated at the deformation front, and appear to have overprinted this primary fabric of deformation. This interpretation is supported by GLORIA sonographs presented elsewhere in this report (Figs 3a,b), which show that the thrust stack extends over 100 km along the North Scotia Ridge.

Convergent deformation of this kind is characteristic of foreland terrains and forearc accretionary wedges. At its western limit, the Falkland Trough is floored by continental crust (e.g. Ludwig *et al.* 1968), and convergent deformation identified along its axis has been attributed to foreland tectonics associated with the Magallanes fold-thrust belt of southern South America (Platt & Philip 1995). However, previous studies (Ewing *et al.* 1971; Ludwig *et al.* 1978b) suggest that farther east, the Falkland Trough is floored by oceanic crust, and that the North Scotia Ridge sediment wedge represents a forearc accretionary prism, formed in connection with southward subduction of the South American plate (Ludwig & Rabinowitz 1982; Barker *et al.* 1991). In a study of the Banda arc collision zone, Audley-Charles (1986) noted that foredeeps are: (1) underlain by continental crust; (2) overlain by a sedimentary cover of detritus derived from the erosion of the uplifted orogenic zone; and (3) located between strongly deformed cover rocks of the orogenic zone, and relatively undeformed cover rocks of the craton. Data presented in this study permit the distinction

between foreland terrain and forearc accretionary wedge to be made in this case. In particular, gravity and MCS data suggest that near 46°W, the Falkland Trough is floored by oceanic thickness crust, and that the Falkland Plateau Basin to the north is floored by intermediate thickness crust of probable Middle Jurassic age (and is not therefore regarded as cratonic). On these grounds, the eastern Falkland Trough is interpreted as a relict subduction zone (as proposed by Ludwig & Rabinowitz 1982).

Timing of north–south convergence. Although MCS profiles clearly describe convergent deformation within the Falkland Trough, an absence of reliable age control means that the timing of Falkland Plateau–North Scotia Ridge convergence remains uncertain. MCS profiles show that most of the FPUS (presumed Cretaceous–Tertiary in age) has been incorporated within the sediment wedge, which suggests that collision probably occurred during the Tertiary. Since the MCS profiles do not show a continuous unconformity between the EFTD and FPUS, some of the youngest FPUS sediments may have been coeval with those of the sediment drift, and might have been deposited after the cessation of convergence. A Tertiary-age collision was also inferred by the Lamont group (Ludwig & Rabinowitz 1982; Ludwig 1983) on the grounds that the Cretaceous–Tertiary unconformity identified on the Falkland Plateau ('U4' of Lorenzo & Mutter 1988) had been incorporated within the North Scotia Ridge accretionary prism. Unfortunately, MCS profiles presented in this study fail to describe a regional unconformity at equivalent depth; while unconformity 'U4' may locally coincide with the FPBR, the FPBR itself is not regarded as a chronostratigraphic surface.

MCS profiles suggest that oldest EFTD sediments may have been incorporated within the North Scotia Ridge accretionary prism. However, at shallower depth, youngest EFTD strata show no indications of recent tectonism, which indicates that north–south convergence has ceased at the toe of the accretionary prism near 46°W (supported by 3.5 kHz sub-bottom profile A–A' shown in Fig. 24 of this report). These findings conflict with the interpretation of Ludwig & Rabinowitz (1982) who inferred active convergence in the eastern Falkland Trough from the 'buckling, folding and uplift of Falkland trough sediments'. In this study, the wavy, mounded, migrating-wave and lenticular acoustic facies apparent in eastern

Falkland Trough sediments are attributed to passive draping of folded topography, or to current control of sedimentation. In the absence of reliable age control, the timing of the cessation of north–south convergence in the eastern Falkland Trough remains uncertain. Barker *et al.* (1984, 1991) suggest that the northward migration of the North Scotia Ridge ceased *c.* 6 Ma ago, when sea-floor spreading stopped in the Central Scotia Sea and Drake Passage. This estimate is compatible with interpretations presented in this study.

Current-influenced sedimentation

MCS profiles show a thick succession of mounded, highly reflective sediments developed along the Falkland Trough axis east of 48°W (EFTD, Figs 11–13). EFTD sediments exhibit a range of internal reflection configurations including: regular, parallel to sub-parallel, divergent, wavy and migrating-wave acoustic facies. The MCS data also show that EFTD strata thin progressively away from the crest of the mound, which suggests that its mounded external form results from a long-term lateral variation in sedimentation rate. This is confirmed by an accompanying 3.5 kHz sub-bottom profile (profile A–A', shown in chapter 4 of this report) which shows pinch-out of near-surface reflections at the thinning edges of the mound, and non-deposition along its flanking depressions. The gently asymmetric, convex-upward external form of the mound resembles that of 'confined' contourite sediment drifts reported in studies of the Mediterranean and Sumba forearc (Reed *et al.* 1987; Marani *et al.* 1993), and is interpreted as an indication of deposition in the presence of ambient bottom currents. Piston cores (Jordan & Pudsey 1992) obtained from the surface of the mound show that EFTD sediments are predominantly biogenic in composition, and show no evidence (sedimentary structures or grading) of deposition by turbidity flows. Hence, on these grounds, the EFTD is interpreted as a contourite sediment drift, formed as a result of prolonged pelagic-hemipelagic sedimentation in the presence of ambient bottom currents.

Migrating sediment waves. MCS profiles (Figs 11 and 13) show a field of migrating sediment waves buried at intermediate depth within the EFTD near 47°W. The waves have apparent wavelengths of 3.8–4.6 km (on east–west profile BAS923–S26, Fig. 13) and amplitudes of

up to 90 m (assuming a formation velocity of 1800 m.s^{-1}), and are therefore comparable in size to migrating bedforms reported in the Argentine Basin (Flood & Shor 1988). Existing data are insufficient to determine the trend of these bedforms, although comparison between MCS profiles BAS878-03 and BAS923-S26 suggests that the wave crests may be more closely aligned with north-south profile BAS878-03. The sediment waves show a consistent east component of migration on east-west profile BAS878-S26. Farther east, 3.5 kHz sub-bottom profiles presented in chapter 4 of this report (profiles B-B' and C-C', Fig. 25) show a separate field of active sediment waves at the surface of the EFTD near $44^{\circ}30'W$, which have formed in the presence of westward-flowing southern-origin bottom water. The buried sediment waves apparent in the MCS data may have also formed in the presence of westward-flowing ambient bottom currents.

3.7 CONCLUSIONS

MCS profiles and gravity measurements presented in this study provide insights into the tectonic and sedimentary development of the Falkland Plateau-North Scotia Ridge collision zone near $46^{\circ}W$. Some specific findings are listed below:

1) MCS profiles show extended Falkland Plateau basement overlain by a thick sedimentary succession of presumed Middle Jurassic-Tertiary age. Correlations between these data and published LDEO profiles suggest that basement extension had begun by the Middle Jurassic, and may have continued until the Lower Cretaceous. Basement faulting probably occurred in connection with the opening of the Falkland Plateau Basin to the north, or the rifting of the southern flank of the plateau from its congruent margin in the Weddell Sea. Results of gravity modelling suggest intermediate thickness crust beneath the southern Falkland Plateau Basin (9-13 km thickness, when modelled as an oceanic section), consistent with previous studies (e.g. Lorenzo & Mutter 1988).

2) MCS profiles show Falkland Plateau basement overlain by a thick sedimentary succession containing two principal acoustic stratigraphic sequences (FPLS and FPUS). The

FPLS (presumed Middle–Upper Jurassic age, and correlated with sequence ‘1’ of Lorenzo & Mutter 1988) is characterised by high-amplitude, laterally-continuous reflections. Deposition of this sequence accompanied extension of Falkland Plateau basement, and was controlled in part by basement topography. The overlying FPUS (presumed Cretaceous–Tertiary age, and correlated with sequences ‘2’, ‘3’ and ‘4’ of Lorenzo & Mutter 1988) is characterised by diverse, discontinuous internal reflection configurations, interpreted as an indication of current control of sedimentation. Basement tectonism may have accompanied the deposition of the FPUS during the Lower Cretaceous. Previous studies (e.g. Barker, Dalziel *et al.* 1976; Lorenzo & Mutter 1988) describe a Cretaceous–Tertiary unconformity which extends across the Falkland Plateau Basin to the north. However, MCS profiles presented here fail to show an equivalent surface. A widespread but discontinuous reflection identified at comparable depth (FPBR) is interpreted as a silica diagenetic boundary (e.g. Lonsdale 1990). The FPBR may coincide in places with the Cretaceous–Tertiary unconformity identified in the Falkland Plateau Basin, but if such an association exists, it is of local extent.

3) Results of gravity modelling suggest oceanic-thickness crust (up to 6.4 km thick, when modelled as an oceanic section) beneath the southern Falkland Trough and the northern flank of the North Scotia Ridge near 46°W. This is consistent with previous studies (Ewing *et al.* 1971; Ludwig *et al.* 1978b) suggesting an oceanic origin for the central Falkland Trough.

4) MCS profiles show that the Aurora Bank section of the North Scotia Ridge is formed principally of uplifted, accreted sediment, overriding a dense, north-dipping basement backstop. Results of gravity modelling suggest that the northern flank of Aurora Bank is underlain by sediments with a total thickness exceeding 9 km. This interpretation is consistent with previous studies which have shown thick sediments elsewhere beneath the North Scotia Ridge (e.g. Davey 1972), and with gravity data (Sandwell *et al.* 1995) which show that the northern slope of Aurora Bank coincides with a large amplitude (exceeding –150 mGal) negative free-air gravity anomaly.

5) MCS profiles show compressional deformation in the Falkland Trough, where sediments of the Falkland Plateau and the EFTD have been uplifted, deformed, and incorporated within the North Scotia Ridge accretionary prism. At shallower depth, youngest EFTD sediments show no signs of recent tectonism, indicating that north–south convergence has ceased at the toe of the accretionary prism. This interpretation conflicts with results of Ludwig & Rabinowitz (1982) who inferred continued convergence from the ‘buckling, folding and uplift of Falkland trough sediments’. The timing of the cessation of Falkland Plateau–North Scotia Ridge convergence remains uncertain, although the *c.* 6 Ma estimate of Barker *et al.* (1984, 1991) is compatible with the results of this study. The existence of intermediate-to-oceanic thickness crust beneath the southern Falkland Plateau and Falkland Trough (near 46°W) supports the notion that the North Scotia Ridge sediment wedge represents a forearc accretionary prism, formed in connection with southward subduction of the South American plate (as suggested by Ludwig & Rabinowitz 1982; Barker *et al.* 1991).

6) MCS profiles show that the eastern Falkland Trough is occupied by a well-formed contourite sediment drift (EFTD). Diverse seismic reflection patterns within the drift are attributed to current control of deposition, or to sediment drape across the deformed topography of the North Scotia Ridge accretionary prism. This interpretation conflicts with the results of Ludwig & Rabinowitz (1982), who interpreted the reflection character of EFTD sediments as an indication of active tectonic convergence. Near 47°W, MCS profiles reveal migrating sediment waves buried at intermediate depth within the drift, which show a consistent east component of migration. The sediment drift and the buried bedforms may have formed in the presence of ambient bottom currents associated with the northward transit of southern-origin bottom water.

Chapter 4

3.5 kHz sub-bottom profile and bathymetry investigation of the eastern Falkland Trough

4.1 SYNOPSIS

The North Scotia Ridge controls the eastward and northward flow of the Antarctic Circumpolar Current emerging from Drake Passage. Existing physical oceanographic data in this region are sparse and do not define the flow pattern of Circumpolar Deep Water within the Antarctic Circumpolar Current, or of Weddell Sea Deep Water heading northward beneath it, in the region of the North Scotia Ridge and Falkland Trough. 3.5 kHz reflection profiles show sediment waves at the surface of a sediment drift along the axis of the eastern Falkland Trough that have a consistent northeast–southwest alignment and are migrating southeast, indicating persistent westward bottom-current flow along the trough axis. Sediment thinning and non-deposition at the southern drift margin indicate intensified westward flow, considered to be Weddell Sea Deep Water from the Malvinas Outer Basin to the east. This flow probably continues to 48°W, but beyond there its fate is unknown. Similar non-deposition along the northern margin of the drift is considered to result from intensified eastward return flow of Weddell Sea Deep Water, or from Circumpolar Deep Water. The sediment wave geometry appears to extend to at least 400-m depth within the drift, which therefore probably contains a record of southern-origin bottom water (presently Weddell Sea Deep Water) extending back for several million years.

4.2 INTRODUCTION

The Falkland Trough is an east–west bathymetric deep extending 1300 km from the continental margin of South America to the Malvinas Outer Basin in the western South Atlantic (see chapter 2, Fig. 1c). Between 56°W and 41°W, the floor of the trough lies 3000–4000 m below sea level (Tectonic Map 1985), and the slopes of the trough are formed by the southern flank of the Falkland Plateau, and the northern flank of the North Scotia Ridge. Falkland Plateau sea floor dips gently into the trough axis with gradients of about 0.5°, whereas the North Scotia Ridge is an area of appreciable bathymetric relief: summit regions lie above 1000 m below sea level, and submarine slopes exceed 10° along its northern flank.

Oceanographic setting

The Falkland Trough lies in the path of Circumpolar Deep Water within the Antarctic Circumpolar Current, which is constrained to flow east through Drake Passage (Fig. 19), but then diverges as topography permits: shallow Circumpolar Deep Water flows northeast over the western North Scotia Ridge and Falkland Plateau as the Falkland Current (Peterson & Whitworth 1989; Peterson 1992), but deeper Circumpolar Deep Water is retained within the Scotia Sea until Shag Rocks passage, a gap in the ridge at 48°W with a sill depth of 3000 m. Thereafter, Circumpolar Deep Water flows north through the gap, and then east, along the southern flank of the Falkland Plateau. A more southerly component of the Antarctic Circumpolar Current flows eastward within the Scotia Sea (Peterson & Whitworth 1989; Grose *et al.* 1995).

At greater depths, cold, fresh Weddell Sea Deep Water (potential temperature (θ) = -0.7°C to $+0.2^{\circ}\text{C}$) flows north through gaps in the South Scotia Ridge into the Scotia Sea, where it underlies the Antarctic Circumpolar Current at a sub-horizontal interface (Locarnini *et al.* 1993). This surface lies *c.* 1000 m below sea level across the South Scotia Ridge, and descends northward to meet the sea floor at 3000 to 4000 m depth in the northern Scotia Sea

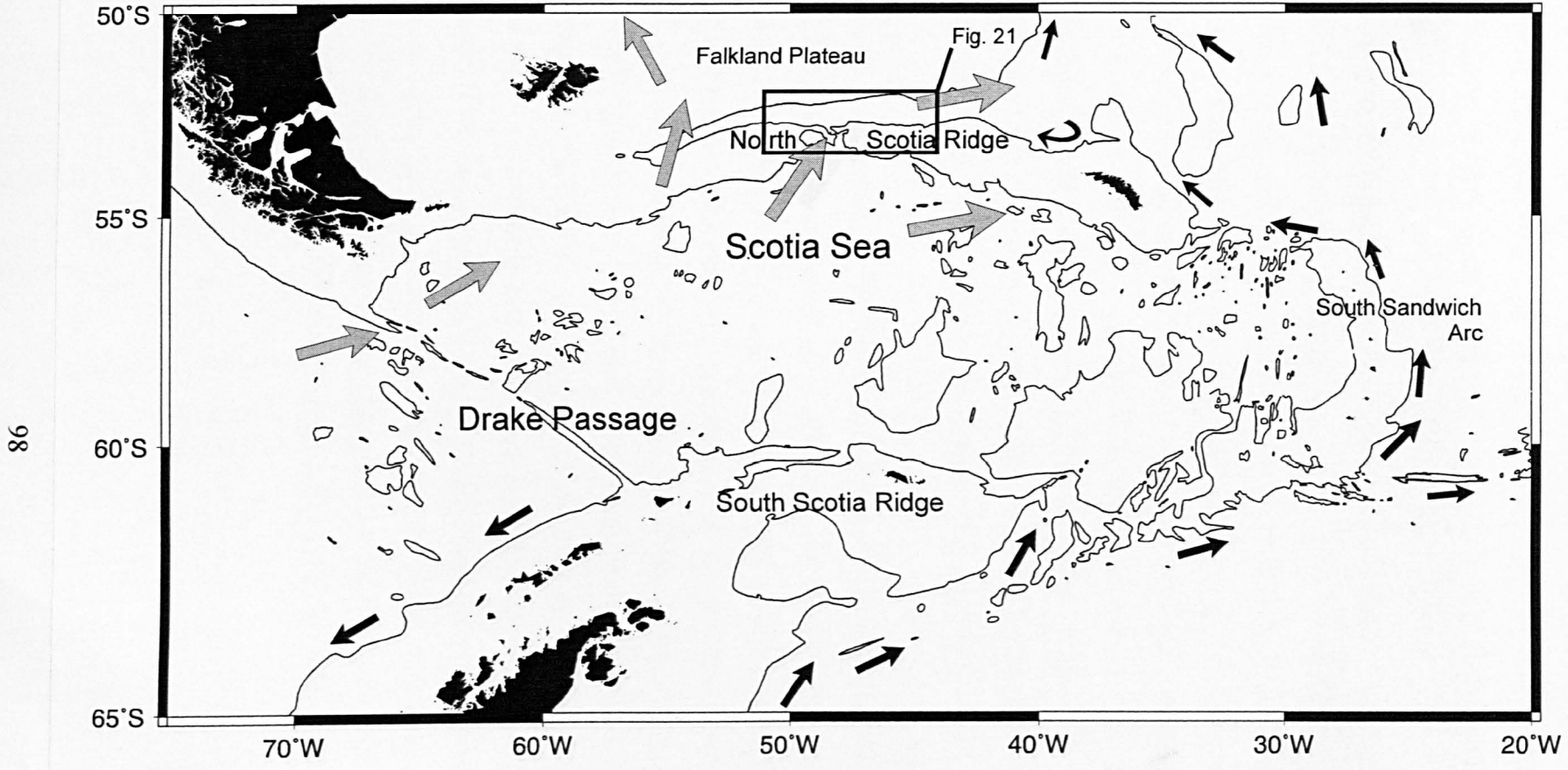


Fig. 19 The western South Atlantic Ocean, with 3000 m isobath. Bottom-flow directions described by Gordon (1966), Hollister & Elder (1969), Georgi (1981), Nowlin & Zenk (1988) and Locarnini *et al.* (1993) shown by grey arrows (Antarctic Circumpolar Current) and black arrows (Weddell Sea Deep and Bottom Water). Area shown in Figs 21-23 is outlined.

(Fig. 20). Farther east, Weddell Sea Deep Water flows northward along the South Sandwich Trench, through the Malvinas Outer Basin, and eventually into the Argentine Basin and beyond (Hollister & Elder 1969; Georgi 1981; Mantyla & Reid 1983, and Fig. 19).

Direct oceanographic measurements in the vicinity of the Falkland Trough and North Scotia Ridge are few. Zenk (1981) and Wittstock & Zenk (1983) reported results of a year-long current meter mooring *M259* directly on the 3000-m sill of Shag Rocks passage at 52°52'S, 48°19'W (located in Fig. 23). Bottom potential temperatures varied between -0.2°C and +0.7°C, and current speeds reached 60 cm.s⁻¹: there was a strong correlation between low potential temperature and strong west-northwest bottom-current flow at speeds above 15 cm.s⁻¹. On these grounds, Zenk (1981) argued for strong northwestward overflow events involving 'Scotia Sea bottom water', derived from Weddell Sea Deep Water, after mixing with Circumpolar Deep Water within the Antarctic Circumpolar Current.

More recently, Locarnini *et al.* (1993) showed bottom potential temperatures decreasing both eastward along the Falkland Trough and southward across the Scotia Sea, from a local high just above +0.2°C in Shag Rocks passage (Fig. 20). These results suggested that Weddell Sea Deep Water flowing northward in the Scotia Sea fails to reach Shag Rocks passage, since the +0.2°C contour which describes the northern limit of Weddell Sea Deep Water meets the North Scotia Ridge c. 110 km farther east. Furthermore, re-examination of the data of Zenk (1981) suggested that the cold overflow events detected in the gap were more closely correlated with westward flow than northward flow. On these grounds, Locarnini *et al.* (1993) inferred westward flow of Weddell Sea Deep Water along the Falkland Trough from the Malvinas Outer Basin, and cast doubt on the existence of northwestward 'Scotia Sea bottom water' flow through Shag Rocks passage. However, there was significant scatter in the aggregated data, and the bottom-current regime in the Falkland Trough remains unresolved.

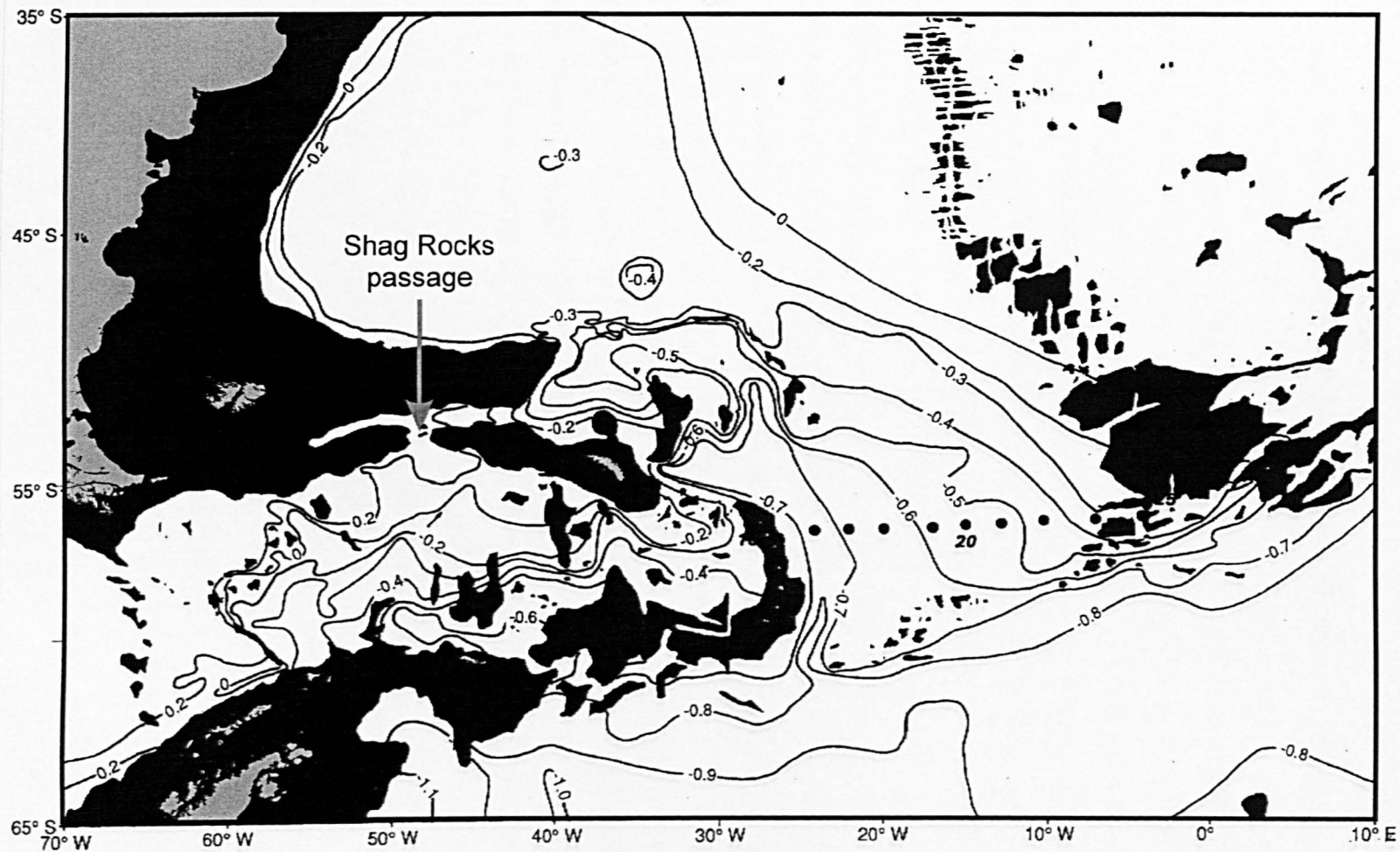


Fig. 20 Bottom potential temperature (in degrees celsius) in the western South Atlantic showing the spread of cold waters from the Weddell Sea. $+0.2^{\circ}\text{C}$ contour describes the northern extent of Weddell Sea Deep Water in the Scotia Sea. Depths less than 3000 m are shaded (from Locarnini *et al.* 1993)

Depositional setting

Although the Antarctic Circumpolar Current is wind-forced at the sea surface, existing studies suggest that Antarctic Circumpolar Current flow extends in many places to the sea floor. Seismic reflection profiles crossing Drake Passage (Barker & Burrell 1977) and the northern Scotia Sea (Pudsey & Howe 1998) show sediment accumulation in isolated banks, under strong bottom current control, and piston cores show pre-Quaternary sediments widely exposed across the Falkland Plateau, where vigorous Antarctic Circumpolar Current bottom currents inhibit modern sedimentation (Burckle & Hays 1974; Saito *et al.* 1974; Howe *et al.* 1997). Similarly, studies based on results of DSDP drilling (Barker, Dalziel *et al.* 1976) have shown that the Falkland Plateau has been a site of prolonged non-deposition or erosion since the inception of the Antarctic Circumpolar Current in the early Miocene. As a consequence, young, fine-grained sediments deposited in the path of the Antarctic Circumpolar Current are best preserved in deep, sheltered parts of the Falkland Trough and Malvinas Outer Basin where bottom currents have remained slack. At these sites, considerable thicknesses of pelagic-hemipelagic sediment have accumulated in the presence of comparatively weak bottom currents, associated with the northward transit of southern-origin bottom water, or deepest Antarctic Circumpolar Current flow. Ciesielski *et al.* (1982) described the eastern Falkland Trough as 'relatively protected' from strong Antarctic Circumpolar Current flow, and showed that post-Miocene sediments were best developed within the trough axis. Similarly, Barker, Dalziel *et al.* (1976) described a sequence of Oligocene–Pleistocene diatomaceous oozes which attains a thickness of >1.5 km at the mouth of the Falkland Trough, and inferred a minimum post-Eocene sedimentation rate of 40 m.my⁻¹.

In this study, I present bathymetry data and 3.5 kHz sub-bottom profiles which describe the distribution and extent of young contourite drift sediments deposited in the eastern Falkland Trough (east Falkland Trough sediment drift, EFTD).

4.3 GEOPHYSICAL DATA ACQUISITION AND PROCESSING

Bathymetry data

As part of this study, a detailed bathymetry map of the central and eastern Falkland Trough (shown in Fig. 23) has been produced to delineate better the subdued topography of the trough floor. The new map is derived from bathymetric soundings held in the British Antarctic Survey archive and the National Geophysical Data Centre *GEODAS* database (NGDC 1996). Bathymetry data (shown in Fig. 21) were obtained during 20 scientific cruises between 1968 and 1990. All soundings were corrected to true depth (Carter 1980), and positioned with TRANSIT or GPS satellite navigation systems. Corrected depths were posted on a Mercator projection (true scale=1:1,875,000 at 57°S), and isobaths were drafted by hand at intervals of 200 m for water depths of < 3000 m, and 100 m for depths of > 3000 m, to accentuate the subdued topography of the Falkland Trough floor.

3.5 kHz sub-bottom profiles

Figure 22 shows tracks of 3.5 kHz high-resolution profiles crossing the eastern Falkland Trough. These data were obtained by the British Antarctic Survey using an Institute of Oceanographic Sciences (IOS) sub-bottom profiler during RRS *Discovery* cruises 154 (D154, 1985) and 172 (D172, 1988), RRS *Charles Darwin* cruise 37 (CD37, 1989) and RRS *James Clark Ross* cruise 04 (JR04, 1993). During operation, the IOS profiler transmitted a swept acoustic pulse (3000–4000 Hz, 28 ms duration) through an array of towed or hull-mounted transducers, and the reflected signal was bandpass filtered, and cross-correlated with a reference pulse to obtain a trace of the sea floor and near-surface geology. 3.5 kHz profiles reproduced in this study (A–A', B–B' and C–C', located in Fig. 23 and shown in Figs 24,25) are unprocessed shipboard records (bandpass filtered, with no additional digital enhancement).

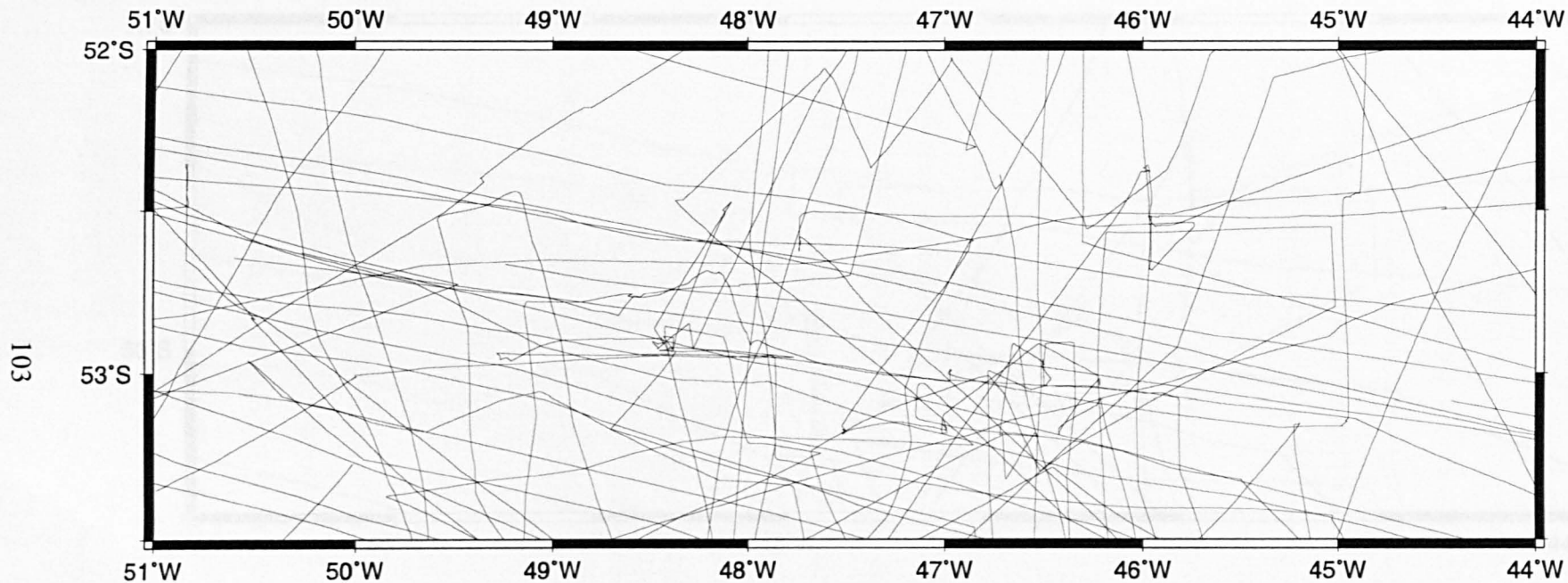


Fig. 21 Bathymetry ship tracks crossing the central and eastern Falkland Trough. Data were obtained during 20 scientific cruises (1968-1990), and are held in the British Antarctic Survey archive. Accompanying bathymetry soundings have been corrected to true depth (Carter 1980) and located with the aid of satellite navigation systems.

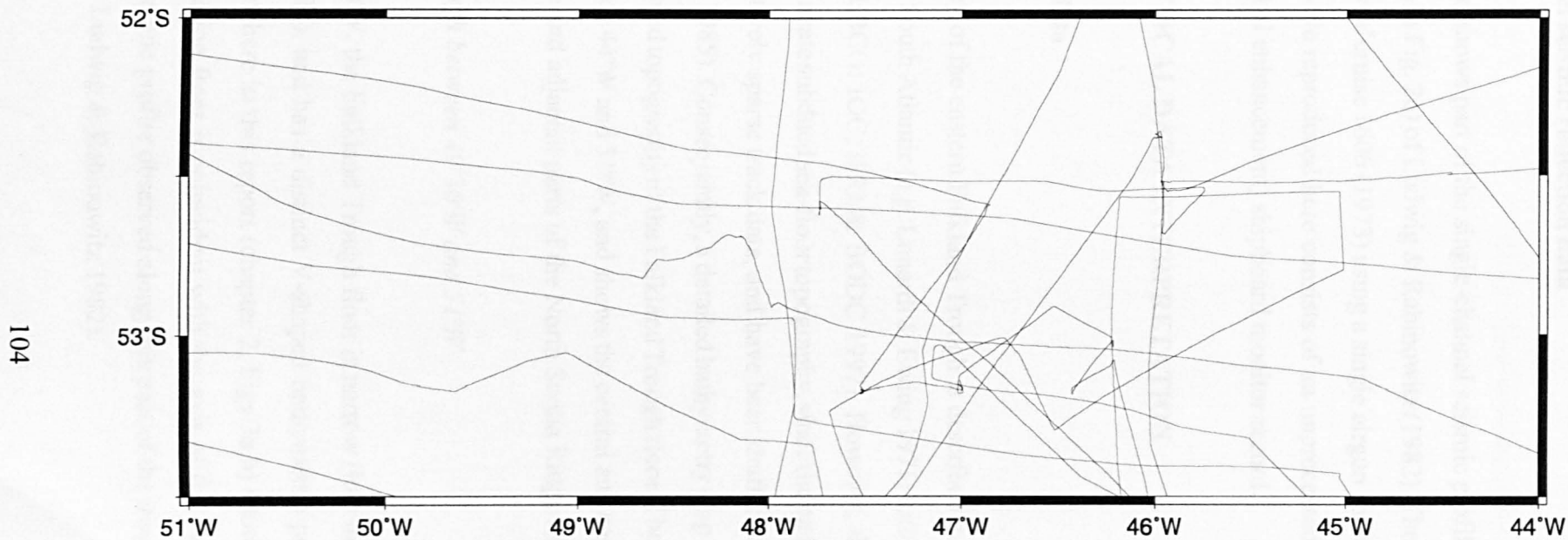


Fig. 22 3.5 kHz high-resolution sub-bottom profile tracks crossing the central and eastern Falkland Trough. These data were obtained by the British Antarctic Survey during four scientific cruises between 1985 and 1993.

Single-channel seismic reflection data

This study also shows part of the single-channel seismic profile 'B' (labelled D-D' in Fig. 23, and shown in Fig. 26) of Ludwig & Rabinowitz (1982). These data were obtained during *Robert D Conrad* cruise 1606 (1973) using a single airgun source (chamber capacity = 0.41 l), and the profile reproduced here consists of an unprocessed (bandpass-filtered, with no additional digital enhancement) shipboard monitor record.

4.4 GEOPHYSICAL DATA INTERPRETATION

Bathymetry data

The topography of the eastern Falkland Trough is described in existing bathymetry studies of the western South Atlantic (e.g. Lonardi & Ewing 1971; Rabinowitz *et al.* 1978; Tectonic Map 1985; GEBCO: IOC, IHO & BODC 1997). However, these regional studies do not accurately delineate subdued sea-floor topography, since the bathymetry contours are derived from comparatively sparse track data, and have been drafted at large intervals (e.g. 250 m, Tectonic Map 1985). Consequently, a detailed bathymetry map has been produced to define better the subdued topography of the Falkland Trough floor. The new map (shown in Fig. 23) extends between 44°W and 51°W, and shows the central and eastern Falkland Trough, Shag Rocks passage and adjacent parts of the North Scotia Ridge and Falkland Plateau.

Falkland Trough between 49°30'W and 51°W

West of 49°30'W, the Falkland Trough floor is narrow (less than 9 km wide at the 3600 m isobath, Fig. 23), and has a distinct V-shaped bathymetric profile. GLORIA sonographs presented elsewhere in this report (chapter 2, Figs 3a,b) show that here, the North Scotia Ridge deformation front is coincident with the axis of the Falkland Trough, and that the angular bathymetric profile observed along this part of the trough is tectonically controlled (noted also by Ludwig & Rabinowitz 1982).

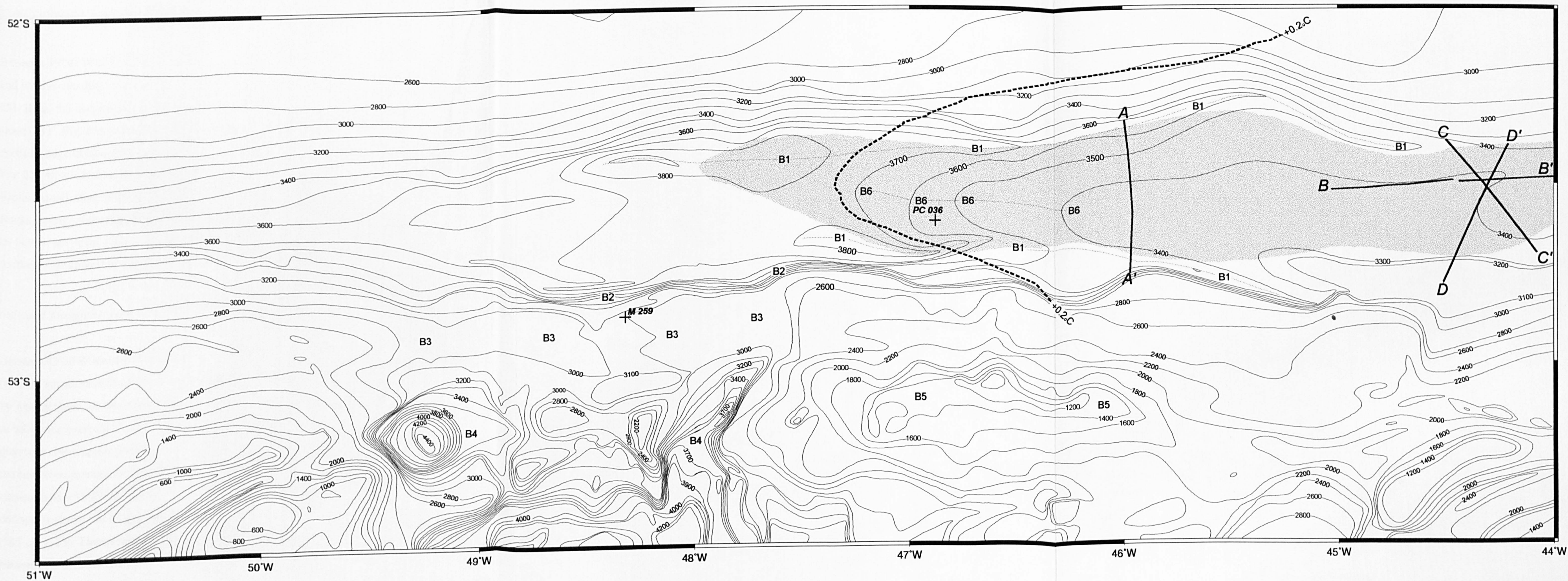


Fig. 23 Bathymetry map of the central and eastern Falkland Trough. Isobaths are drafted at 100 m intervals for depths of > 3000 m, and at 200 m intervals for depths of < 3000 m. Shaded sea floor describes area of east Falkland Trough sediment drift deduced from 3.5 kHz profiles (located in Fig. 22). Heavy dashed line (+0.2°C bottom potential temperature contour of Locarnini *et al.* 1993) describes the western limit of Weddell Sea Deep Water in the Falkland Trough. 3.5 kHz profiles A-A', B-B' and C-C' (shown in Figs 24 and 25), and seismic reflection profile D-D' (shown in Fig. 26) are located. M 259 locates current meter mooring of Zenk (1981), and PC 036 locates piston core 036 of Jordan & Pudsey (1992).

Falkland Trough between 49°30'W and 47°30'W

Between 49°30'W and 47°30'W, the floor of the Falkland Trough has subdued topography and widens steadily eastward (to *c.* 55 km width at the 3600 m isobath near 47°30'W, Fig. 23). Here, the deepest parts of the trough extend along the northern and southern base of slope ('B1', Fig. 23), and the southern trough slope is breached by Shag Rocks passage. The northern edge of Shag Rocks passage is described by a flat-topped bathymetric ridge ('B3', Fig. 23), which defines the sill depth of the gap at *c.* 3000 m. The northern flank of the ridge forms a small, steep north-facing scarp ('B2', Fig. 23). Farther south, sea floor within Shag Rocks passage shows considerable relief, with small steep-sided basins extending to >3800 m below sea level ('B4', Fig. 23). The steep flanks of these basins commonly trend northeast-southwest or northwest-southeast, and are probably tectonically controlled.

Falkland Trough between 47°30'W and 44°W

Between 47°30'W and 44°W, the floor of the Falkland Trough continues to widen eastward (to *c.* 60 km width at the 3600 m isobath near 45°30'W, Fig. 23), and is flanked to the south by Aurora Bank, an elevated component of the North Scotia Ridge which shoals to < 1200 m below sea level ('B5', Fig. 23). Here, Falkland Trough sea floor at >3200 m depth has a distinct convex-upward curvature, described by looped bathymetry contours which open to the east (crest marked by 'B6', Fig. 23). The isobaths show that the trough floor has greatest curvature near 46°45'W. The elevated trough axis is bounded to the north and south by well-defined bathymetric deeps, described by tightly looped isobaths which open to the west ('B1', Fig. 23). These features were first described by Lonardi & Ewing (1971) as 'marginal bathymetric depressions', and the northern depression can be traced in the bathymetry over 170 km. East of 46°W, the curved profile of the trough floor becomes more subdued and increasingly asymmetric, and is not clearly apparent in bathymetry at 44°30'W.

3.5 kHz high-resolution reflection profiles

Figure 22 shows 3.5 kHz profile tracks crossing the eastern Falkland Trough. These data have been used to map the acoustic penetration and character of near-surface sediments, and to describe bedforms preserved at the sea floor. This section describes three profiles (A–A', B–B' and C–C', Figs 24 and 25) which form part of this data set.

3.5 kHz sub-bottom profile A–A'

3.5 kHz profile A–A' (located in Fig. 23, and shown in Fig. 24) was obtained with MCS profile BAS878–04 (described in chapter 3 of this report) and crosses the southern Falkland Plateau, Falkland Trough and the North Scotia Ridge near 46°W.

The northernmost part of profile A–A' crosses the southern flank of the Falkland Plateau. Here, A–A' shows low acoustic penetration, and erosional truncation of a steep, south-dipping reflection beneath the base of slope, which suggests that this part of the Falkland Plateau is presently non-depositional.

At the base of slope, the 3.5 kHz profile shows a bathymetric deep, which corresponds to the northern marginal depression described by regional bathymetry (northernmost 'B1', Fig. 23). Here, the 3.5 kHz data show a southward increase in acoustic penetration, which suggests that the axis of the depression marks the northern limit of recent sedimentation. Within the depression, non-depositional Falkland Plateau sea floor is replaced to the south by exceptionally smooth Falkland Trough sea floor, with coherent, laterally-persistent reflections extending to the limit of 3.5 kHz penetration. Farther south, thick, acoustically-stratified sediments extend continuously across the floor of the Falkland Trough, but thin and pinch-out again at the southern marginal depression (southernmost 'B1', Fig. 23). The southern depression shows hyperbolic echoes, suggesting an irregular sea floor, and is interpreted as an area of non-deposition. Farther south, profile A–A' crosses the steep, irregular northern flank of the North Scotia Ridge which shows hyperbolic echoes. A similar

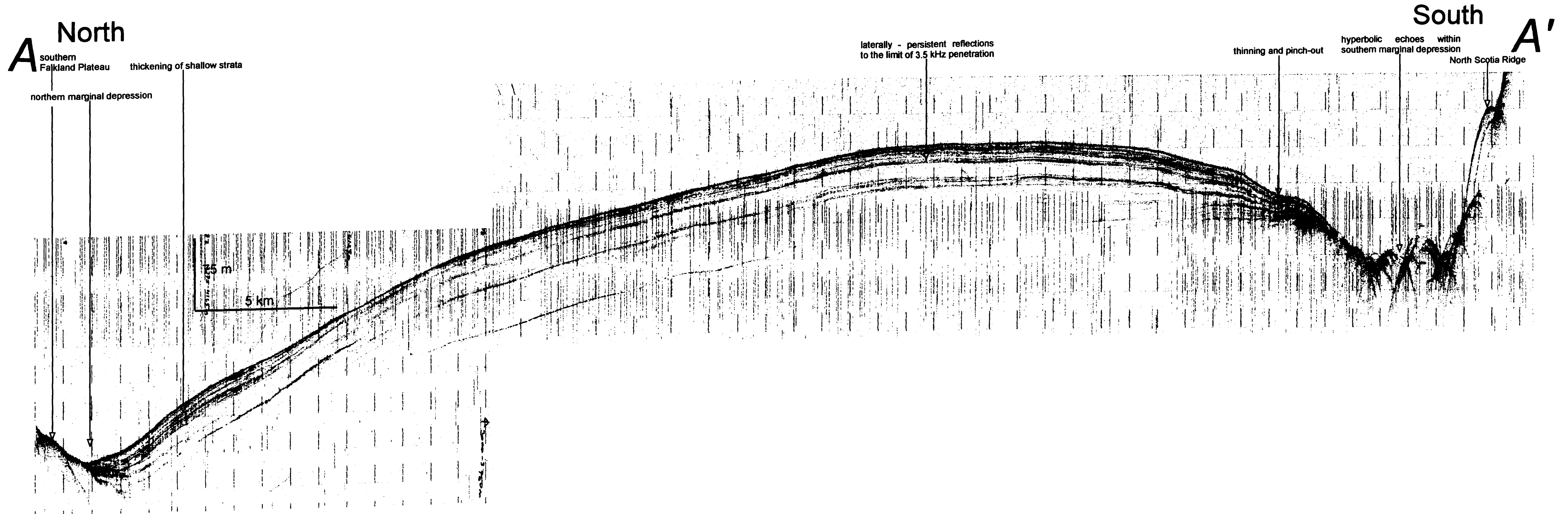


Fig. 24. 3.5 kHz sub-bottom profile A-A' (located in Fig. 23). Vertical exaggeration = c. 34:1 at the sea floor.

echo character has been reported for the northern flank of the North Scotia Ridge to the west (Howe *et al.* 1997).

3.5 kHz profiles (located in Fig. 22) have been used to map the extent of young, acoustically-stratified sediments within the eastern Falkland Trough (shown with new bathymetry, Fig. 23). These stratified strata are confined to water depths of >3300 m, and extend continuously along the eastern Falkland Trough between 48°W and 43°30'W.

3.5 kHz sub-bottom profiles B–B' and C–C': migrating sediment waves

Figures 25a,b show two additional 3.5 kHz profiles (B–B' and C–C', located in Fig. 23) which lie along 266°T and 141°T respectively, and cross within the Falkland Trough. These profiles show migrating bedforms developed at the surface of the sediment mound in the vicinity of 44°20'W. The bedforms are comparable in size and morphology to abyssal sediment waves, described by Flood *et al.* (1993) as 'large-scale, quasi-sinusoidal, current-related sedimentary features (or bedforms) that develop in fine-grained cohesive sediments'. Profiles B–B' and C–C' intersect within the sediment wave field, so that the true orientation and wavelength of individual sediment waves may be determined. Continuous GPS navigation on both cruises provided positions accurate to *c.* 100 m (Hofmann-Wellenhof *et al.* 1992), leading to only minor uncertainties in bedform orientation. I have assumed that the larger bedforms are continuous over a maximum distance of 14 km when correlating between profiles, but recognise that additional data may be required to verify this, as sediment waves are known to have limited strike extent (Flood & Shor 1988). The correlation of five prominent sediment wave crests between profiles B–B' and C–C' (M1, M2, M4, M5 and M6, Figs 25a,b) reveals consistent northeast–southwest crestral alignments between 045°T and 051°T. The M3 wave crest on profile B–B' is represented on profile C–C' by two smaller, distinct wave crests (M3a and M3b, Fig. 25b). M3 may therefore be discontinuous along strike and has been excluded from estimates of bedform orientation. The northwest–southeast trending profile C–C' (Fig. 25b) lies almost orthogonal to the dominant sediment wave trend, so bedform wavelengths on this profile approximate true wavelengths.

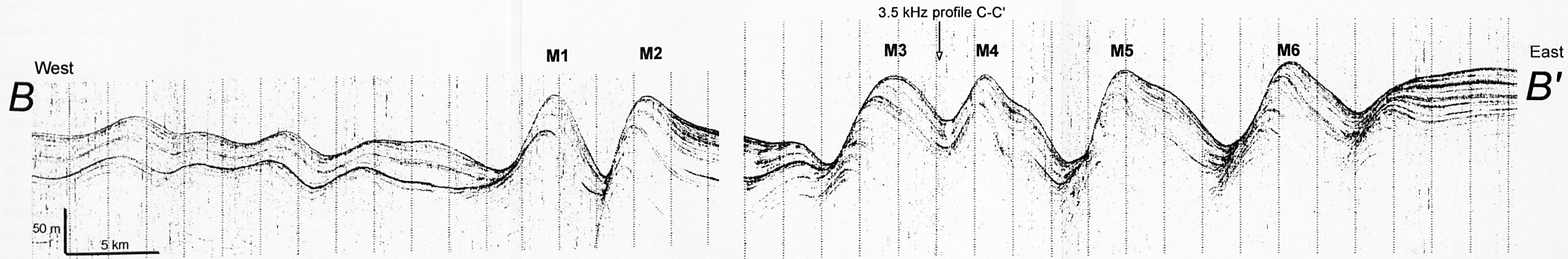


Fig. 25 (a) 3.5 kHz sub-bottom profile B-B' (located in Fig. 23). Vertical exaggeration = *c.* 48:1 in water. Intersection with 3.5 kHz profile C-C' is marked.

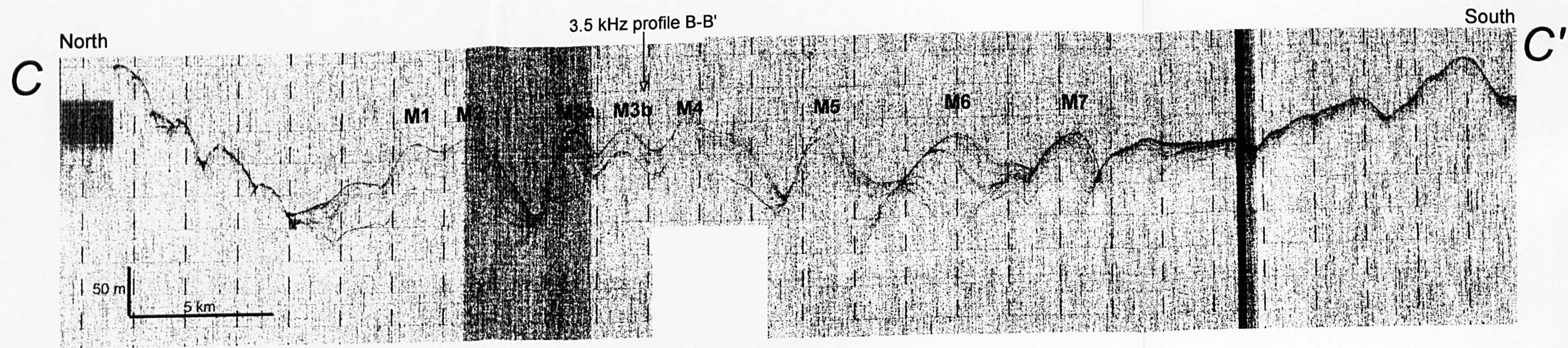


Fig. 25 (b) 3.5 kHz sub-bottom profile B-B'. Vertical exaggeration = *c.* 32:1 in water. Intersection with 3.5 kHz profile B-B' is marked.

Measurements between sediment wave peaks M1 to M7 show true wavelengths between 2.0 and 5.0 km and peak-to-trough heights between 10 and 95 m. These are similar to the dimensions of sediment waves observed in the Argentine Basin (Flood & Shor 1988).

Sub-bottom reflections show a greater accumulation of sediment on the southeastern flanks of most bedforms (e.g. M1 to M6, profile B-B', Fig. 25a), which has resulted in the net migration of bedforms to the south and east. The sediment waves show varying degrees of asymmetry from 'symmetrical' (e.g. M1 and M2, profile C-C', Fig. 25b) through 'preferential-depositional' (e.g. bedforms to the west of M1, profile B-B', Fig. 25a) to 'depositional-erosional' forms which show truncation of near-surface reflections at the sea bed (e.g. M3, profile B-B', Fig. 25a). Similar variations in wave symmetry have been reported in the Argentine Basin by Flood & Shor (1988). On both 3.5 kHz profiles, bedform migration directions remain consistently toward the south and east in all areas where migration is clearly discernible.

Profile C-C' (Fig. 25b) also shows that the sediment waves become increasingly symmetric to the north; symmetric bedforms are considered by Flood & Shor (1988) to reflect a reduction in asymmetric deposition, resulting perhaps from reduced bottom current speeds, or from alternating deposition between the opposing sediment wave flanks. There is no evidence of ponding within the sediment wave troughs or recent erosion of higher accumulation sediment wave flanks which suggests that the processes maintaining these bedforms were active recently and may remain active today.

Seismic reflection data

3.5 kHz profiles B-B' and C-C' show that the sediment wave morphology extends to the limit of 3.5 kHz penetration. Furthermore, a single-channel seismic reflection profile D-D' (located in Fig. 23, and shown in Fig. 26) crosses both 3.5 kHz profiles within the sediment wave field, and shows that the sediment waves extend to greater depths. Though of limited stratigraphic resolution, profile D-D' appears to show migrating bedforms

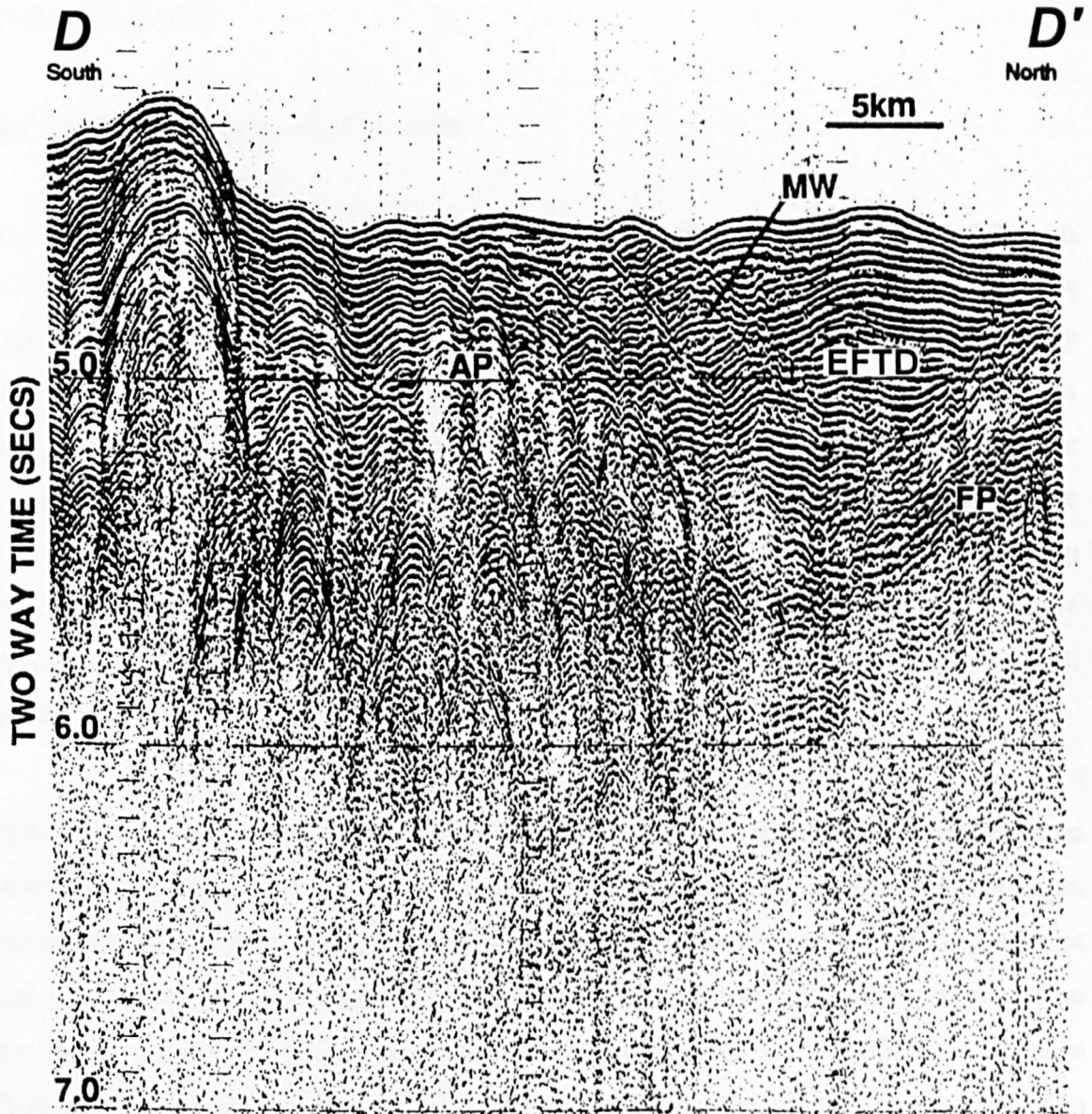


Fig. 26 Single-channel seismic reflection profile D-D' (located in Fig. 23, part of LDEO profile B of Ludwig & Rabinowitz 1982). AP, deformed surface of North Scotia Ridge accretionary prism; EFTD, undeformed drift sediments; FP, Falkland Plateau sediments; MW, migrating-wave acoustic facies.

(labelled 'MW', Fig. 26) extending to a depth of at least 400 ms two-way-time (equivalent to 360 m assuming a speed of sound in sediments of 1800 m.s⁻¹).

4.5 DISCUSSION

East Falkland Trough sediment drift

3.5 kHz sub-bottom profiles show that between 48 and 44°W, the eastern Falkland Trough is occupied by a thick, elongate mound of acoustically stratified sediment. On profiles crossing the mound, sub-bottom reflections (beyond the sediment wave field) are usually concordant with the sea floor and extend to the limit of 3.5 kHz penetration, which suggests that the mound is a site of modern deposition. This is confirmed by piston core data (core PC 036 of Jordan & Pudsey 1992) which show that the youngest mound sediments are Holocene in age, with an average diatom content of 70–80%, 10 % carbonate near the top and the base of the core, and a small terrigenous component. The composition of these sediments reflects abundant siliceous productivity in the vicinity of the Antarctic Polar Front, and a virtual absence of local terrigenous sources.

Thinning and pinch-out of near-surface strata at the edges of the mound are interpreted as an indication of intensified bottom current flow toward the northern and southern base of slope, and toward Shag Rocks passage. Similarly, divergent sub-bottom reflections suggest that external geometry of the mound results from a prolonged, lateral variation in sedimentation rate across its flanks. This is seen also at lower resolution on MCS profiles presented in chapter 3 of this report (Figs 11 and 12). On these grounds, the mound is interpreted as an elongate contourite sediment drift, resulting from prolonged pelagic-hemipelagic sedimentation in the presence of ambient bottom currents.

Migrating sediment waves

Migrating sediment waves have been associated with ambient thermohaline current flow across sediment drifts (Flood *et al.* 1993) and turbidity current flow across deep-sea channel levees (e.g. Damuth 1979; Normark *et al.* 1980; Carter *et al.* 1990). No sediment samples or current measurements have been obtained from the sediment wave site in the eastern Falkland Trough, and consequently, the origin of these bedforms remains uncertain. However, I surmise that the sediment waves were formed in the presence of westward flowing ambient bottom currents on the basis of their regional setting and likely lithology. The bedforms have formed at the surface of a sediment drift: the mounded geometry of this feature is attributed to deposition in the presence of ambient bottom currents. Furthermore, sediment cores obtained nearby support an ambient bottom-current origin for the sediment waves. In particular, piston core PC 036 (located in Fig. 23) of Jordan & Pudsey (1992) is largely biogenic in composition and shows no evidence (sedimentary structures or grading) of turbidity flows. This is also apparent in unpublished data from two additional cores obtained at the drift margins (C.J. Pudsey, personal communication). These cores may be expected to contain turbidites if the nearby sediment waves were recently maintained by thick turbidity flows such as those described by Normark *et al.* (1980). Existing studies have not yet resolved the bottom current regime in the Falkland Trough. However, there is evidence of northward flow of Weddell Sea Deep Water nearby to the east (Georgi 1981), and a westward flow of Weddell Sea Deep Water along the eastern Falkland Trough has been inferred from bottom potential temperature measurements (Locarnini *et al.* 1993).

Migrating sediment waves have been associated with persistent bottom current flow over fine-grained sediment drifts, at velocities in the range 9–30 cm.s⁻¹ (Flood 1988). Recent studies (project MUDWAVES: Flood *et al.* 1993) suggest that southern-hemisphere sediment waves which develop in ambient bottom currents will form at an angle anti-clockwise from the prevailing bottom-flow direction, and will migrate up-current and to the left of the current. The 3.5 kHz profiles B–B' and C–C' (Figs 25a,b) show sediment waves orientated in a northeast-southwest direction which have clearly migrated toward the south and east.

3.5 kHz sub-bottom profile and bathymetry survey of the eastern Falkland Trough

Although profile D–D' (Fig. 26) has limited seismic resolution, it appears to show a south component of sediment wave migration which is compatible with the 3.5 kHz profiles. If a principal sediment wave migration direction to the southeast is assumed, the results of Flood *et al.* (1993) predict a prevailing westward flow of bottom water along the axis of the Falkland Trough. Sediment thinning and non-deposition along the southern flank of the trough (the northern margin of the North Scotia Ridge) is presumed related to an intensification of this westward flow. These observations are consistent with the flow of Weddell Sea Deep Water from the Malvinas Outer Basin as suggested by Locarnini *et al.* (1993), with intensification along the boundary. The west–northwest flow reported at the northern edge of Shag Rocks passage by Zenk (1981), that becomes colder as it intensifies to 60 cm.s^{-1} , may be the same feature resulting from westward flow in the trough, rather than from northward overflow into the trough. The velocities measured at the mooring ranged higher than those usually associated with sediment wave formation ($9\text{--}30 \text{ cm.s}^{-1}$: Flood 1988), and are compatible with the non-deposition observed at the southern trough margin.

The origin of the thinning and non-deposition along the northern margin of the sediment drift is less certain. The more symmetric sediment waves apparent on Profile C–C' (Fig. 25b) suggest a northward reduction in westward velocity, leading perhaps to eastward flow at the northern drift margin. Locarnini *et al.* (1993) suggest eastward return flow of Weddell Sea Deep Water to the Malvinas Outer Basin along this margin. However, it has long been suggested that non-deposition over the Falkland Plateau results from strong bottom currents associated with the Antarctic Circumpolar Current (eg. Saito *et al.* 1974; Barker, Dalziel *et al.* 1976). Thus, non-deposition at the northern margin of the drift may be caused by returning Weddell Sea Deep Water, or by eastward-flowing Circumpolar Deep Water within the Antarctic Circumpolar Current.

Sediment waves are recognised as a long-term response to quasi-stable environmental conditions, and studies suggest that individual bedforms require tens to hundreds of thousands of years to develop (Flood & Shor 1988). The single-channel seismic profile D–D' (Fig. 26) suggests that a migrating sediment wave morphology extends through much of the

east Falkland Trough drift. Similarly, MCS profiles presented in chapter 3 of this report (Figs 11 and 13) show sediment waves buried at intermediate depth within the drift near 47°W, which also show a consistent east-component of migration. Hence, a westward flow of southern-origin bottom water may have persisted through several glacial cycles and for much of the life of the drift. The age of onset of drift deposition along the trough axis is uncertain, but some loose constraint is available. Seismic reflection profiles presented in chapter 3 of this report show the drift overlying and perhaps coeval with deformed sediments of the North Scotia Ridge accretionary prism. Barker *et al.* (1984, 1991) suggest that the northward migration of the North Scotia Ridge, that generated the accretionary prism, ceased *c.* 6 Ma ago, when sea-floor spreading stopped in the Central Scotia Sea and Drake Passage. It seems likely therefore, that the drift and the migrating stratigraphy within it, provide a depositional record of southern-origin bottom water extending back for several million years.

4.6 CONCLUSIONS

In summary, 3.5 kHz and seismic reflection profiles show sediment waves developed on a contourite sediment drift in the eastern Falkland Trough. An active sediment wave morphology preserved at the seabed suggests persistent westward flow that probably continues today; non-deposition at the southern drift margin suggests intensified flow. This is consistent with the westward flow of Weddell Sea Deep Water along the Falkland Trough from the Malvinas Outer Basin, as suggested by Locarnini *et al.* (1993), and may also explain the westward flow recorded in Shag Rocks passage by Zenk (1981). However, the fate of the west-flowing Weddell Sea Deep Water in the Falkland Trough, and the cause of scour along the northern margin of the drift, remain uncertain. The sediment waves extend several hundred metres beneath the sea floor, and provide a long-term depositional record of southern-origin bottom water, and its possible interaction with the Antarctic Circumpolar Current.

Appendices

APPENDIX A

The following pages contain copies of publications associated with the work of this thesis in the order set out below.

Peer-reviewed papers

- 1) Cunningham, A.P., Barker, P.F. & Tomlinson, J.S. 1998. Tectonics and sedimentary environment of the North Scotia Ridge region revealed by side-scan sonar. *Journal of the Geological Society of London*, **155**, 941–956.
- 2) Howe, J.A., Pudsey, C.J. & Cunningham, A.P. 1997. Contourite deposition under the Antarctic Circumpolar Current, western Falkland Trough. *Marine Geology*, **138**, 27–50.
- 3) Cunningham, A.P. & Barker, P.F. 1996. Evidence for westward-flowing Weddell Sea Deep Water in the Falkland Trough, western South Atlantic. *Deep-Sea Research*, **43**, 643–654.

Abstracts

- 4) Barker, P.F., Cunningham, A.P., Larter, R.D. 1994. Sediment records of Antarctic Circumpolar Current variability and Weddell Sea Deep Water interaction in the northern Scotia Sea and Falkland Trough. *Berichte aus dem Fachbereich Geowissenschaften, Universität Bremen*, 17.

- 5) Barker, P.F. & Cunningham, A.P. 1995. Sediment records of long-term variation in Antarctic Circumpolar Current flow, and interaction with southern-origin bottom water, in the Scotia Sea and SW Atlantic. *Abstracts, 5th International Conference on Paleoceanography, Halifax, Nova Scotia*, 152.
- 6) Cunningham, A.P., Woollett, R.W., Tomlinson, J.S. & Barker, P.F. 1992a. The structure of Aurora Bank (47°W,53°S), *Annales Geophysicae*, **10**, suppl. 1, 71.
- 7) Cunningham, A.P., Tomlinson, J.S. & Barker, P.F. 1992b. The disposition of pelagic-hemipelagic sediments in the Falkland Trough and implications for palaeo-circulation. *Eos. Transactions of the American Geophysical Union*, **73**, suppl., 286.
- 8) Cunningham, A.P. & Barker, P.F. 1995. Evidence for westward-flowing Weddell Sea Deep Water in the Falkland Trough, western South Atlantic. *Abstracts, 5th International Conference on Paleoceanography, Halifax, Nova Scotia*, 155.
- 9) Tomlinson, J.S., Cunningham, A.P. & Barker, P.F. 1992. GLORIA imagery of the North Scotia Ridge, *Annales Geophysicae*, **10**, suppl. 1, 77.

Tectonics and sedimentary environment of the North Scotia Ridge region revealed by side-scan sonar

ALEX P. CUNNINGHAM¹, PETER F. BARKER¹ & JEREMY S. TOMLINSON^{1,2}

¹British Antarctic Survey, High Cross, Madingley Road, Cambridge CB3 0ET, UK
(e-mail: a.cunningham@bas.ac.uk)

²Present address: PGS Tensor (UK) Ltd, PGS House, Mayfield Road, Walton-on-Thames KT12 5PL, UK

Abstract: The North Scotia Ridge is a series of islands and submarine ridges extending 2000 km from Tierra del Fuego to South Georgia in the western South Atlantic. The ridge forms the elevated northern tectonic margin of the Scotia Sea, and accommodates E–W sinistral strike-slip motion at the South American–Scotia plate boundary. Existing studies have shown that the northern flank of the North Scotia Ridge is a large and continuous accretionary prism, formed during presumed mid–late Cenozoic N–S convergence. In this study, we present long-range side-scan sonar (GLORIA) images and seismic reflection profiles which show the structural style of the accretionary prism for the first time. The youngest accreted sediments show a uniform fabric of initial deformation (symmetric–gently asymmetric folds of 1–4 km wavelength), which has been subsequently disrupted at shallower depths by additional shortening and uplift. Between 52°45'W and 50°30'W, the deformation front is exposed at the sea floor, and the Falkland Trough retains the appearance of an active convergent margin. Elsewhere, however, the deformation front is buried beneath younger, undeformed drift sediments indicating that convergence has ceased. GLORIA sonographs also show geological features consistent with current-control of sedimentation, non-deposition, and erosion beneath the Antarctic Circumpolar Current. In particular, this study describes current-influenced sedimentation in the Falkland Trough, and steep-sided, eroded depressions and diffuse slope-parallel fabric on the elevated Falkland Plateau.

Keywords: GLORIA, Scotia Ridge, South Atlantic, accretionary wedges.

Studies of arc accretion have shown that arc–continent collision may lead to a cessation of convergent deformation in an accretionary prism, and relocation of the zone of convergence elsewhere. The Banda arc collision zone provides an example of this process (Genrich *et al.* 1996; Snyder *et al.* 1996), where the locus of convergence between the Australian and SE Asian plates may have moved from a site south of Timor to the Wetar thrust after collision. This study describes the similar development of the North Scotia Ridge in the western South Atlantic (Fig. 1a), where mid–late Cenozoic north–south convergence of the South American and Scotia plates led to collision of an E–W limb of the Scotia arc with the partly continental Falkland Plateau. Here, GLORIA and seismic reflection profiles show clearly that convergence has ceased, and reveal the style of pre-collision deformation. The Banda arc remains in a convergent tectonic setting, but collision of the North Scotia Ridge with the Falkland Plateau has given way to east–west strike-slip motion some 50–100 km south of the original deformation front.

Tectonic setting

The North Scotia Ridge consists of a series of islands and submarine ridges extending 2000 km from Tierra del Fuego to South Georgia, in the western South Atlantic (Fig. 1a). Submerged parts of the ridge have appreciable bathymetric relief: summit regions lie above 1000 m, and slopes exceed 15° along its southern margin (BAS 1985). The North Scotia Ridge is bordered to the N by the Falkland Trough, an E–W bathymetric deep extending from the South American continental margin to the Malvinas Outer Basin, and to the S, by ocean floor exceeding 3000 m depth. The southern flank of the ridge forms the northern topographic boundary of the Scotia Sea.

The North Scotia Ridge is a component of the Scotia arc, an eastward-closing loop of submarine ridges and islands which connects the Andean Cordillera of South America to the Antarctic Peninsula, and encloses the Scotia Sea (Barker & Dalziel 1983; Barker *et al.* 1991). The ridge is principally composed of small, discrete crustal blocks, partly overlain and flanked to the N by an appreciable thickness of sediment (e.g. Ludwig *et al.* 1968; Davey 1972). The largest crustal blocks (Burdwood Bank, the Shag Rocks block and South Georgia, located in Fig. 1a, c) are continental in origin, and once formed part of a continuous continental connection between southern South America and the Antarctic Peninsula (e.g. Dalziel *et al.* 1975; Tanner 1982; Barker & Dalziel 1983, and references therein). However, the origin of smaller blocks identified between 55°W and 44°W remains uncertain.

Tectonic reconstructions (Barker & Griffiths 1972; Hill & Barker 1980; Barker *et al.* 1984, 1991) suggest that the modern North Scotia Ridge formed in connection with the eastward growth of the Scotia Sea during the Cenozoic. In these models, the dispersal of crustal blocks along the Scotia Ridge was accomplished by back-arc spreading (between 28 and 6 Ma), coupled to westward subduction at ancestors of the South Sandwich Trench. The initiation of westward subduction, and subsequent growth of the Scotia Sea, are viewed as complications of otherwise simple South American–Antarctic plate motion.

North Scotia Ridge accretionary prism

Seismic refraction studies showed considerable thicknesses of sediment beneath the northern flank of the North Scotia

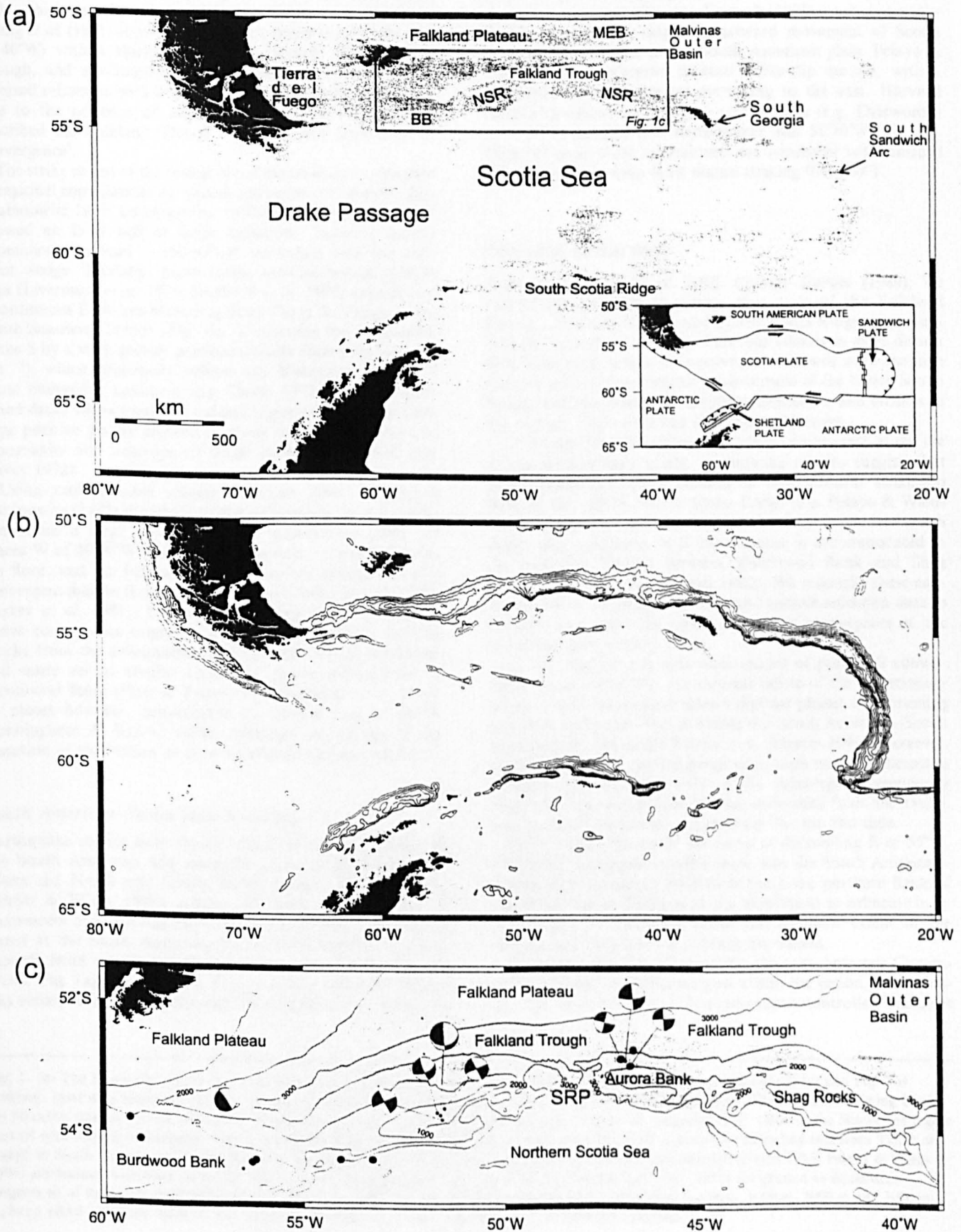


Fig. 1.

Ridge. Ludwig *et al.* (1968) identified sedimentary layers with a combined thickness exceeding 8 km beneath Burdwood Bank (compressional-wave velocity $v \leq 4.76 \text{ km s}^{-1}$), and layers with a thickness of 4 km at 49°W ($v \leq 4.0 \text{ km s}^{-1}$). Similarly, Ewing *et al.* (1971) showed sedimentary layers ($v \leq 3.0 \text{ km s}^{-1}$ at 40°W) with a thickness of 4 km beneath the Falkland Trough, and attributed high velocities ($v = 7.1 \text{ km s}^{-1}$, unreversed refraction measurement at 50°W) beneath the trough axis to the presence of oceanic crust. Ewing *et al.* (1971) described the Falkland Trough as 'a tectonic expression of convergence'.

The strike extent of the wedge of sediments became apparent in regional compilations of seismic refraction and gravity data (Rabinowitz 1977; Ludwig *et al.* 1978a, b). Rabinowitz (1977) showed an E-W belt of large amplitude, negative gravity anomalies (less than -150 mGal) coinciding with the sediment wedge. Similarly, more recent satellite-derived gravity data (Livermore *et al.* 1994; Sandwell *et al.* 1995) have shown a continuous E-W low extending from Tierra del Fuego to the South Sandwich Trench (Fig. 1b). The gravity low is bounded to the S by a steep gravity gradient (locally exceeding 10 mGal km^{-1}), which principally reflects the N-dipping surface of dense underlying basement (e.g. Davey 1972; Barker unpublished data). More southerly summit regions of the ridge show large positive gravity anomalies which coincide with elevated topography and outcrops of dense basement material (e.g. Davey 1972).

Using multi-channel seismic reflection data, Ludwig & Rabinowitz (1982) showed that the deformed sediment wedge constitutes a large and continuous accretionary prism. In places W of $50^\circ 30'\text{W}$, the deformation front is exposed at the sea floor, and the Falkland Trough has the appearance of a convergent margin (Ludwig & Rabinowitz 1982; Ludwig 1983; Barker *et al.* 1991). Ludwig & Rabinowitz (1982) inferred active convergence extending from Burdwood Bank to Shag Rocks from the deformation of Falkland Trough sediments, and more recent studies confirmed active deformation at Burdwood Bank (Platt & Philip 1995; Richards *et al.* 1996). In places however, convergence has ceased (e.g. at 46°W , Cunningham & Barker 1996), although the timing of the cessation of subduction at these localities remains uncertain.

South American–Scotia plate boundary

Earthquake studies have shown that E–W relative motion of the South American and Antarctic plates is partitioned between the North and South Scotia Ridges (Forsyth 1975; Pelayo & Wiens 1989). Along the North Scotia Ridge, a component of South American–Antarctic motion is accommodated at the South American–Scotia plate boundary, which extends from continental South America to South Georgia (inset, Fig. 1a). In Tierra del Fuego, South American–Scotia slip occurs at fault zones crossing the Magallanes foreland fold

and thrust belt (Winslow 1982; Klepeis 1994; Klepeis & Austin 1997). Farther east, the plate boundary lies beneath the North Scotia Ridge, although sparse seismicity does not permit its detailed delineation (Fig. 1c). Forsyth (1975) attributed earthquakes beneath the ridge to eastward movement of Scotia sea floor with respect to the South American plate. Pelayo & Wiens (1989) confirmed sinistral strike-slip motion, with a component of convergence increasing to the east. Harvard centroid moment tensor focal mechanisms (e.g. Dziewonski *et al.* 1995) describe four earthquakes near $51^\circ 30'\text{W}$ (Fig. 1c). Three of these focal mechanisms are consistent with sinistral strike-slip along steep fault planes striking $070\text{--}250^\circ\text{T}$.

Objectives of this study

During cruise CD37 of RRS *Charles Darwin* (1989), we conducted a GLORIA survey of a part of the Falkland Plateau, Falkland Trough and North Scotia Ridge, opportunistically on passage from the Falkland Islands to more distant GLORIA target areas. This survey has allowed us to examine the past and present tectonic environment of the North Scotia Ridge, and the pattern of sediment deposition and erosion in this region. This paper has four main objectives.

(1) To describe the extent of modern convergence at the toe of the accretionary prism: earthquake studies suggest that South American–Scotia motion is now sinistral strike-slip beneath the central North Scotia Ridge (e.g. Pelayo & Wiens 1989). However, these results are contrary to studies which imply that significant N–S convergence is accommodated in the Falkland Trough between Burdwood Bank and Shag Rocks (Ludwig & Rabinowitz 1982). We reconcile these conflicting views by using GLORIA and seismic reflection data to identify, and assess the extent of modern convergence at, the toe of the accretionary prism.

(2) To describe the structural record of past N–S convergence preserved within the tectonic fabric of the accretionary prism. Field studies have shown distinct phases of shortening and later strike-slip motion across the South American–Scotia boundary in Tierra del Fuego (e.g. Klepeis 1994). However, prior to this study, marine geophysical data were insufficient to establish the structural style of the submerged accretionary prism. We use sonographs to map individual folds and faults, and elucidate structural relationships for the first time.

(3) To constrain better the locus of decoupling E of 55°W . Although earthquake studies show that the South American–Scotia plate boundary extends beneath the northern flank of the North Scotia Ridge, data are insufficient to delineate it. In this study, we constrain better the northern extent of the neotectonic zone from its surface expression.

(4) To examine the effects of the vigorous Antarctic Circumpolar Current on sedimentation within the region. In particular, we describe young bottom-current-controlled sediment

Fig. 1. (a) The Scotia Sea region of the western South Atlantic. Sea floor above 3000 m is shaded, and the area shown in (c) and Fig. 2 is outlined. Inset map shows the tectonic setting of the Scotia Sea. NSR, North Scotia Ridge; BB, Burdwood Bank; MEB, Maurice Ewing Bank. (b) Negative free-air gravity anomalies (contour range 0 to -250 mGal , contour interval 25 mGal ; Sandwell *et al.* 1995) in the Scotia Sea region plotted with 3000 m bathymetry. The North Scotia Ridge accretionary prism is marked by the E–W gravity low extending east from Tierra del Fuego to South Georgia. (c) North Scotia Ridge region of the western South Atlantic. Earthquake epicentres (Forsyth 1975; Pelayo & Wiens 1989) are marked with black dots, and Harvard centroid moment tensor solutions (e.g. Dziewonski *et al.* 1995) are plotted as equal-area projections of the lower focal hemisphere, with solid quadrants representing compressional *P* wave first motions. 1000 m, 2000 m and 3000 m isobaths (BAS 1985) are marked, and the area of GLORIA survey is shaded. SRP, Shag Rocks passage.

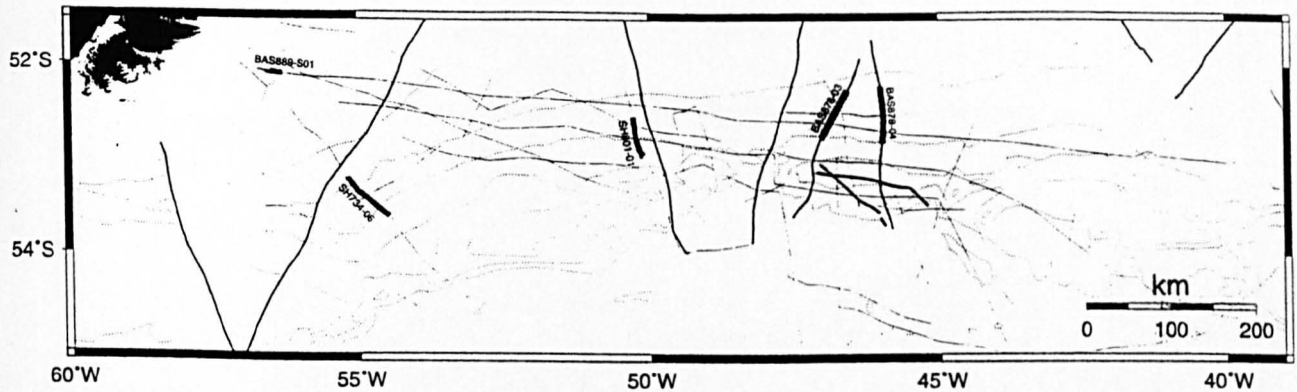


Fig. 2. Single-channel seismic and multi-channel seismic tracks (seismic data sources described in the text). Thin tracks correspond to single-channel seismic reflection profiles. Bold tracks correspond to multi-channel seismic reflection profiles, and profiles reproduced in Figs 6 and 7a–d are labelled. 1000 m, 2000 m and 3000 m isobaths are marked with dotted lines, and the area of the GLORIA survey is shaded.

drift deposits in the Falkland Trough, and surficial structures and bedforms in more elevated areas of non-deposition.

GLORIA side-scan sonar data acquisition and processing

During cruise CD37, the British Antarctic Survey conducted the first long-range side-scan sonar survey of the North Scotia Ridge (Tomlinson *et al.* 1992) using the GLORIA Mk II side-scan sonar (Somers *et al.* 1978). GLORIA data were acquired along four principal ship tracks extending ESE across the Falkland Plateau, Falkland Trough and North Scotia Ridge (Fig. 1c). The data constitute c. 11 days of continuous GLORIA survey, and cover an area exceeding 100 000 km². During CD37, the GLORIA swath width was 45 km (30 s recording), and survey speeds of 15–18 km h⁻¹ resulted in cross-line spatial sampling resolutions of c. 45 m, and in-line resolutions of c. 120 m at close range, degrading to c. 900 m at far range (Searle *et al.* 1990). Cruise CD37 also acquired gravity and magnetic data, 3.5 and 10 kHz echo soundings, and two-channel seismic reflection profiles. Seismic reflection profiles from published studies and the British Antarctic Survey archive (Fig. 2) have also been used to support our interpretations.

GLORIA side-scan sonar data processing

GLORIA data were initially corrected for ray path geometry (slant-range correction), variations in ship speed (anamorphic correction), and beam sensitivity and refraction effects (shading correction: Searle *et al.* 1990). Pixel positions were transformed onto a Lambert Conformal Conic projection, and coincident sonographs were digitally edited and combined using Mini Image Processing Software (Chavez 1986). A linear contrast stretch was applied before display.

Artefacts and inherent limitations of the GLORIA image are few, but should be noted. Along-track resolution is decreased at far range, and artefacts may appear along track, either from the poorly synchronised output pulse of a different acoustic system (air gun, 3.5 kHz) or as interference fringes from path distortion at extreme range. The ship track appears as a diffuse central zone, resulting from the zero sensitivity of the system in the vertical plane. When interpreting the image, care must be taken to consider the insonification direction, which will generally change between adjacent swaths and across the

ship track, and the insonification angle, which will vary from the centre to edge of a swath. Fabric perpendicular to track will be relatively poorly insonified.

For convenience, the GLORIA mosaic has been split at 50°W into western and eastern parts. Figure 3(a and b) shows the separate parts of the mosaic, plotted so that areas of high backscatter appear bright, and areas of low backscatter appear dark. Figure 3(a and b) also includes interpreted line drawings of features apparent in the sonographs. In general, these lineaments mark boundaries separating areas of contrasting backscatter, discontinuities in fabric, and narrow areas of very high backscatter.

Interpretation of GLORIA and seismic reflection data

GLORIA sonographs have been interpreted with reference to Birmingham University and British Antarctic Survey seismic reflection profiles (Fig. 2) obtained during RRS *Shackleton* cruises 734, 756 and 801 (1973–1981), RRS *Discovery* cruise 172 (1988), cruise CD37 (1989) and RRS *James Clark Ross* cruise JR04 (1993). We also refer to profiles acquired by the Lamont-Doherty Earth Observatory (Ludwig & Rabinowitz 1982) during RV *Robert D. Conrad* cruises 1606 (1973) and 2106 (1978). These data help to determine the internal structure and origin of sea-floor features apparent in the sonographs. Figures 3–5 show interpreted GLORIA lineaments with seismic tracks, regional bathymetry (BAS 1985) and satellite-derived gravity anomalies (Sandwell *et al.* 1995).

This study is concerned principally with tectonic fabric, but we also describe bottom current-related bedforms and sediment drift deposits, which are prominent in the sonographs. The GLORIA mosaic includes four distinct geological provinces: the Falkland Plateau, Falkland Trough, North Scotia Ridge and northern Scotia Sea (Fig. 1c).

Falkland Plateau

The GLORIA survey extends across a triangular area of the Falkland Plateau, SE of the Falkland Islands. This area lies

Fig. 3. Digital mosaic of GLORIA sonographs acquired (a) west of 50°W, (b) east of 50°W. Insets show interpreted lineaments traced from the GLORIA data. Labels locate sea-floor features described in the text, and tracks of seismic reflection profiles (Figs 6 and 7a–d) are labelled. Solid black areas on insets correspond to areas of very high backscatter in the side-scan sonographs. Dotted lines on insets are locations of GLORIA survey tracks.

Figs 3a,b of Cunningham *et al.* 1998 shown on pages 11 and 12 of this report.

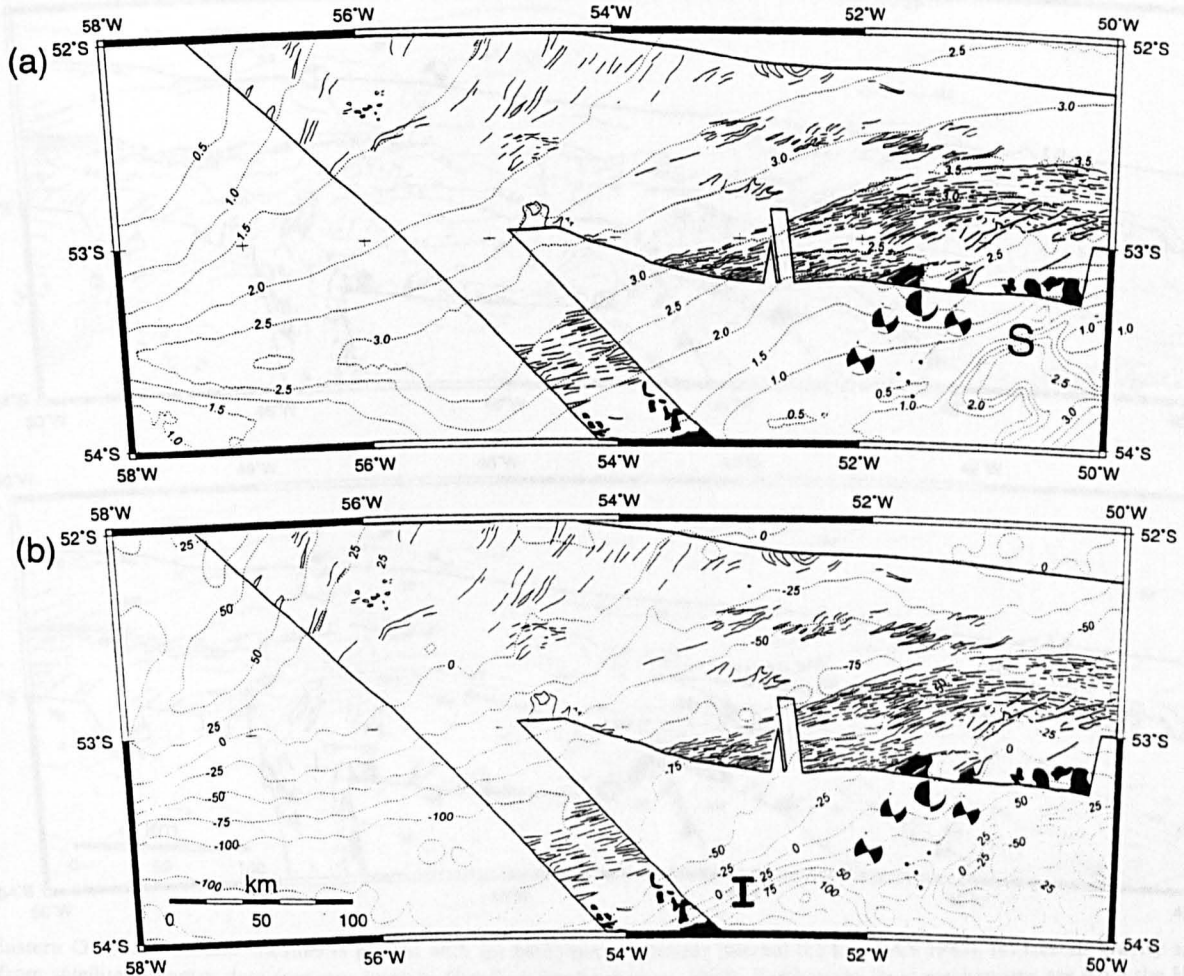


Fig. 4. Western GLORIA mosaic lineaments plotted with (a) bathymetry (contour interval 0.5 km; BAS 1985), (b) free-air gravity anomaly derived from satellite altimetry data (contour interval 25 mGal; Sandwell *et al.* 1995). Earthquake focal mechanisms are from the Harvard centroid moment tensor catalogue (e.g. Dziewonski *et al.* 1995). Solid black areas correspond to areas of very high backscatter in sonographs.

almost entirely within the western mosaic, N of the Falkland Trough (Fig. 1c). Here, Falkland Plateau sea floor is smooth, and dips southeastward with gradients of up to 0.8° (Fig. 4a). Sonographs show a strongly-textured sea floor, with broad areas of moderate backscatter, adjacent shadow and prominent lineaments. Most lineaments are sub-parallel to the bathymetric contours (Fig. 4a).

FP1 acoustic fabric. A group of bright lineaments ('FP1a', Fig. 3a) lies near the western limit of survey at 800–1400 m depth. FP1a are elongate areas of very high backscatter, broadly aligned with the bathymetric contours. The most prominent FP1a lineament can be traced over 17 km in the sonographs. Single-channel seismic reflection and 3.5 kHz profiles (Fig. 6, and profile SHA734–6, Barker unpublished data) show that this particular lineament is a steep-sided asymmetric depression, created by differential erosion at the thinning up-slope termination of a sediment sequence that is widespread over the Falkland Plateau slope. The agent of erosion is the Antarctic Circumpolar Current, although seismic reflection profile BAS889-S01 (Fig. 6) shows that the locus of the depression is probably geologically controlled.

Other geological boundaries that crop out are seen down-slope on seismic reflection profile SHA734–6, but are not

similarly eroded. The more subdued FP1a lineaments do not have this origin: on CD37 seismic reflection and 3.5 kHz profiles they appear as changes in surface roughness, but the 3.5 kHz profiles are acoustically-opaque (indicating a hard sea floor) and the seismic profiles show no systematic changes in sediment thickness. We therefore consider the other, contour-following FP1a lineations to be caused by bottom flow, with an orientation parallel to the current direction. If they are influenced by sea floor geology, it is on a scale smaller than the seismic profiles display.

Broad, diffuse areas of moderate backscatter and adjacent shadow ('FP1b', Fig. 3a) are seen in deeper water between 55°W and 53°W . Although bright areas of FP1b sea floor have poorly defined, gradational edges, they are closely aligned with bathymetric contours. They appear similar to the majority of FP1a. Taking FP1a and FP1b together, we conclude that Falkland Plateau sea floor above 2250 m depth has a slope-parallel acoustic grain, attributed to scouring by vigorous contour currents flowing within the Antarctic Circumpolar Current (Fig. 3a, and Howe *et al.* 1997).

FP2 lineaments. Prominent ENE-striking lineaments ('FP2', Fig. 3a) extend along the Falkland Plateau slope at 2500–3500 m depth, between $53^\circ30'\text{W}$ and $50^\circ30'\text{W}$. The largest FP2

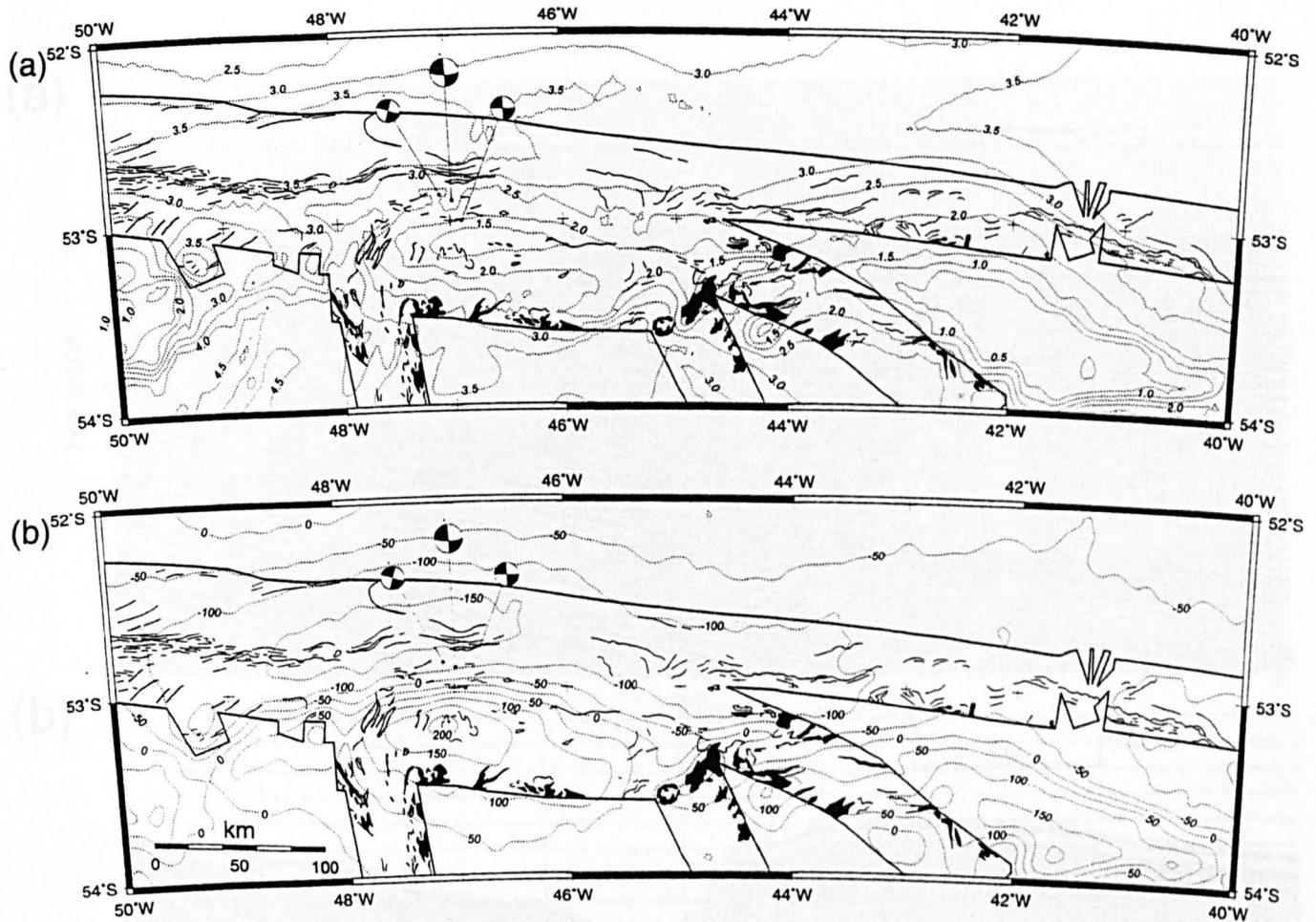


Fig. 5. Eastern GLORIA mosaic lineaments plotted with (a) bathymetry (contour interval 0.5 km: BAS 1985), (b) free-air gravity anomaly derived from satellite altimetry data (contour interval 50 mGal: Sandwell *et al.* 1995). Earthquake focal mechanisms are from the Harvard centroid moment tensor catalogue (e.g. Dziewonski *et al.* 1995). Solid black areas correspond to areas of very high backscatter in sonographs.

lineaments are broad lines of very high backscatter and adjacent shadow, extending over 25 km in the sonographs (Fig. 3a). Some FP2 lineaments show bifurcation toward the NE (e.g. 'FP2a', Fig. 3a). FP2 lineaments straddle an E-W boundary between GLORIA swaths, and appear consistently brighter on the more southerly (up-slope) sonograph (Fig. 3a). This may reflect over compensation of backscatter amplitude at far range during processing, since the farthest ranges were preserved on the southernmost swath during editing. However, these characteristics are also consistent with backscatter from steep, S-facing bathymetric scarps.

FP2 fabric is crossed obliquely by one 3.5 kHz profile, and by two Lamont-Doherty single-channel seismic reflection profiles (cruises RC1606 and IO1578). The 3.5 kHz profile (Howe *et al.* 1997, fig. 5a) shows a S-facing fault scarp (c. 75 m height). Similarly, the seismic profiles show sea-floor scarps with comparable scale and asymmetry (steeper flank to the S), but are not sufficiently well-displayed to show faulting. It is possible that faulting of the sedimentary succession has resulted from downwarping of the northern margin of the Falkland Trough, and the resulting fabric has been preserved by ambient bottom currents.

Falkland Trough

The Falkland Trough part of the GLORIA survey comprises a strip of sea floor extending NE-SW across the western mosaic, and most sea floor N of 52°45'S within the eastern mosaic (Fig. 1c). Here, the trough axis lies at 3000–4000 m depth (Figs 4a & 5a), and shows large variations in backscatter. Areas of dark, smooth sea floor are seen in the trough at the western and northern limits of survey, whereas intervening sections of the trough show bright sea floor and prominent lineaments.

Sediment drift deposition in the Falkland Trough. The western Falkland Trough, from the western limit of survey to about 53°W, shows extremely low backscatter ('FT1', Fig. 3a). At 54°30'W, FT1 contrasts with the bright, textured sea floor of the adjacent Falkland Plateau and North Scotia Ridge, and can be traced eastward across a gap in sonographs over 160 km. The low backscatter suggests a smooth, well-sedimented sea floor, since a rough surface buried beneath weakly-scattering sediment may yield significant backscatter to c. 20 m depth (at 6.5 kHz, Mitchell 1993). Between 54°W and 53°W, FT1 widens to the east and shows steadily increasing

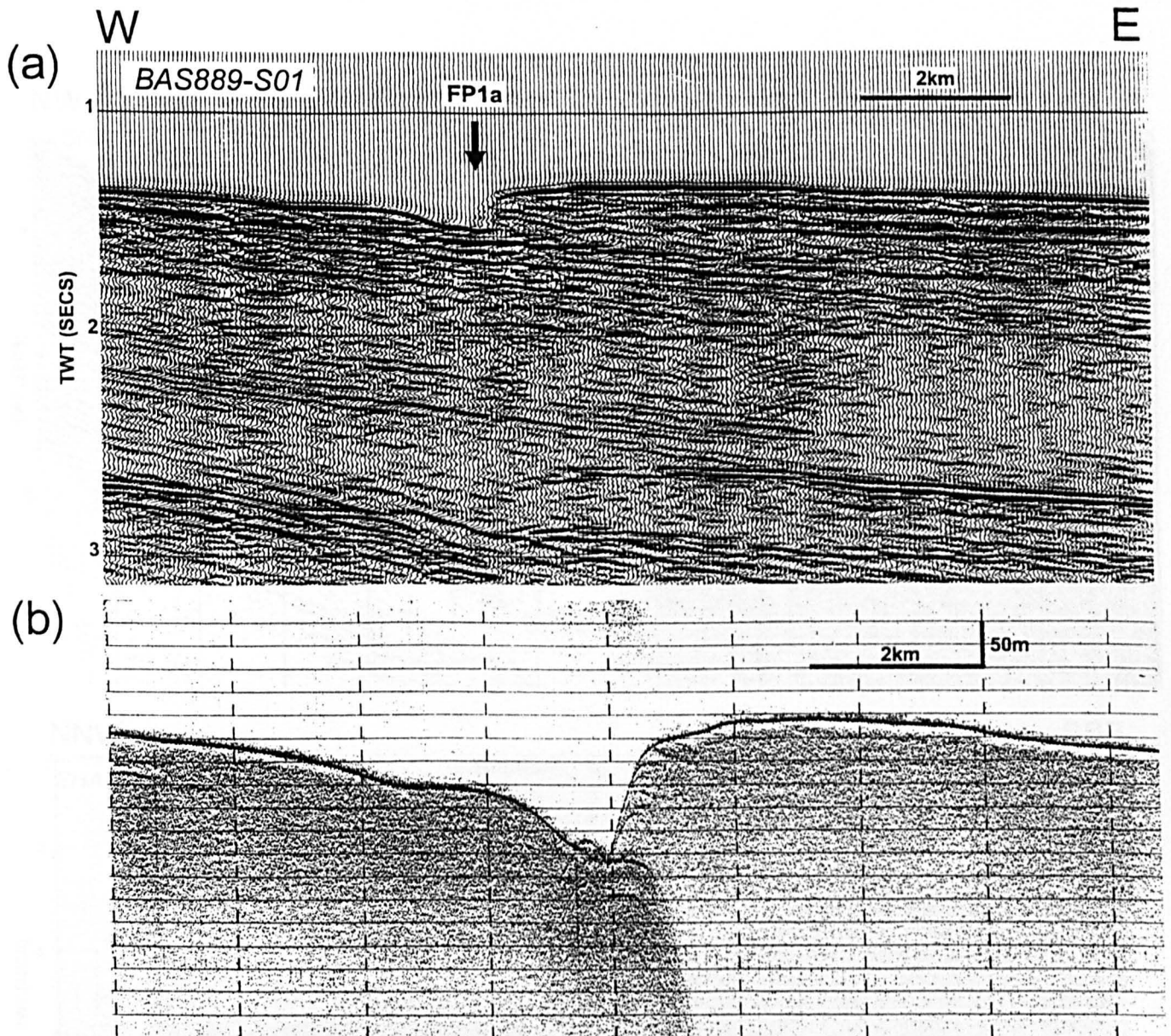


Fig. 6. (a) Single-channel seismic reflection profile BAS889-S01 (located in Fig. 3a inset, vertical exaggeration (VE)=4:1 in water) showing eroded depression on Falkland Plateau sea floor (FP1a, Fig. 3a). (b) Coincident 3.5 kHz sub-bottom profile (VE=10:1 in water).

backscatter. Coincident 3.5 kHz profiles show thinning of surficial trough sediments to the east (Howe *et al.* 1997). The thinning eastern end of FT1 lies on the northern trough slope, adjacent to a separate, flat-bottomed deep ('FT3', Fig. 3a).

Seismic reflection profile SHA734-6 (Fig. 7a) shows that FT1 corresponds to the surface of a thick, mounded sequence characterized by bright, fairly continuous reflectors. These data show also, that FT1 is confined between marginal bathymetric depressions ('D', Fig. 7a), and has the appearance of a current-controlled hemipelagic sediment drift. This is supported by 3.5 kHz profiles (Howe *et al.* 1997) which show thinning and non-deposition at the drift margins in response to intensified bottom-current flow at the base of slope. Beneath

the southern flank of the trough, FT1 sediments overlie deformed, acoustically-opaque sediments of the North Scotia Ridge accretionary prism. At greater depths, the boundary between drift and accretionary prism becomes indistinct, and some older drift sediments may have been incorporated within the accretionary prism. To the N, FT1 sediments overlie acoustically-stratified, S-dipping sediments of the Falkland Plateau (Fig. 7a).

At the northern limit of survey, the Falkland Trough is occupied by a separate pelagic-hemipelagic drift ('FT2', Fig. 3b and Cunningham & Barker 1996). FT2 appears in sonographs as a faint but discernible eastward reduction in backscatter near 47°30'W (Fig. 3b). Multi-channel seismic reflection profiles BAS878-03 and BAS878-04 (Fig. 7c, d)

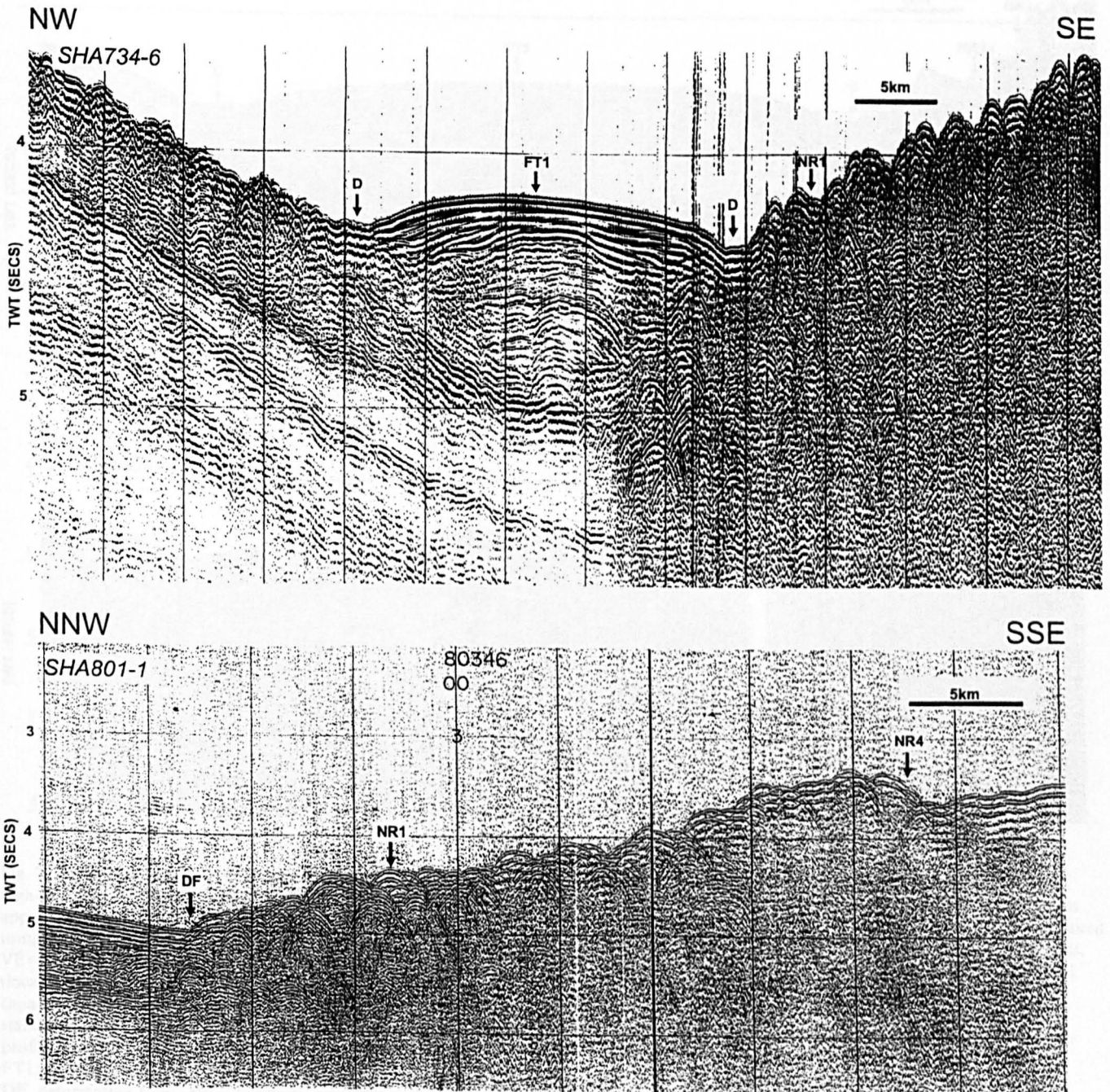


Fig. 7. (a and b)

show thick, acoustically laminated FT2 sediments confined between marginal bathymetric depressions ('D', Fig. 7c, d, and Lonardi & Ewing 1971), and coincident 3.5 kHz profiles show thinning and non-deposition at the drift margins (Cunningham & Barker 1996). On these grounds, we attribute the mounded external geometry of FT2 to bottom current-control of deposition.

Between the FT1 and FT2 drifts lies an area of the Falkland Trough with moderate to high backscatter, in which such lineaments as are seen are characteristic of the Falkland

Plateau. This area probably has only a thin and patchy cover of modern sediments. At the eastern end of FT1, the rougher sea floor of the Falkland Trough deep ('FT3', Fig. 3a) is also Falkland Plateau sediment, essentially unburied.

North Scotia Ridge

North Scotia Ridge sea floor extends E-W through central and southern parts of the survey area (Fig. 1c). Here, the ridge

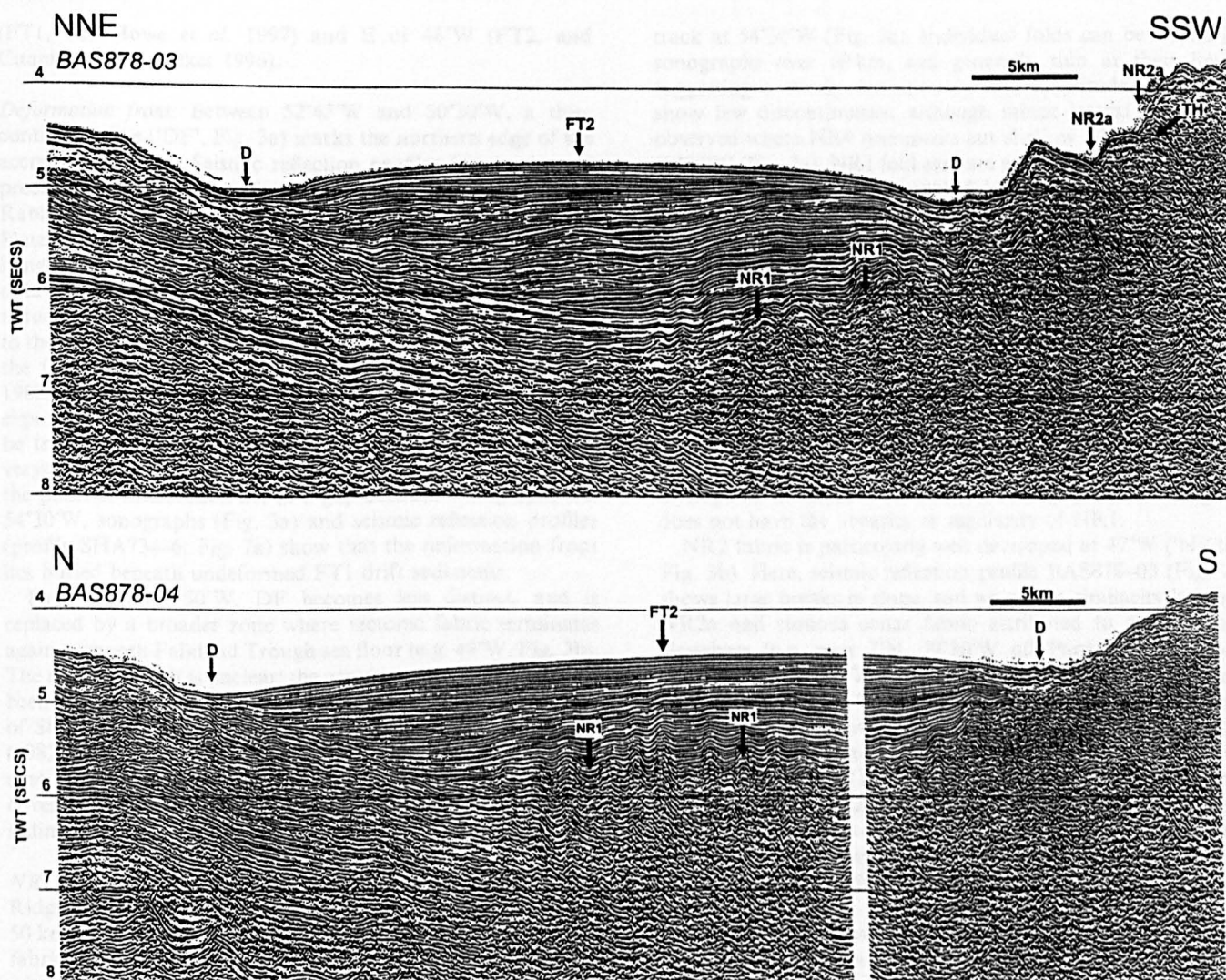


Fig. 7 (c and d)

Fig. 7. (a) Single-channel seismic reflection profile SHA734-6 (located in Fig. 3a inset, VE=18:1 at the sea floor). Broad, shallow, high-amplitude reflections which parallel the sea floor beneath FT1 are airgun source bubble reverberations; primary geological reflections appear as higher frequency arrivals which cut across these events. Profile shown is a bandpass filtered single-channel monitor record acquired using a single Bolt 1500C airgun (chamber capacity=4.8 l). (b) Single-channel seismic reflection profile SHA801-1 (located in Fig. 3a inset, VE=6:1 at the sea floor). Acquisition and processing procedures as for SHA734-6. (c) Multi-channel seismic reflection profile BAS878-03 (located in Fig. 3b inset, VE=6:1 at the sea floor). BAS878-03 was acquired using a source of 3 Bolt 1500C airguns (combined chamber capacity=15.1 l) and a 48-channel hydrophone streamer (50 m group interval), and processed to 24-fold common-mid-point stack using standard procedures. The profile shown has been imaged using a Stolt F-K time migration algorithm. (d) Multi-channel seismic reflection profile BAS878-04 (located in Fig. 3b inset, VE=6:1 at the sea floor). Acquisition and processing procedures as for BAS878-03. FT1, western Falkland Trough sediment drift; FT2, eastern Falkland Trough sediment drift; D, marginal bathymetric depressions; DF, deformation front; NR1, fabric of initial deformation; NR2a, outcrops of thrust faults; NR4, young southward-dipping fault scarp; TH, thrust fault plane reflection.

has considerable bathymetric relief, and most lineaments are parallel or slightly oblique to the bathymetric contours (Figs 4a & 5a).

North Scotia Ridge accretionary prism. Sonographs show linear-curvilinear fabric, attributed to backscatter from folds, faults and breaks in slope at the surface of the North Scotia Ridge accretionary prism. Fold fabric and fault traces are particularly well preserved across the northernmost 50 km of the accretionary prism. In contrast, sonographs crossing

more southerly, elevated terrains show irregular areas of high backscatter, low backscatter and shadow. These regions are characterized by rough sea-floor topography, and areas with outcrops of dense basement material.

Between 52°45'W and 50°30'W, the deformation front of the North Scotia Ridge accretionary prism is exposed at the sea floor, and the Falkland Trough axis retains the appearance of a convergent margin (Ludwig & Rabinowitz 1982; Ludwig 1983; Barker *et al.* 1991). Elsewhere, however, the deformation front is buried beneath undeformed drift sediments W of 53°W

(FT1, and Howe *et al.* 1997) and E of 48°W (FT2, and Cunningham & Barker 1996).

Deformation front. Between 52°45'W and 50°30'W, a thin, continuous line ('DF', Fig. 3a) marks the northern edge of the accretionary prism. Seismic reflection profiles (single-channel profile SHA801-1, Fig. 7b and profile 143 of Ludwig & Rabinowitz 1982) show that DF separates smooth Falkland Plateau sea floor from rougher North Scotia Ridge sea floor lying to the south (marked with diffractions in Fig. 7b). These data show also, that DF is accompanied by a southward reduction in the continuity of near-surface reflectors, attributed to the deformation and uplift of Falkland Plateau sediments at the foot of the North Scotia Ridge (Ludwig & Rabinowitz 1982; Ludwig 1983; Barker *et al.* 1991). Hence, DF marks the exposed deformation front of the accretionary prism, which can be traced in sonographs over 250 km. Near 54°W, DF converges to the west with sediment drift FT1 (Fig. 3a), although the point of intersection lies in a gap between sonographs. At 54°30'W, sonographs (Fig. 3a) and seismic reflection profiles (profile SHA734-6, Fig. 7a) show that the deformation front lies buried beneath undeformed FT1 drift sediments.

East of about 50°W, DF becomes less distinct, and is replaced by a broader zone where tectonic fabric terminates against smooth Falkland Trough sea floor (e.g. 49°W, Fig. 3b). The reason for this is unclear: the accretionary prism may have been eroded by strong bottom currents flowing in the vicinity of Shag Rocks passage, as inferred by Ludwig & Rabinowitz (1982) from their nearby seismic reflection profile 142. However, it is also possible that DF may lie buried beneath a thin cover of recent sediment extending westward from the FT2 sediment drift.

NR1 acoustic fabric. Sonographs of the western North Scotia Ridge show a striped acoustic fabric ('NR1', Fig. 3a) within 50 km of the deformation front (below 2000 m depth). NR1 fabric is characterised by very bright, sub-parallel lineaments which are closely aligned with the bathymetric contours (Fig. 4a). NR1 lineaments can be traced across a gap in sonographs from 48°30'W to the western limit of survey.

Migrated seismic reflection profiles crossing exposed NR1 fabric were not available for this study. However, time-migrated data obtained farther east help to describe this fabric. Profiles BAS878-03 and BAS878-04 (Fig. 7c, d) obtained between 47°W and 46°W show a wavy reflection configuration within the lower layers of the FT2 drift ('NR1', Fig. 7c, d), which we attribute to drape across well-formed, open, symmetric-gently asymmetric folds developed at the surface of the accretionary prism. Farther W, these folds are unburied, and are represented in sonographs by NR1 (Fig. 3a, b). The striped fabric results from large, regular variations in acoustic grazing angle across successive folds; bright lineaments correspond to fold limbs facing the insonification direction, and opposing fold limbs occupy intervening areas of low backscatter. The lack of dependence of brightness on insonification direction suggests that the folds are symmetric-gently asymmetric. Hence, NR1 represents a broad area of regular folds extending S from the deformation front, and in this respect, resembles the most recently accreted sections of the Makran accretionary prism (e.g. White & Ross 1979) and the Barbados Ridge accretionary prism (Biju-Duval *et al.* 1982; Stride *et al.* 1982; Brown & Westbrook 1987).

NR1 fold wavelengths are between 1 and 4 km, and appear consistently larger (c. 3.5 km) on the westernmost GLORIA

track at 54°30'W (Fig. 3a). Individual folds can be traced in sonographs over 20 km, and generally thin at their limit, suggesting a steady reduction in fold amplitude. The folds show few discontinuities, although minor lateral offsets are observed where NR4 lineaments cut shallow NR1 fabric near 50°30'W (Fig. 3a). NR1 fold axes are generally aligned with the bathymetric contours, although folds appear slightly oblique to bathymetric strike near 54°30'W (Fig. 4a). There is little variation in fold trend with distance from the deformation front, across any given section of the accretionary prism.

NR2 acoustic fabric. Near 48°W, NR1 fabric is replaced to the E by a thin band of sinuous acoustic fabric ('NR2', Fig. 3b) extending along the North Scotia Ridge to the Shag Rocks block at 2000–3500 m depth. NR2 is characterized by sinuous, curvilinear bands of moderate and low backscatter, parallel or slightly oblique to the bathymetric contours (Fig. 3b). This fabric is attributed to backscatter from folds, faults and breaks in slope at the surface of the accretionary prism, although it does not have the linearity or regularity of NR1.

NR2 fabric is particularly well developed at 47°W ('NR2a', Fig. 3b). Here, seismic reflection profile BAS878-03 (Fig. 7c) shows large breaks in slope, and we note a similarity between NR2a and sinuous sonar fabric attributed to slope breaks elsewhere (e.g. near 7°N, 79°30'W off Panama, Westbrook *et al.* 1995, plate 2). The breaks in slope mark the surface trace of S-dipping thrust faults, with faint thrust plane reflections apparent in the near surface ('TH', Fig. 7c). Hence, NR2a represents backscatter from the exposed surface of thrust fault-bound slices of accreted sediment, resulting from secondary (post-NR1) uplift and shortening within the accretionary prism. Thrust fault-controlled breaks in slope have been associated with compressional loading of the foreland N of Burdwood Bank (Platt & Philip 1995), and are a common feature of accreting forearc terrains (e.g. in the W Gulf of Oman, White & Ross 1979; Middle America Trench, Moore & Shipley 1988; Nankai Trough, Moore *et al.* 1990).

On profile BAS878-03 (Fig. 7c), NR2a structures mark the southern limit of NR1 folds. From this, we infer that the regularity of NR1 generated at the frontal fold has been disrupted at shallower depths by secondary deformation and uplift. Also, BAS878-03 and BAS878-04 (Fig. 7c, d) show that NR1 sea floor is entirely buried beneath FT2 drift sediments between 47°W and 46°W. Therefore, the transition from NR1 to NR2 fabric observed in sonographs at 48°W reflects the burial of NR1 folds E of 48°W, and does not necessarily indicate a change in structural style.

Similar but smaller lineaments ('NR2b', Fig. 3b) extend at 2250–3000 m depth along the northern slope of the Shag Rocks block. Here, Ludwig & Rabinowitz (1982) described incipient thrusting and uplift of near-surface sediments. On these grounds, we suggest that NR2c may represent backscatter from convergent deformation at the surface of the accretionary prism.

East of 42°W, the tectonic environment is different: to the north lies thick ponded sediment overlying ocean floor of the Malvinas Outer Basin, rather than the narrow Falkland Trough and (probably continental) eastern Falkland Plateau. Here, sonographs show a prominent fabric ('NR2c', Fig. 3b) along the NE flank of the Shag Rocks block, attributed to backscatter from slopes steepened by shortening and uplift of the accretionary prism. NR2c fabric is separated from adjacent dark sedimented ocean floor by a lobate boundary which runs close to the base of slope. The lobate character of NR2c

appears similar to that observed in sonographs of active deformation fronts (e.g. Masson & Scanlon 1991; Maldonado *et al.* 1994; Westbrook *et al.* 1995).

NR3 acoustic fabric. Above 2250 m depth, the North Scotia Ridge shows chaotic fabric ('NR3', Fig. 3a, b), with irregular areas of high backscatter, low backscatter and shadow. Near 44°30'W, bright NR3 fabric coincides with broad, steep-sided summit ridges (Fig. 5a). Narrow, very bright NR3 lineaments near 42°30'W may represent backscatter from fault scarps along the southern flank of the Shag Rocks block ('NR3a', Fig. 3b). The brightness of NR3 owes something to the virtual absence of sedimentation over the crest of the North Scotia Ridge under the influence of a vigorous Antarctic Circumpolar Current.

NR4 lineaments. Near 50°30'W, a set of faint lineaments ('NR4', Fig. 3a) extends across the North Scotia Ridge at 2000–3000 m depth. NR4 lineaments appear as thin, faint but continuous lines, with 060–240°T trending curvilinear trajectories which cut NR1 folds. This subdued fabric crosses shallowest NR1 sea floor and adjacent NR3 sea floor near 50°30'W. Individual NR4 structures can be traced in sonographs over 35 km. Near 52°50'S, NR4 structures have an échelon pattern and terminate *c.* 20 km S of the deformation front (Fig. 3a).

Seismic reflection profile SHA801–1 crosses NR4 structures near 52°30'S (Fig. 3a) where they define a horst, with a S-facing scarp at its southern end ('NR4', Fig. 7b). On these grounds, we interpret NR4 lineaments as fault traces which cut North Scotia Ridge tectonic fabric. The faults are broadly aligned with ENE–WSW trends in gravity and bathymetry; in particular, the nearby southern flank of the North Scotia Ridge ('S', Fig. 4a), and the steep gravity gradient ('T', Fig. 4b), that in places corresponds to the northern flank of North Scotia Ridge basement (e.g. Barker unpublished data).

The linearity and continuity of NR4 suggest that the faults are young, relative to the development of the accretionary prism, and possibly active. Nearby earthquakes showing sinistral strike-slip along near-vertical fault planes (oriented at 070–250°T, Fig. 4) suggest that this section of the ridge is being actively dissected by South American–Scotia motion. NR4 faults are closely aligned with the fault planes (Fig. 4), although an absence of GLORIA data in the vicinity of the earthquakes means that their relationship with NR4 remains uncertain. The NR4 faults and earthquakes could reflect separate components of slip, occurring near the northern and southern boundaries of basement.

Alternatively, NR4 could reflect merely a stage in the continued uplift and deformation of sediments within the accretionary prism, following NR1. The faults lie 40 km N of the few published earthquakes which describe South American–Scotia slip, and they die out steadily northeastward, which is more a feature of normal faulting than of strike-slip. They might be oblique to NR1 here because of the curve in the overall trend of the accretionary prism, but more commonly aligned with NR1, and therefore almost impossible to detect.

South American–Scotia plate boundary. West of 50°W, earthquakes show South American–Scotia slip south of the survey area (Fig. 1c). Across Aurora Bank however, earthquakes lie within the survey area (Fig. 5, and Pelayo & Wiens 1989), allowing any sea-bed fabric associated with South American–Scotia motion to be examined. Here, an E–W zone of short

(up to 10 km), curvilinear, low-amplitude lineaments extends across the epicentres. It can be traced only with difficulty, possibly from 48°W to 45°W along the same line. The northern (down-slope) edge of the zone is indistinct, lying close to a swath boundary, and possibly merging with NR2 fabric. Up-slope to the S the seabed appears smooth. In summary, seabed fabric in the epicentral region is minor, not warranting specific identification in Fig. 3b.

Northern Scotia Sea

The GLORIA data include two swaths within the eastern mosaic that extend S onto Scotia Sea ocean floor (S of 53°30'S and W of 44°W, Fig. 3b). Bathymetric relief within this area is subdued, and ocean floor ages range between 28 and 18 Ma in the vicinity of the westernmost swath (BAS 1985).

Sonographs show bright, chaotic fabric, lying adjacent to broad areas of smooth, almost featureless sea floor ('NSS', Fig. 3b). Unpublished CD37 profile data show that bright NSS fabric coincides with slightly elevated ocean floor, where basement has negligible sediment cover. Intervening, featureless areas have a variable thickness of weakly-scattering sediment.

Discussion

North Scotia Ridge accretionary prism: convergent deformation, and neotectonics of the South American–Scotia plate boundary

Earthquake studies suggest that between 65°W and 31°W, the Scotia Sea is floored by a single, independent Scotia plate, and that the South American–Scotia plate boundary accommodates slow, sinistral, mainly E–W strike-slip motion (Forsyth 1975; Pelayo & Wiens 1989). Sparse seismicity prevents detailed delineation of the South American–Scotia plate boundary beneath the North Scotia Ridge, although we surmise that it lies close to the margins of the crustal fragments which support the accretionary prism, several tens of km S of the deformation front. A tectonic summary map (Fig. 8) shows a possible line of the plate boundary, plotted with the North Scotia Ridge deformation front, 3000 m bathymetry, and small circles of South American–Scotia motion.

Relict North Scotia Ridge deformation front. Seismic profiles have been used to argue that N–S convergence persists, with continued deformation at the toe of the accretionary prism. In particular, Ludwig & Rabinowitz (1982) inferred active convergence extending from Burdwood Bank to Shag Rocks from the deformation of the youngest preserved Falkland Trough sediments. More recent studies (Platt & Philip 1995; Richards *et al.* 1996) confirmed active thrusting of Falkland Trough sediments at Burdwood Bank.

In this study, sonographs and profile data show that the North Scotia Ridge deformation front is buried beneath undeformed drift sediments W of 53°W ('FT1', Fig. 3a) and E of 48°W ('FT2', Fig. 3b). Here, seismic profiles (Fig. 7a, c, d) and 3.5 kHz high-resolution data (Cunningham & Barker 1996; Howe *et al.* 1997) show an exceptionally smooth sea floor, and there are no surficial structures or detachments which might indicate active deformation at the toe of the accretionary prism. This is supported by sonographs which show no evidence of tectonic fabric within the youngest drift

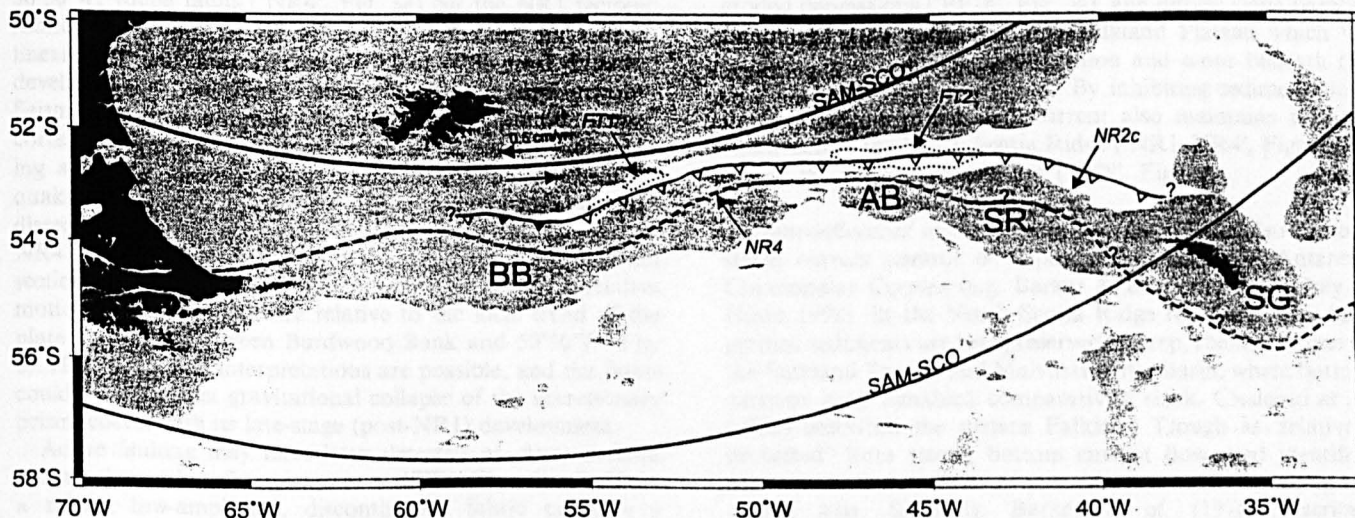


Fig. 8. Tectonic summary of the North Scotia Ridge region. Sea floor above 3000 m is shaded. BB, Burdwood Bank; AB, Aurora Bank; SR, Shag Rocks Block; SG, South Georgia. The position of the North Scotia Ridge deformation front (inferred from sonographs and seismic reflection profiles) is marked with a solid line, with barbs on the overriding plate. Inactive sections of the deformation front are marked with open barbs, and solid barbs delineate active thrusting of Falkland Trough sediments at Burdwood Bank. A possible path of the South American–Scotia plate boundary (inferred from gravity and earthquake data, and adjusted with reference to sonographs) is marked with a bold dashed line. Small circles of South American–Scotia relative motion (pole at 18.7°S, 58.9°W; Pelayo & Wiens 1989) with co-latitudes of 34° and 39° relative to the rotation pole are labelled SAM–SCO. Fine dotted lines (labelled FT1, FT2) enclose areas of known drift deposition in the Falkland Trough. NR4 and NR2c locate tectonic fabric described in the text.

sediments (e.g. 'FT1', Fig. 3a). Hence, we infer that N–S convergence has ceased in the Falkland Trough at 54°30'W, and between 47°W and 46°W.

The timing of the cessation of convergence within the central Falkland Trough remains uncertain, although some loose constraint is available. Barker *et al.* (1984, 1991) suggested that the northward migration of the North Scotia Ridge ceased about 6 Ma ago, when sea-floor spreading stopped in the central Scotia Sea and Drake Passage. Between 47°W and 46°W, seismic reflection profiles (Fig. 7c, d) show that oldest FT2 sediments may have been incorporated within the accretionary prism, whilst younger undeformed sequences onlap or passively drape its surface.

Between 52°45'W and 50°30'W, bottom currents inhibit sedimentation, and young drift sediments are thin or absent within the Falkland Trough (e.g. Howe *et al.* 1997, fig. 3). As a consequence, the deformation front is exposed ('DF' Figs 3a and 7b), and the Falkland Trough axis retains a V-shaped bathymetric profile, sometimes interpreted as an indication of active convergence (Ludwig & Rabinowitz 1982). However, the presence of undeformed drift sediments nearby to the E and W ('FT1', 'FT2', Fig. 3) suggests that the exposed deformation front may be relict, and possibly several million years old. Seismic reflection profile SHA801–1 (Fig. 7b) acquired near 50°30'W shows that the youngest deformed sediments extend S from the Falkland Plateau. Although the age of these sediments is uncertain, piston and gravity cores acquired on this part of the Falkland Plateau have Eocene–Miocene core top ages (Saito *et al.* 1974), showing that Falkland Plateau sea floor has been non-depositional during much of the late Cenozoic. Thus, we suggest that deformation of youngest Falkland Plateau sediments is not necessarily indicative of recent convergence, and that the deformation front is probably inactive at 50°30'W. On the basis of available data, we suggest that an inactive deformation front may extend

eastward from about 54°30'W to the northern margin of South Georgia (marked with open barbs, Fig. 8).

These findings conflict with the conclusions of Ludwig & Rabinowitz (1982) who inferred active convergence within the survey area from the 'buckling, folding and uplift of Falkland Trough sediments', and argued that young Falkland Trough sediments are 'quickly incorporated into the collision complex' where the trough retains a V-shaped bathymetric profile.

Transpression at Burdwood Bank. Multi-channel seismic reflection profiles (Ludwig & Rabinowitz 1982; Platt & Philip 1995; Richards *et al.* 1996) show active thrusting of Falkland Trough sediments at the foot of Burdwood Bank. Because Burdwood Bank lies beyond the western limit of GLORIA survey, we cannot properly account for this apparent change in the stress regime at the toe of the accretionary prism. However, we speculate that this region may accommodate a northerly component of South American–Scotia slip (marked with solid barbs, Fig. 8), possibly associated with a change in the trend of the plate boundary inferred near 55°W (eastward from 058–238°T to 103–283°T, Fig. 8).

Convergent deformation style. Sonographs show E–W variation in convergent deformation style. West of 48°W, regular NR1 fabric records the northward advance of the frontal fold, whereas farther E, NR1 is replaced by sinuous, less continuous NR2 fabric (Fig. 3b). Near 47°W, this reflects the eastward burial of NR1 beneath the FT2 sediment drift, where NR2 represents a subsequent stage of deformation. East of 42°W, lobate NR2c fabric resembles that of a modern deformation front, although Fig. 8 shows that it lies midway between the inferred positions of the North Scotia Ridge deformation front and the South American–Scotia plate boundary. Additional profile data are required to determine if NR2c represents relict tectonic fabric, or fabric related to modern plate motion.

Young faults within the North Scotia Ridge accretionary prism.

Sonographs provide little evidence of recent tectonic activity at the surface of the accretionary prism. However, near 50°30'W, young faults ('NR4', Fig. 3a) cut the NR1 tectonic fabric. The faults have well-defined, fairly continuous curvilinear traces, suggesting that they are young relative to the development of the accretionary prism, and possibly active. Seismic reflection profiles show that a prominent NR4 trace corresponds to a normal fault scarp ('NR4', Fig. 7b), suggesting an extensional component of slip. Also, nearby earthquakes show that this part of the ridge is being actively dissected by South American–Scotia motion (Fig. 4a). Hence, NR4 faults may accommodate slip across a transtensional section of the North Scotia Ridge, where the vector of relative motion is rotated clockwise relative to the local trend of the plate boundary (between Burdwood Bank and 50°30'W, Fig. 8). However, other interpretations are possible, and the faults could merely reflect gravitational collapse of the accretionary prism, coeval with its late-stage (post-NR1) development.

Active faulting may have been detected on Aurora Bank around the earthquake epicentres at 47°W (Figs. 3b, 5). Here, a minor, low-amplitude, discontinuous fabric occupies a median zone of the accretionary prism, where sediments are several km thick (unpublished British Antarctic Survey data). It is difficult to reconcile this subdued fabric with continued E–W strike-slip motion at this locality over 6 Ma or so (at 0.5 cm a⁻¹, Pelayo & Wiens 1989), producing a total offset of c. 30 km. Possibly, sediment sliding down slope has buried older surface fabric, or the locus of strike-slip may have migrated to this region only recently. Alternatively, South American–Scotia motion could be distributed diffusely across this section of the ridge. In Fig. 8, the South American–Scotia plate boundary has been drawn through the earthquake epicentres on Aurora Bank and the NR4 fault zone (north of earthquakes, Fig. 4a).

Controls on sedimentation

Oceanographic data show that the North Scotia Ridge lies in the path of Circumpolar Deep Water within the Antarctic Circumpolar Current, which flows eastward through Drake Passage, and then northward across the North Scotia Ridge, Falkland Trough and Falkland Plateau (e.g. Nowlin & Klinck 1986; Peterson & Whitworth 1989; Peterson 1992; Orsi *et al.* 1995). The elevated topography of the North Scotia Ridge forms a barrier to Circumpolar Deep Water flow: shallower water flows across the western North Scotia Ridge as the Falkland Current (Peterson 1992), whereas deeper water remains confined within the northern Scotia Sea until Shag Rocks passage (located in Fig. 1c). Estimates of Antarctic Circumpolar Current flow through Drake Passage average 134 Sv (e.g. Grose *et al.* 1995).

Non-deposition beneath the Antarctic Circumpolar Current.

Although the Antarctic Circumpolar Current is principally wind-driven, studies demonstrate the influence of Antarctic Circumpolar Current bottom flow on sedimentation in the North Scotia Ridge region. Piston and gravity cores show pre-Quaternary sediments exposed across the Falkland Plateau (Saito *et al.* 1974; Ciesielski *et al.* 1982; Howe *et al.* 1997), where vigorous bottom currents inhibit sedimentation. Similarly, DSDP cores show that the Falkland Plateau sea floor has been subject to prolonged non-deposition or erosion since the

inception of the Antarctic Circumpolar Current in the early Miocene (Barker *et al.* 1976).

In this study, sonographs and profile data show steep-sided, eroded depressions ('FP1a', Fig. 3a), and diffuse slope-parallel fabric ('FP1b', Fig. 3a) on the Falkland Plateau which we attribute to persistent non-deposition and scour beneath the Antarctic Circumpolar Current. By inhibiting sedimentation, the Antarctic Circumpolar Current also maintains tectonic fabric across the North Scotia Ridge ('NR1–NR4', Figs 3a, b) and in the northern Scotia Sea ('NSS', Fig. 3b).

Current-influenced sedimentation. Existing studies also demonstrate current control of deposition beneath the Antarctic Circumpolar Current (e.g. Barker & Burrell 1977; Pudsey & Howe 1998). In the North Scotia Ridge region, young, fine-grained sediments are best preserved in deep, sheltered areas of the Falkland Trough and Malvinas Outer Basin, where bottom currents have remained comparatively slack. Ciesielski *et al.* (1982) described the eastern Falkland Trough as 'relatively protected' from strong bottom current flow, and identified thickest accumulations of post-Miocene sediment along the trough axis. Similarly, Barker *et al.* (1976) described Oligocene–Pleistocene diatomaceous oozes with a thickness exceeding 1.5 km at the mouth of the Falkland Trough.

Sonographs and profile data crossing the Falkland Trough show young, partly biogenic drift sediments, which have been deposited in the presence of sluggish southern-origin bottom water, or deepest Antarctic Circumpolar Current flow ('FT1' and 'FT2', Fig. 8).

Western sediment drift (FT1). The western Falkland Trough is occupied by a well-developed sediment drift ('FT1', Figs 3a, 7a). Sediment cores obtained at the drift surface contain a 0.1–0.4 m layer of foraminiferal sand, underlain by fine-grained diatomaceous hemipelagites. These incorporate a significant (up to 55%) terrigenous component, of reworked sediment transported down-slope from Burdwood Bank, the Falkland Islands and southern South America, with a small proportion of ice-rafted material (Howe *et al.* 1997). The average sedimentation rate is 3–4 cm ka⁻¹.

Although FT1 drift sediments incorporate a significant terrigenous component, the external geometry of the drift suggests that ambient bottom currents, rather than down-slope flows, have maintained a controlling influence on its formation. At 54°30'W, its bounding bathymetric depressions result from sediment thinning and non-deposition toward the drift margins. Farther east, drift sediments lie not within the deepest part of the trough, but along the Falkland Plateau slope. Profiles crossing the adjacent trough deep show no equivalent accumulations of coarse material as may have been expected if gravity flow maintained a controlling influence on drift formation. In the Falkland Trough, ponded sediments (and mass wasting) occur at 56°W (profile 144 of Ludwig & Rabinowitz 1982; Howe *et al.* 1997, fig. 4c), mounded drift sediments occur at 54°30'W ('FT1', Fig. 7a), and thin plastered drift sediments are seen at 53°30'W ('FT1', Fig. 3a). We attribute this lateral change in depositional style to an eastward increase in bottom current activity, acting on a relatively small volume of terrigenous sediment transported down-slope.

It follows that FT1 drift sediments are confined W of 53°W because bottom currents there have remained sufficiently sluggish to permit prolonged hemipelagic sedimentation. At 54°30'W, the drift flanks are symmetrically disposed within the trough axis, and sediment thinning suggests intensified bottom

current flow toward the base of slope (Howe *et al.* 1997). These characteristics may be explained by sedimentation within a cyclonic loop of Circumpolar Deep Water, with westward flow at the southern margin of the drift, and eastward flow at its northern margin; similar flow has been inferred at shallower depths by Piola & Gordon (1989). Alternatively, FT1 sediments may have been deposited within a loop of Weddell Sea Deep Water, extending even farther westward along the Falkland Trough from the Malvinas Outer Basin than for FT2 (Cunningham & Barker 1996, and below). However, this is considered less likely, since thick drift sediments do not extend continuously across Shag Rocks passage, and Weddell Sea Deep Water appears confined within the eastern Falkland Trough by the Antarctic Circumpolar Current (Locarnini *et al.* 1993).

Howe *et al.* (1997) inferred a reduction in bottom current flow across the FT1 drift, and an increase in terrigenous sedimentation during the Last Glacial Maximum. A reduction in Circumpolar Deep Water flow may have accompanied the fall in sea level at the Last Glacial Maximum, since the ocean section accommodating northward Antarctic Circumpolar Current flow above the western North Scotia Ridge would have been significantly reduced, and parts of Burdwood Bank would have been subaerial. However, existing studies suggest also that Weddell Sea Deep Water activity was reduced, and that Antarctic Circumpolar Current activity increased at glacial maximum (Pudsey 1992; Pudsey & Howe 1998); as a consequence, westward flow of Weddell Sea Deep Water in the Falkland Trough may have been suppressed further by a more vigorous Antarctic Circumpolar Current during the Last Glacial Maximum. Hence, we infer that ambient bottom currents have maintained a controlling influence on drift sedimentation in the western Falkland Trough through the glacial cycle, and that bottom current strength across the drift flanks was reduced during the Last Glacial Maximum. However, the origin of the water mass which controls sedimentation in the western Falkland Trough remains uncertain.

Eastern sediment drift (FT2). The eastern Falkland Trough is occupied by a well-developed sediment drift ('FT2', Figs 3b, 7c, d). Piston core PC 036 of Jordan & Pudsey (1992) shows that youngest FT2 drift sediments are predominantly biogenic, with an average diatom content of 70–80%, 10% carbonate near the top and base of the core, and a small (partly ice-rafted) terrigenous component. This contrasts with the substantial terrigenous component of drift sediments in the western Falkland Trough (e.g. GC062 of Howe *et al.* 1997), and reflects increased biogenic productivity in the vicinity of the Antarctic Polar Front, and the virtual absence of local terrigenous sources. FT2 sediments have a likely sedimentation rate of 5 cm ka⁻¹ (Shimmield *et al.* 1993).

In a recent study, Cunningham & Barker (1996) related mudwaves at the drift surface, and non-deposition at its southern margin, to westward flow of Weddell Sea Deep Water along the Falkland Trough. Non-deposition at the northern margin of the drift was attributed to returning Weddell Sea Deep Water, or eastward-flowing Circumpolar Deep Water. Hence, FT2 drift sediments have been deposited in the presence of comparatively sluggish southern-origin bottom water (presently Weddell Sea Deep Water). An absence of carbonate in the central part of core PC 036 suggests that the Polar Front lay farther N in this region during the Last Glacial Maximum.

Conclusions

New side-scan sonographs and profile data provide insights into the tectonic development of the North Scotia Ridge, and the neotectonics of the South American–Scotia plate boundary. In particular, we assess the extent of modern convergence at the toe of the accretionary prism, and describe relict deformation fabric resulting from past N–S convergence. Also, we describe erosional sea floor fabric, and young sediment drift deposits which are prominent in the sonographs, and discuss controls on sedimentation. More specific findings are listed below.

(1) North–south convergence has ceased along much of the central Falkland Trough. Here, the deformation front is buried beneath undeformed drift sediments west of 53°W and east of 48°W. In the intervening region, where drift sedimentation is thin or absent, the toe of the accretionary prism is preserved at the sea floor, and the trough axis retains the appearance of a convergent margin (e.g. Ludwig & Rabinowitz 1982; Barker *et al.* 1991). However, the exposed deformation front is considered inactive, since the youngest deformed Falkland Plateau sediments may be several million years old, and earthquakes suggest a more southerly locus of slip. These findings conflict with conclusions of previous studies (Ludwig & Rabinowitz 1982) that suggested continuing N–S convergence within the survey area, but do not necessarily conflict with a notion of continued transpression at Burdwood Bank to the west.

(2) Sonographs and seismic reflection profiles show that the North Scotia Ridge accretionary prism has a well-ordered elongate primary deformational fabric created by past N–S convergence of the Scotia Sea and Falkland Plateau. A linear–curvilinear fabric ('NR1', elongate folds of wavelength 1–4 km, up to 20 km in length) extends up to 50 km S of the deformation front (exposed between 52°45'W and 50°30'W), and is also seen buried beneath younger drift sediments. East of 48°W this fabric is replaced by a more sinuous, curvilinear sea-floor fabric, less regular or linear ('NR2'). In this region, NR1 is buried, and it is possible that NR2 developed farther from the frontal fold, overprinting NR1. Along the northern flank of Shag Rocks block (E of 42°W), a prominent lobate fabric ('NR2c', Fig. 3b) lies midway between the inferred line of the deformation front and the South American–Scotia plate boundary. The lobate character of NR2c appears similar to that observed in sonographs of active deformation fronts (e.g. Masson & Scanlon 1991). However, additional profile data are required to determine if NR2c represents relict tectonic fabric, or fabric related to modern plate motion.

(3) East of 52°W, sparse earthquake data suggest that South American–Scotia strike-slip occurs beneath southerly elevated parts of the North Scotia Ridge, close to the fragmented crustal blocks which support the accretionary prism. Near 50°30'W, we identify a set of relatively young faults ('NR4', Fig. 3a) which extend across deformation fabric. The origin of these faults is uncertain; they may result from gravitational collapse of the accretionary prism cœval with its late-stage (post-NR1) development. However, we consider it likely that the faults are active, and accommodate slip across a transtensional part of the South American–Scotia plate boundary. Farther E, on the northern slope of Aurora Bank (47°W) where the locus of strike-slip is defined by earthquake epicentres, its sea-floor expression in the GLORIA image is less prominent than expected, and cannot be followed far.

(4) Sonographs show large, steep-sided depressions ('FP1a', Fig. 3a), and diffuse, slope-parallel acoustic fabric ('FP1b', Fig. 3a) on the Falkland Plateau which reflect persistent non-deposition and scour by bottom currents flowing within the Antarctic Circumpolar Current. Also, these data show well-formed sediment drift deposits in the Falkland Trough east of 48°W and W of 53°W. Here, thick sequences of pelagic and hemipelagic sediment have accumulated in the presence of comparatively sluggish bottom currents associated with southern-origin bottom water, or deepest Antarctic Circumpolar Current flow. The composition of these sediments reflects increased biogenic productivity in the vicinity of the Antarctic Polar Front, and the limited contributions of more westerly sources of terrigenous sediment.

We thank the officers, crew and scientists who participated in RRS *Charles Darwin*, RRS *Shackleton*, RRS *Discovery* and RRS *James Clark Ross* cruises for assistance in obtaining the original data. Research Vessel Services and GLORIA personnel at the Southampton Oceanography Centre provided technical support, and NERC Computer Services at ITE Monks Wood provided image processing facilities. R. Larter and M. Curtis provided comments on the manuscript, and R. Livermore assisted with data preparation. We also thank D. Snyder, D. Masson and two anonymous referees for their constructive reviews. Most figures were produced using the GMT software of Wessel & Smith (1991).

References

- BARKER, P.F. & BURRELL, J. 1977. The opening of Drake Passage. *Marine Geology*, 25, 15–34.
- & DALZIEL, I.W.D. 1983. Progress in geodynamics in the Scotia Arc region. In: CABRE, R. (ed.) *Geodynamics of the eastern Pacific region. Caribbean and Scotia Arcs*. American Geophysical Union, Geodynamics Series, 9, 137–170.
- & GRIFFITHS, D.H. 1972. The evolution of the Scotia Ridge and Scotia Sea. *Philosophical Transactions of the Royal Society of London*, A271, 151–183.
- , BARBER, P.L. & KING, E.C. 1984. An early Miocene ridge crest–trench collision on the South Scotia Ridge near 36°W. *Tectonophysics*, 102, 315–332.
- , DALZIEL, I.W.D. & SHIPBOARD SCIENTIFIC PARTY 1976. Evolution of the southwestern Atlantic Ocean basin: results of Leg 36. Deep Sea Drilling Project. In: BARKER, P.F., DALZIEL, I.W.D. et al. (eds) *Initial reports of the Deep Sea Drilling Project*. US Government Printing Office, Washington, 36, 993–1014.
- , — & STOREY, B.C. 1991. Tectonic development of the Scotia arc region. In: TINGEY, R.J. (ed.) *The geology of Antarctica*. Oxford University Press, New York, Monographs on Geology and Geophysics, 17, 215–248.
- BAS 1985. *Tectonic map of the Scotia Arc*. 1:3 000 000, BAS(Misc) 3. British Antarctic Survey, Cambridge.
- BIJU-DUVAL, B., LE QUELLEC, P., MASCLE, A., RENARD, V. & VALERY, P. 1982. Multibeam bathymetric survey and high resolution seismic investigations on the Barbados Ridge Complex (eastern Caribbean): a key to the knowledge and interpretation of an accretionary wedge. *Tectonophysics*, 86, 275–304.
- BROWN, K.M. & WESTBROOK, G.K. 1987. The tectonic fabric of the Barbados Ridge accretionary complex. *Marine and Petroleum Geology*, 4, 71–81.
- CHAVEZ, P.S. 1986. Processing techniques for digital sonar images from GLORIA. *Photogrammetric Engineering and Remote Sensing*, 52, 1133–1145.
- CIESIELSKI, P.F., LEDBETTER, M.T. & ELLWOOD, B.B. 1982. The development of Antarctic glaciation and the Neogene palaeoenvironment of the Maurice Ewing Bank. *Marine Geology*, 46, 1–51.
- CUNNINGHAM, A.P. & BARKER, P.F. 1996. Evidence for westward-flowing Weddell Sea Deep Water in the Falkland Trough, western South Atlantic. *Deep-Sea Research*, 43, 643–654.
- DALZIEL, I.W.D., DOTT, R.H., WINN, R.D. & BRUHN, R.L. 1975. Tectonic relationships of South Georgia Island to the southernmost Andes. *Geological Society of America Bulletin*, 86, 1034–1040.
- DAVEY, F.J. 1972. Gravity measurements over Burdwood Bank. *Marine Geophysical Researches*, 1, 428–435.
- DZIEWONSKI, A.M., EKSTRÖM, G. & SALGANIK, M.P. 1995. Centroid-moment tensor solutions for July–September 1995. *Physics of the Earth and Planetary Interiors*, 97, 3–13.
- EWING, J.I., LUDWIG, W.J., EWING, M. & EITREIM, S.L. 1971. Structure of Scotia Sea and Falkland Plateau. *Journal of Geophysical Research*, 76, 7118–7137.
- FORSYTH, D.W. 1975. Fault plane solutions and tectonics of the South Atlantic and Scotia Sea. *Journal of Geophysical Research*, 80, 1429–1443.
- GENRICH, J.F., BOCK, Y., MCCAFFREY, R., CALAIS, E., STEVENS, C.W. & SUBARYA, C. 1996. Accretion of the southern Banda arc to the Australian plate margin determined by Global Positioning System measurements. *Tectonics*, 15, 288–295.
- GROSE, T.J., JOHNSON, J.A. & BIGG, G.R. 1995. A comparison between the FRAM (Fine Resolution Antarctic Model) results and observations in the Drake Passage. *Deep-Sea Research*, 42, 365–388.
- HILL, I.A. & BARKER, P.F. 1980. Evidence for Miocene back-arc spreading in the Central Scotia Sea. *Geophysical Journal of the Royal Astronomical Society*, 63, 427–440.
- JORDAN, R.W. & PUDSEY, C.J. 1992. High-resolution diatom stratigraphy of Quaternary sediments from the Scotia Sea. *Marine Micropaleontology*, 19, 201–237.
- HOWE, J.A., PUDSEY, C.J. & CUNNINGHAM, A.P. 1997. Pliocene–Holocene contourite deposition under the Antarctic Circumpolar Current, Western Falkland Trough, South Atlantic Ocean. *Marine Geology*, 138, 27–50.
- KLEPEIS, K.A. 1994. The Magallanes and Deseado fault zones: Major segments of the South American–Scotia transform plate boundary in southernmost South America, Tierra del Fuego. *Journal of Geophysical Research*, 99, 22 001–22 014.
- & AUSTIN, J.A. 1997. Contrasting styles of superimposed deformation in the southernmost Andes. *Tectonics*, 16, 755–776.
- LIVERMORE, R.A., MCAODOO, D. & MARKS, K.M. 1994. Scotia Sea tectonics from high-resolution satellite gravity. *Earth and Planetary Science Letters*, 123, 255–268.
- LOCARNINI, R.A., WHITWORTH, T. III & NOWLIN, W.D. 1993. The importance of the Scotia Sea on the outflow of Weddell Sea Deep Water. *Journal of Marine Research*, 51, 135–153.
- LONARDI, A. G. & EWING, M. 1971. Sediment transport and distribution in the Argentine Basin. 4. Bathymetry of the continental margin, Argentine Basin and other related provinces. Canyons and sources of sediments. In: AHRENS, L.H., RUNCORN, S.K. & UREY, H.C. (eds) *Physics and chemistry of the Earth*. Pergamon Press, Oxford, 8, 18–121.
- LUDWIG, W.J. 1983. Geologic framework of the Falkland Plateau. In: LUDWIG, W.J. & KRASHENNIKOV, V.A. et al. (eds) *Initial Reports of the Deep Sea Drilling Project*. US Government Printing Office, Washington, 71, 281–293.
- & RABINOWITZ, P.D. 1982. The collision complex of the North Scotia Ridge. *Journal of Geophysical Research*, 87, 3731–3740.
- , CARPENTER, G., HOUTZ, R.E., LONARDI, A.G. & RIOS, F.F. 1978a. *Sediment isopach map: Argentine continental margin and adjacent areas*. American Association of Petroleum Geologists, Argentine Map Series.
- , EWING, J.I. & EWING, M. 1968. Structure of Argentine continental margin. *American Association of Petroleum Geologists Bulletin*, 52, 2337–2368.
- , WINDISCH, C.C., HOUTZ, R.E. & EWING, J.I. 1978b. Structure of Falkland plateau and offshore Tierra del Fuego, Argentina. In: WATKINS, J.S. et al. (eds) *Geological and Geophysical Investigations of Continental Margins*. American Association of Petroleum Geologists, Memoirs, 29, 125–137.
- MALDONADO, A., LARTER, R.D. & ALDAYA, F. 1994. Forearc tectonic evolution of the South Shetland Margin, Antarctic Peninsula. *Tectonics*, 13, 1345–1370.
- MASSON, D.G. & SCANLON, K.M. 1991. The neotectonic setting of Puerto Rico. *Geological Society of America Bulletin*, 103, 144–154.
- MITCHELL, N.C. 1993. A model for attenuation of backscatter due to sediment accumulations and its application to determine sediment thicknesses with GLORIA sidescan sonar. *Journal of Geophysical Research*, 98, 22 477–22 493.
- MOORE, G.F. & SHIPLEY, T.H. 1988. Mechanics of sediment accretion in the Middle America Trench. *Journal of Geophysical Research*, 93, 8911–8927.
- , —, STOFFA, P.L., KARIG, D.E., TAIRA, A., KURAMOTO, S., TOKUYAMA, H. & SUYEHRO, K. 1990. Structure of the Nankai Trough accretionary zone from multichannel seismic reflection data. *Journal of Geophysical Research*, 95, 8753–8765.
- NOWLIN, W.D. & KLINCK, J.M. 1986. The physics of the Antarctic Circumpolar Current. *Reviews of Geophysics*, 24, 469–491.
- ORSI, A. H., WHITWORTH, T. III & NOWLIN, W. D. 1995. On the meridional extent and fronts of the Antarctic Circumpolar Current. *Deep-Sea Research*, 42, 641–673.

- PELAYO, A.M. & WIENS, D.A. 1989. Seismotectonics and relative plate motions in the Scotia Sea region. *Journal of Geophysical Research*, **94**, 7293–7320.
- PETERSON, R.G. 1992. The boundary currents in the western Argentine Basin. *Deep-Sea Research*, **39**, 623–644.
- & WHITWORTH, T. III. 1989. The Subantarctic and Polar Fronts in relation to deep water masses through the southwestern Atlantic. *Journal of Geophysical Research*, **94**, 10 817–10 838.
- PIOLA, A.R. & GORDON, A.L. 1989. Intermediate waters in the southwest South Atlantic. *Deep-Sea Research*, **36**, 1–16.
- PLATT, N.H. & PHILIP, P.R. 1995. Structure of the southern Falkland Islands continental shelf: initial results from new seismic data. *Marine and Petroleum Geology*, **12**, 759–771.
- PUDSEY, C.J. 1992. Late Quaternary changes in Antarctic Bottom Water velocity inferred from sediment grain size in the northern Weddell Sea. *Marine Geology*, **107**, 9–33.
- & HOWE, J.A. 1998. Quaternary history of the Antarctic Circumpolar Current: evidence from the Scotia Sea. *Marine Geology*, **148**, 83–112.
- RABINOWITZ, P.D. 1977. *Free-air gravity anomalies bordering the continental margin of Argentina*. American Association of Petroleum Geologists, Argentine Map Series.
- RICHARDS, P.C., GATCLIFF, R.W., QUINN, M.F., WILLIAMSON, J.P. & FANNIN, N.G.T. 1996. The geological evolution of the Falkland Islands continental shelf. In: STOREY, B.C., KING, E.C. & LIVERMORE, R.A. (eds) *Weddell Sea Tectonics and Gondwana Break-up*. Geological Society, London, Special Publications, **108**, 105–128.
- SAITO, T., BURCKLE, L.H. & HAYS, J.D. 1974. Implications of some pre-Quaternary sediment cores and dredgings. In: HAY, W.W. (ed.) *Studies in paleo-oceanography*. Society of Economic Paleontologists and Mineralogists, Tulsa, Special Publications, **20**, 6–35.
- SANDWELL, D.T., YALE, M.M. & SMITH, W.H.F. 1995. Gravity anomaly profiles from ERS-1, Topex, and Geosat Altimetry. *Eos, Transactions, American Geophysical Union*, **76**, S89.
- SEARLE, R.C., LEBAS, T.P., MITCHELL, N.C., SOMERS, M.L., PARSON, L.M. & PATRIAT, P.H. 1990. GLORIA Image Processing: The State of the Art. *Marine Geophysical Researches*, **12**, 21–39.
- SHIMMIELD, G., DERRICK, S., PUDSEY, C., BARKER, P., MACKENSEN, A., GROBE, H. 1993. The use of inorganic chemistry in studying palaeoceanography of the Weddell Sea. In: HEYWOOD, R.B. (ed.) *University Research in Antarctica, 1989–1992. Proceedings of the British Antarctic Survey Antarctic Special Award Scheme Round 2*. British Antarctic Survey, Cambridge, 99–108.
- SNYDER, D.B., PRASETYO, H., BLUNDELL, D.J., PIGRAM, C.J., BARBER, A.J., RICHARDSON, A. & TIKOSAPROETRO, S. 1996. A dual doubly vergent orogen in the Banda Arc continent-arc collision zone as observed on deep seismic reflection profiles. *Tectonics*, **15**, 34–53.
- SOMERS, M.L., CARSON, R.M., REVIE, J.A., EDGE, R.H., BARROW, B.J. & ANDREWS, A.G. 1978. GLORIA II – an improved long-range side-scan sonar. In: *Oceanology International, Proceedings, Offshore Instrumentation and Communications*. Institute of Electrical Engineers, New York, 16–24.
- STRIDE, A.H., BELDERSON, R.H. & KENYON, N.H. 1982. Structural grain, mud volcanoes and other features on the Barbados Ridge complex revealed by GLORIA long-range side-scan sonar. *Marine Geology*, **49**, 187–196.
- TANNER, P.W.G. 1982. Geology of Shag Rocks, part of a continental block on the north Scotia Ridge, and possible regional correlations. *British Antarctic Survey Bulletin*, **51**, 125–136.
- TOMLINSON, J.S., CUNNINGHAM, A.P. & BARKER, P.F. 1992. GLORIA imagery of the North Scotia Ridge (Abs.). *Annales Geophysicae*, **10**, suppl. 1, C77.
- WESSEL, P. & SMITH, W.H.F. 1991. Free software helps map and display data. *Eos, Transactions, American Geophysical Union*, **72**, 441–445.
- WESTBROOK, G.K., HARDY, N.C. & HEATH, R.P. 1995. Structure and tectonics of the Panama–Nazca plate boundary. In: MANN, P. (ed.) *Geologic and Tectonic Development of the Caribbean Plate Boundary in Southern Central America*. Geological Society of America, Special Papers, **295**, 91–109.
- WHITE, R.S. & ROSS, D.A. 1979. Tectonics of the Western Gulf of Oman. *Journal of Geophysical Research*, **84**, 3479–3489.
- WINSLOW, M. A. 1982. The structural evolution of the Magallanes Basin and neotectonics in the southernmost Andes. In: CRADDOCK, C. (ed.) *Antarctic Geoscience*. University of Wisconsin Press, Madison, 143–154.

Received 6 November 1997; revised typescript accepted 7 April 1998.

Scientific editing by David Snyder.

Pliocene–Holocene contourite deposition under the Antarctic Circumpolar Current, Western Falkland Trough, South Atlantic Ocean

John A. Howe *, Carol J. Pudsey, Alex P. Cunningham

British Antarctic Survey, High Cross, Madingley Rd. Cambridge, CB3 0ET, UK

Received 14 June 1996; accepted 19 December 1996

Abstract

The eastward-flowing Antarctic Circumpolar Current (ACC) has influenced sedimentation on the slope and floor of the western Falkland Trough, where the axis of the current is topographically constrained. Deep-water flow (below 3000 m) has produced a symmetrical sediment drift on the trough floor, with non-depositional margins indicating higher current velocities at the base of slope. To the southeast of the Falkland Islands there is a gap in the North Scotia Ridge, north of which the floor of the trough is swept clean of sediment by the ACC. Both echo character mapping and GLORIA side-scan data indicate that currents follow the bathymetric contours along the slope, redistributing sediment and locally eroding furrows. From six cores on the drift and on the northern slope, two styles of contourite deposition have been identified. On the drift, Holocene biogenic sandy contourites overlie Last Glacial Maximum muddy contourites and fine-grained diatomaceous hemipelagites. Sedimentation rates here average 3–4 cm ka⁻¹. The sandy contourites present in four of the cores from the sediment drift are sharply underlain by the finer-grained, diatomaceous hemipelagites. The lack of a coarsening upward sequence, commonly associated with an increase in current velocity may be indicative of high current activity eroding away the finer (negative) sequence. Pliocene and Mid-Pleistocene glaucony-rich sandy contourites containing radiolaria characterise the Falkland Plateau and the floor of the trough near the gap in the North Scotia Ridge. We suggest that the glaucony is derived from a combination of authigenic formation and erosion of locally outcropping Cretaceous and Tertiary strata; this is supported by dinoflagellate analysis. Sedimentation rates in these current-swept areas average <1 cm ka⁻¹. © 1997 Elsevier Science B.V.

Keywords: Glacial; Interglacial; Antarctic Circumpolar Current; Glaucony; Contourites

1. Introduction

Contourites have long been recognised as the product of a major style of sedimentation on the world ocean floors, resulting from deposition by

along-slope bottom-currents [see Hollister (1993) for review]. Contourite sequences provide a sedimentary record of local changes in ambient bottom water flow, and therefore a source of proxy indicators for climatic variation. In a recent synthesis, Faugères and Stow (1993) suggested that the main problems facing modern contourite research included the expansion of the facies model, to

* Corresponding author. Fax: +1223.362616,
e-mail: jaho@pcmail.nerc-bas.ac.uk

include more recently described contourite types, the recognition of along-slope seismic characteristics and the relationship between bottom-current activity and climate change. In a mid-high-latitude marginal setting, these problems are compounded with a constant “background” of glaciomarine processes and sedimentation. Modern contourite research is also concerned with the recognition of diagnostic features that can be used to identify both modern and ancient examples (Stow, 1994). Characteristics such as cross bedding, upward fining and erosive contacts are not uniquely the product of down-slope turbidity currents, having been attributed in some instances to bottom-current reworking of pre-existing turbidites (Stanley, 1993).

In this study, we describe mid-high-latitude contourites sampled along the Falkland Trough, an east–west elongated bathymetric deep that separates the Falkland Plateau from the North Scotia Ridge in the western South Atlantic (Fig. 1). Sedimentation in this region takes place in the presence of vigorous bottom currents associated with the eastward and northward flow of the Antarctic Circumpolar Current (ACC) emerging from Drake Passage. Although the ACC is principally a wind-driven current (i.e., forced at the surface, with flow extending to the seabed), oceanographic measurements provide ample evidence for appreciable ACC bottom flow about bathymetric highs and along bathymetric contours in this area. We have cored silty–sandy contourites deposited along the flanks of the western Falkland Trough which lie in the path of these contour currents, and this study aims to document the sedimentary record of ACC variability contained within these sediments. We describe the provenance, evolution and present-day disposition of these sediments, and discuss implications for the facies model.

Previous work in this area has been limited to a single Eltanin gravity core on the Falkland Plateau and some seabed photographs from the area (Goodell, 1964). This study is part of the British Antarctic Survey’s ‘HILATS’ project, which entails the understanding of ACC flow during the last 30–40 Ma. Other studies from the literature on the role of bottom current activity and sediment distribution have concentrated on

the Weddell and Scotia Seas, examining the variation in Antarctic Bottom Water. In these studies it was deduced that bottom current activity was weaker during the Last Glacial Maximum (Pudsey et al., 1988; Pudsey, 1992; Shimmield et al., 1994).

2. Regional setting

The Falkland Trough consists of an east–west bathymetric deep extending 1300 km from the South American continental margin to the Malvinas Outer Basin in the western South Atlantic (Fig. 1). The axis of the Falkland Trough is between 3000 and 4000 m below sea level from 56° to 41°W, and is bordered by the Falkland Plateau to the north and the North Scotia Ridge to the south. The Falkland Plateau is an area of gentle slope, up to 0.5° steepening slightly at its western limit. The North Scotia Ridge is an area of considerable bathymetric relief: shallow components of the ridge lie at depths of <1000 m below sea level, and appreciable bathymetric gradients of ~5° are observed along much of its southern margin, decreasing to 1.5° on the northern flank. The North Scotia Ridge and Falkland Trough lie in the path of Circumpolar Deep Water (CDW), the >2000-m-deep mass within the ACC, which flows eastward through Drake Passage, and thereafter east through the northern Scotia Sea and northeast across the North Scotia Ridge and Falkland Trough (Grose et al., 1995). The topographic relief of the North Scotia Ridge strongly influences the flow of CDW across the western Falkland Trough.

Shallower components of the ACC flow directly across the North Scotia Ridge and Falkland Trough, with increased flow along the Antarctic Polar Front. Oceanographic data show that ACC flows directly across the western Falkland Trough as the Falkland (Malvinas) Current, and then continues northward along the South American continental slope into the western Argentine Basin (Peterson and Whitworth, 1989; Piola and Gordon, 1989; Peterson, 1992). Direct velocity measurements using surface drifters in the Falkland Current confirm this and demonstrate appreciable flow parallel to bathymetric strike (Peterson and Johnson, 1994). Deeper components

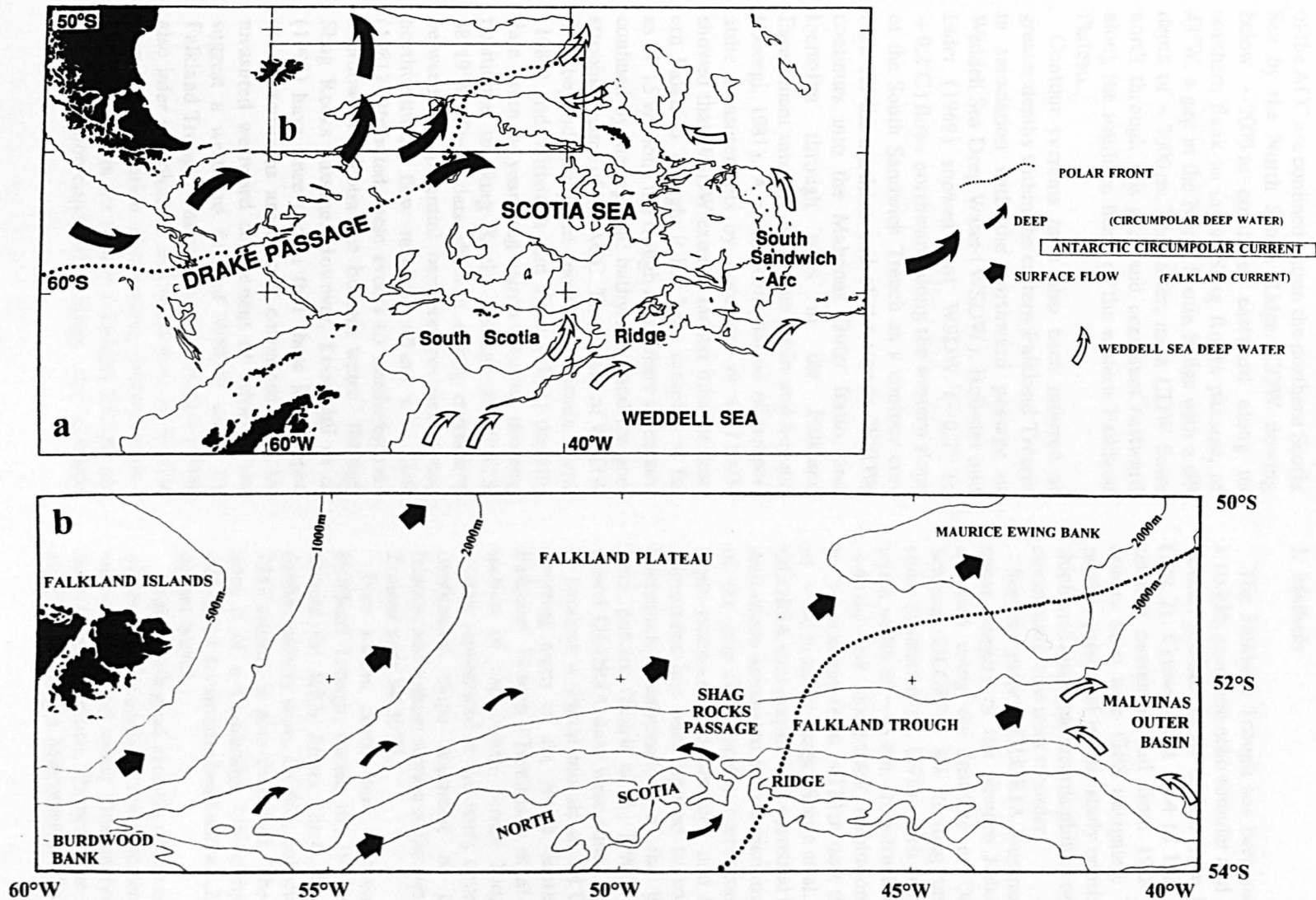


Fig. 1. Main map (a) shows the 3000-m isobath and bottom-current flow directions of the southwestern Atlantic from Gordon (1966), Hollister and Elder (1969), Georgi (1981), Nowlin and Zenk (1988), and Locarnini et al. (1993). Inset (b) shows the location of the Falkland Trough. The two main water masses that influence the area are the Antarctic Circumpolar Current (ACC) and, to a lesser extent, Weddell Sea Deep Water (WSDW). Two components of ACC circulate within the trough; Intermediate-Surface water flows across the Falkland Plateau to the northeast, as the Falkland Current, and at deeper levels (>2000 m), deep water enters the Falkland Trough via Shag Rocks passage, through the North Scotia Ridge termed Circumpolar Deep Water (CDW). Bathymetric contours in metres. Polar Front = Antarctic Polar Front. (Adapted from Cunningham and Barker, 1996.)

of the ACC are confined within the northern Scotia Sea by the North Scotia Ridge: CDW flowing below ~2000 m continues eastward along its southern flank as far as Shag Rocks passage, at 48°W, a gap in the North Scotia Ridge with a sill depth of ~3000 m. Thereafter, most CDW flows north through this gap, and continues eastward along the southern flank of the eastern Falkland Plateau.

Contour currents have also been inferred at greater depths within the eastern Falkland Trough in association with the northward passage of Weddell Sea Deep Water (WSDW). Hollister and Elder (1969) showed that WSDW (-0.7° to $+0.2^{\circ}\text{C}$) flows northward along the western slope of the South Sandwich Trench as a contour current. At the northern end of the trench, WSDW continues into the Malvinas Outer Basin, and thereafter through gaps in the Falkland Escarpment into the Argentine Basin and beyond (Georgi, 1981). A recent compilation of temperature measurements by Locarnini et al. (1993) showed that WSDW extends farther into the eastern Falkland Trough; it has been sampled as far as 47°15'W along the trough axis, where it remains confined by the regional bathymetry and the geostrophic regime of the ACC. The nature of WSDW flow beyond this point remains uncertain. Zenk (1981) and Wittstock and Zenk (1983) describe data from a year-long current meter mooring positioned in Shag Rocks passage at 52°52'S, 48°19'W. These data show a strong correlation between low potential temperatures and strong northwestward flow reaching 60 cm s^{-1} . Zenk (1981) attributed these events to northwestward overflow of "Scotia Sea bottom water" through Shag Rocks passage. However, Locarnini et al. (1993) have since shown that these low-temperature excursions are closely correlated with the measured westward component of velocity, and suggest a westward flow of WSDW along the Falkland Trough. Cunningham and Barker (1996) also infer a prolonged westward flow of WSDW from the disposition of migrating mudwaves on a sediment drift in the eastern Falkland Trough and persistent non-deposition along the southern margin.

3. Methods

The Falkland Trough has been surveyed using a 10-kHz precision echo sounder and 3.5-kHz sub-bottom profiler on six cruises from 1984 to 1995 (Fig. 2). Cruises from 1984 to 1987 were transit satellite navigated and from 1988 onwards all cruises have been GPS navigated. The 3.5-kHz profiles presented in this study consist of original shipboard analogue records plotted on a Raytheon electrostatic line scan recorder.

We also present GLORIA long-range side-scan sonar imagery of the western Falkland Trough acquired using the Institute of Oceanographic Sciences GLORIA *Mk II* long-range side-scan sonar (Somers et al., 1978) which provided a sonar swath width of ~44 km, cross-track resolutions of ~45 m, and along-track resolutions (at 16 km h^{-1}) increasing from ~120 m near the ship track to ~900 m at far range (Searle et al., 1990). Raw GLORIA sonographs were corrected for geometric distortions associated with variations in the speed of the ship (anamorphic correction) and water depth (slant-range correction), and an additional adjustment has been applied to correct for the inadequate compensation of the uneven sonar beam pattern (Searle et al., 1990). The pre-processed GLORIA data were edited and assembled to produce a digital mosaic of GLORIA images covering parts of the North Scotia Ridge and Falkland Trough (Tomlinson et al., 1992). The section of the North Scotia Ridge GLORIA mosaic reproduced in this study covers part of the continental slope southeast of the Falkland Islands, and a short section of the western Falkland Trough near 54°30'W.

Five kasten cores were recovered from the Falkland Trough, during the 1995 coring season aboard the RRS *James Clark Ross* (Fig. 2). A further gravity core, GC062, collected during the 1993 season, is also described. The kasten corer used is of a Cambridge University design, and utilises a 1-tonne core head and a $3.25\text{ m} \times 0.15\text{ m}$ square barrel.

Sedimentological analysis of the cores consisted of particle size analysis, measurement of magnetic susceptibility and smear slide analysis for terrigenous-biogenic ratios. Particle size analysis was conducted using a Micromeritics SediGraph 5100

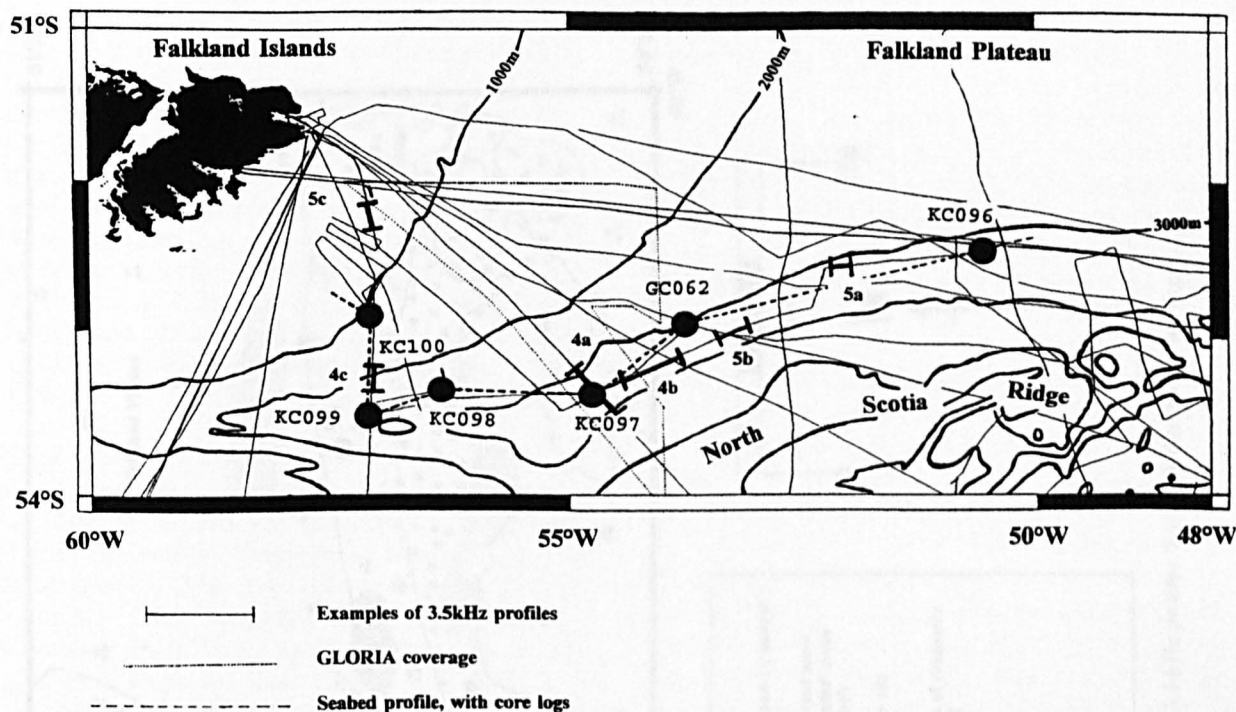


Fig. 2. 3.5-kHz tracks across the western Falkland Trough, used to compile the 3.5-kHz character map. Core locations are indicated by shaded circles, illustrated 3.5-kHz profiles highlighted in bold; (see Figs. 4 and 5). Seabed profile for Fig. 7 is shown as dashed line. GLORIA coverage as dotted area. Contour intervals are 1000 m.

for the $<63\text{-}\mu\text{m}$ fraction. The sand fraction was analysed by settling tube at the School of Ocean Sciences, Bangor University, and by dry sieving at BAS. A Bartington magnetic susceptibility meter MS2 was used to measure magnetic susceptibility every 2 cm on gravity cores and on channel subsamples for the kasten cores. Percent calcium carbonate was measured gravimetrically by dilute HCl dissolution. Biogenic silica was measured in smear slides by point counting (Pudsey, 1993). Sand-fraction slides were prepared, usually at 20-cm intervals, using the random-settling technique of Moore (1973); these slides were used for: (1) petrographic grain counts; and (2) radiolarian species counts to determine relative abundance of *Cycladophora davisiana*. Carbonate-free sand fractions were prepared by HCl dissolution of the foram-rich sands, to facilitate radiolarian identification. Those sands which contained very few radiolarians were separated into a light and a heavy fraction using sodium polytungstate solution made up to a density of 2.25 g cm^{-3} , and the light

fraction was used for radiolarian analysis. The diatom zonation of Gersonde and Burckle (1990) and the radiolarian zonation of Lazarus (1990) were used. Glaucony was examined in two ways; by SEM with energy-dispersive X-ray analysis of individual grains, and by bulk XRF analysis of $\sim 1\text{ g}$ of crushed glaucony-rich sand.

4. Acoustic character of the seabed

4.1. 3.5-kHz Echo character

We have compiled 3.5-kHz sub-bottom profiles acquired across the Falkland Trough west of 48°W , and used these data to generate a new echo character map of this area. Echo types were identified on 3.5-kHz records and plotted on a bathymetric basemap; the western part of this new map is reproduced in Fig. 3 with accompanying bathymetry. The echo character mapped across the study

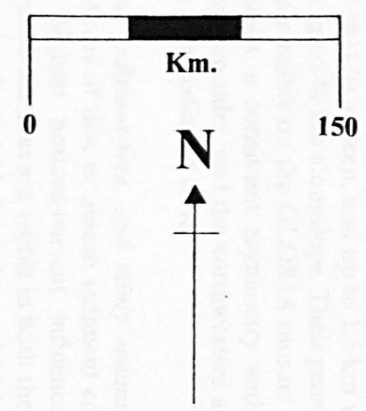
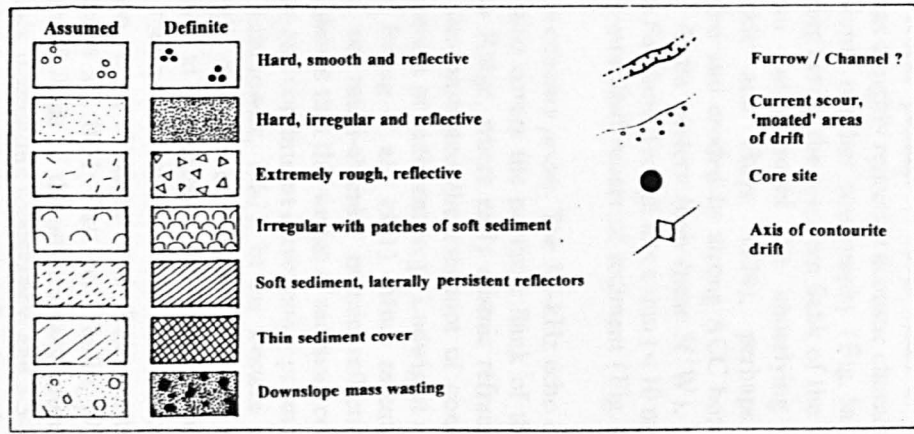
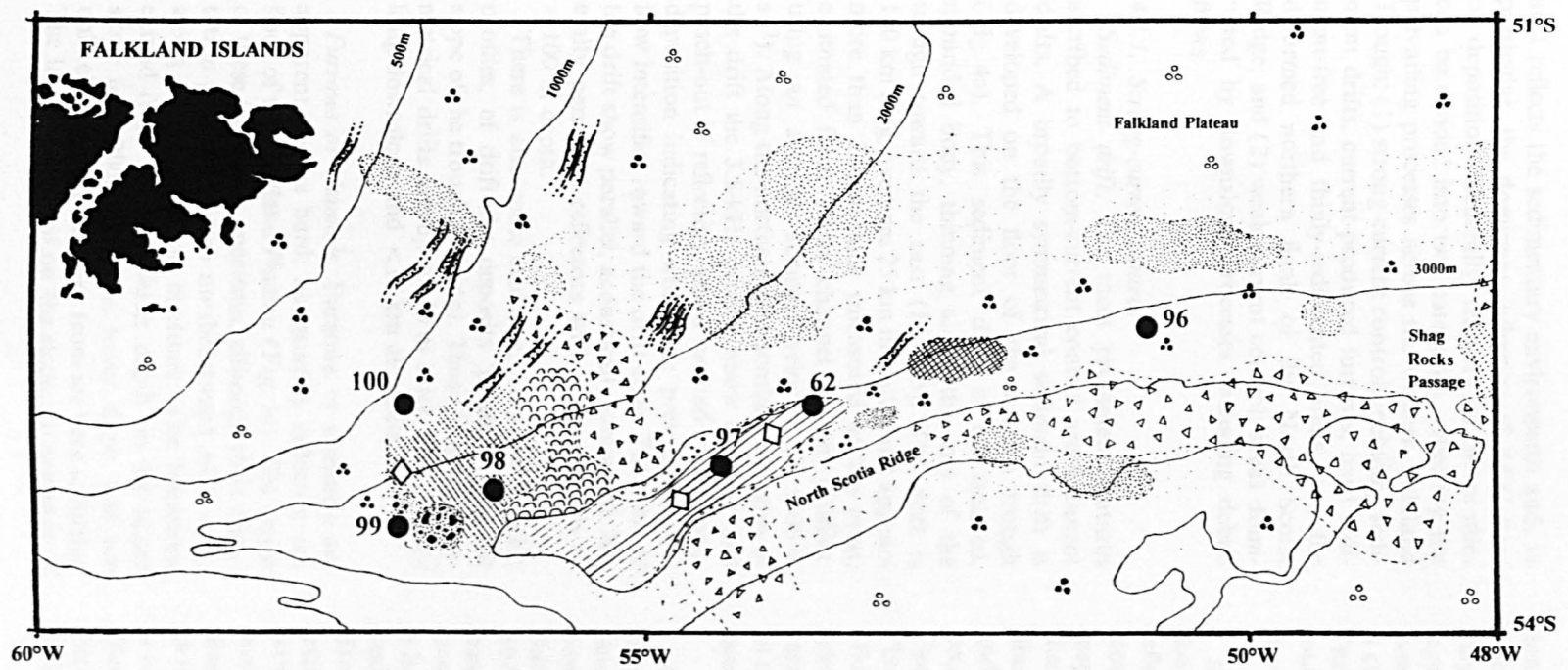


Fig. 3. Echo character map of the western Falkland Trough, compiled from 3.5-kHz profiles. For track distribution see Fig. 2.

area reflects the sedimentary environment and, in particular, the dominant influence of ACC flow on deposition. Generally, features on the profiles can be divided into two categories, reflecting the prevailing processes across the western Falkland Trough: (1) strong-current control, including sediment drifts, current-produced furrows, hard sediment-free and thinly-sedimented areas, and the deformed northern flank of the North Scotia Ridge; and (2) weak-current control; areas dominated by downslope processes including debris flows.

4.1.1. Strong-current control

Sediment drift. The most prominent features ascribed to bottom-current control are sediment drifts. A broadly symmetrical sediment drift is developed on the floor of the western trough (Fig. 4a). This sediment drift is an isolated, mounded body, thinning along the axis of the trough toward the east (Fig. 4b). The drift is 150 km long, averages 25 km in width, and appears more than 200 m thick (measured at the crest, estimated from single channel seismic profiles, using an average acoustic velocity of 1600 m s^{-1}). Along the northern and southern margins of the drift the 3.5-kHz profiles show thinning and pinch-out of reflectors, and a moated area of non-deposition indicating where the prevailing ACC flow intensifies toward the drift edge. The crest of the drift show parallel, acoustically-laminated, laterally persistent reflectors with a penetration to $\sim 100 \text{ m}$ depth.

There is also some evidence, from the 3.5-kHz profiles, of drift-like deposits 'plastered' on the slope of the trough (Fig. 4c). These smaller, asymmetrical drifts are up to 50 m thick and 3–5 km long downslope and $< 15 \text{ km}$ alongslope.

Furrows or channels. Furrows or channels are apparent on the hard, acoustically reflective sea floor of the Falkland Plateau (Fig. 5c). The origin of these features is uncertain, although their orientation parallels known northeastward ACC flow, along the bathymetric contours. The lineations extend from $< 500 \text{ m}$ water depth on the upper slope to $> 2000 \text{ m}$ on the lower slope, and are unlikely therefore to result from ice berg scouring. The lack of sediment on the slope, no evidence of

downslope disturbance and no glide plane visible from seismic profiles all suggest that the features may not be slump scarps. The furrows are commonly 35–130 m deep, and up to 1.5 km wide and extend up to 40 km alongslope. Their general trend is clearly visible on the GLORIA mosaic (Fig. 6). They show a consistent asymmetry with steeper southeastern sides, and the northwestern sides may have a thin sediment cover.

Hard, sediment-free, and thinly sedimented sea floor. Areas of thin or absent sediment cover may reflect highest bottom-current influence, where along-slope features are visible in both the 3.5-kHz map (as hard, smooth-irregular and highly reflective) and the GLORIA mosaic. The area north of Shag Rocks passage is swept clean of sediment and has a highly reflective acoustic character, with occasional rougher topography (Fig. 5a and b). Faulting across the southern flank of the Falkland Plateau has exposed the underlying bedrock (Burckle and Hays, 1974), perhaps further revealed and eroded by strong ACC bottom currents. At its western limit (near 56°W), the floor of the Falkland Trough has a thin ($< 10 \text{ m}$), acoustically-stratified veneer of sediment (Fig. 4c).

Accretionary prism. The 3.5-kHz echo character map also covers the northern flank of the North Scotia Ridge, where early seismic refraction surveys demonstrated the existence of considerable thicknesses of sediment (e.g., Ludwig et al., 1968, 1979; Ewing et al., 1971). More recent studies, based on multi-channel seismic reflection data, have shown that this wedge of sediment constitutes a large and continuous accretionary prism (Ludwig and Rabinowitz, 1982). In the western Falkland Trough, the toe of the accretionary prism is exposed at the seabed, and parts of the trough axis retain the aspect of an active convergent margin (e.g., Ludwig and Rabinowitz, 1982; Barker et al., 1991; Platt and Phillip, 1995). The deformed folds of the accretionary prism present a rough, undulating topography, and 3.5-kHz profiles show hyperbolic, rough reflective echoes, with little evidence of recent sedimentation in this area (Fig. 4a).

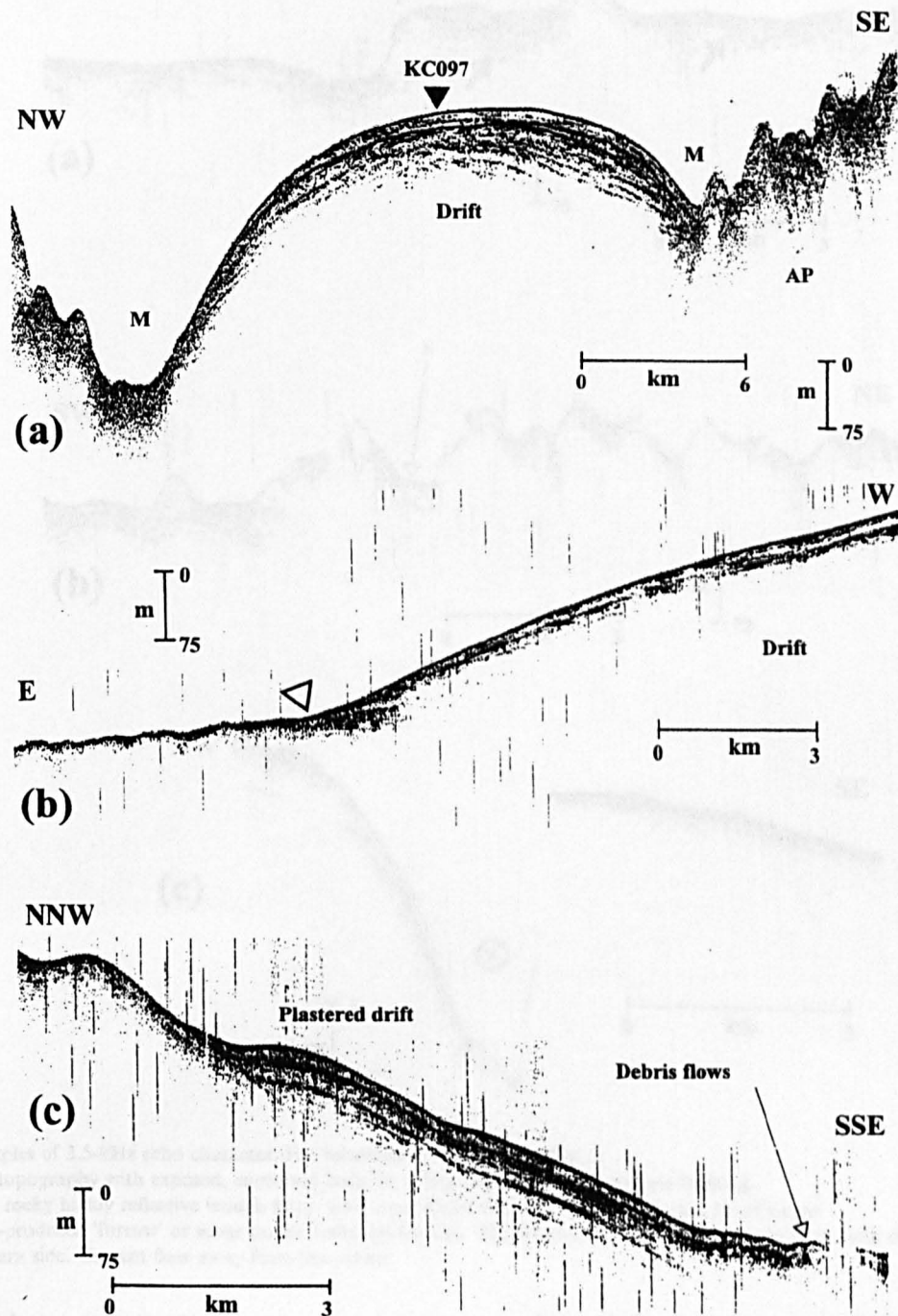


Fig. 4. Examples of 3.5-kHz profiles across the main drift and slope sediments.

a. Mounded drift on the floor of the western trough (*M*=moated erosional areas on either margin; *AP*=accretionary prism). Also shown is the location of core KC097.

b. Profile across the western drift showing the relationship between the distal drift edge (*arrow*) and the reflective, current-swept floor of the trough.

c. Plastered slope sediments with laterally equivalent downslope debris flows encroaching onto the floor of the trough.

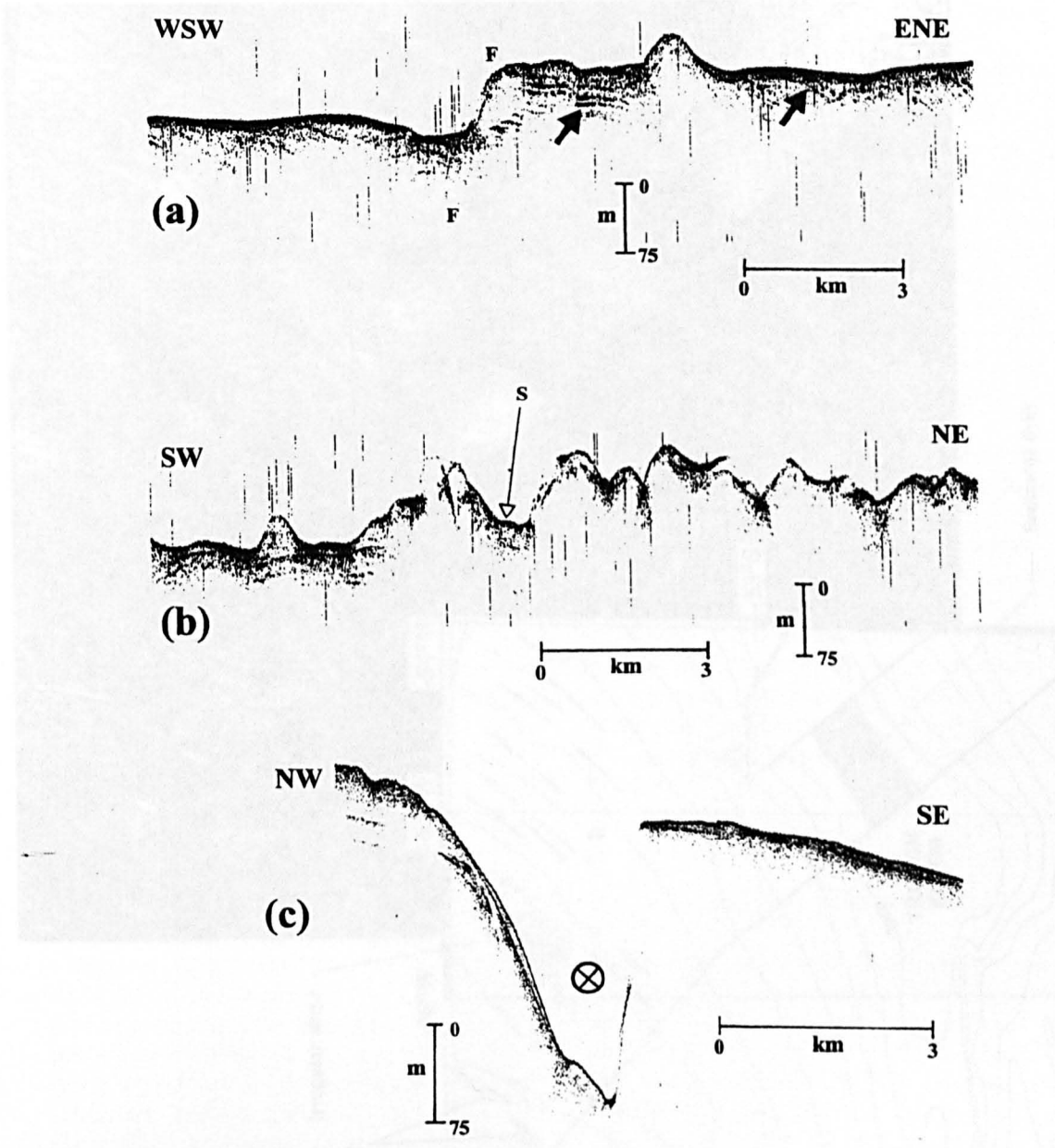


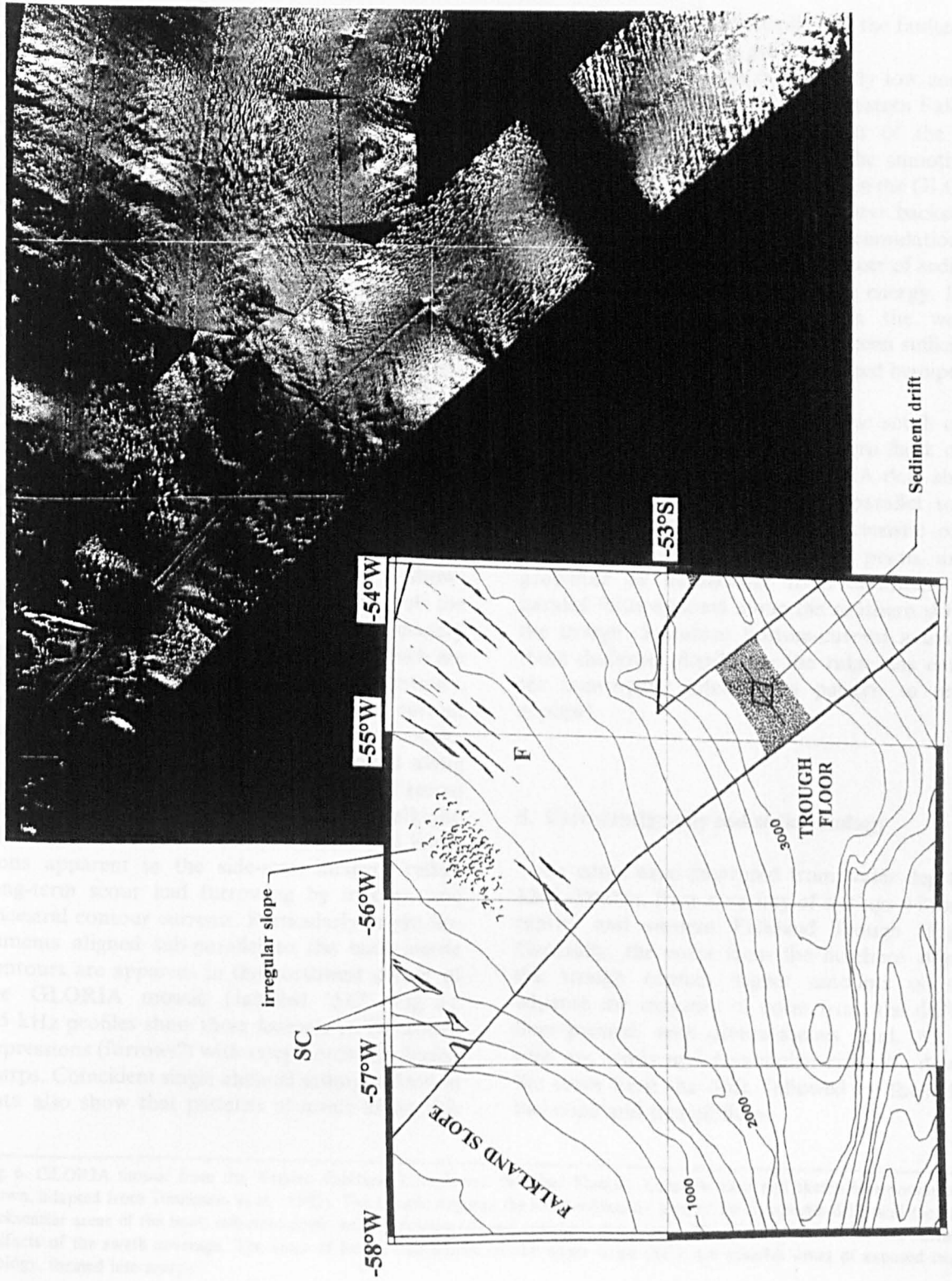
Fig. 5. Examples of 3.5-kHz echo character. For locations of the lines see Fig. 2:

- a. Rough topography with exposed, contorted bedrock strata (arrows). F-F=seafloor faulting.
- b. Rough, rocky highly reflective trough floor, with some slight sediment cover (S) in the lee of ridges.
- c. Current-produced 'furrow' or scour on the Falkland Plateau. The feature shows a marked asymmetry, with the steeper slope on its southeastern side. Current flow away from the reader.

4.1.2. Weak current control

The 3.5-kHz sub-bottom profiles also display features that can be attributed to processes other than the influence of the ACC.

Downslope processes: Debris flows. Some features can be attributed to downslope mass-wasting activity. A small area of debris flows is visible on the extreme western trough floor (Fig. 4c). Here



the flows are laterally continuous with the 'plastered', current-influenced sediments on the slope. The 3.5-kHz profile across the debris flow displays an acoustically chaotic to transparent 'raft' of sediment extending downslope into a localised depression on the floor of the trough. There is some suggestion of internal reflectors, concordant with the plastered slope sediments, which indicate a failure of these units 'en masse', and only moderate disturbance during subsequent deposition in the trough axis. The thickness of the flow is 15–20 m, with a lateral extent of ~3 km. A possible source of the flows is the nearby steep slope of Burdwood Bank to the southwest.

4.2. GLORIA long-range side-scan sonar imagery

Fig. 6 shows a digital mosaic of GLORIA long-range side-scan sonar images (Tomlinson et al., 1992) acquired across the western Falkland Trough, with accompanying bathymetry.

The area of the mosaic north of 53°S shows part of the continental slope southeast of the Falkland Islands. Here, the side-scan imagery reveals acoustic shadows and lineaments which are aligned with the regional bathymetric contours, and located in an area of known contour current activity (labelled 'F', Fig. 6). Unpublished single-channel seismic reflection profiles acquired along the GLORIA tracks show little evidence of recent tectonic activity on this part of the Falkland Plateau, and we infer that the textures and lineations apparent in the side-scan imagery reflect long-term scour and furrowing by modern and ancestral contour currents. Particularly bright lineaments aligned sub-parallel to the bathymetric contours are apparent in the northwest corner of the GLORIA mosaic (labelled 'SC', Fig. 6). 3.5-kHz profiles show these features to be eroded depressions (furrows?) with steep northwest-facing scarps. Coincident single-channel seismic reflection data also show that patterns of scour along this

slope may in part be controlled by the faulted and contorted outcropping geology.

Fig. 6 shows an area of extremely low acoustic backscatter along the axis of the western Falkland Trough, which defines the extent of the axial sediment drift described above. The smooth surface of the drift appears featureless in the GLORIA side-scan imagery, and the very low backscatter implies appreciable sediment accumulation, as topography obscured by a thin veneer of sediment may still scatter incident side-scan energy. Long-term bottom-current flow across the western Falkland Trough appears to have been sufficiently weak at ~3000 m to permit prolonged hemipelagic deposition onto the drift.

The area of the GLORIA mosaic south of the drift shows a section of the northern flank of the North Scotia Ridge. Here, GLORIA data show a distinct striping, orientated sub-parallel to the bathymetry. This fabric is characteristic of the North Scotia Ridge accretionary prism, and is generated by backscatter from deformed, sub-parallel folds exposed along the southern slope of the trough. Sustained bottom-current activity at these shallower depths on the ridge has enabled the convergent deformation pattern to remain exposed.

5. Core stratigraphy and sedimentology

Six cores were recovered from water depths of 1200–3800 m, from a variety of settings within the central and western Falkland Trough (Fig. 7). Generally, the cores from the northern slope of the trough contain higher amounts of sand, whereas the majority of cores from the drift are finer-grained, with diatomaceous mud. All core tops are sandy and foraminifer-rich. We describe the cores from the drift, followed by those from the slope and trough floor.

Fig. 6. GLORIA mosaic from the Western Falkland Trough and Falkland Plateau. Location map and sketch interpretation also shown, adapted from Tomlinson et al. (1992). The mosaic displays the low-backscatter area of the contourite drift, and the higher-backscatter areas of the hard, reflective slope, with furrowing (F) and rougher topography. The black 'pie slices' on the mosaic are artifacts of the swath coverage. The areas of bright backscatter on the upper slope (SC), are possible areas of exposed bedrock geology, formed into scarps.

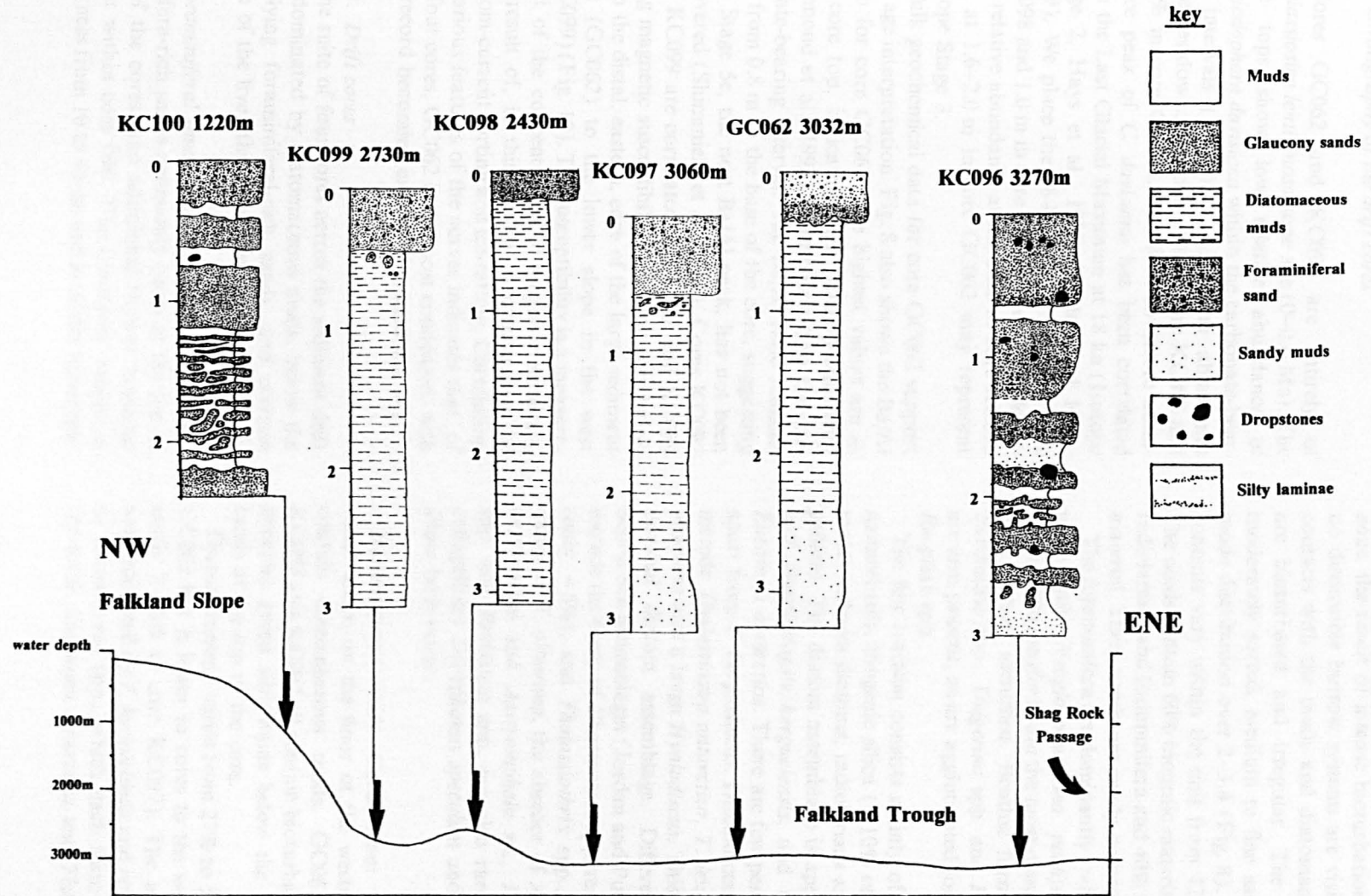


Fig. 7. Core logs on a seabed profile across the floor of the Western Falkland Trough (dashed line in Fig. 2). Vertical and lateral distribution of lithofacies reflects the influence of the ACC on sedimentation. Condensed sequences of sandy contourites are found in cores KC100 and KC096.

5.1. Stratigraphy of the drift cores

Cores GC062 and KC098 are entirely of *Thalassiosira lentiginosa* zone age (0–0.6 Ma). The core tops show low relative abundance of *Cycladophora davisiana* within the carbonate-bearing intervals (Fig. 9). *C. davisiana* abundance increases downcore, to 8–12% in core KC098 and 4–6% in core GC062. The first downcore abundance peak of *C. davisiana* has been correlated with the Last Glacial Maximum at 18 ka (Isotope Stage 2, Hays et al., 1976; Morley and Hays, 1979). We place the 18-ka level at 1.4 m in core KC098 and 1.0 m in core GC062. Lower *C. davisiana* relative abundance at the base of core KC098 and at 1.6–2.0 m in core GC062 may represent Isotope Stage 3.

Bulk geochemical data for core GC062 support this age interpretation. Fig. 8 also shows the Ba/Al ratio for core GC062. The highest values are at the core top, indicating high palaeoproductivity (Dymond et al., 1992) corresponding to the carbonate-bearing interval. The Ba/Al ratio remains low from 0.8 m to the base of the core, suggesting that Stage 5e, the next Ba/Al peak, has not been recovered (Shimmield et al., 1994). Cores KC097 and KC099 are correlated to GC062 and KC098 using magnetic susceptibility, allowing correlation from the distal, eastern, edge of the large sediment drift (GC062) to the lower slope in the west (KC099) (Fig. 10). The susceptibility is a measurement of the concentration of magnetic minerals, the result of, in this locality, a combination of bottom-current sorting and ice-rafting. Correlation of various features of the curves indicates that, of the four cores, GC062 is the most condensed, with the record becoming expanded toward the west.

5.1.1. Drift cores

The suite of four cores across the sediment drift are dominated by diatomaceous muds, below the overlying foraminiferal-rich sands, and contain three of the five lithofacies found in all the cores.

Foraminiferal sands. Pale cream-coloured, foraminifera-rich sands commonly occur at the top of all of the cores, and additional thinner horizons occur within core 096. This lithofacies ranges in thickness from 10 to 40 cm and is totally homogen-

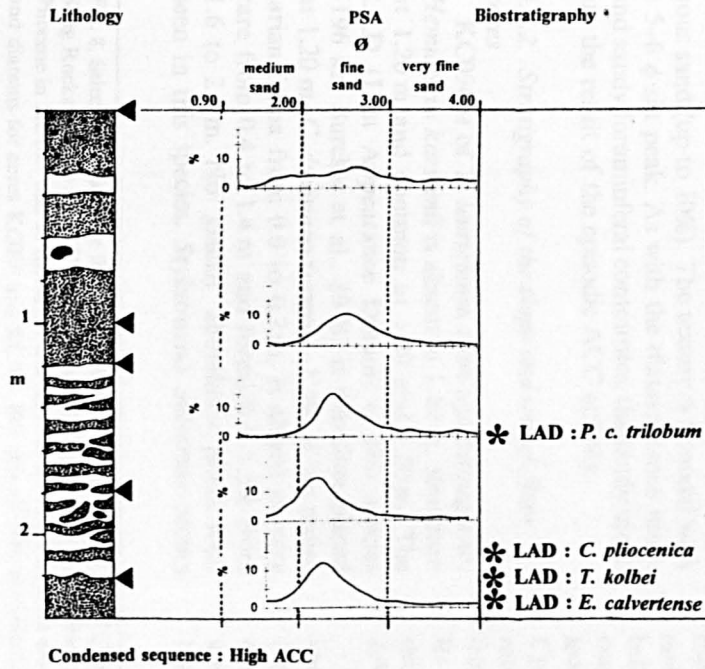
eous, the result of intense bioturbation, although no discernible burrow systems are visible. Lower contacts with the muds and diatomaceous muds are bioturbated and irregular. The sands are moderately sorted, medium to fine sands with a mode distribution over 2–3 ϕ (Fig. 8). Carbonate contents vary within the unit from 42% to 84%. The sands contain 60% biogenic material, diatoms, radiolarians and foraminifera and 40% terrigenous material. These sands are sandy contourites.

The foraminifera are dominantly (>80%) planktonic with *Neogloboquadrina pachyderma* and *Globigerina conglomerata* the most common planktonic species identified. Benthic forms, such as *Pulvinulina* spp., *Uvigerina* spp. and *Lagena* spp. are also present, as are agglutinated forms such as *Reophax* spp.

The fine fraction consists mainly of calcareous nannofossils. Biogenic silica (~10% of total sediment) includes diatoms, radiolarians and silicoflagellates. The diatom assemblage is approximately half *Fragilariopsis kerguelensis*, and up to 10% *Eucampia antarctica*. There are few pennate forms apart from *F. kerguelensis*. Discoid centric species include *Thalassiosira antarctica*, *T. lentiginosa*, *T. oliverana* and a large *Hyalodiscus*. This is a rather unusual diatom assemblage. Differences from Scotia Sea assemblages (Jordan and Pudsey, 1992) include the rarity of *Chaetoceros* spp. resting spores (only ~5%), and *Thalassiothrix* spp., the abundance of *T. oliverana*, the absence of *Actinocyclus actinochilus* and *Asteromphalu* sp., *Rhizosolenia* spp. and *Proboscia* spp. are also rare. The silicoflagellates *Distephanus speculum* and *Dictyocha fibula* both occur.

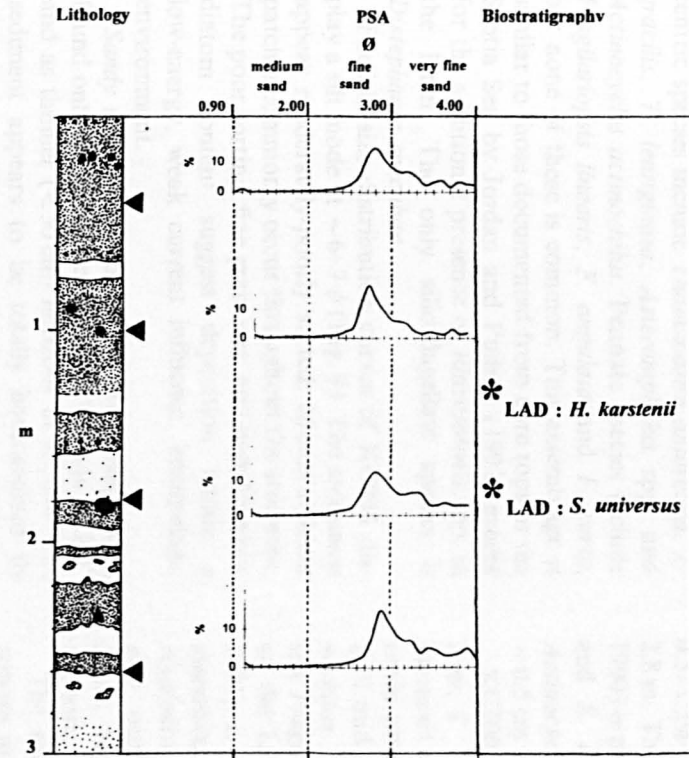
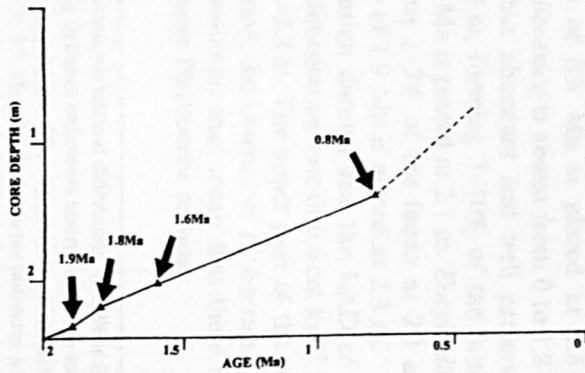
Diatomaceous muds. Cores from the deeper water areas, on the floor of the western trough, contain diatomaceous muds; GC062, KC099, KC098 and KC097 all contain bioturbated, homogeneous, green silty muds below the <0.5 m of sands at the top of the core.

Diatom content varies from 27% to 52% in core GC062 but is lower in cores to the west (consistently 8–10% in core KC097). The assemblages are dominated by *F. kerguelensis* and resting spores of *Chaetoceros* spp., which each form ~33% of the total. *Eucampia antarctica* and *Thalassiothrix*



KC100

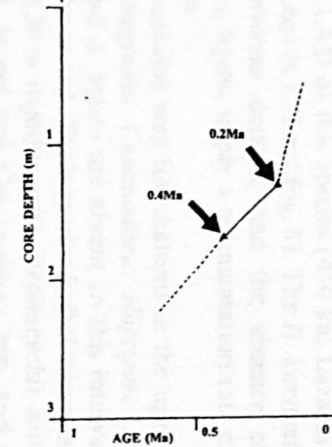
Hard, thin, slope sediments
Falkland Slope



Condensed sequence : High ACC

KC096

Hard, thin sediment cover
Falkland Trough floor



Sedimentation Rate < 1 cm / Ka

spp. each form ~5% of the assemblage. Discoid centric species include *Thalassiosira antarctica*, *T. gracilis*, *T. lentiginosa*, *Asteromphalus* spp. and *Actinocyclus actinochilus*. Pennate species include *Fragilariopsis linearis*, *F. angulata* and *F. curta*, but none of these is common. This assemblage is similar to those documented from core tops in the Scotia Sea by Jordan and Pudsey (1992) except for the additional presence of *Rhizosolenia* spp. in the latter. The only silicoflagellate species is *Distephanus speculum*.

Particle size distribution curves of KC098 display a silt mode at ~6–7 ϕ (Fig. 9). The sediments appear moderately-poorly sorted. Monosulphidic patches commonly occur throughout the sediment. The poor sorting, fine grain size, and high biogenic diatom content suggest deposition within a low-energy, weak current influence, hemipelagic environment.

Sandy muds. These occur less frequently; being found only at the base of cores GC062 and KC097 and as thinner (<50 cm) horizons in KC096. The sediment appears to be totally homogenised by bioturbation. Grain size distribution is similar to the diatomaceous muds but with more fine terrigenous sand (up to 10%). The texture is bimodal with a 5–6 ϕ silt peak. As with the diatomaceous muds and sandy foraminiferal contourites, the sandy muds are the result of the episodic ACC activity.

5.1.2. Stratigraphy of the slope and trough floor cores

KC096 is of *T. lentiginosa* zone age throughout. *Hemidiscus karstenii* is absent at 1.10 m, abundant at 1.20 m and common at 1.30 and 1.50 m. The LAD (Last Appearance Datum) of this species (196 ka; Burckle et al., 1978) is therefore placed at 1.20 m. *C. davisiana* forms 1–1.5% of the radiolarian fauna from 0.0 to 0.2 m, is absent or very rare from 0.4 to 1.4 m and forms 0.5–1.5% from 1.6 to 2.8 m. No 'glacial' abundance peaks were seen in this species. *Stylatractus universus* occurs

rarely at 1.2 and 1.4 m and consistently forms 0.5–1.5% of the radiolarian fauna from 1.8 to 2.8 m. The LAD of this species (410 ka; Lazarus, 1990) is placed at 1.75 m (Fig. 8). The *H. karstenii* and *S. universus* datums, and the absence of *Actinocyclus ingens*, imply a sedimentation rate of ~0.5 cm ka⁻¹.

KC100 contains very few diatoms in the upper 2 m; *T. lentiginosa*, *Coscinodiscus elliptipora*, *H. karstenii* and *A. ingens* are absent so this interval could not be zoned. *Thalassiosira kolbei* occurs at 2.10 and 2.30 m together with *Actinocyclus actinochilus*, *A. ingens* and *Coscinodiscus* spp. and a few *Fragilariopsis* spp. *T. kolbei* is absent at 2.0 m so the LAD of this species (~1.8 Ma; Fenner, 1991) is placed at 2.10 m. The limited diatom assemblage in the upper 2 m is dominated by *Hyalodiscus* sp.; *E. antarctica* and *F. kerguelensis* also occur, with the silicoflagellate *Dictyocha fibula*. Sponge spicules are common throughout the core.

The radiolarian fauna contains no diagnostic species in the upper 1.4 m. *Stylatractus universus* was not seen and many of the common Antarctic forms are rare or absent in this interval. *Antarctissa denticulata* and *A. strelkovi* are common only below 0.8 m. *Pterocanium charybdeum trilobum* occurs at 1.6 and 1.8 m, and rarely below this level; its LAD of 0.8 Ma is placed at 1.6 m. *Cycladophora pliocenica* is absent from 0 to 1.8 m, rare at 2.0 m but abundant and well preserved from 2.1 to 2.4 m, forming 3–10% of the fauna. Its LAD of 1.6 Ma is placed at 2.1 m. *Eucyrtidium calvertense* forms 1–2% of the fauna at 2.3 and 2.4 m; its LAD of 1.9 Ma is placed at 2.3 m.

These radiolarian datums and the LAD of *T. kolbei* give a sedimentation rate of 0.6 cm ka⁻¹ for the interval 1.6–2.3 m. The upper part of the core could not be dated; the absence of *H. karstenii*, *A. ingens* and *S. universus* may mean that there is a hiatus in the upper Pleistocene section.

Fig. 8. Selected particle size frequency curves for cores KC096 and KC100 showing the downcore textural differences. KC096 is from Shag Rocks passage and KC100 from the Falkland Plateau Slope. Biostratigraphic dating indicates sediments extending down to the Pliocene in KC100, and to the Mid-Pleistocene in KC096. Displayed are the LAD (Last Appearance Datum) positions of radiolaria and diatoms for cores KC096 and KC100. For core KC096: *Hemidiscus karstenii* LAD at 0.2 Ma and *Stylatractus universus* at 0.4 Ma; for core KC100: *Pterocanium charybdeum trilobum* LAD at 0.8 Ma, *Cycladophora pliocenica* LAD at 1.6 Ma, *Thalassiosira kolbei* LAD at 1.8 Ma and *Eucyrtidium calvertense* LAD at 1.9 Ma. Key for the lithologies same as Fig. 7.

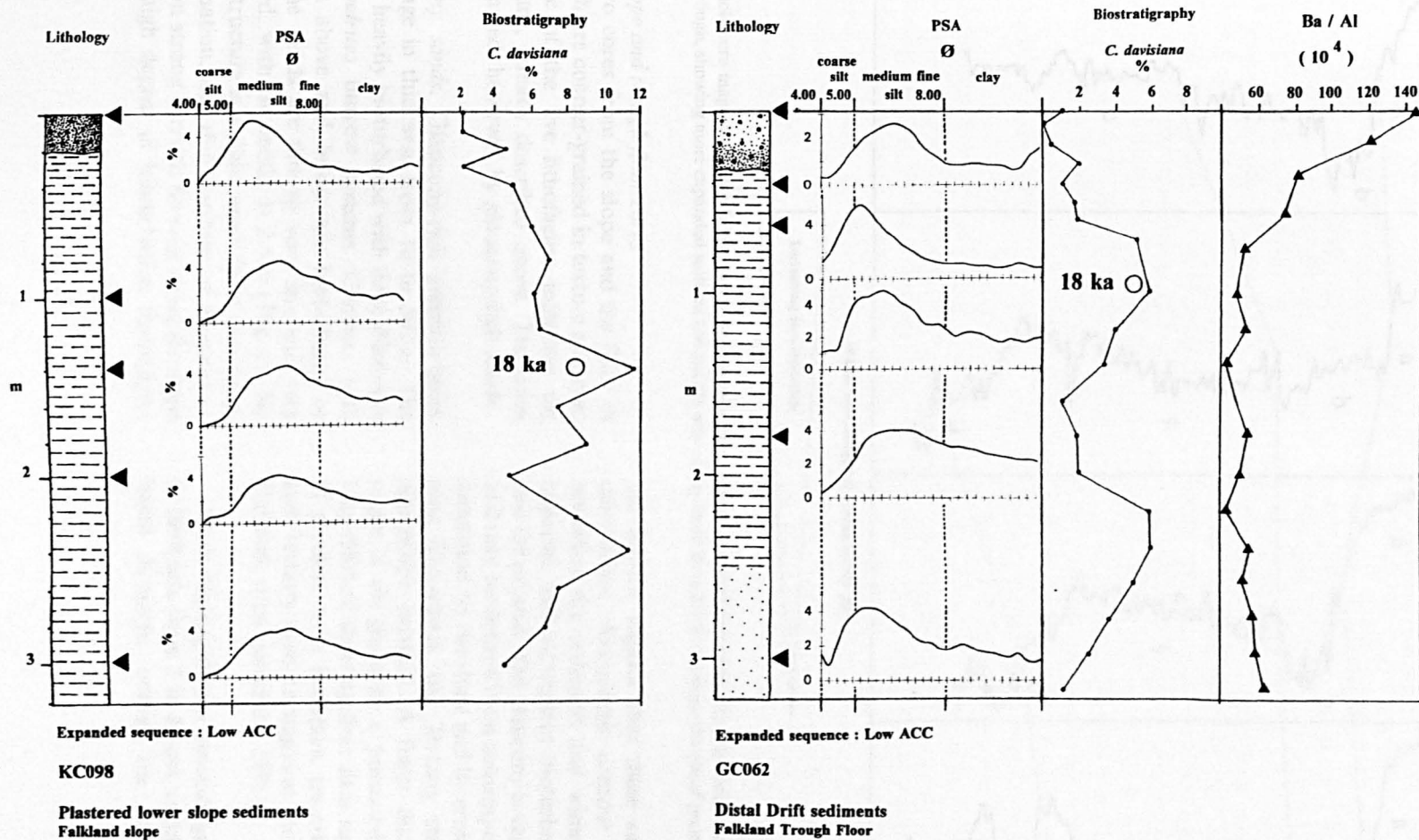


Fig. 9. Particle size frequency curves and core logs of cores KC098 and GC062, from the lower slope and the distal drift sediments on the floor of the trough. Also shown are *Cycladophora davisiana* curves (2–12%) for both cores and the Ba/Al ratio for core GC062. The diatom *Hemidiscus karstenii* LAD, present in the more condensed cores, is absent here, suggesting sediments younger than 0.2 Ma. Key for the lithologies is same as for Fig. 7.

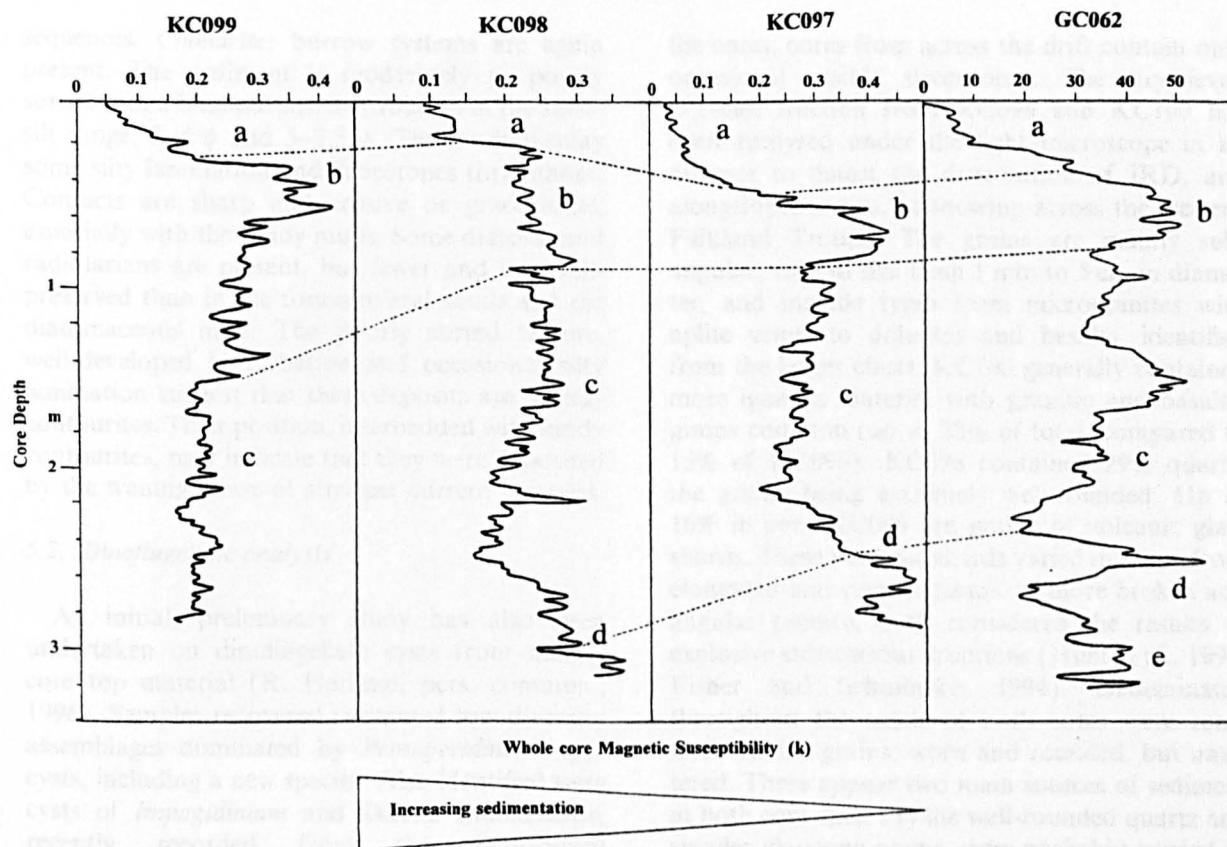


Fig. 10. Whole core magnetic susceptibility curves and correlations (units a–e) across four cores from the drift and lower slope of the Falkland Trough, showing more expanded sections toward the west, away from Shag Rocks passage, the site of main flow of deep ACC.

5.1.3. Slope and trough floor cores

The two cores from the slope and the floor of the trough are coarser-grained in texture and contain three of the five lithofacies; including the sandy muds, already described above. The cores are dominated, however, by glaucony-rich sands.

Glaucony sands. Glaucony-rich greenish-black sands range in thickness from 10 to 50 cm. The sands are heavily bioturbated with large *Planolites* and *Chondrites* burrow systems. Contacts with sediments above and below are bioturbated or sharp. The sands are fine to very fine and very well sorted, with the mode at 2.5 ϕ (Fig. 8). No internal structure is visible, apart from rare mud-dier lamination, and thin horizons of dropstones. The known strong currents flowing along the slope and the high degree of bioturbation throughout

the deposit suggest that these sands are sandy contourites. Alongslope contour currents have reworked the sediment and winnowed the finer material, and subsequent bioturbation homogenised the deposit. The glaucony is very well-rounded and may be derived from contemporary authigenic formation on the slope and by erosion of outcropping Cretaceous and Tertiary strata by strong alongslope currents. A fuller discussion on the origin of the glaucony is presented in Section 6.1. Unpublished dinoflagellate data supports the idea of erosion, with abundant reworked Cretaceous and Tertiary cysts throughout the sediments (R. Harland, pers. commun., 1996).

Muds. Homogeneous greenish-grey muds range in thickness from 5 to 60 cm, occurring as bioturbated horizons within the sandy contourite

sequences. *Chondrites* burrow systems are again present. The sediment is moderately to poorly sorted with a bimodal size distribution in the sand-silt range; 2–4 ϕ and 5–7.5 ϕ . The muds display some silty lamination and dropstones throughout. Contacts are sharp and erosive or gradational, especially with the sandy muds. Some diatoms and radiolarians are present, but fewer and less well-preserved than in the foraminiferal sands and the diatomaceous mud. The poorly sorted texture, well-developed bioturbation and occasional silty lamination suggest that these deposits are muddy contourites. Their position, interbedded with sandy contourites, may indicate that they were deposited by the waning phase of stronger current episodes.

5.2. Dinoflagellate analysis

An initial, preliminary study has also been undertaken on dinoflagellate cysts from mainly core top material (R. Harland, pers. commun., 1996). Samples recovered contained low diversity assemblages dominated by *Protoperidinium* spp. cysts, including a new species. Also identified were cysts of *Impagidinium* and *Dalella chathamense*, recently recorded from the Subtropical Convergence around Chatham Rise, New Zealand (McMinn and Sun, 1994). The dinoflagellate assemblages also contained abundant reworked cysts of Late Cretaceous–Palaeogene age, which appear to increase in number toward the Falkland Islands (R. Harland, pers. commun., 1996).

6. Sediment provenance

Ice-rafted debris (IRD) was assumed to be more common in the sandier slope and trough floor cores, due to the highly condensed sequences in

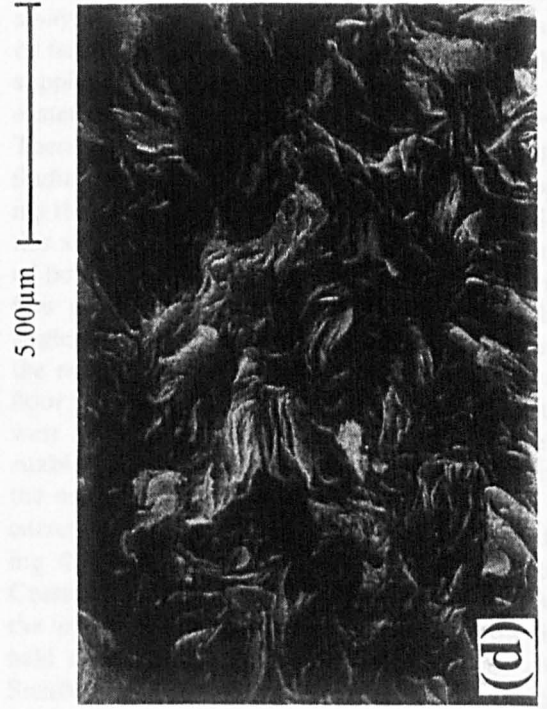
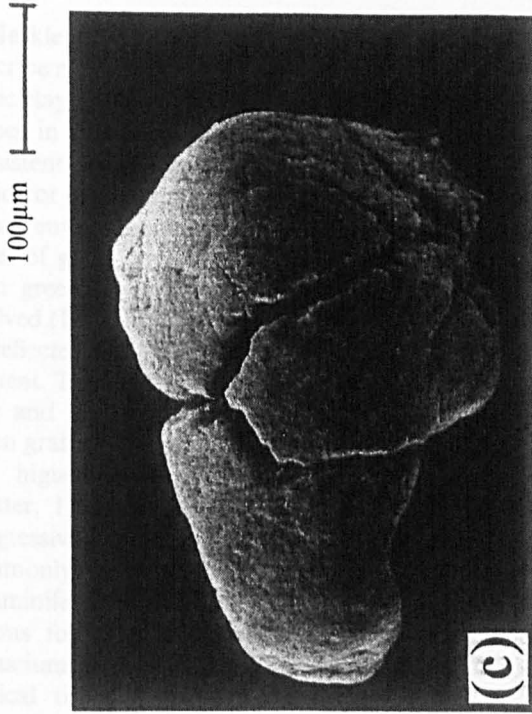
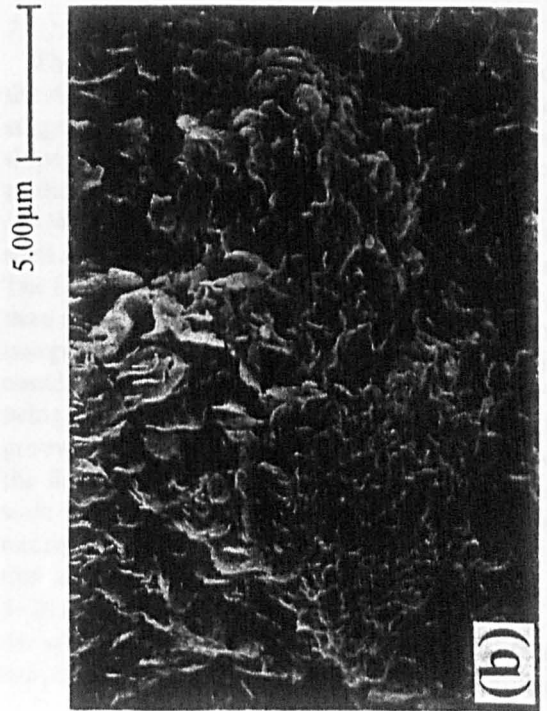
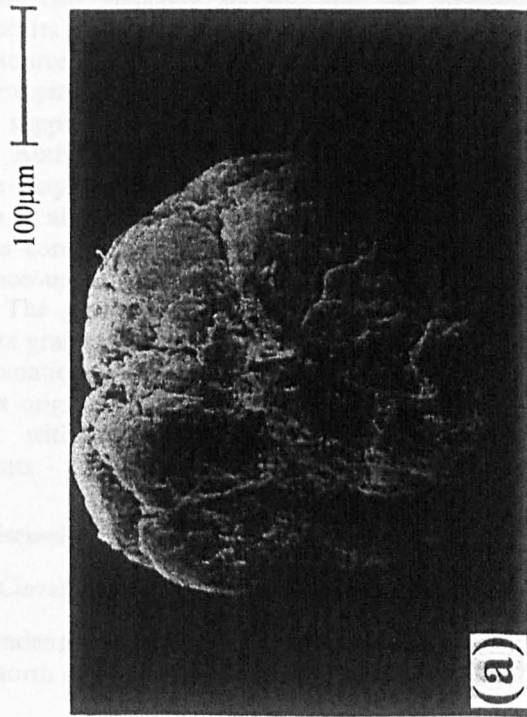
the cores, cores from across the drift contain only occasional visible dropstones. The dry-sieved >1-mm fraction from KC096 and KC100 has been analysed under the light microscope in an attempt to detect the distribution of IRD, and alongslope, in-situ, winnowing across the western Falkland Trough. The grains are mainly sub-angular, vary in size from 1 mm to 5 cm in diameter, and include types from microgranites with aplite veins, to dolerites and basalts, identified from the larger clasts. KC100 generally contained more igneous material with granitic and basaltic grains common (up to 22% of total, compared to 15% of KC096). KC096 contained 29% quartz, the grains being extremely well-rounded. Up to 16% in core KC096 are grains of volcanic glass shards. These volcanic shards varied in shape from elongated and cusped forms, to more broken and angular pumice, both considered the results of explosive subaqueous eruptions (Hunt et al., 1995; Fisher and Schmincke, 1994). Disseminated throughout the sands of both cores were some fresh olivine grains, worn and rounded, but unaltered. There appear two main sources of sediment at both core sites: (1) the well-rounded quartz and smaller glaucony grains, were probably carried as bedload by alongslope currents, the product of shelf spillover and in situ winnowing; and (2) the more exotic, angular, granitic and metamorphic grains were probably dropped by melting sea ice or possibly reworked from a parent glaciomarine deposit. In view of the present-day ACC flow to the east, an Antarctic Peninsula source of IRD seems unlikely, the majority of sea-ice being the product of ice calving from the Ronne and Larsen Ice Shelves in the Weddell Sea. Present-day surface currents transport ice to the northeast, bypassing the northern Scotia Sea and Falkland Islands area. A South American ice source seems the most plausible.

Plate I

Scanning electron micrographs of glaucony grains of different maturities.

- Whole view of evolved, light-green, glaucony grain. Sample from KC096 1–60-m core depth ($\times 220$ magnification).
- Detailed view of the same evolved grain, displaying the internal rosette structure indicative of a K_2O content of 6.5%. ($\times 5000$ magnification).
- Whole view of highly evolved, dark-green, glaucony grain. Sample from KC100 2–10-m core depth ($\times 240$ magnification).
- Detailed view of the same highly evolved grain, displaying an internal lamellar structure, indicative of a K_2O content of >8%. ($\times 8000$ magnification). (Terminology adapted from Odin and Matter, 1981.)

PLATE I



6.1. *Glaucony*

Heckle (1974) and Odin and Fullagar (1988) describe modern glaucony as a shallow-water authigenic clay mineral occurring typically on cold water slopes in <2000-m depth with a well-established, persistent current regime. It is well known as an indicator of very slow sedimentation or non-depositional environments on continental margins. Two types of grain have been identified from the cores; light green or evolved, and dark green or highly evolved (Plate Ia and c). The maturity of the grains is reflected in their internal structure and K₂O content. The light-green grains have a rosette structure and K₂O contents of 6.5% (Plate Ib). Dark-green grains commonly contain a lamellar structure and higher K₂O amounts of >8% (Odin and Matter, 1981) (Plate Id). Glaucony is formed by progressive growth and alteration of a parent grain, commonly carbonate, argillaceous faecal pellets, foraminiferal tests or lithic fragments. Optimal conditions for formation are a source of iron and potassium and low depositional rates or winnowing. Typical times for formation of the light-green, evolved grains are 0.1 Myr and for the dark-green, highly evolved grains are up to 1 Myr (Odin and Matter, 1981; Amorosi, 1995). From the presence of the two glaucony species, and the different timescales for formation we speculate that there are two sources for the glaucony. Erosion of the locally outcropping bedrock by vigorous bottom-currents may supply the older dark-green highly evolved type. Authigenic glaucony formed on the modern slope may provide the light-green evolved type. Saito et al. (1974) described pre-Pleistocene sediments cored from the Falkland Plateau, of Late Cretaceous (possibly Maastrichtian) and Tertiary age. The glaucony pellets and the well-rounded quartz grains are probably locally derived, from a combination of shelf spillover and downslope processes originating from the shelf break and upper slope with subsequent reworking by bottom currents.

7. Discussion

7.1. *Current-influenced sedimentation and erosion*

Condensed contourite sequences on the slope and north of Shag Rocks passage are the result of

high-velocity, sustained, ACC flow winnowing away the fines. Sediment removed from this area, or held in suspension in a nepheloid layer may be supplying the sediment drifts and waves in the eastern trough (Cunningham and Barker, 1996). There is also the possibility of some ACC flow finding its way into the western trough and supplying the western sediment drift. High current velocities are maintained by the topographic influences of both the narrow passage funnelling deep-water flow and the intensifying effects of steeper slope angles across the western trough. The location of the main drift, at the western limit of the trough floor, does suggest that ACC flow from the south-west across Burdwood Bank is relatively stable, enabling the drift to form. The enclosed slopes to the north and the west funnel and accelerate the current across the margins of the trough, producing the moated areas at the base of the slope. Current velocities away from the slope, towards the axis of the trough decrease and allow the fines held in suspension to settle over the drift crest. Smaller isolated 'patch' drifts on the slope may have arisen as a result of meandering cores of current or separated eddies flowing across the irregular topography of the mid-lower slope.

7.1.1. *Origin of the furrows*

The persistence of lineations or 'furrows' along the slope into deeper water on the Falkland Plateau suggests they may have resulted from an along-slope current process similar to the helical flows in the benthic boundary layer discussed by Flood (1994) rather than from alternative possibilities such as ice-berg scouring, faulting, or slump scars. The furrows described here are 10–100 times larger than those discussed by Flood (1994). Continental margin furrowing is initiated by secondary helical circulation in the benthic boundary layer, debris being swept along lineations on the seabed, cutting grooves which subsequently influence and enhance the flow to produce furrowing. Flood describes a wide furrow geometry as common in a predominantly erosional setting; the features observed in this study are up to 1.5 km wide, compared to 5–20 m of other studies. Other disparities lie in the consistent asymmetry of the furrows, with the steeper slope oriented downslope; in the southern

hemisphere the Coriolis force pushes water masses to the left, the steeper slope should therefore be on the northwestern flank. Some of the features described in this study are pre-existing scarps and outcropping bedrock, that were subsequently accentuated by vigorous alongslope currents. The features are probably not fault-related as there appears no evidence from unpublished BAS single-channel seismic lines of any dislocation of the underlying strata. The furrows may be related to outcropping bedrock on the seabed. The origin of these features remains unknown, but in view of their location in an area of high current activity an origin by current-enhanced scouring/‘furlowing’ seems most likely.

7.2. ACC paleoflow history

The cores clearly indicate changes in the intensity of the ACC through time, within the western Falkland Trough, with highly condensed sequences of sandy contourites on the Falkland Plateau slope, and near to the main influx of deep ACC flow, through Shag Rocks passage. Underlying the sandy contourites at the top of the cores across the drift, are younger, more expanded sequences of finer-grained muddy diatom-rich sediments.

7.2.1. Holocene

Interglacial conditions produced a relatively uniform style of sedimentation across the entire western trough and slope. Foraminifera-rich sandy contourites are present throughout the Holocene record, at the top of the cores in this area. The number of foraminifera in the sediment varies from the thickest capping on the cores across the drift to a much thinner veneer in the two slope and Shag Rocks passage cores. This suggests open marine conditions with ACC flow across the northern slope and plateau and sustained stronger flow across the drift. The presence of the silicoflagellate *Dictyocha fibula* attests to relatively warm surface water (Ciesielski, 1975). Glaucony is present within the sediment across all the core sites, although in smaller quantities than seen in the older sandy contourites of the slope and trough floor, suggesting that the degree of winnowing and in situ erosion may be less than during deposition of the

older sediments, and by inference, the ACC flow is less vigorous than during the deposition of the Plio-Pleistocene condensed sandy contourites.

7.2.2. Late Pleistocene

During the Late Pleistocene (late Stage 2), the ACC was weak below 2500 m within the trough. Fine-grained, diatomaceous sediments were deposited on the floor of the trough, with weak ACC maintaining the western sediment drift. The similarity of the diatom flora to the Holocene Scotia Sea flora (Jordan and Pudsey, 1992), and the absence of *D. fibula*, both suggest that during Stage 2, surface waters were cooler than today, with the Polar Front lying to the north of the sites. At <2000-m water depth, on the slope, more vigorous circulation continued, reworking the glaucony-rich sands as sandy contourites. Periodic reduction in energy allowed the deposition of muddier contourites, interbedded with the sands. A reduction in Weddell Sea Deep Water production during glaciation (Pudsey et al., 1988) would have led to reduced entrainment in the ACC and, therefore, helped to repress the inflow of Circumpolar Deep Water into the eastern trough. The upper and intermediate waters, the Falkland Current, on the slope, being predominantly wind-driven, remained unaffected. Throughout this time ice bergs were present and dropstones were occasionally released into the sediment, becoming concentrated by the winnowing action of bottom-currents. Provenance of the granitic and basaltic clasts is unknown although a South American source is most plausible with northeastward-flowing surface currents transporting ice across the Northern Scotia Sea.

7.2.3. Late Pliocene–Middle Pleistocene

Cores KC100 and KC096 represent highly condensed contourite sequences, indicative of sustained periods of non-deposition and erosion across the floor of the trough, near Shag Rocks Passage, and on the Falkland Plateau slope. Core KC100 recovered sediments of Late Pliocene age and it is clear that the lowest sedimentation rate and therefore the highest ACC activity has been on the Falkland Plateau slope. Thinly bedded sequences of glaucony-rich sandy and silty

contourites, subsequently bioturbated, indicate a fluctuating core of high-velocity ACC on the mid-lower slope during the Late Pliocene. Current instability may have extended into the Early–Mid-Pleistocene in both the deeper and intermediate waters flowing through Shag Rocks passage and across the slope with erosive contacts and coarsening and fining sequences in the contourites. Occasional ice bergs were also present with dropstones released onto the seabed. The deposition of sediment in both areas during this time was minimal, either as an indirect result of sediment bypass and non deposition due to strong bottom current activity, or as a direct result of minimal sediment supply. The presence of two species of glaucony may be an indication of in-situ winnowing of glaucony-rich Cretaceous bedrock and alongslope reworking of old authigenic deposits, with along-slope transportation and shelf spillover of authigenic, younger glaucony.

7.3. *Implications for the contourite facies model*

The glauconitic sandy contourites from the western Falkland Trough generally conform to the contourite facies model proposed by Stow and Piper (1984). Similar Holocene sandy contourites to those seen in the Falkland Trough cores have been observed from studies of the late Quaternary across the Hebrides Slope in the Rockall Trough, northeast Atlantic (Akhurst, 1991; Howe, 1995; Stoker et al., 1997). The deposition of sandy contourites involves winnowing, erosion and removal of underlying lower fine-grained sequences, leaving the sandy contourites remaining, indicative of highest current speeds only. This style of deposition has been termed a 'mid-only' contourite sequence by Stoker et al. (1997), meaning only the middle sandy sequence of the facies model is preserved. In the Falkland Trough the sands appear to be structureless and more massive, with no suggestion of any vertical or progressive sequence. Possibly current activity was not continuous, but rather a series of interrupted phases of high current flow winnowing and eroding the lower, finer contourite sequence. Episodic periods of quiescence allowed bioturbation to fully homogenise the sands further. Current meter evidence, from the Scotia Sea, has shown that deep-water

ACC flow is not continuous and unidirectional but far more sporadic, with high-energy 'benthic storm' events punctuating more subdued background sluggish bottom-currents (Pudsey and Howe, 1997). High-energy current events have the potential to erode away any evidence of earlier deposition. The reverse (+ve) sequences or waning phase of a period of high current activity will therefore have a far greater potential for preservation, as current strengths decrease and the coarser sediment is overlain by an input of fines.

8. Conclusions

A contourite sediment drift has been identified at a depth of 3000 m on the floor of the western Falkland Trough. The drift is 150 km long, averages 35 km wide and is >200 m thick; the drift crest axis trends east-northeast to west-southwest. Bottom-current flow at the margins of the drift has produced non-depositional moats, suggesting an intensification of flow. Strong current velocities from the inflow of ACC deep water (Circumpolar Deep Water) has maintained the floor of the trough to the north of Shag Rocks passage, the gap in the North Scotia Ridge, sediment free. On the Falkland slope ACC intermediate and shallow flow (the Falkland Current) follows the bathymetric contours eroding furrows and reworking sediment.

Six cores across the drift, slope and the floor of the trough indicate two styles of contourite deposition. In four cores across the sediment drift muddy contourites and hemipelagites of Last Glacial Maximum age overlie Holocene sandy biogenic contourites. On the floor of the trough and the slope, condensed sequences of sandy, glaucony-rich contourites of Pliocene and Mid-Pleistocene age are present. The glaucony originates from the reworking of exposed Cretaceous and Tertiary age bedrock by vigorous bottom-currents, and by authigenic formation and spillover on the slope.

ACC flow during the Late Pliocene–Mid-Pleistocene was characterised by unstable but periodically vigorous flow, with occasional sea ice in the Pleistocene. Late Pleistocene flow was weak below 2500 m on the drift; however, upper and intermediate water flow on the slope was

unaffected and remained strong. Surface water conditions were cool with the Polar Front to the north of its present position. ACC flow in the Holocene was uniform at all depths, with normal open marine conditions and relatively warm surface waters.

Acknowledgements

The authors wish to thank the officers and crew of the RRS *James Clark Ross* for an enjoyable and productive cruise in the face of adversity. Steven Evans assisted with sample preparation and John Smellie helped identify some of the dropstones. We thank Rex Harland for the dinoflagellate analysis; Sarah Jones at the School of Ocean Sciences, Bangor, for the use of the sand settling tube; Jerry Lee at Royal Holloway and Bedford New College, London, for help with the Sedigraph; and Peter F. Barker and Richard V. Dingle for reading an early draft of the manuscript. The paper was greatly improved by the reviews of Jean-Claude Faugères and David J.W. Piper.

References

- Akhurst, M.C., 1991. Aspects of late Quaternary sedimentation in the Faeroe–Shetland Channel, Northwest UK continental margin. *Br. Geol. Surv., Tech. Rep. WB/91/2*.
- Amorosi, A., 1995. Glaucony and sequence stratigraphy: A conceptual framework of distribution in siliciclastic sequences. *J. Sediment. Res. B* 65 (4), 419–425.
- Barker, P.F., Dalziel, I.W.D., Storey, B.C., 1991. Tectonic development of the Scotia arc region. In: Tingey, R.J. (Ed.), *The Geology of Antarctica. Oxford Monographs on Geology and Geophysics*, Vol. 17, Oxford University Press, New York, NY, pp. 215–248.
- Burckle, L.H., Hays, J.D., 1974. Pre-Pleistocene sediment distribution and evolution of the Argentine continental margin & Falkland Plateau. *Geol. Soc. Am., Prog. Abstr.* 6, 673–674.
- Burckle, L.H., Clarke, D.B., Shackleton, N.J., 1978. Isochronous last appearance datum of the diatom *Hemidiscus karsenii* in the subantarctic. *Geology* 6, 243–246.
- Ciesielski, P.F., 1975. Biostratigraphy and palaeoecology of Neogene and Oligocene silicoflagellates recovered from cores during Antarctic Leg 28. In: *Proceedings of the Deep Sea Drilling Project*, Vol. 28. U.S. Gov. Print. Off., Washington, DC, pp. 625–691.
- Cunningham, A.P., Barker, P.F., 1996. Evidence for westward-flowing Weddell Sea Deep Water in the Falkland Trough, western South Atlantic. *Deep-Sea Res.* 43 (5), 643–654.
- Dymond, J., Suess, E., Lyle, M., 1992. Barium in deep-sea sediments: A geochemical proxy for palaeoproductivity. *Paleoceanography* 7, 163–181.
- Ewing, J.I., Ludwig, W.J., Ewing, M., Eittrheim, S.L., 1971. Structure of the Scotia Sea and Falkland Plateau. *J. Geophys. Res.* 76 (29), 7118–7137.
- Faugères, J.-C., Stow, D.A.V., 1993. Bottom-current controlled sedimentation: a synthesis of the contourite problem. *Sediment. Geol.* 82 (1/4), 287–299.
- Fenner, J.M., 1991. Late Pliocene–Quaternary quantitative diatom stratigraphy in the Atlantic sector of the Southern Ocean. In: Ciesielski, P.F., Kristofferson, Y., et al. (Eds.), *Proceedings of the Ocean Drilling Program, Scientific Results*, Vol. 114. Ocean Drill. Prog., College Station, TX, pp. 97–121.
- Fisher, R.V., Schmincke, H.-U., 1994. Volcaniclastic sediment transport and deposition. In: Pye, K. (Ed.), *Sediment Transport and Depositional Processes*. Blackwell, London, 397 pp.
- Flood, R.D., 1994. Abyssal bedforms as indicators of changing bottom current flow: Examples from the U.S. East Coast continental rise. *Paleoceanography* 9, 1049–1060.
- Georgi, D.T., 1981. Circulation of bottom waters in the southwestern South Atlantic. *Deep-Sea Res.* 28 A, 959–979.
- Gersonde, R., Burckle, L.H. 1990. Neogene diatom biostratigraphy of ODP Leg 113, Weddell Sea (Antarctic Ocean). In: Barker, P.F., Kennett, J.P. (Eds.), *Proceedings of the Ocean Drilling Program, Scientific Results*, Vol. 113. Ocean Drill. Prog., College Station, TX, pp. 761–791.
- Goodell, H.G., 1964. Marine geology of Drake Passage, Scotia Sea and South Sandwich Trench. USNS Eltanin, Mar. Geol. Rep., Dep. Geol., Florida State University, Tallahassee, FL.
- Gordon, A.L., 1966. Potential temperature, oxygen and circulation of bottom water in the Southern Ocean. *Deep-Sea Res.* 13, 1125–1138.
- Grose, T.J., Johnson, J.A., Bigg, G.R., 1995. A comparison between the FRAM (Fine Resolution Antarctic Model) results and observations in the Drake Passage. *Deep-Sea Res.* 42 (3), 365–388.
- Hays, J.D., Lozano, J.A., Shackleton, N.J., Irving, G., 1976. Reconstruction of the Atlantic and western Indian Ocean sectors of the 18,000 B.P. Antarctic Ocean. In: Cline, R.M., Hays, J.D. (Eds.), *Investigation of Late Quaternary Paleocceanography and Paleoclimatology*. *Geol. Soc. Am. Mem.* 145, 337–372.
- Heckle, P.H., 1974. Recognition of ancient shallow marine environments. In: Rigby, J.K., Hamblin, W.K. (Eds.), *Recognition of Ancient Sedimentary Environments*. *Soc. Econ. Paleontol. Mineral., Spec. Publ.* 16, 226–242.
- Hollister, C.D., 1993. The concept of deep-sea contourites. *Sediment. Geol.* 82 (1/4), 5–15.
- Hollister, C.D., Elder, R.B., 1969. Contour currents in the Weddell Sea. *Deep-Sea Res.* 16, 99–101.
- Howe, J.A., 1995. Sedimentary processes and variations in slope-current activity during the last Glacial–Interglacial episode on the Hebrides Slope, northern Rockall Trough, North Atlantic Ocean. *Sediment. Geol.* 96, 201–230.
- Hunt, J.B., Fannin, N.G.T., Hill, P.G., Peacock, J.D., 1995.

- The tephrochronology and radiocarbon dating of North Atlantic, Late Quaternary sediments: an example from the St. Kilda Basin. In: Scrutton, R.A., Stoker, M.S., Shimmield, G.B., Tudhope, A.W. (Eds.), *The Tectonics, Sedimentation and Palaeoceanography of the North Atlantic Region*. Geol. Soc. London, Spec. Publ. 90, 227–248.
- Jordan, R.W., Pudsey, C.J., 1992. High-resolution diatom stratigraphy of Quaternary sediments from the Scotia Sea. *Mar. Micropaleontol.* 19, 201–237.
- Lazarus, D., 1990. Middle Miocene to Recent radiolarians from the Weddell Sea, Antarctica, O.D.P. Leg 113. In: Barker, P.F., Kennett, J.P., et al. (Eds.), *Proceedings of the Ocean Drilling Program, Scientific Results, Vol. 113*. Ocean Drill. Prog., College Station, TX, pp. 709–727.
- Locarnini, R.A., Whitworth III, T., Nowlin, W.D., 1993. The importance of the Scotia Sea on the outflow of Weddell Sea Deep Water. *J. Mar. Res.* 51, 135–153.
- Ludwig, W.J., Rabinowitz, P.D., 1982. The collision complex of the North Scotia Ridge. *J. Geophys. Res.* 87, 3731–3740.
- Ludwig, W.J., Ewing, J.I., Ewing, M., 1968. Structure of Argentine continental margin. *Bull. Am. Assoc. Pet. Geol.* 52 (12), 2337–2368.
- Ludwig, W.J., Windisch, C.C., Houtz, R.E., Ewing, J.I., 1979. Structure of Falkland Plateau and offshore Tierra del Fuego, Argentina. In: Watkins, J.S., Montadert, L., Wood Dickerson, P. (Eds.), *Geological and Geophysical Investigations of Continental Margins*. Am. Assoc. Pet. Geol. Mem. 29, 125–137.
- McMinn, A., Sun, X., 1994. Recent dinoflagellate cysts from the Chatham Rise, Southern Ocean, east of New Zealand. *Palynology* 18, 41–53.
- Moore, Jr., T.C., 1973. Method of randomly distributing grains for microscopic examination. *J. Sediment. Petrol.* 43, 904–906.
- Morley, J.J., Hays, J.D., 1979. *Cycladophora davisiana*: a stratigraphic tool for the Pleistocene North Atlantic and inter-hemispheric correlation. *Earth Planet. Sci. Lett.* 44, 383–389.
- Nowlin, W.D., Zenk, W., 1988. Westerward bottom currents along the margin of the South Shetland Island Arc. *Deep-Sea Res.* 35, 269–301.
- Odin, G.S., Fullagar, P.D., 1988. The geological significance of the glaucony facies. In: Odin, G.S. (Ed.), *Green Marine Clays. Developments in Sedimentology*, Vol. 45. Elsevier, Amsterdam, pp. 295–332.
- Odin, G.S., Matter, A., 1981. De glauconiarum origine. *Sedimentology* 28, 611–641.
- Peterson, R.G., 1992. The boundary currents of the western Argentine Basin. *Deep-Sea Res.* 39, 623–644.
- Peterson, R.G., Johnson, C.S., 1994. Direct velocity measurements in the Malvinas Current. *Ber. Fachbereich Geowiss. Univ. Bremen* 52, 114 (abstract).
- Peterson, R.G. and Whitworth III, T., 1989. The Subantarctic and Polar Fronts in relation to deep water masses through the southwestern Atlantic. *J. Geophys. Res.* 94, 10817–10835.
- Piola, A.R., Gordon, A.L., 1989. Intermediate waters in the southwest South Atlantic. *Deep-Sea Res.* 36, 1–16.
- Platt, N.H., Phillip, P.R., 1995. Structure of the southern Falkland Islands continental shelf: initial results from new seismic data. *Mar. Petr. Geol.* 12 (7), 759–771.
- Pudsey, C.J., 1992. Late Quaternary changes in Antarctic Bottom Water velocity inferred from sediment grain size in the northern Weddell Sea. *Mar. Geol.* 107, 9–33.
- Pudsey, C.J., 1993. Calibration of a point counting technique for estimation of biogenic silica in marine sediments. *J. Sediment. Petrol.* 63, 760–762.
- Pudsey, C.J., Howe, J.A., 1997. Quaternary sedimentation in the Scotia Sea. *Mar. Geol.* (submitted).
- Pudsey, C.J., Barker, P.F., Hamilton, N., 1988. Weddell Sea abyssal sediments a record of Antarctic Bottom Water flow. *Mar. Geol.* 81, 289–314.
- Saito, T., Burckle, L.H., Hays, J.D., 1974. Implications of some pre-Quaternary sediment cores and dredgings. In: Hay, W.W. (Ed.), *Studies in Paleo-oceanography*. Soc. Econ. Paleontol. Mineral., Spec. Publ. 20, 6–35.
- Searle, R.C., Le Bas, T.P., Mitchell, N.C., Somers, M.L., Parson, L.M., Patriat, P.H., 1990. GLORIA image processing: the state of the art. *Mar. Geophys. Res.* 12, 21–39.
- Shimmield, G., Derrick, S., Mackensen, A., Grobe, H., Pudsey, C., 1994. The history of barium, biogenic silica and organic carbon accumulation in the Weddell Sea and Antarctic Ocean over the last 150,000 years. In: Zahn, R. (Ed.), *Carbon Cycling in the Glacial Ocean: Constraints on the Ocean's Role in Global Change*. NATO, ASI Ser. 117, 555–574.
- Somers, M.L., Carson, R.M., Revie, J.A., Edge, R.H., Barrow, B.J., Andrews, A.G., 1978. GLORIA II — an improved long-range side-scan sonar. In: *Proceedings of the IEEE/IERE Subconference on Offshore Instrumentation*. Oceanology International '78, Technical Session J, London, BPS Exhibitions Ltd., pp. 16–24.
- Stanley, D.J., 1993. Model for turbidite to contourite continuum and multiple process transport in deep marine settings: examples in the rock record. *Sediment. Geol.* 82 (1/4), 241–257.
- Stoker, M.S., Akhurst, M.C., Howe, J.A., Stow, D.A.V., 1997. Sediment drifts and contourites off north-west Britain. *Sediment. Geol.* (in press).
- Stow, D.A.V., 1994. Deep-sea processes of sediment transport and deposition. In: Pye, K. (Ed.), *Sediment Transport and Depositional Processes*. Blackwell, London, 397 pp.
- Stow, D.A.V., Piper, D.J.W., 1984. Deep-water fine-grained sediments: facies models. In: Stow, D.A.V., Piper, D.J.W. (Eds.), *Fine-grained Sediments: Deep-water Processes and Facies*. Geol. Soc. London, Spec. Publ. 15, 611–646.
- Tomlinson, J.S., Cunningham, A.P., Barker, P.F., 1992. GLORIA imagery of the North Scotia Ridge. *Ann. Geophys.* 10, Suppl. 1, 77.
- Wittstock, R.R., Zenk, W., 1983. Some current observations and surface T/S distributions from the Scotia Sea and Bransfield Strait during the early austral summer, 1980/81. "Meteor" *Forschungsergeb. Reihe A/B*, 24, 77–86.
- Zenk, W., 1981. Detection of overflow events in the Shag Rocks Passage, Scotia Ridge. *Science* 213, 1113–1114.



Evidence for westward-flowing Weddell Sea Deep Water in the Falkland Trough, western South Atlantic

ALEX P. CUNNINGHAM* and PETER F. BARKER*

(Received 13 February 1995; in revised form 9 January 1996; accepted 21 January 1996)

Abstract—The North Scotia Ridge controls the eastward and northward flow of the Antarctic Circumpolar Current (ACC) emerging from Drake Passage. Existing physical oceanographic data in this region are sparse and do not define the flow pattern of Circumpolar Deep Water (CDW) within the ACC, or of Weddell Sea Deep Water (WSDW) heading northward beneath it, in the region of the North Scotia Ridge and Falkland Trough. 3.5-kHz reflection profiles show mudwaves at the surface of a sediment drift along the axis of the eastern Falkland Trough that have a consistent NE–SW alignment and are migrating SE, indicating persistent westward bottom-current flow along the trough axis. Sediment thinning and non-deposition at the southern drift margin indicate intensified westward flow, considered to be Weddell Sea Deep Water from the Malvinas Outer Basin to the east. This flow probably continues to 48°W, but beyond there its fate is unknown. Similar non-deposition along the northern margin of the drift is considered to result from intensified eastward return flow of WSDW, or from CDW. The mudwave geometry appears to extend to at least 400-m depth within the drift, which therefore most probably contains a record of southern-origin bottom water (presently WSDW) extending back for several million years. Copyright © 1996 Elsevier Science Ltd

INTRODUCTION

The Falkland Trough is a west–east elongated deep that separates the Falkland Plateau from the North Scotia Ridge in the western South Atlantic (Fig. 1). Extending 1300 km from the South American continental shelf to the Malvinas Outer Basin, its floor is between 3000 m and 4000 m below sea level from 56°W to 41°W. It lies in the path of Circumpolar Deep Water (CDW) within the Antarctic Circumpolar Current (ACC), which is constrained to flow east through Drake Passage but then diverges as sea-bed topography permits: the shallow water flows northeast over the western North Scotia Ridge and Falkland Plateau as the Falkland Current (Peterson and Whitworth, 1989), but the deeper water is retained within the Scotia Sea until Shag Rocks Passage, a gap in the North Scotia Ridge at 48°W with a sill depth of 3000 m. Thereafter some of the ACC flows north through the gap and eastward, south of the elevated eastern Falkland Plateau. A more southerly component of the ACC continues eastward within the Scotia Sea.

Some of the much colder Weddell Sea Deep Water (WSDW, -0.7°C to $+0.2^{\circ}\text{C}$) flows north through gaps in the South Scotia Ridge into the Scotia Sea, where it underlies the ACC at a sub-horizontal interface (Locarnini *et al.*, 1993). This interface lies at about 1-km depth across the South Scotia Ridge and descends northward to meet the sea bed at 3–4-km depth in the northern Scotia Sea. Other WSDW flows north along the South Sandwich

* British Antarctic Survey, High Cross, Madingley Road, Cambridge CB3 0ET, U.K.

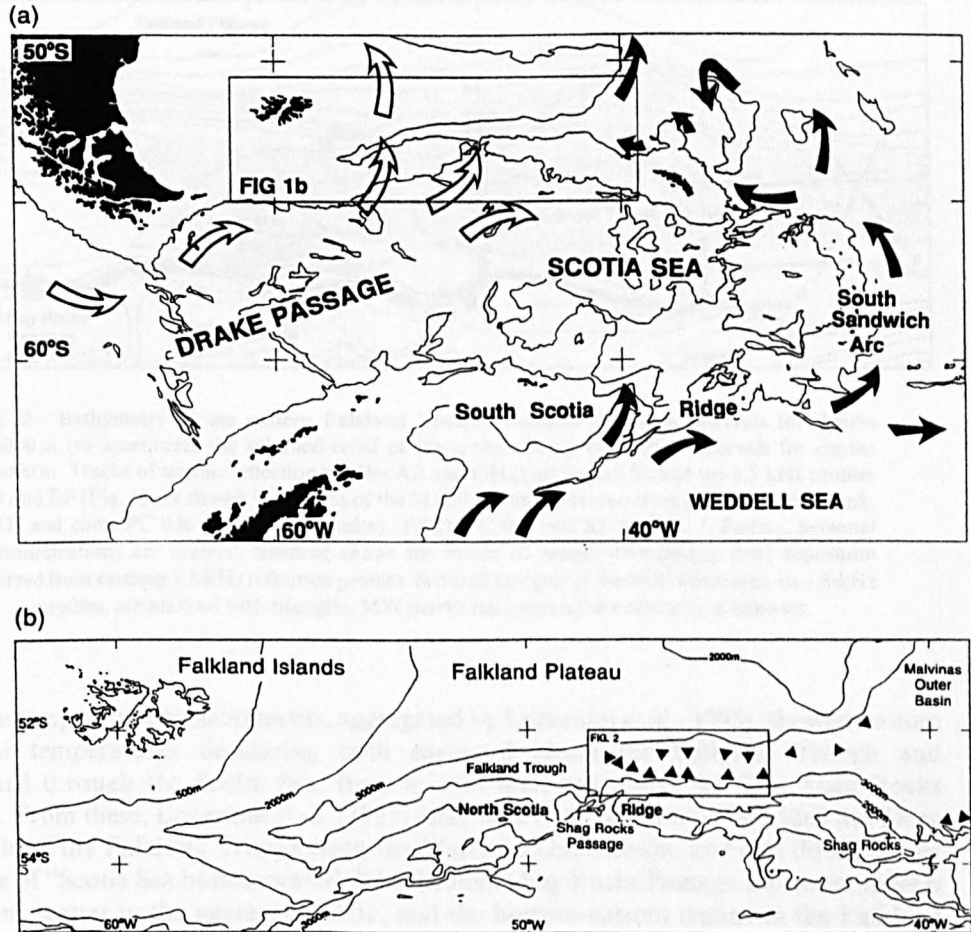


Fig. 1. (a) The western South Atlantic Ocean, with 3000-m isobath. Bottom-flow directions described by Gordon (1966), Hollister and Elder (1969), Georgi (1981), Nowlin and Zenk (1988) and Locarnini *et al.* (1993) shown by open arrows (Antarctic Circumpolar Current) and closed arrows (Weddell Sea Deep and Bottom Water). (b) The Falkland Trough region of the western South Atlantic Ocean, with 500-m, 2000-m and 3000-m isobaths. The area shown in Fig. 2 is outlined and scoured margins of sediment bodies seen on 3.5-kHz profiles are marked with triangles.

Trench and through the Malvinas Outer Basin, also beneath the ACC (Fig. 1a), and eventually into the Argentine Basin and beyond (Georgi, 1981; Mantyla and Reid, 1983).

Direct oceanographic measurements in the vicinity of the Falkland Trough and North Scotia Ridge are few. Zenk (1981) and Wittstock and Zenk (1983) report the results of a year-long current meter mooring (M 259) directly on the 3000-m sill of Shag Rocks Passage at 52°52'S, 48°19'W (Fig. 2). Bottom potential temperatures varied between -0.2°C and $+0.7^{\circ}\text{C}$, and current speeds reached 60 cm s^{-1} ; there was a strong correlation between low potential temperature and strong WNW bottom-current flow at speeds above 15 cm s^{-1} . Zenk (1981) argued for strong northwestward overflow events involving "Scotia Sea bottom water", derived from WSDW after mixing with CDW within the Scotia Sea.

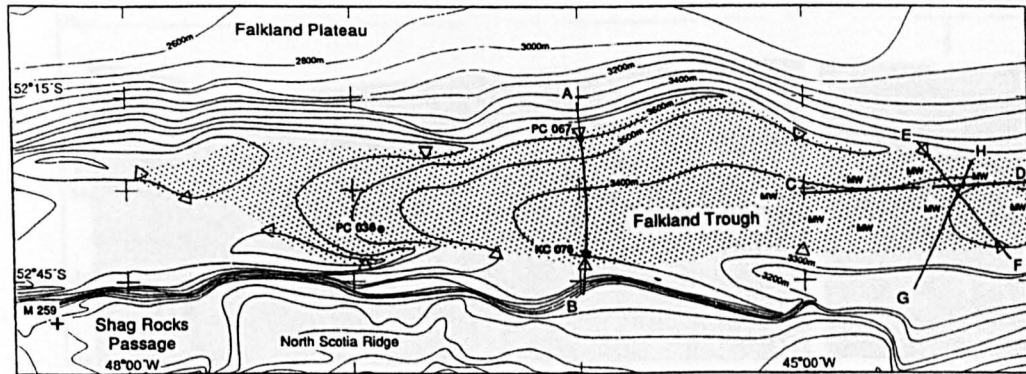


Fig. 2. Bathymetry of the eastern Falkland Trough. Isobaths at 100-m intervals for depths > 3000 m (to accentuate the subdued relief of the trough floor) and 200-m intervals for depths < 3000 m. Tracks of seismic reflection profiles AB and GH (Figs 3a and 5), and the 3.5-kHz profiles CD and EF (Fig. 4) are shown. Locations of the M 259 current meter mooring (Wittstock and Zenk, 1983) and cores PC 036 (Jordan and Pudsey, 1992), PC 067 and KC 075 (C. J. Pudsey, personal communication) are marked. Shading shows the extent of pelagic-hemipelagic drift deposition inferred from existing 3.5-kHz reflection profiles. Scoured margins of the drift, where seen on 3.5-kHz profiles, are marked with triangles. MW marks the approximate extent of mudwaves.

Sparse temperature measurements, aggregated by Locarnini *et al.* (1993), showed bottom potential temperatures decreasing both eastward along the Falkland Trough and southward through the Scotia Sea, from a local high just above 0.2°C in Shag Rocks Passage. From these, Locarnini *et al.* (1993) inferred a westward flow of Weddell Sea Deep Water along the Falkland Trough from the Malvinas Outer Basin, and cast doubt on the existence of "Scotia Sea bottom water" flow through Shag Rocks Passage. However, there is significant scatter in the aggregated data, and the bottom-current regime in the Falkland Trough remains unresolved.

Our own interest is in understanding bottom-current control of sedimentation in this region, and in finding and sampling sedimentary bodies that contain a record of the history of development of the ACC and of southern-origin bottom water (represented now by WSDW). We present here 3.5 kHz high-resolution and seismic-reflection profiles from the Falkland Trough which provide evidence for persistent westward bottom-current flow.

DATA ACQUISITION AND INTERPRETATION

Figure 2 shows a 300-km section of the Falkland Trough located between Shag Rocks Passage and the western margin of the Malvinas Outer Basin (Fig. 1b). Here, the Falkland Trough is approximately 80 km wide at the 3000-m isobath, and its floor lies between 3400- and 3850-m depth. A multichannel seismic (MCS) reflection profile AB (located in Fig. 2 and displayed in Fig. 3a) was acquired during R.R.S. *Discovery* Cruise 172 in 1987. This profile lies along 180°T and crosses the Falkland Trough near 46°W. The 3.5-kHz profile along the southern part of the same track forms Fig. 3b. Two additional 3.5-kHz high-resolution reflection profiles CD, and EF (located in Fig. 2 and displayed in Fig. 4) were acquired during R.R.S. *James Clark Ross* Cruise 04 in 1993 and R.R.S. *Discovery* Cruise

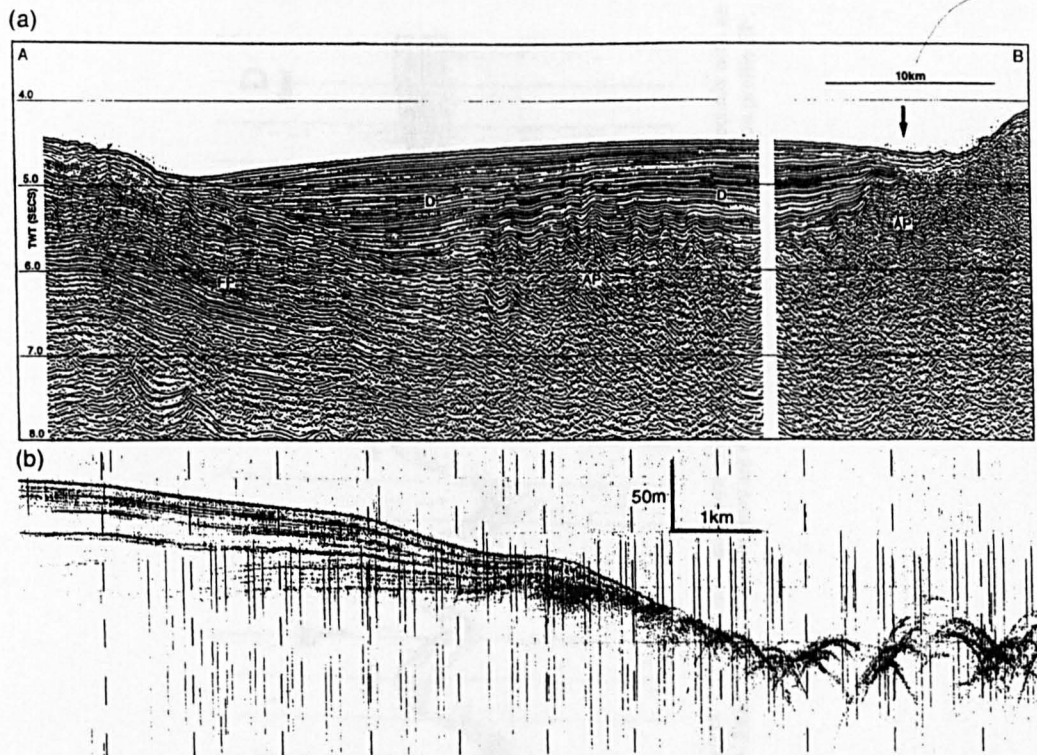


Fig. 3. (a) The MCS reflection profile AB (BAS878-04, VE 7:1 in water). These data were processed to 24-fold common-mid-point stack using standard procedures and imaged using a Stolt F-K time migration algorithm. AP, North Scotia Ridge accretionary prism; D, pelagic-hemipelagic drift sediments; FP, Falkland Plateau sediments. A vertical arrow marks the location of 3.5-kHz data shown in (b). (b) 3.5 kHz high-resolution seismic reflection profile acquired along AB (VE 18:1 in water) showing the southern scour margin of the drift.

172. Profile CD lies along 266°T , coincident with the trough axis. Profile EF lies along 141°T , at a high angle to the east-west trend of the Falkland Trough, and intersects CD on the trough floor near $44^{\circ}20'\text{W}$.

Falkland Trough sediment drift

The floor of the Falkland Trough between 48°W and 42°W is occupied by a well-developed sediment drift. The MCS reflection profile AB (Fig. 3a) shows that this section of the Falkland Trough is underlain by a thick mounded sequence characterised by bright, fairly continuous reflectors (labelled "D", Figs 3 and 5). Towards the southern flank of the trough, these younger sediments overlie the North Scotia Ridge accretionary prism (Ludwig and Rabinowitz, 1982 and labelled "AP", Figs 3 and 5). The older sediments of this thick, mounded sequence, undeformed in the north, may to the south, have been incorporated into the accretionary prism. Towards the north, these sediments lap onto older, southward-dipping sediments of the Falkland Plateau, characterised by bright, coherent but

(a)

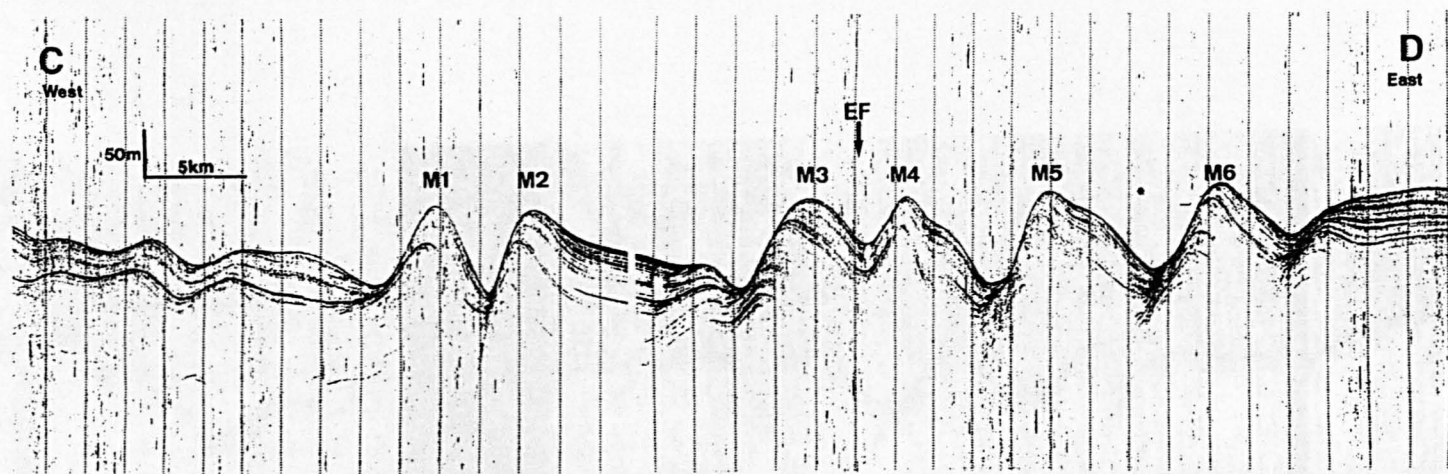
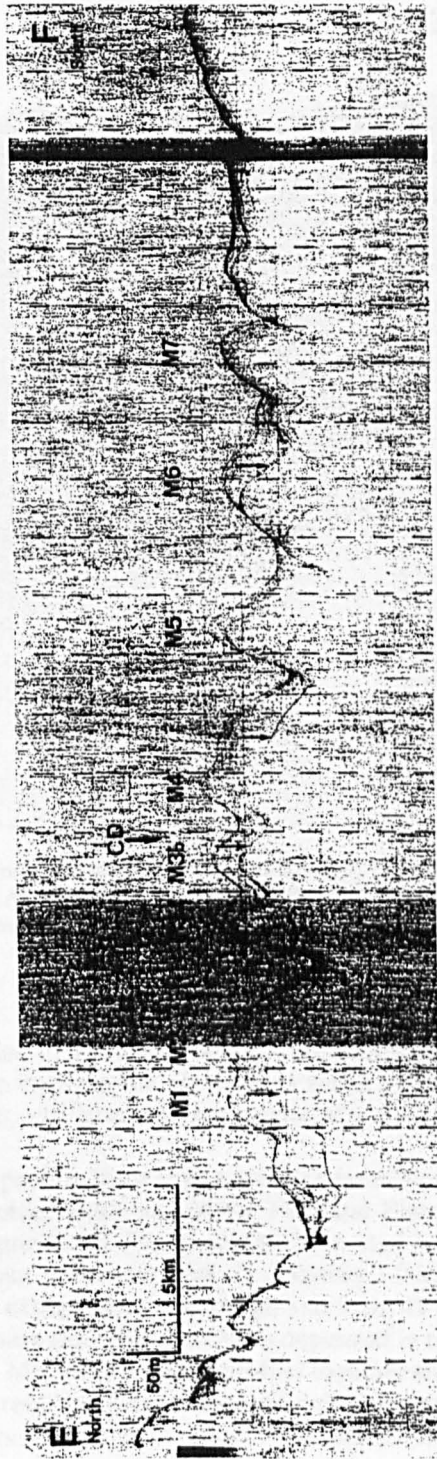


Fig. 4. The 3.5-kHz profiles (a) CD (VE 48:1 in water) and (b) EF (VE 32:1 in water). The point of intersection of these profiles is marked on both records with an annotated vertical arrow. Profile CD contains a recording gap between M2 and M3. Faint sub-bottom reflectors are marked with small vertical arrows on profile EF.



(b)

Fig. 4(b).

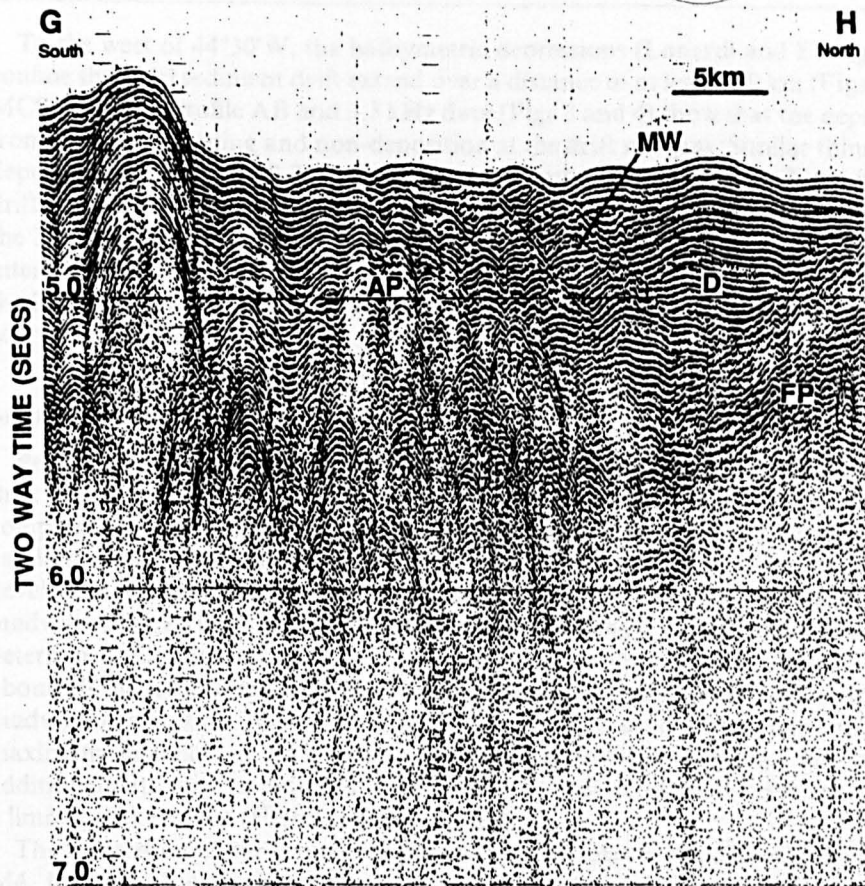


Fig. 5. Single-channel seismic reflection profile GH acquired during R.V. *Robert D. Conrad* Cruise 1606 in 1973 (VE 20:1 in water). AP, deformed surface of North Scotia Ridge accretionary prism; D, pelagic-hemipelagic drift sediments; FP, Falkland Plateau sediments; MW, migrating mudwave stratigraphy.

discontinuous reflectors (labelled "FP", Figs 3 and 5). On profile AB also, the mounded sediments are confined between bathymetric depressions which lie along the northern and southern margins of the trough, and have the appearance of a current-controlled pelagic-hemipelagic sediment drift.

Higher-resolution (3.5 kHz) profiles show high acoustic penetration across the mounded sediments, in contrast to the older sediments of the Falkland Plateau and North Scotia Ridge accretionary prism (e.g. profile EF, Fig. 4), and we have used 3.5-kHz data to map the distribution of these more recent sediments (Fig. 2). Existing 3.5-kHz profiles show that pelagic-hemipelagic sediments extend along the trough axis from 48°W to 43°W. Figures 2 and 3a also demonstrate that these sequences have been deposited in the form of an elongate mound to the west of 44°30'W. MCS and 3.5-kHz profiles together show this feature to be a well-developed sediment drift resulting from prolonged pelagic-hemipelagic deposition in the presence of bottom currents (Cunningham *et al.*, 1992; Barker *et al.*, 1994).

To the west of 44°30'W, the bathymetric depressions (Lonardi and Ewing, 1971) which confine the axial sediment drift extend over a distance of at least 160 km (Figs 2 and 3). The MCS reflection profile AB and 3.5 kHz data (Figs 3 and 4) show that the depressions result from sediment thinning and non-deposition at the drift margins. Similar thinning and non-deposition are seen on all 3.5-kHz profiles crossing the drift (Fig. 2). Towards the east the drift ends, but 3.5 kHz-profiles also show peripheral scouring along the southern margin of the Malvinas Outer Basin (Fig. 1b). We attribute this thinning and non-deposition to an intensification of flow at the base of slope, all along the northern and southern margins of the Falkland Trough and along the eastward continuation of that southern margin into the Malvinas Outer Basin.

Migrating mudwaves

Profiles CD and EF cross a field of migrating bedforms on the surface of the sediment drift within the Falkland Trough in the vicinity of 44°20'W (Fig. 4). These bedforms are comparable in size and morphology to abyssal mudwaves, described by Flood *et al.* (1993) as "large-scale, quasi-sinusoidal, current-related sedimentary features (or bedforms) that develop in fine-grained cohesive sediments". Profiles CD and EF intersect within the mudwave field, so that the true orientation and wavelength of individual mudwaves may be determined. Continuous GPS navigation on both cruises provided positions accurate to about 100 m (Hofmann-Wellenhof *et al.*, 1992), leading to only minor uncertainties in mudwave orientation. We have assumed that the larger bedforms remain continuous over a maximum distance of 14 km when correlating between profiles, but recognise that additional data may be required to verify this, as individual mudwaves are known to have a limited strike extent (Flood and Shor, 1988).

The correlation of five prominent mudwave peaks between profiles CD and EF (M1, M2, M4, M5, M6, Fig. 4) reveals consistent NE–SW crestal alignments between 045°T and 051°T. The M3 mudwave peak on profile CD is represented on profile EF by two smaller and quite distinct mudwave peaks (M3a and M3b). M3 may therefore be discontinuous along strike and has been excluded from estimates of bedform orientation. The NW–SE trending profile EF (Fig. 4) lies almost orthogonal to the dominant mudwave trend, so bedform wavelengths apparent in profile EF are less than those measured on other profiles and are taken as true wavelengths. A seismic-reflection profile GH (Fig. 5) acquired nearly parallel to the wave crests shows very long wavelengths. Measurements between mudwave peaks M1 and M7 show true wavelengths between 2.0 and 5.0 km and peak-to-trough heights between 10 and 95 m. These are similar to the dimensions of mudwaves observed in the Argentine Basin (Flood and Shor, 1988).

Sub-bottom reflectors show a greater accumulation of sediment on the southeastern flanks of most mudwaves (e.g. M1 to M6, profile CD, Fig. 4), which has resulted in the net migration of individual bedforms to the south and east. Mudwaves within the study area show varying degrees of asymmetry from "symmetrical" (e.g. M1 and M2, profile EF, Fig. 4) through "preferential-depositional" (e.g. mudwaves to the west of M1, profile CD, Fig. 4) to "depositional-erosional" forms, which show erosional truncation of near-surface reflectors at the sea bed (e.g. M3, profile CD, Fig. 4). Similar variations in wave symmetry are seen by Flood and Shor (1988) in the Argentine Basin. However, bedform migration directions remain consistently toward the south and east in all areas where migration is clearly discernible. Although mudwaves with heights of 95 m are seen only along Section

CD of the axial 3.5-kHz profile, a similar eastward component of migration is seen consistently within smaller bedforms (heights of < 50 m) elsewhere on this profile.

Profile EF also shows that mudwaves become increasingly symmetric to the north (Fig. 4): symmetric bedforms are considered by Flood and Shor (1988) to reflect a reduction in asymmetric deposition, perhaps from reduced bottom-current speeds or perhaps by alternating deposition between mudwave flanks. There is no evidence of sediment ponding within existing mudwave troughs or recent erosion of higher accumulation mudwave flanks, and we conclude that the processes maintaining these bedforms were active recently and may remain active today.

Profile CD shows buried mudwave reflectors to the limit of 3.5-kHz penetration in this area (e.g. M3, profile CD, Fig. 4). Furthermore, a single-channel seismic-reflection profile (Profile GH, located in Fig. 2 and displayed in Fig. 5) acquired across the mudwave field during R.V. *Robert D. Conrad* Cruise 1606 suggests that a mudwave morphology extends to greater depths. Though of limited stratigraphic resolution, profile GH appears to show migrating bedforms (labelled "MW", Fig. 5) extending to a depth of at least 400 ms two-way-time (equivalent to 400 m, assuming a speed of sound in sediments of 2000 m s^{-1}), which is a significant proportion of the recent pelagic-hemipelagic section (labelled "D", Fig. 5).

DISCUSSION AND CONCLUSIONS

Mudwaves have been associated with ambient thermohaline current flow across sediment drifts (Flood *et al.*, 1993) and turbidity current flow across deep-sea channel levees (Damuth, 1979; Normark *et al.*, 1980). At present, no sediment samples or current measurements have been obtained from the mudwave site in the eastern Falkland Trough. However, we consider it probable that the mudwaves were formed by ambient westward bottom-current flow on the basis of their regional setting and likely lithology.

The mudwaves have formed at the surface of a sediment drift, and we interpret the mounded geometry of this feature as being consistent with deposition from ambient bottom currents. Although existing studies have not yet resolved the bottom-current regime in the Falkland Trough, there is evidence of northward flow of WSDW nearby to the east (Georgi, 1981), and the westward flow of WSDW along the eastern Falkland Trough has been inferred from oceanographic measurements (Locarnini *et al.*, 1993). Furthermore, sediment cores obtained nearby support an ambient bottom-current origin for the mudwaves. Piston core PC 036 (Fig. 2) obtained from the sediment drift is largely biogenic in composition and shows no evidence (sedimentary structures or grading) of turbidity flows (Jordan and Pudsey, 1992). This is also apparent in unpublished data from two additional cores (PC 067 and KC 075, Fig. 2) obtained at the drift margins (C. J. Pudsey, personal communication). We consider it likely that these cores would contain turbidites if the nearby mudwaves were recently maintained by thick turbidity flows such as those described by Normark *et al.* (1980).

Migrating mudwaves have been associated with persistent bottom-current flow over fine-grained sediment drifts, at velocities in the range $9\text{--}30 \text{ cm s}^{-1}$ (Flood, 1988). Recent models of mudwave dynamics (Blumsack and Weatherly, 1989; Blumsack, 1993) derived from the lee-wave model of Flood (1988) predict that mudwaves growing in the southern hemisphere will form at an angle anti-clockwise from the prevailing bottom-flow direction, and will migrate up-current and to the left of the current (Flood *et al.*, 1993). The 3.5-kHz profiles

CD and EF show mudwaves presently orientated in a NE–SW direction which have clearly migrated toward the south and east (Fig. 4). The seismic-reflection profile GH (Fig. 5) has limited seismic resolution and does not show small-scale features clearly. However, profile GH shows an apparent S component of mudwave migration which is compatible with the 3.5-kHz profiles. If a principal mudwave migration direction to the southeast is assumed, the models predict a prevailing westward flow of bottom water along the axis of the Falkland Trough. Sediment thinning and non-deposition along the southern flank of the trough (the northern margin of the North Scotia Ridge) is presumed related to an intensification of this westward flow. These observations are consistent with the flow of WSDW from the Malvinas Outer Basin as suggested by Locarnini *et al.* (1993), with intensification along the boundary. The WNW flow reported at the northern edge of Shag Rocks Passage (Fig. 2) by Zenk (1981), which becomes colder as it intensifies to 60 cm s^{-1} , may be the same feature resulting from westward flow in the trough, rather than from northwestward overflow into the trough. The velocities measured at the mooring ranged higher than those usually associated with mudwave formation, and are compatible with the non-deposition observed along the southern trough margin.

The origin of the similar thinning and non-deposition seen on all crossings of the northern margin of the Falkland Trough drift is less certain. The more symmetric mudwaves towards the northern margin on Profile EF (Fig. 4) suggest a northward reduction in westward velocity, leading perhaps to eastward flow at the northern margin. Locarnini *et al.* (1993) suggest eastward return flow of WSDW to the Malvinas Outer Basin along this margin. However, it has long been suggested that non-deposition over the Falkland Plateau resulted from strong bottom currents associated with the ACC (e.g. Saito *et al.*, 1974; Barker *et al.*, 1976), and no other drift, which might reflect a more northerly locus of slack water, is seen. Thus, non-deposition at the northern margin of the Falkland Trough may be caused by returning WSDW, or by eastward-flowing CDW within the ACC.

Mudwaves are recognised as a long-term response to quasi-stable environmental conditions, and studies suggest that individual bedforms require tens to hundreds of thousands of years to develop (Flood and Shor, 1988). Figure 4 demonstrates that a mudwave morphology extends to depths of at least 100 m below the present-day seafloor. Furthermore, the single-channel seismic-reflection profile GH (Fig. 5) suggests that a migrating mudwave morphology extends through much of the reflective pelagic-hemipelagic drift developed within the eastern Falkland Trough. The westward flow of southern-origin bottom water may have persisted through several glacial cycles and for much of the life of the drift. The age of onset of drift deposition along the trough axis is uncertain, but some loose constraint is available. Seismic-reflection profiles show the drift overlying and perhaps coeval with deformed sediments of the North Scotia Ridge accretionary prism (Ludwig and Rabinowitz, 1982). Barker *et al.* (1984, 1991) suggest that the northward migration of the North Scotia Ridge, which generated the accretionary prism, ceased about 6 Ma ago, when seafloor spreading stopped in the Central Scotia Sea and Drake Passage. It seems likely, therefore, that the drift and the migrating stratigraphy within it, apparent in Figs 4 and 5, provide a depositional record of southern-origin bottom water extending back for several million years.

In summary, 3.5-kHz and seismic-reflection profiles show a mudwave field developed within a sediment drift in the eastern Falkland Trough. An active mudwave morphology preserved at the present-day seabed suggests persistent westward flow that probably continues today; non-deposition at the southern drift margin suggests intensified flow. This

is consistent with the westward flow of WSDW along the Falkland Trough from the Malvinas Outer Basin, as suggested by Locarnini *et al.* (1993), and may also explain the westward flow recorded in Shag Rocks Passage by Zenk (1981). However, the fate of the west-flowing WSDW in the Falkland Trough, and the cause of scour along the northern margin of the drift, remain uncertain. The mudwaves extend several hundred metres beneath the sea floor, and provide a long-term depositional record of southern-origin bottom water and its possible interaction with the ACC.

Acknowledgements—We thank the officers, crew and scientists who participated in R.R.S. *Discovery* Cruise 172 and R.R.S. *James Clark Ross* Cruise 04 for assistance in obtaining the original data, and Research Vessel Services, Barry for technical support. The R.V. *Robert D. Conrad* Cruise 1606 profile was kindly supplied by the ODP Data Bank at the Lamont-Doherty Earth Observatory. We also thank Ricardo Locarnini and Marion Barber for advice on the physical oceanography and Rob Larter for comments on the interpretations. Carol Pudsey and John Howe provided additional advice on piston cores. We also wish to express our gratitude for comments provided by two anonymous reviewers.

REFERENCES

- Barker P. F., P. L. Barber and E. C. King (1984) An early Miocene ridge crest–trench collision on the South Scotia Ridge near 36°W. *Tectonophysics*, **102**, 315–332.
- Barker P. F., A. P. Cunningham, R. D. Larter and C. J. Pudsey (1994) Sediment records of ACC variability and WSDW interaction in the northern Scotia Sea and Falkland Trough (abs.). *Berichte aus dem Fachbereich Geowissenschaften, Universität Bremen*, **52**, 17.
- Barker P. F., I. W. D. Dalziel and B. C. Storey (1991) Tectonic development of the Scotia arc region. In: *The geology of Antarctica*, Oxford monographs on geology and geophysics, Vol. 17, R. J. Tingey, editor, Oxford University Press, New York, pp. 215–248.
- Barker P. F., I. W. D. Dalziel and Shipboard Scientific Party (1976) Evolution of the southwestern Atlantic Ocean basin: results of Leg 36, Deep Sea Drilling Project. In: *Initial reports of the Deep Sea Drilling Project*, Vol. 36, P. F. Barker, I. W. D. Dalziel *et al.*, editors, U.S. Government Printing Office, Washington, DC, pp. 993–1014.
- Blumsack S. (1993) A model for the growth of mudwaves in the presence of time-varying currents. *Deep-Sea Research I*, **40**, 963–974.
- Blumsack S. and G. L. Weatherly (1989) Observations and growth mechanisms for mudwaves. *Deep-Sea Research*, **36**, 1327–1339.
- Cunningham A. P., J. S. Tomlinson and P. F. Barker (1992) The disposition of pelagic hemipelagic sediments in the Falkland Trough and implications for palaeo-circulation (abs.). *Eos. Transactions of the American Geophysical Union*, **73**(suppl.), 286.
- Damuth J. E. (1979) Migrating sediment waves created by turbidity currents in the northern South China Basin. *Geology*, **7**, 520–523.
- Flood R. D. (1988) A lee wave model for deep-sea mudwave activity. *Deep-Sea Research*, **35**, 973–983.
- Flood R. D. and A. N. Shor (1988) Mud waves in the Argentine Basin and their relationship to regional bottom circulation patterns. *Deep-Sea Research*, **35**, 943–971.
- Flood R. D., A. N. Shor and P. D. Manley (1993) Morphology of abyssal mudwaves at Project Mudwaves sites in the Argentine Basin. *Deep-Sea Research II*, **40**, 859–888.
- Georgi D. T. (1981) Circulation of bottom waters in the southwestern South Atlantic. *Deep-Sea Research*, **28A**, 959–979.
- Gordon A. L. (1966) Potential temperature, oxygen and circulation of bottom water in the Southern Ocean. *Deep-Sea Research*, **13**, 1125–1138.
- Hofmann-Wellenhof B., H. Lichtenegger and J. Collins (1992) *Global positioning system theory and practice*. Springer, Vienna, 326 pp.
- Hollister C. D. and R. B. Elder (1969) Contour currents in the Weddell Sea. *Deep-Sea Research*, **16**, 99–101.
- Jordan R. W. and C. J. Pudsey (1992) High-resolution diatom stratigraphy of Quaternary sediments from the Scotia Sea. *Marine Micropaleontology*, **19**, 201–237.

- Locarnini R. A., T. Whitworth III and W. D. Nowlin (1993) The importance of the Scotia Sea on the outflow of Weddell Sea Deep Water. *Journal of Marine Research*, **51**, 135-153.
- Lonardi A. G. and M. Ewing (1971) Sediment transport and distribution in the Argentine Basin. 4. Bathymetry of the continental margin, Argentine Basin and other related provinces. Canyons and sources of sediments. In: *Physics and chemistry of the Earth*, Vol. 8, L. H. Ahrens, S. K. Runcorn and H. C. Urey, editors, Pergamon Press, Oxford, pp. 18-121.
- Ludwig W. J. and P. D. Rabinowitz (1982) The collision complex of the North Scotia Ridge. *Journal of Geophysical Research*, **87**, 3731-3740.
- Mantyla A. W. and J. L. Reid (1983) Abyssal characteristics of the world ocean waters. *Deep-Sea Research*, **30**, 805-833.
- Normark W. R., G. R. Hess, D. A. V. Stow and A. J. Bowen (1980) Sediment waves on the Monterey Fan levee: a preliminary physical interpretation. *Marine Geology*, **37**, 1-18.
- Nowlin W. D. and W. Zenk (1988) Westward bottom currents along the margin of the South Shetland Island Arc. *Deep-Sea Research*, **35**, 269-301.
- Peterson R. G. and T. Whitworth III (1989) The Subantarctic and Polar Fronts in relation to deep water masses through the southwestern Atlantic. *Journal of Geophysical Research*, **94**, 10,817-10,838.
- Saito T., L. H. Burckle and J. D. Hays (1974) Implications of some pre-Quaternary sediment cores and dredgings. In: *Studies in paleo-oceanography*, Society of Economic Paleontologists and Mineralogists Special Publication, No. 20, W. W. Hay, editor, SEPM, Tulsa, pp. 6-35.
- Wittstock R.-R. and W. Zenk (1983) Some current observations and surface T/S distribution from the Scotia Sea and the Bransfield Strait during early austral summer 1980/1981. *Meteor Forschungs-Ergebnisse, Reihe A/B*, **24**, 77-86.
- Zenk W. (1981) Detection of overflow events in the Shag Rocks Passage, Scotia Ridge. *Science*, **213**, 1113-1114.

SEDIMENT RECORDS OF ACC VARIABILITY & WSDW INTERACTION IN THE NORTHERN SCOTIA SEA AND FALKLAND TROUGH

P.F. Barker, A.P. Cunningham & R.D. Larter

British Antarctic Survey, Madingley Road, Cambridge CB3 0ET, UK

The Antarctic Circumpolar Current (ACC) is the main means of interchange of water between the Pacific, Atlantic and Indian Oceans, and appears also to control the degree of isolation of the Antarctic water masses from others farther north. Although in the past other channels (eg. Panama, N of Australia) may have been significant, the ACC has performed these functions ever since a deep-water pathway was created at Drake Passage and through the Scotia Sea, in the early Miocene.

The ACC axis runs eastward through northern Drake Passage, striking north through the North Scotia Ridge near 48°W and continuing east along the Falkland Trough, where it interacts with northward-flowing Weddell Sea Deep Water - WSDW. In much of this region, the ACC is sufficiently vigorous to prevent deposition, or to cause major re-erosion. However, areas have been identified in the Scotia Sea and Falkland Trough where deposition appears continuous but varied, reflecting changes in the strength of the ACC and its interaction with southern-origin bottom waters, over several million years. We present here a preliminary interpretation of seismic reflection and GLORIA sidescan data from three areas in particular: a bank near 54°S, 48°W in the northern Scotia Sea, a well-developed drift between 48°W and 45°W in the Falkland Trough and the eastern margin of the Falkland Plateau near 52°S, 41°W, where ACC and WSDW interact. A complementary poster describes sediment cores from the same areas.

In particular, mud waves at the seabed near 44°W in the Falkland Trough indicate westward flow, probably a loop of WSDW. A separate, buried field of mud waves within the drift near 47°W, with a similar polarity, reflects a period in the past when westward penetration of northward-flowing bottom water along the Falkland Trough was more marked.

SEDIMENT RECORDS OF LONG-TERM
VARIATION IN ANTARCTIC CIRCUMPOLAR
CURRENT FLOW, AND INTERACTION WITH
SOUTHERN-ORIGIN BOTTOM WATER, IN THE
SCOTIA SEA AND SW ATLANTIC

Barker, P.F. and Cunningham, A.P., British Antarctic
Survey, Madingley Road, Cambridge CB3 0ET, UK.

We have examined a range of depositional environments in the Scotia Sea and SW Atlantic, that might contain a record of long-term variation of the Antarctic Circumpolar Current (ACC) and its interaction with Southern-origin Bottom Water (SOBW). Seismic reflection profiles and GLORIA data are used to describe these sediment bodies, and the evidence of piston cores and moored current meters (see complementary posters, Howe and Pudsey; Pudsey and Howe; Cunningham and Barker) helps define their origins. The ACC flows rapidly east and northeast through the constriction of Drake Passage and along the southern margin of the North Scotia Ridge. Where it can, it swings north across the North Scotia Ridge, into the Falkland Trough and eastward over the Falkland Plateau. Sedimentation beneath the ACC is confined mainly to current-bounded drift deposits; we have examined three such, in the northern Scotia Sea and Falkland Trough, and along the southeast margin of the Falkland Plateau. In the northern Scotia Sea, a current-bounded drift deposit contains a 700 m-thick sequence on 24 Myr old ocean floor. Along the axis of the eastern Falkland Trough, a symmetric drift contains a high-resolution record of ACC-SOBW interaction extending back over 10 Myr or more, in a sequence up to 2 km thick. The southeastern margin of the Falkland Plateau shows a significant (>15:1) contrast in rates of sedimentation between a thick abyssal section controlled by a sluggish SOBW circulation and a thinner slope section controlled by the ACC, on basement more than 90 Myr old. The history of this interaction, extending back in theory to before the presumed 36 Ma origin of SOBW, is well-defined by the sediment geometry. In combination, these three drift deposits contain a record of ACC and SOBW flow since their inception, in proximal positions directly downstream from Drake Passage, the presumed final barrier to complete circumpolar deep-water flow.

THE STRUCTURE OF AURORA BANK (47W,53S).

A.P. Cunningham, R.W. Woollett, J.S. Tomlinson and P.F. Barker, British Antarctic Survey, High Cross, Madingley Road, Cambridge CB3 0ET, U.K.

The B.A.S. Marine Geophysics Section is presently concerned with problems relating to Scotia Sea evolution and palaeo-circulation with particular emphasis on the initiation and development of the Antarctic Circumpolar Current (ACC). Models of Scotia Sea evolution have established the importance of the Aurora Bank section of the North Scotia Ridge (NSR) to the initiation of the ACC during the early Miocene. The NSR consists of a series of islands and submarine ridges that broadly delineate the boundary between the Scotia and South American Plates to the South and East of the Falkland Islands. Present relative motion along this boundary is predominantly sinistral strike-slip. GLORIA sidescan sonar images acquired during RRS *Charles Darwin* Cruise 37 confirm the existence of an accretionary prism associated with northward convergent motion across this boundary during the Cenozoic. Complementary multichannel seismic reflection data suggest Aurora Bank itself to consist of a basement block largely obscured by uplifted and deformed sediment. The large and continuous gravity low revealed by Geosat data demonstrates the continuity of the accretionary prism. Refined gravity data from Aurora Bank have been used in conjunction with the multichannel seismic reflection data to investigate the nature and extent of both the basement and uplifted sediments that together constitute this section of the NSR.

0310-8 1030h

The Disposition of Pelagic-Hemipelagic Sediments in the Falkland Trough and Implications for Palaeo-Circulation

A P Cunningham J S Tomlinson and P F Barker (British Antarctic Survey, High Cross, Madingley Road, Cambridge CB3 0ET, UK.)

Scotia Sea reconstructions have already established the importance of a deep gap in the North Scotia Ridge at 49W to the development of the Antarctic Circumpolar Current (ACC). This gap together with the adjacent Falkland Trough now constitutes an established pathway for the ACC. GLORIA sidescan sonar data acquired during R.R.S. Charles Darwin Cruise 37 and accompanying seismic reflection data suggest a central part of the Falkland Trough to be non-depositional, functioning largely as a conduit for terrigenous sediments derived from the South American continental margin. Multichannel seismic reflection profiles suggest the axis of the Falkland Trough to become progressively buried to the East of 49W by a mound of younger, partly biogenic sediment. The mound locally exhibits a complex fill seismic facies and up-sequence changes in facies type suggest variations in bottom current velocity. High resolution 3.5KHz reflection profiles suggest the mound consists of finer-grained material than the underlying Falkland Trough sediments exposed at the seabed to the West. In both composition and form, this overburden reflects the influence of an evolving ACC.

EVIDENCE FOR WESTWARD-FLOWING
WEDDELL SEA DEEP WATER IN THE
FALKLAND TROUGH, WESTERN SOUTH
ATLANTIC

Cunningham, A. P. and P. F. Barker, British Antarctic Survey, Madingley Road, Cambridge CB3 0ET, United Kingdom.

The North Scotia Ridge controls the eastward and northward flow of the Antarctic Circumpolar Current (ACC) emerging from Drake Passage. Existing physical oceanographic data in this region are sparse, and do not define the flow pattern of Circumpolar Deep Water (CDW) within the ACC, or of Weddell Sea Deep Water (WSDW) heading northward beneath it, in the region of the North Scotia Ridge and Falkland Trough. 3.5 kHz reflection profiles show mudwaves at the surface of a sediment drift along the axis of the eastern Falkland Trough, that have a consistent NE-SW alignment and are migrating SE, indicating persistent westward bottom current flow along the trough axis. Sediment thinning and non-deposition at the southern drift margin indicate intensified westward flow, considered to be Weddell Sea Deep Water from the Malvinas Outer Basin to the east. This flow probably continues to 48°W, but beyond there its fate is unknown. Similar non-deposition along the northern margin of the drift is considered to result from eastward flow of CDW. Companion posters (Howe and Pudsey, Pudsey and Howe, Barker and Cunningham) show core data from this drift, and evidence of buried mudwaves that demonstrate the persistence of the factors controlling drift formation.

GLORIA IMAGERY OF THE NORTH SCOTIA RIDGE

I.S. Tomlinson, A.P. Cunningham and P.F. Barker, British Antarctic Survey, High Cross, Madingley Road, Cambridge CB3 0ET, U.K.

A GLORIA mosaic covering part of the North Scotia Ridge, Falkland Trough and Falkland Plateau was built up using passage lines to and from the Falkland Islands during *RRS Charles Darwin* Cruise 37, in 1989. The North Scotia Ridge (NSR) is a series of islands and submarine ridges that form the present boundary between the South American and Scotia plates. Present relative motion is largely east-west strike-slip, but an accretionary prism on the northern flank of the NSR, marked by a large and continuous free-air gravity low, results from northward convergent motion across this boundary during much of the Cenozoic. The GLORIA image shows well-developed folding in its western part, within sediment probably derived largely from South America. Farther east the folding dies out: MCS profiles show the deformed sediment buried beneath a mound of younger, partly biogenic sediment. In both composition and form, this overburden reflects the northward transit of the NSR by the Polar Front and Antarctic Circumpolar Current axis, through a gap in the NSR at 49°W.

APPENDIX B

MAP_SYS map projection software

In the course of this study, a geophysical data plotting program 'MAP_SYS' was written by the author and Richard Woollett (formerly of British Antarctic Survey Geoscience Division, BASGD) to plot shotpoint navigation, bathymetry, gravity, magnetic and satellite altimetry data on a series of standard geographical maps (including Mercator, Lambert conformal conic, polar stereographic and azimuthal equidistant projections). The computer program was written in standard FORTRAN 77 for use with the Graphical Kernel System graphics library, and consists of more than 11000 lines of original source code. Before the introduction of the GMT package of Wessel & Smith (1991), MAP_SYS was the principal software package used by BASGD marine geoscientists to plot marine geophysical data. This appendix includes the MAP_SYS header program, and some published examples of MAP_SYS maps.

```

C
C Program Map_sys.for
C -----
C
C Program Map_sys.for is intended to be a general
C purpose plotting program.
C
C
C Program details
C -----
C
C OS VMS
C Language Fortran 77 + GKS + sub_lib
C
C Authors R.W.Woollett, A.P.Cunningham
C Date 4 th April 1990
C
C
C--- SET NUMBER OF CRUISES + SECTIONS OF
C--- CRUISES TO BE ACCOMMODATED
C
C PARAMETER ( NCRUMX = 99, NSCTMX = 50, NCOL = 10, IATLMX = 5000,
1 ICNMAX = 495, NGEOMX = 100 )
C
C--- DEFINE VARIABLE TYPES
C
C CHARACTER*10 ELNAME
C
C CHARACTER*40 BTHFIL( 60 ), FILNAM( NCRUMX ), QFILE1, QFILE2,
1 SHOTFL( 50 ), GEOINF, ATLFIL( 60 ), GEOFIL( 200 ),
2 DRGFIL
C
C INTEGER DEVNUM, TIMINT, WIGINT
C
C INTEGER NSECT(NCRUMX), STRTDY( NCRUMX, NSCTMX),
1 ENDDY( NCRUMX, NSCTMX), ICOLOR( NCOL ),
2 SHOTAN, SHOTMK
C
C LOGICAL ANNOT, HEADR, JULI, ORIENT, PARAMS, SHPTRK, STYLE, TIME,
1 TIMELT, TRACK, WIGGLE, BATHMY, QFLAG, SHFLAG, GEOSAT,
2 GEOCYC, GEOCLP, ATLDAT, TECMAP, CRUPLT, SHDDIF, DREDGE
C
C REAL NLAT
C
C REAL STRTFR( NCRUMX, NSCTMX ), ENDFR( NCRUMX, NSCTMX ),
1 ANGLES( NCRUMX, NSCTMX ), ATLLAT( IATLMX ),
2 ATLLON( IATLMX ), XATS( ICNMAX ), YATS( ICNMAX ),
3 XGEOS( NGEOMX ), YGEOS( NGEOMX )
C
C REAL*8 OLAT, OLON, SLAT1, SLAT2, CSFACT,
1 CLAT1, CLON1, CLAT2, CLON2, AZIM,
2 EQRAD, ECC
C
C--- DEFINE PROGRAM UNITS COMMON BLOCK
C
C COMMON /UNITS/ LGIN, LGOUT, LGDEV, LGDAT
C
C--- DEFINE COLOUR SCHEME COMMON BLOCK

```

```

C
COMMON /COLOUR/ ICOLOR
C
C---- DEFINE MAP PROJECTION COMMON BLOCKS
C
COMMON /PROJ/ IPROJ, IELPSE, SCALE, SCALMM
COMMON /MAPC01/ OLAT, OLON, SLAT1, SLAT2, CSFACT
COMMON /MAPC02/ CLAT1, CLON1, CLAT2, CLON2, AZIM
COMMON /SPHCON/ EQRAD, ECC
C
C---- DEFINE DEVICE COMMON BLOCK
C
COMMON /DEVICE/ META, DEVNUM, DVSIZX, DVSIZY, SIZXMM, SIZYMM
C
C---- DEFINE MARKER CHARACTERISTICS COMMON BLOCK
C
COMMON /MARK/ MRKTYP, SIZMRK
C
C---- DEFINE MAP REGION COMMON BLOCK
C
COMMON /AREA/ WLON, ELON, SLAT, NLAT, XMIN, XMAX, YMIN, YMAX
COMMON /SHIFT/ XORIGN, YORIGN, XSHIFT, YSHIFT
COMMON /BNDRY/ IBDR, IBDRWD, IBRINT
COMMON /GRDDEF/ IGRAT, IDGMN, TICKSZ
COMMON /GRDINT/ IGRDLT, IGRDLN, IGRDCH
COMMON /ANNOA/ ANNOT
COMMON /ANNOX/ ANNTHT
C
C---- DEFINE SHIP TRACK COMMON BLOCK
C
COMMON /CRUSCT/ NCRUIS
COMMON /TRCK/ SHPTRK, TRACK, TIME, TIMELT, JULI, PARAMS,
1 WIGGLE, ORIENT, STYLE, CRUPLT, SHDDIF
COMMON /PARAM/ MODE, IFRMT, IDATA, TIMINT, SCALPM, ZERO, XSEPA,
1 YSEPA, WIGINT
COMMON /CENTRY/ ICENT
C
C---- DEFINE GEBCO BATHYMETRY COMMON BLOCK
C
COMMON /GEBCOF/ BTHFIL
COMMON /GEBCOI/ IBTHFL
COMMON /GEBCOL/ BATHMY
C
C---- DEFINE EARTHQUAKE DATA COMMON BLOCKS
C
COMMON /EQUAKE/ QFLAG
COMMON /FQUAKE/ QFILE1, QFILE2
C
C---- DEFINE SHOT POINT LOCATION COMMON BLOCKS
C
COMMON /FSHOT/ SHOTFL
COMMON /ISHOT/ NSHOTF, SHOTAN, SHOTMK
COMMON /LSHOT/ SHFLAG
C
C---- DEFINE GEOSAT COMMON BLOCKS
C
COMMON /GEOSTC/ GEOINF
COMMON /GEOSTI/ IGEOFM, IGEOCY

```

```

COMMON /GEOSTL/ GEOSAT, GEOCYC, GEOCLP
COMMON /GEOSFL/ GEOFIL
COMMON /GEOPLT/ IGEOTP, GEOSCL, GEOSEP, GEOLIM
C
C---- DEFINE ATLAS FORMAT COMMON BLOCKS
C
COMMON /ATLASF/ ATLFIL
COMMON /ATLASI/ IATLFL
COMMON /ATLASL/ ATLDAT, TECMAP
COMMON /ATLASM/ HIMARK
C
C---- DEFINE DREDGE PLOT COMMON BLOCKS
C
COMMON /DRDGEL/ DREDGE
COMMON /DRDGEF/ DRGFIL
C
C---- MISCELLANEOUS COMMON BLOCKS
C
COMMON /HDR/ HEADR
C
C---- DEFINE PROGRAM UNITS
C
DATA LGIN, LGOUT, LGDEV, LGDAT / 5, 6, 7, 8 /
C
C---- DEFINE DEFAULT MARKER CHARACTERISTICS
C
DATA MRKTYP, SIZMRK / 1, 2.0 /
C
C---- DEFINE ORIGIN SHIFT
C
DATA XSHIFT, YSHIFT / 30.0, 25.0 /
C
C---- DEFINE CENTURY OF SHIP TRACK DATA
C
DATA ICENT /1900/
C
C---- OUTPUT INTRODUCTORY MESSAGE
C
CALL INTRO
C
C---- INPUT COMMAND FILE
C
CALL MAPRD( NCRUMX, NSCTMX, FILNAM, NSECT, STRTDY, ENDDY,
1 STRTFR, ENDFR, ANGLES )
C
C---- INITIALIZE GRAPHICS
C
CALL SETGKS( IGKSNO )
C
C---- DEFINE ELLIPSOID
C
CALL ELSOID( IELPSE, ELNAME )
C
C---- DETERMINE SIZE OF GRATICULE
C
CALL CORNER
C
C---- DEFINE PLOT ORIGIN

```

```

C
CALL ORIGIN
C
C--- PLOT GRID
C
CALL GRIDPT
C
C--- WRITE PARAMETERS TO HEADER
C
IF(HEADR)THEN
CALL HEADER( ELNAME )
END IF
C
C--- PLOT SHIP'S TRACK + PARAMETERS
C
IF(SHPTRK)THEN
CALL TRCKPT( NCRUMX, NSCTMX, FILNAM, NSECT, STRTDY, ENDDY,
1 STRTFR, ENDFR, ANGLES )
END IF
C
C--- PLOT GEBCO BATHYMETRY
C
IF(BATHMY)THEN
CALL GEBPLT
END IF
C
C--- PLOT SHOT POINT LOCATIONS
C
IF(SHFLAG)THEN
CALL SNPLOT
END IF
C
C--- PLOT EARTHQUAKE LOCATIONS
C
IF(QFLAG)THEN
CALL QPLOT
END IF
C
C--- PLOT GEOSAT DATA
C
IF(GEOSAT)THEN
C
IF(IGEOFM.EQ.1)THEN
C
C--- PLOT LEEDS DATA
C
CALL GEOSLD( XGEOS, YGEOS, NGEOMX )
C
ELSE IF(IGEOFM.EQ.2)THEN
C
C--- PLOT OXFORD DATA
C
CALL GEOSOX( XGEOS, YGEOS, NGEOMX )
C
END IF
C
END IF
C

```

```
C--- PLOT ATLAS FORMAT DATA
C
C   IF(ATLDAT)THEN
C     CALL ATLAS( ATLLAT, ATLLON, IATLMX, XATS, YATS, ICNMAX )
C   END IF
C
C--- PLOT DREDGE SITES
C
C   IF(DREDGE)THEN
C     CALL DRGPLT
C   END IF
C
C--- CLOSE GRAPHICS
C
C   CALL CLSGKS
C
C   STOP
C   END
```

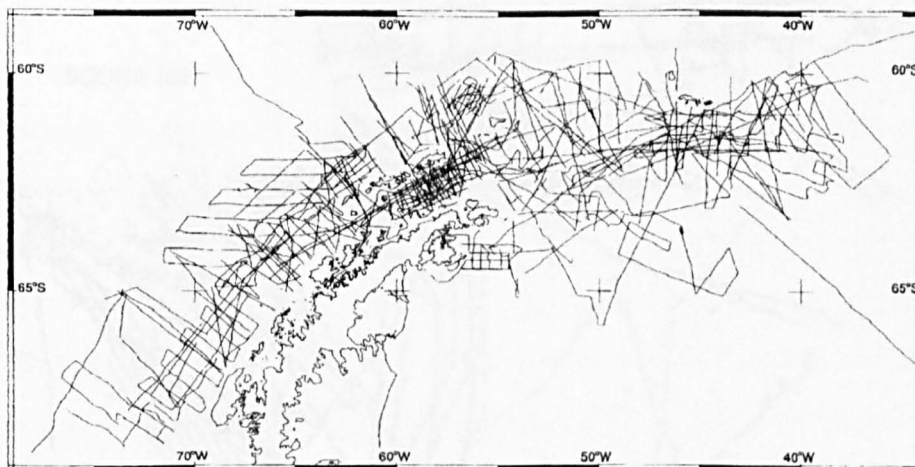


Fig. 1. The ANTOSTRAT Antarctic Peninsula Regional Working Group digital navigation compilation shown with a coastline taken from the Antarctic Digital Database [BAS, SPRI and WCMC, 1993]. These data illustrate the distribution of single and multichannel seismic reflection data acquired across and adjacent to the continental margin of the Antarctic Peninsula by 12 participating agencies (Table 1).

From: Cunningham, A.P., Vanneste, L.E. & the ANTOSTRAT APRWG 1995. The ANTOSTRAT Antarctic Peninsula Regional Working Group digital navigation compilation. In: Cooper, A.K. & Barker, P.F. (eds), *Geology and Seismic Stratigraphy of the Antarctic Margin*, AGU Antarctic Research Series, 68, A297.

292

PETER F. BARKER

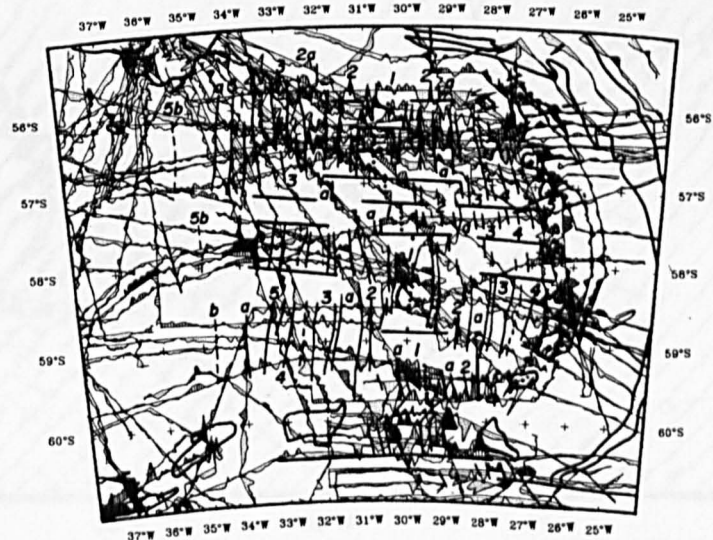


FIGURE 7.6. Magnetic anomalies in the East Scotia Sea region, projected along ship tracks (solid line ornament for positive values). Identified anomalies are marked and major anomalies numbered. For ease of identification, the ridge crest is dotted, where seen on bathymetric profiles or in Fig. 7.5, and anomalies 3A and 5B are dashed. Comparisons with synthetic anomalies are shown in Figs. 7.10 and 7.11. Thicker, straight lines are transform faults and fault traces. The 1000-m and 6000-m contours from Fig. 7.4 are used to identify the South Sandwich Islands, other submarine elevations, and the South Sandwich Trench. Lambert Conical Orthomorphic projection.

From: Barker, P.F. 1995. Tectonic framework of the East Scotia Sea. In: Taylor, B. (ed), *Backarc Basins: Tectonics and Magmatism*, Plenum Press, New York, 281-314.

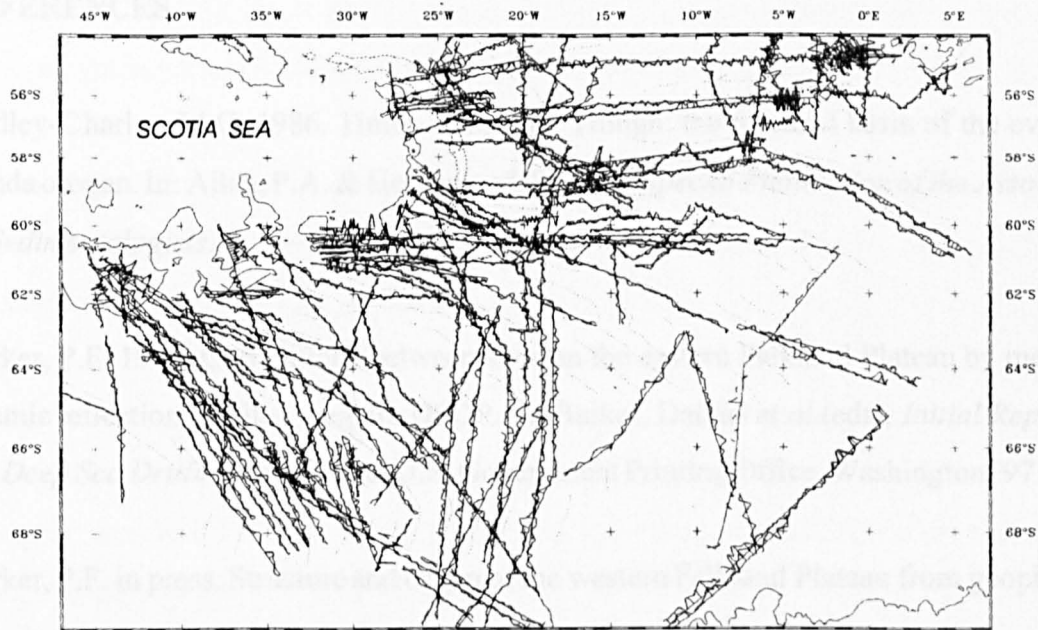


Fig. 5. Summary map of magnetic anomaly profiles used to identify isochrons in the Weddell Sea and adjacent areas. Bathymetric contours from GEBCO Sheet 5.16 are shown at 2000 m (solid) and 6000 m (dotted). Feint, dotted lines in the Weddell Sea represent picked flowlines (see text).

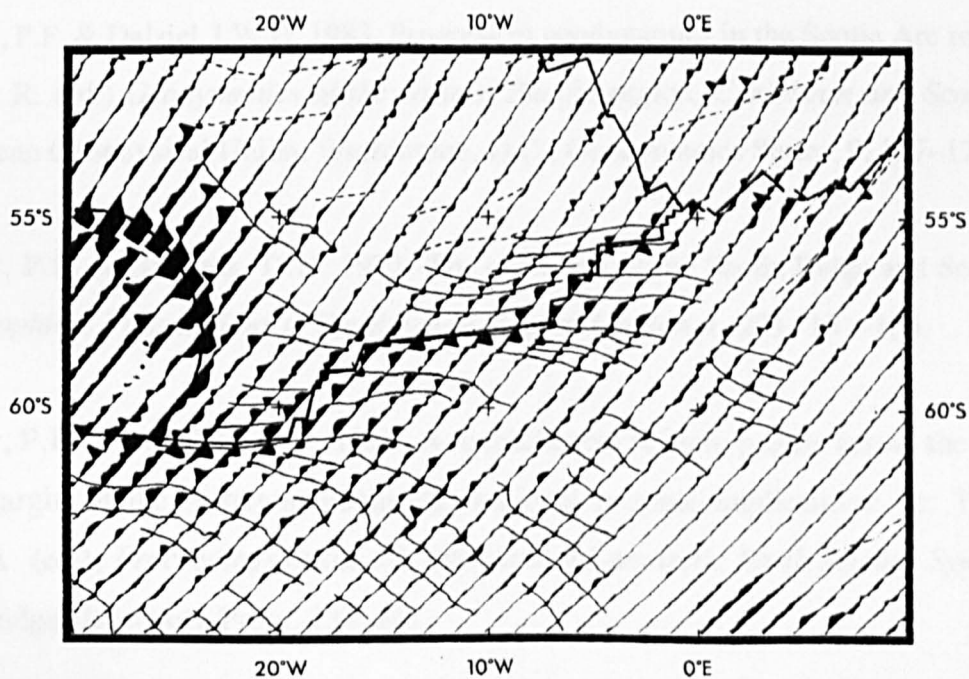


Fig. 4. Plot of along-track gravity anomalies derived from stacked deflection of the vertical data for descending ERM passes. The anomaly wiggle trace has been clipped at ± 100 mGal to preserve clarity. Superimposed are approximate flowlines of SAM-ANT (solid lines), ANT-AFR (composite dashed and dotted lines) and SAM-AFR (dashed lines) relative plate motion.

From: Livermore, R.A. & Woollett, R.W. 1993. Seafloor spreading in the Weddell Sea and southwest Atlantic since the Late Cretaceous, *Earth and Planetary Science Letters*, **117**, 475-495.

REFERENCES

- Audley-Charles, M.G. 1986. Timor–Tanimbar Trough: the foreland basin of the evolving Banda orogen. In: Allen, P.A. & Homewood, P. (eds), *Special Publication of the Association of Sedimentologists*, **8**, 91–102.
- Barker, P.F. 1976. Correlations between sites on the eastern Falkland Plateau by means of seismic reflection profiles, Leg 36, DSDP. In: Barker, Dalziel *et al.* (eds), *Initial Reports of the Deep Sea Drilling Project*, **36**, U.S. Government Printing Office, Washington, 971–990.
- Barker, P.F. in press. Structure and origin of the western Falkland Plateau from geophysical measurements, *Journal of the Geological Society, London*.
- Barker, P.F. & Burrell, J. 1977. The opening of Drake Passage. *Marine Geology*, **25**, 15–34.
- Barker, P.F. & Dalziel, I.W.D. 1983. Progress in geodynamics in the Scotia Arc region. In: Cabre, R. (ed.) *Geodynamics of the eastern Pacific region, Caribbean and Scotia Arcs*. American Geophysical Union, Washington, D.C., Geodynamics Series, **9**, 137–170.
- Barker, P.F. & Griffiths, D.H. 1972. The evolution of the Scotia Ridge and Scotia Sea. *Philosophical Transactions of the Royal Society of London A*, **271**, 151–183.
- Barker, P.F. & Lonsdale, M.J. 1991. A multichannel seismic profile across the Weddell Sea margin of the Antarctic Peninsula: regional tectonic implications. In: Thomson, M.R.A. (ed.), *Proceedings of the 5th International Antarctic Earth Science Symposium*, Cambridge University Press, 237–241.
- Barker, P.F., Barber, P.L. & King, E.C. 1984. An early Miocene ridge crest–trench collision on the South Scotia Ridge near 36°W. *Tectonophysics*, **102**, 315–332.
- Barker, P.F., Dalziel, I.W.D. & Shipboard Scientific Party 1976. Evolution of the

southwestern Atlantic Ocean basin: results of Leg 36, Deep Sea Drilling Project. In: Barker, P.F., Dalziel, I.W.D. *et al.* (eds) *Initial Reports of the Deep Sea Drilling Project*. US Government Printing Office, Washington, **36**, 993–1014.

Barker, P.F., Dalziel, I.W.D. & Storey, B.C. 1991. Tectonic development of the Scotia arc region. In: Tingey, R.J. (ed.) *The geology of Antarctica*. Oxford University Press, New York, monographs on geology and geophysics, **17**, 215–248.

Biju-Duval, B., Le Quellec, P., Mascle, A., Renard, V. & Valery, P. 1982. Multibeam bathymetric survey and high resolution seismic investigations on the Barbados Ridge Complex (eastern Caribbean): a key to the knowledge and interpretation of an accretionary wedge. *Tectonophysics*, **86**, 275–304.

British Antarctic Survey 1988. RRS *Discovery* 172 cruise report, marine geology and geophysics in the Scotia Sea, Weddell Sea and southeast Pacific. Unpublished report, British Antarctic Survey, Cambridge, 46 pp.

British Antarctic Survey 1993. RRS *James Clark Ross* 04 cruise report, marine geology and geophysics, Scotia and Bellingshausen Seas. Unpublished report, British Antarctic Survey, Cambridge, 57 pp.

Brown, K.M. & Westbrook, G.K. 1987. The tectonic fabric of the Barbados Ridge accretionary complex. *Marine and Petroleum Geology*, **4**, 71–81.

Burckle, L.H. & Hays, J.D. 1974. Pre-Pleistocene sediment distribution and evolution of the Argentine continental margin and Falkland Plateau (abs.) Geological Society of America, Abstracts with Programs, **6**, 673–674.

Carlson, R.L. & Raskin, G.S. 1984. Density of the ocean crust. *Nature*, **311**, 555–558.

Carlson, R. L., Gangi, A.F. & Snow, K.R. 1986. Empirical reflection travel time versus depth and velocity versus depth functions for the deep sea sediment column, *Journal of*

Geophysical Research, **91**, 8249-8266.

Carter, D.J.T. 1980. *Echo-sounding correction tables*. Hydrographic Department, Ministry of Defence, Taunton, pp. 150.

Carter, L., Carter, R.M., Nelson, C.S., Fulthorpe, C.S. & Neil, H.L. 1990. Evolution of Pliocene to Recent abyssal sediment waves on Bounty Channel levees, New Zealand. *Marine Geology*, **95**, 97-109.

Chavez, P.S. 1986. Processing techniques for digital sonar images from GLORIA. *Photogrammetric Engineering and Remote Sensing*, **52**, 1133-1145.

Ciesielski, P.F. & Wise, S.W. 1977. Geologic history of the Maurice Ewing Bank of the Falkland Plateau (Southwest Atlantic sector of the southern ocean) based on piston and drill cores, *Marine Geology*, **25**, 175-207.

Ciesielski, P.F., Ledbetter, M.T. & Ellwood, B.B. 1982. The development of Antarctic glaciation and the Neogene palaeoenvironment of the Maurice Ewing Bank. *Marine Geology*, **46**, 1-51.

Dalziel, I.W.D., Dott, R.H., Winn, R.D. & Bruhn, R.L. 1975. Tectonic relationships of South Georgia Island to the southernmost Andes. *Geological Society of America Bulletin*, **86**, 1034-1040.

Damuth, J.E. 1979. Migrating sediment waves created by turbidity currents in the northern South China Basin. *Geology*, **7**, 520-523.

Davey, F.J. 1972. Gravity measurements over Burdwood Bank. *Marine Geophysical Researches*, **1**, 428-435.

deWit, M.J. 1977. The evolution of the Scotia arc as a key to the reconstruction of southwestern Gondwanaland. *Tectonophysics*, **37**, 53-81.

Diraison, M., Cobbold, P.R., Gapais, D. & Rossello, E.A. 1997. Magellan Strait: Part of a Neogene rift system. *Geology*, **25**, 703–706.

Dix, C.H. 1956. Seismic velocities from surface measurements. *Geophysics*, **20**, 68–86.

Dziewonski, A.M., Ekström, G. & Salganik, M.P. 1995. Centroid-moment tensor solutions for July–September 1995. *Physics of the Earth and Planetary Interiors*, **97**, 3–13.

Ewing, J.I., Ludwig, W.J., Ewing, M. & Eittrheim, S.L. 1971. Structure of Scotia Sea and Falkland Plateau. *Journal of Geophysical Research*, **76**, 7118–7137.

Flood, R.D. 1988. A lee-wave model for deep-sea mudwave activity. *Deep-Sea Research*, **35**, 973–983.

Flood, R.D. & Shor, A.N. 1988. Mud waves in the Argentine Basin and their relationship to regional bottom circulation patterns. *Deep-Sea Research*, **35**, 943–971.

Flood, R.D., Shor, A.N. & Manley, P.D. 1993. Morphology of abyssal mudwaves at Project MUDWAVES sites in the Argentine Basin. *Deep-Sea Research II*, **40**, 859–888.

Forsyth, D.W. 1975. Fault plane solutions and tectonics of the South Atlantic and Scotia Sea. *Journal of Geophysical Research*, **80**, 1429–1443.

Genrich, J.F., Bock, Y., McCaffrey, R., Calais, E., Stevens, C.W. & Subarya, C. 1996. Accretion of the southern Banda arc to the Australian plate margin determined by Global Positioning System measurements. *Tectonics*, **15**, 288–295.

Georgi, D.T. 1981. Circulation of bottom waters in the southwestern South Atlantic. *Deep-Sea Research*, **28A**, 959–979.

Gordon, A.L. 1966. Potential temperature, oxygen and circulation of bottom water in the Southern Ocean. *Deep-Sea Research*, **13**, 1125–1138.

- Grose, T.J., Johnson, J.A. & Bigg, G.R. 1995. A comparison between the FRAM (Fine Resolution Antarctic Model) results and observations in the Drake Passage. *Deep-Sea Research I*, **42**, 365–388.
- Hill, I.A. 1978. A marine geophysical study of the crustal structure and evolution of the central Scotia Sea, South Atlantic. Unpublished Ph.D. thesis, University of Birmingham, Birmingham, England. 215 pp.
- Hill, I.A. & Barker, P.F. 1980. Evidence for Miocene back-arc spreading in the Central Scotia Sea. *Geophysical Journal of the Royal Astronomical Society*, **63**, 427–440.
- Hofmann-Wellenhof, B., Lichtenegger, H. & Collins, J. 1992. *Global Positioning System Theory and Practice*. Springer-Verlag, Vienna, 326 pp.
- Hollister, C.D. & Elder, R.B. 1969. Contour currents in the Weddell Sea. *Deep-Sea Research*, **16**, 99–101.
- Howe, J.A., Pudsey, C.J. & Cunningham, A.P. 1997. Pliocene–Pleistocene contourite deposition under the Antarctic Circumpolar Current, western Falkland Trough, South Atlantic Ocean. *Marine Geology*, **138**, 27–50.
- IOC, IHO & BODC. 1997. GEBCO–97: The 1997 edition of the GEBCO digital atlas, published on behalf of the Intergovernmental Oceanographic Commission and the International Hydrographic Organization as part of the General Bathymetric Chart of the Oceans (GEBCO), British Oceanographic Data Centre, Birkenhead.
- Jordan, R.W. & Pudsey, C.J. 1992. High-resolution diatom stratigraphy of Quaternary sediments from the Scotia Sea. *Marine Micropaleontology*, **19**, 201–237.
- Klepeis, K.A. 1994. The Magallanes and Deseado fault zones: Major segments of the South American–Scotia transform plate boundary in southernmost South America, Tierra del Fuego. *Journal of Geophysical Research*, **99**, 22001–22014.

Klepeis, K.A. & Austin, J.A. 1997. Contrasting styles of superimposed deformation in the southernmost Andes. *Tectonics*, **16**, 755–776.

Livermore, R.A. & Hunter, R.J. 1996. Mesozoic sea-floor spreading in the southern Weddell Sea. In: Storey, B.C., King, E.C. & Livermore, R.A. (eds), *Weddell Sea Tectonics and Gondwana Break-up*, Geological Society, London, Special Publication, **108**, 227–241.

Livermore, R.A., McAdoo, D. & Marks, K.M. 1994. Scotia Sea tectonics from high-resolution satellite gravity. *Earth and Planetary Science Letters*, **123**, 255–268.

Locarnini, R.A., Whitworth III, T. & Nowlin, W.D. 1993. The importance of the Scotia Sea on the outflow of Weddell Sea Deep Water. *Journal of Marine Research*, **51**, 135–153.

Lonardi, A. G. & Ewing, M. 1971. Sediment transport and distribution in the Argentine Basin. 4. Bathymetry of the continental margin, Argentine Basin and other related provinces. Canyons and sources of sediments. In: Ahrens, L.H., Runcorn, S.K. & Urey, H.C. (eds) *Physics and chemistry of the Earth*. Pergamon Press, Oxford, **8**, 18–121.

Lonsdale, M.J. 1990. The relationship between silica diagenesis, methane, and seismic reflections on the South Orkney microcontinent. In: Barker, P.F., Kennet, J.P., *et al.*, *Proceedings of the Ocean Drilling Program, Scientific Results*, **113**, 27–37.

Lorenzo, J.M. & Mutter, J.C. 1988. Seismic stratigraphy and tectonic evolution of the Malvinas/Falkland plateau. *Revista Brasileira de Geociências*, **18**, 191–200.

Ludwig, W.J. 1983. Geologic framework of the Falkland Plateau. In: Ludwig, W.J. & Krasheninnikov, V.A., *et al.*, *Initial Reports of the Deep Sea Drilling Project*. U.S. Government Printing Office, Washington, **71**, 281–293.

Ludwig, W.J. & Krasheninnikov, V.A., *et al.* 1983. *Initial Reports of the Deep Sea Drilling Project*. US Government Printing Office, Washington, **71**, 1187 pp.

- Ludwig, W.J. & Rabinowitz, P.D. 1980. Seismic stratigraphy and structure of Falkland Plateau. (Abs.). *American Association of Petroleum Geologists Bulletin*, **64**, 742.
- Ludwig, W.J. & Rabinowitz, P.D. 1982. The collision complex of the North Scotia Ridge. *Journal of Geophysical Research*, **87**, 3731–3740.
- Ludwig, W.J., Carpenter, G., Houtz, R.E., Lonardi, A.G. & Rios, F.F. 1978a. Sediment isopach map: Argentine continental margin and adjacent areas. American Association of Petroleum Geologists, Tulsa, *Argentine Map Series*.
- Ludwig, W.J., Ewing, J.I. & Ewing, M. 1968. Structure of Argentine continental margin. *American Association of Petroleum Geologists Bulletin*, **52**, 2337–2368.
- Ludwig, W.J., Nafe, J.E. & Drake, C.L. 1970. Seismic refraction. In: Maxwell, A.E. (ed.), *The Sea, Ideas and Observations in the Study of the Seas*, Wiley, New York, 53–84.
- Ludwig, W.J., Windisch, C.C., Houtz, R.E. & Ewing, J.I. 1978b. Structure of Falkland plateau and offshore Tierra del Fuego, Argentina. In: Watkins, J.S. *et al.*, *Geological and Geophysical Investigations of Continental Margins*. American Association of Petroleum Geologists, Tulsa, Oklahoma, *Memoirs*, **29**, 125–137.
- Maldonado, A., Larter, R.D. & Aldaya, F. 1994. Forearc tectonic evolution of the South Shetland Margin, Antarctic Peninsula. *Tectonics*, **13**, 1345–1370.
- Marani, M., Argnani, A., Roveri, M. & Trincardi, F. 1993. Sediment drifts and erosional surfaces in the central Mediterranean: seismic evidence of bottom-current activity. *Sedimentary Geology*, **82**, 207–220.
- Marshall, J.E.A. 1994. The Falkland Islands: A key element in Gondwana palaeogeography. *Tectonics*, **13**, 499–514.
- Martin, K.A., Hartnady, C.J.H. & Goodlad, S.W. 1981. A revised fit of South America and

south central Africa. *Earth and Planetary Science Letters*, **54**, 293–305.

Masson, D.G. & Scanlon, K.M. 1991. The neotectonic setting of Puerto Rico. *Geological Society of America Bulletin*, **103**, 144–154.

Mantyla, A.W. & Reid, J.L. 1983. Abyssal characteristics of the world ocean waters. *Deep-Sea Research*, **30**, 805–833.

Mitchell, N.C. 1993. A model for attenuation of backscatter due to sediment accumulations and its application to determine sediment thicknesses with GLORIA sidescan sonar. *Journal of Geophysical Research*, **98**, 22477–22493.

Mitchum, R.M., Vail, P.R. & Sangree, J.B. 1977. Seismic stratigraphy and global changes in sea level, part 6: stratigraphic interpretation of seismic reflection patterns in depositional sequences. In: Payton, C.E. (ed.), *Seismic stratigraphy – Applications to Hydrocarbon Exploration*, American Association of Petroleum Geologists, memoirs, **26**, 117–134.

Moore, G.F. & Shipley, T.H. 1988. Mechanics of sediment accretion in the Middle America Trench. *Journal of Geophysical Research*, **93**, 8911–8927.

Moore, G.F., Shipley, T.H., Stoffa, P.L., Karig, D.E., Taira, A., Kuramoto, S., Tokuyama, H. & Suyehiro, K. 1990. Structure of the Nankai Trough accretionary zone from multichannel seismic reflection data. *Journal of Geophysical Research*, **95**, 8753–8765.

NGDC. 1996. Marine geophysical trackline data (GEODAS/TRACKDAS). Data announce 96-MGG-01. NOAA, U.S. Department of Commerce, Boulder, Colorado.

Normark, W.R., Hess, G.R., Stow, D.A.V. & Bowen, A.J. 1980. Sediment waves on the Monterey Fan levee: a preliminary physical interpretation. *Marine Geology*, **37**, 1–18.

Nowlin W.D. & Zenk W. 1988. Westward bottom currents along the margin of the South Shetland Island Arc, *Deep-Sea Research*, **35**, 269–301.

- Nowlin, W.D. & Klinck, J.M. 1986. The physics of the Antarctic Circumpolar Current. *Reviews of Geophysics*, **24**, 469–491.
- Orsi, A. H., Whitworth, T., III & Nowlin, W. D. 1995. On the meridional extent and fronts of the Antarctic Circumpolar Current. *Deep-Sea Research*, **42**, 641–673.
- Pelayo, A.M. & Wiens, D.A. 1989. Seismotectonics and relative plate motions in the Scotia Sea region. *Journal of Geophysical Research*, **94**, 7293–7320.
- Peterson, R.G. 1992. The boundary currents in the western Argentine Basin. *Deep-Sea Research*, **39**, 623–644.
- Peterson, R.G. & Whitworth III, T. 1989. The Subantarctic and Polar Fronts in relation to deep water masses through the southwestern Atlantic. *Journal of Geophysical Research*, **94**, 10817–10838.
- Piola, A.R. & Gordon, A.L. 1989. Intermediate waters in the southwest South Atlantic. *Deep-Sea Research*, **36**, 1–16.
- Platt, N.H. & Philip, P.R. 1995. Structure of the southern Falkland Islands continental shelf: initial results from new seismic data. *Marine and Petroleum Geology*, **12**, 759–771.
- Pudsey, C.J. 1992. Late Quaternary changes in Antarctic Bottom Water velocity inferred from sediment grain size in the northern Weddell Sea. *Marine Geology*, **107**, 9–33.
- Pudsey, C.J. & Howe, J.A. 1998. Quaternary history of the Antarctic Circumpolar Current: evidence from the Scotia Sea. *Marine Geology*, **148**, 83–112.
- Rabinowitz, P.D. 1977. Free-air gravity anomalies bordering the continental margin of Argentina. American Association of Petroleum Geologists, Tulsa, Oklahoma, *Argentine Map Series*.

- Rabinowitz, P.D., Delach, M., Truchan, M. & Lonardi, A. 1978. Bathymetry of the Argentine continental margin and adjacent areas. American Association of Petroleum Geologists, Tulsa, Oklahoma, *Argentine Map Series*.
- Reed, D.L., Meyer, A.W., Silver, E.A. & Prasetyo, H. 1987. Contourite sedimentation in an intraoceanic forearc system: eastern Sunda arc, Indonesia. *Marine Geology*, **76**, 223–241.
- Rex, D.C. & Tanner, P.W.G. 1982. Precambrian age for gneisses at Cape Meredith in the Falkland Islands. In: Craddock, C. (ed.), *Antarctic Geoscience*. University of Wisconsin Press, Madison, 107–110.
- Richards, P.C., Gatliff, R.W., Quinn, M.F., Williamson, J.P. & Fannin, N.G.T. 1996. The geological evolution of the Falkland Islands continental shelf. In: Storey, B.C., King, E.C. & Livermore, R.A. (eds) *Weddell Sea Tectonics and Gondwana Break-up*. Geological Society, London, Special Publications, **108**, 105–128.
- Saito, T., Burckle, L.H. & Hays, J.D. 1974. Implications of some pre-Quaternary sediment cores and dredgings. In: Hay, W.W. (ed.) *Studies in palaeo-oceanography*. Society of Economic Palaeontologists and Mineralogists, Tulsa, Special Publications, **20**, 6–35.
- Sandwell, D.T., Yale, M.M. & Smith, W.H.F. 1995. Gravity anomaly profiles from ERS-1, Topex, and Geosat Altimetry. *Eos, Transactions, American Geophysical Union*, **76**, S89.
- Searle, R.C., LeBas, T.P., Mitchell, N.C., Somers, M.L., Parson, L.M. & Patriat, P.H. 1990. GLORIA Image Processing: The State of the Art. *Marine Geophysical Researches*, **12**, 21–39.
- Shimmield, G., Derrick, S., Pudsey, C., Barker, P., Mackensen, A., Grobe, H. 1993. The use of inorganic chemistry in studying palaeoceanography of the Weddell Sea. In: Heywood, R.B. (ed.) *University Research in Antarctica, 1989–1992. Proceedings of the British Antarctic Survey Antarctic Special Award Scheme Round 2*. British Antarctic Survey, Cambridge, 99–108.

- Shipley, T.H., Houston, M.H., Buffler, R.T., Shaub, F.J., McMillen, K.J., Ladd, J.W. & Worzel, J. L. 1979. Seismic evidence for widespread possible gas hydrate horizons on continental slopes and rises. *American Association of Petroleum Geologists Bulletin*, **63**, 2204–2213.
- Snyder, D.B., Prasetyo, H., Blundell, D.J., Pigram, C.J., Barber, A.J., Richardson, A. & Tjokosaproetro, S. 1996. A dual doubly vergent orogen in the Banda Arc continent-arc collision zone as observed on deep seismic reflection profiles. *Tectonics*, **15**, 34–53.
- Somers, M.L., Carson, R.M., Revie, J.A., Edge, R.H., Barrow, B.J. & Andrews, A.G. 1978. GLORIA II - an improved long-range side-scan sonar. In: *Oceanology International, Proceedings, Offshore Instrumentation and Communications*. Institute of Electrical Engineers, New York, 16–24.
- Stride, A.H., Belderson, R.H. & Kenyon, N.H. 1982. Structural grain, mud volcanoes and other features on the Barbados Ridge complex revealed by GLORIA long-range side-scan sonar. *Marine Geology*, **49**, 187–196.
- Tanner, P.W.G. 1982. Geology of Shag Rocks, part of a continental block on the north Scotia Ridge, and possible regional correlations. *British Antarctic Survey Bulletin*, **51**, 125–136.
- Tectonic Map of the Scotia Arc, 1985. 1:3 000 000, BAS(Misc) 3. British Antarctic Survey, Cambridge.
- Tomlinson, J.S., Cunningham, A.P. & Barker, P.F. 1992. GLORIA imagery of the North Scotia Ridge (Abs.). *Annales Geophysicae*, **10**, suppl. 1, C77.
- UKOOA-P1/90. 1991. P1/90 post-plot positioning data format. *First Break*, **9**, 172–178.
- Wessel, P. & Smith, W.H.F. 1991. Free software helps map and display data. *Eos, Transactions, American Geophysical Union*, **72**, 441–445.

- Westbrook, G.K., Hardy, N.C. & Heath, R.P. 1995. Structure and tectonics of the Panama–Nazcaplate boundary. In: Mann, P. (ed.) *Geologic and Tectonic Development of the Caribbean Plate Boundary in Southern Central America*. Geological Society of America, Boulder, Colorado, Special Papers, **295**, 91–109.
- White, R.S & Ross, D.A. 1979. Tectonics of the Western Gulf of Oman. *Journal of Geophysical Research*, **84**, 3479–3489.
- Winslow, M. A. 1982. The structural evolution of the Magallanes Basin and neotectonics in the southernmost Andes. In: Craddock, C. (ed.), *Antarctic Geoscience*. University of Wisconsin Press, Madison, 143–154.
- Wise, S.W., Ciesielski, P.F., MacKenzie, D.T., Wind, F.H., Busen, K.E., Gombos, A.M., Haq, B.U., Lohmann, G.P., Tjalsma, R.C., Harris, W.K., Hedlund, R.W., Beju, D.N., Jones, D.L., Plafker, G. & Sliter, W.V. 1982. Palaeontologic and palaeoenvironmental synthesis for the southwest Atlantic Ocean basin based on Jurassic to Holocene faunas and floras from the Falkland Plateau. In: Craddock, C. (ed.), *Antarctic Geoscience*. University of Wisconsin Press, Madison, 155–163.
- Wittstock, R.-R. & Zenk, W. 1983. Some current observations and surface T/S distribution from the Scotia Sea and the Bransfield Strait during early austral summer 1980/1981. *Meteor Forschungs-Ergebnisse, Reihe A/B*, **24**, 77–86.
- Woollard, G.P. 1979. The new gravity system—changes in international gravity base values and anomaly values. *Geophysics*, **44**, 1352–1366.
- Worzel, J.L. 1974. Standard oceanic and continental structure. In: Burk, C.A. and Drake C.L. (eds.), *The Geology of Continental Margins*, Springer-Verlag, New York, 59–66.
- Zenk, W. 1981. Detection of overflow events in the Shag Rocks Passage, Scotia Ridge. *Science*, **213**, 1113–1114.

